

AD-757 762

QUANTUM MECHANICAL CALCULATIONS ON LIGHT
DIATOMIC HYDRIDES

Juergen Hinze

Chicago University

Prepared for:

Army Research Office-Durham
Advanced Research Projects Agency

January 1973

DISTRIBUTED BY:

NTIS

National Technical Information Service
U. S. DEPARTMENT OF COMMERCE
5285 Port Royal Road, Springfield Va. 22151

AD 757762

D D C
RECEIVED
APR 3 1973
RECEIVED
B

Reproduced by
NATIONAL TECHNICAL
INFORMATION SERVICE
U S Department of Commerce
Springfield VA 22151

FINAL TECHNICAL REPORT



UNCLASSIFIED

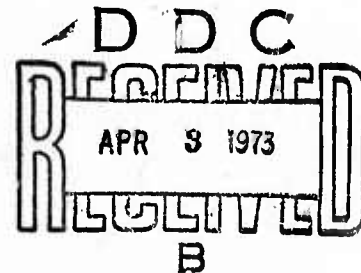
"QUANTUM MECHANICAL CALCULATIONS ON LIGHT
DIATOMIC HYDRIDES"

For the period:
12 June 1970 to 11 June 1971
Army Research Office
Contract DAHC 04-70-C-0037

For the period:
1 October 1971 to 30 September 1972
Army Research Office
Grant DA-ARO-D-31-124-72-G78

Sponsored by
Advanced Research Projects Agency
ARPA Order No. 1482 and 1482 Am. 4

Approved for public release
distribution unlimited



The views and conclusions contained in this document are those of the authors and should not be interpreted as necessarily representing the official policies, either expressed or implied, of the Advanced Research Projects Agency or the U. S. Government.

ARPA Order Number	1482 and 1482 Am. 4
Program Code Number	6230ID
Grantee	The University of Chicago Chicago, Illinois 60637 Tel.: (312) 753-3051
Effective Date	Contract: 12 June 1970 Grant: 1 October 1971
Expiration Date	Contract: 11 June 1971 Grant: 30 September 1972
Amount of Contract	\$55,000
Amount of Grant	\$44,000
Contract Number	DAHC 04-70-C-0037
Grant Number	DA-ARO-D-31-124-72-G78
Principal Investigator	Professor Juergen Hinze Department of Chemistry Tel.: (312) 753-8288
Project Scientist	Dr. Robert Mace (Durham) Tel.: (919) 286-2285
Date	January 1973

Personnel Assigned to Project

Faculty

Juergen Hinze, Assistant Professor of Chemistry, Principal Investigator

Clemens C. J. Roothaan, Professor of Physics, Consultant through June 1971

Research Assistants

John H. Detrich, Physics Ph.D. candidate, through June 1971

Kate K. Docken, Chemistry Ph.D. candidate, through February 1972

George Lie, Chemistry Ph.D. candidate, through September 1972

Shiaw-Shin Liu, Physics Ph.D. candidate, through June 1971

Edward Sachs, Chemistry Ph.D. candidate

Hideo Sambe, Physics Ph.D. candidate, through June 1971

Kenneth J. Schwartz, Chemistry Ph.D. candidate, through July 1972

Zoran Sibincic, Physics Ph.D. candidate, through June 1971

George A. Soukup, Physics Ph.D. candidate, through June 1971

Frank Tobin, Chemistry Ph.D. candidate

Edward Weiss, Physics Ph.D. candidate, through June 1971

Secretarial Staff

Rosie Glass

TABLE OF CONTENTS

1.	Kate K. Docken and Juergen Hinze, "LiH Potential Curves and Wavefunctions for $X^1\Sigma^+$, $A^1\Sigma^+$, $B^1\Pi$, $3\Sigma^+$ and 3Π ." J. Chem. Phys. <u>57</u> , 4928 (1972).	1
2.	Kate K. Docken and Juergen Hinze, "LiH Properties, Rotation-Vibrational Analysis, and Transition Moments for $X^1\Sigma^+$, $A^1\Sigma^+$, $B^1\Pi$, $3\Sigma^+$ and 3Π ." J. Chem. Phys. <u>57</u> , 4936 (1972).	10
3.	George C. Lie, Juergen Hinze and Bowen Liu, "Calculated $a^4\Sigma^-$, $A^2\Delta$, $B^2\Sigma^-$ States of CH," J. Chem. Phys. <u>57</u> , 625 (1972).	27
4.	George C. Lie, Juergen Hinze and Bowen Liu, "Valence Excited States of CH. I. Potential Curves." J. Chem. Phys. <u>58</u> , 0000 (1973).	34
5.	George C. Lie, Juergen Hinze and Bowen Liu, "Valence Excited States of CH. II. Properties." J. Chem. Phys. <u>58</u> , 0000 (1973).	83
6.	Juergen Hinze, "MCSCF I. The Multi-Configuration Self-Consistent-Field Method," J. Chem. Phys. <u>58</u> , 0000 (1973).	126
7.	Juergen Hinze, "Large CI versus MCSCF". Proceedings of the Theoretical Chemistry Conference, Boulder 1972.	153

8. Zoran Sibincic, "Multiconfiguration Self-Consistent-Field Calculations for Several States of Boron." Phys. Rev. A5, 1150 (1972). 162
9. John Detrich, "Pauli Approximation in Many-Electron Atoms." Phys. Rev. A5, 2014 (1972). 172
10. Hideo Sambe, "Steady States and Quasi-Energies of a Quantum-Mechanical System in an Oscillating Field." Phys. Rev. A7, 000 (1973). 186
11. Hideo Sambe, "Effective Charge Tensors of Atoms in a Molecule and Electric Dipole Shielding of Nuclei." J. Chem. Phys. 58, 0000 (1973). 226
12. Hideo Sambe, "Induced Electron Current Density of a Molecule under a Static Magnetic Field." J. Chem. Phys. 58, 0000 (1973). 239
13. George Andrew Soukup, "Self-Consistent Field Calculations for the Elastic Scattering of Electrons from Hydrogen-Like Systems." Phys. Rev. A7, 0000 (1973). 248

LiH Potential Curves and Wavefunctions for $X^1\Sigma^+$, $A^1\Sigma^+$, $B^1\Pi$, $^3\Sigma^+$, and $^3\Pi^*$

KATE K. DOCKEN† AND JUERGEN HINZE

Department of Chemistry, University of Chicago, Chicago, Illinois 60637

(Received 3 August 1972)

Ab initio multiconfiguration self-consistent-field calculations are reported for the potential curves and electronic wave functions of the states $X^1\Sigma^+$, $A^1\Sigma^+$, $B^1\Pi$, $^3\Sigma^+$, and $^3\Pi$ of LiH. In this calculation, the outer two electrons are correlated, while the 1σ shell, essentially a K shell on Li, is left uncorrelated. The obtained dissociation energies, with the known experimental values in parentheses, are $D_e(X^1\Sigma^+) = 2.411(2.5154)$ eV, $D_e(A^1\Sigma^+) = 1.048(1.0765)$ eV, $D_e(B^1\Pi) = 0.017(0.035)$ eV and $D_e(^3\Pi) = 0.226$ eV.

INTRODUCTION

As the smallest neutral heteropolar molecule, LiH has been a favorite molecule for theoretical investigation. Since a reasonable amount of accurate spectroscopic data is available for LiH, detailed calculations can give a good assessment of a given computational procedure, and at the same time, information which can aid in the understanding of the observed data. Until recently, most theoretical work done on LiH (and on molecules in general) concentrated on describing the ground state and its properties only. The experimental information available goes beyond this and a more complete theoretical study should include the calculation of wavefunctions, potential curves, and properties of ground as well as excited states. It is with this aim that we set out to compute the five valence excited states $X^1\Sigma^+$, $A^1\Sigma^+$, $B^1\Pi$, $^3\Sigma^+$, and $^3\Pi$ of LiH. This allows one to evaluate the capability of the multiconfiguration self-consistent-field (MCSCF) method to yield accurate potential curves, term values and molecular properties for ground and excited states. In addition one can expect to obtain a more detailed understanding of some of the observed anomalies in the LiH spectrum.

A careful spectroscopic analysis of the $A^1\Sigma^+-X^1\Sigma^+$ band system of LiH and LiD by Crawford and Jorgensen^{1,2} revealed that the $G(v)$ and B_v values of the $A^1\Sigma^+$ state do not show the normally expected decrease with increasing v . Instead they rise initially, before the normal decrease sets in, yielding anomalous negative values for $\omega_e x_e$ and α_e . The same anomaly is observed for the $A^1\Sigma^+$ states of other alkali hydrides. On the basis of their observation, Crawford and Jorgensen concluded that this anomaly must be ascribed to peculiarities of the potential energy curve of the $A^1\Sigma^+$ state alone.³ Mulliken⁴ explained the exceptional shape of the $A^1\Sigma^+$ potential curve as being due to an avoided crossing of the zero-order curves of LiH and Li^+H^- . However, more recently Jenč⁵ argued that the anomalous character of the $A^1\Sigma^+$ states of the alkali hydrides should be ascribed to nonadiabatic effects, i.e., a breakdown of the Born-Oppenheimer approximation.

In addition to the $A^1\Sigma^+-X^1\Sigma^+$ band system, Velasco⁶ identified in 1957 the $B^1\Pi-X^1\Sigma^+$ system, characterizing the $B^1\Pi$ state as weakly bound ($D_e = 0.03$ eV). No theoretical study to date has yielded a bound potential

curve for this state. Also the corresponding $^3\Pi$ state, which is expected to lie below the singlet state has not as yet been identified.

In the following paragraphs we will give a brief outline of the MCSCF method used in the present calculations, together with some computational details such as basis function choice and selection of configurations. This will be followed by a presentation and discussion of the calculated wavefunctions, potential curves and expectation values of various one electron operators. A more detailed spectroscopic analysis, including the calculation of rotation-vibrational wavefunctions, energies, term values and vibrationally averaged properties will be presented in a forthcoming publication.

THE MCSCF METHOD

It is essential in a computation of the present scope to obtain correlated electronic wavefunctions and energies, since the correlation energy is expected to be significantly different at different internuclear distances as well as for the different states. It is well known that a configuration interaction (CI) type wavefunction

$$\Psi = \sum_I C_I \Phi_I \quad (1)$$

is capable of representing correlation effects exactly, provided the CI expansion is carried far enough. It is obvious that the convergence of this CI expansion will depend critically on the appropriateness of the expansion functions Φ_I . In the conventional CI methods as here, the Φ 's are configuration state functions (CSF's), i.e., specific linear combinations of Slater determinants (SD's), such that they are eigenfunctions of the symmetry operators of the system. The SD's themselves are constructed from symmetry adapted orbitals. The expansion functions Φ_I and thus the convergence of (1) will depend therefore on the type of orbitals which are used in their construction, as well as on the detailed functional shape of the orbitals. It is here where the difference between conventional CI and MCSCF lies. In conventional CI only the expansion coefficients C_I are optimized variationally, while the MCSCF also optimizes variationally the detailed shape of all the orbitals entering the total wavefunction. Thus one obtains a wavefunction which will give the lowest possible energy with the given number and type of CSF's.

The procedure for computation is then to

- (1) select initial orbitals and configuration types,
- (2) solve the CI problem for the state desired,
- (3) construct the SCF equations from the first and second order density matrices of the selected state of (2);
- (4) solve the SCF equations.

Steps (2)–(4) are iterated to convergence. If we select in (2) always the K th lowest root, then one will obtain an upper bound to the true energy of the K th state of a given symmetry. Unfortunately this process does not always work except for the lowest state of a given symmetry. The reason for this is as follows. Since the orbitals are optimized in the field corresponding to state K , this state will be described better and its energy lowered. However if one of the lower states, for instance, state J , has a very different charge distribution than state K , thus requiring quite different orbitals, it follows that the orbitals obtained for state K will be poorer for state J . Thus the energy of state J , originally below state K , will be raised. This may eventually lead to a flipping of the energy order of these two states, preventing convergence of the MCSCF process. Such a state flipping will always happen when the excited state desired has a state of the same symmetry only a little lower in energy, but with a substantially different charge distribution. This is exactly the case for the $A\ ^1\Sigma^+$ state of LiH, the $X\ ^1\Sigma^+$ state being lower by only a few eV. It is possible in this case to optimize the orbitals in the averaged field of both states, obtaining compromise orbitals which will describe both states equally well, however neither optimally. Fortunately it is possible to make up for the deficiency in these compromise orbitals by the addition of a few singly excited configurations. This will become clear in the discussion on configuration selection. The details of the MCSCF method as well as the "averaged field method" are described explicitly elsewhere.⁷

CHOICE OF CONFIGURATIONS

It appears reasonable that in LiH the correlation energy of the 1σ shell, essentially the K shell of lithium, remains nearly constant as the potential curves are traversed and as the outer electrons are excited. Therefore we have chosen to correlate only the outer two valence electrons, which simplifies the problem significantly. In the two electron correlation problem singly excited configurations do not contribute; therefore it is possible to account for the correlation energy of the $B\ ^1\Pi$, $^3\Pi$ and $^3\Sigma^+$ states by using only doubly excited configurations. The particular ones chosen for these three states are presented in Table I, where the bold configuration signifies the dominant one in each state for all internuclear distances calculated.

The configuration choice for the averaged field calculation of $X\ ^1\Sigma^+$ and $A\ ^1\Sigma^+$ is not as straightforward.

TABLE I. Types of valence configurations used.

$X\ ^1\Sigma^+$ and	$1\sigma^2(2\sigma^2+4\sigma^2+5\sigma^2+6\sigma^2+1\pi^2+2\pi^2+1\delta^2+2\delta^2)$
$A\ ^1\Sigma^+$	$2\sigma 3\sigma+4\sigma 5\sigma+4\sigma 3\pi+5\sigma 3\sigma+6\sigma 3\sigma+1\pi 2\pi+1\delta 2\delta$
$B\ ^1\Pi$	$1\sigma^2(2\delta 1\pi+3\sigma 2\pi+4\sigma 3\pi+2\pi 1\delta+3\pi 1\delta)$
$^3\Pi$	$1\sigma^2(2\delta 1\pi+3\sigma 2\pi+4\sigma 3\pi+2\pi 1\delta+3\pi 1\delta)$
$^3\Sigma^+$	$1\sigma^2(2\delta 3\sigma+4\sigma 5\sigma+1\pi 2\pi+1\delta 2\delta)$

Fifteen configurations were used and are given in Table I. The lowest energy configuration of $^1\Sigma^+$ symmetry at intermediate R values is $1\sigma^2 2\sigma^2$, and of necessity ionic (Li^+H^-). The 2σ is a $1s\ \text{H}^-$ type orbital. The configuration of next lowest energy in the intermediate R range is $1\sigma^2 2\sigma 3\sigma$. In this case the 2σ orbital is a much more contracted $1s\ \text{H}$ -like orbital, and the 3σ is a diffuse $2s-2p$ hybrid on Li. Because of the double occupation in the ground state, the 2σ orbital determined in the averaged field calculations is essentially that for the ground state. Thus it is too diffuse in nature to describe adequately the 2σ orbital in the $A\ ^1\Sigma^+$ state. The purpose of the thirteen additional configurations was to correlate the ground and first excited state and to make up for the 2σ orbital deficiency in the excited state. Because of the doubly occupied configurations, the 4σ , 5σ , and 6σ orbitals essentially contribute to in-out and left-right correlation of the ground state. By not including a $3\sigma^2$ configuration which would attempt to correlate the ground 2σ also, we tried to make the 3σ orbital an orbital of the excited state only. By considering $2\sigma_A\ ^1\Sigma^+=2\sigma_X\ ^1\Sigma^++4\sigma+5\sigma+6\sigma$ in order to make up for orbital deficiency, the configurations $3\sigma 4\sigma$, $3\sigma 5\sigma$, and $3\sigma 6\sigma$ arise. The doubly occupied π and δ configurations primarily introduce angular correlation into the ground state, while the $1\pi 2\pi$ and $1\delta 2\delta$ configurations are more effective in correlating the $A\ ^1\Sigma^+$ state. A discussion of the orbitals and important configurations in the wavefunctions of these two $^1\Sigma^+$ states at several internuclear distances is postponed until the next section.

It was found both convenient and time saving to move across the potential curves in one direction using the converged orbital coefficients for each state at the preceding internuclear distance to begin the calculation at each point. No convergence difficulties in solving the SCF equations were encountered in the calculation of the $B\ ^1\Pi$, $^3\Pi$ and $^3\Sigma^+$ states. These states retained the same dominant configuration all across the potential curves, the orbitals of the additional configurations being solely used to correlate the valence electrons. In the averaged field calculation of the $A\ ^1\Sigma^+$ and $X\ ^1\Sigma^+$ states, convergence difficulties, characterized mainly by orbital flipping among the valence sigma orbitals, could be avoided when the R step size through the curve-crossing regions was made small enough. It is

TABLE II. Basis set of Slater-type orbitals: $23\sigma \times 8\pi \times 4\delta$.

		<i>N</i>	<i>L</i>	<i>M</i>	<i>K</i>	Zeta
1	1	1	0	0	1	4.6351
2	2	1	0	0	1	2.4730
3	3	2	0	0	1	1.0330
4	4	2	0	0	1	0.8237
5	5	2	0	0	1	0.5100
6	6	3	0	0	1	2.6811
7	7	2	1	0	1	3.9004
8	8	2	1	0	1	2.1109
9	9	2	1	0	1	1.0758
10	10	2	1	0	1	0.7359
11	11	2	1	0	1	0.5100
12	12	2	1	0	1	0.3500
13	13	3	2	0	1	1.4974
14	14	3	2	0	1	0.9866
15	15	4	3	0	1	1.7748
16	16	1	0	0	2	1.9583
17	17	1	0	0	2	1.0000
18	18	1	0	0	2	0.7000
19	19	1	0	0	2	0.4000
20	20	2	0	0	2	2.2425
21	21	2	1	0	2	1.0633
22	22	2	1	0	2	0.5480
23	23	3	2	0	2	1.5774
24	1	2	1	1	1	1.5600
25	2	2	1	1	1	0.7800
26	3	2	1	1	1	0.5472
27	4	2	1	1	1	0.3500
28	5	3	2	1	1	1.0000
29	6	2	1	1	2	2.0000
30	7	2	1	1	2	1.0000
31	8	3	2	1	2	2.1000
32	1	3	2	2	1	1.0000
33	2	3	2	2	1	0.5000
34	3	3	2	2	2	2.0000
35	4	3	2	2	2	1.0000

felt that the dual role of these orbitals—that of correlating the ground state 2σ and making up for deficiencies in the excited state 2σ —imposed a strain. The valence sigma orbitals were attempting to optimize simultaneously in several different regions of space.

CHOICE OF BASIS SET

The importance of choosing a good basis set cannot be underestimated in a multiconfiguration technique, for, in the limit that all configurations are included, the basis set determines the quality of the calculation. Since the same basis set of Slater-type functions (STF's) was used for four of the five states of LiH, the following factors were considered important in selecting it:

- (1) how well it reproduced the ground state Hartree-Fock
- (2) how adequate it was for description of correlating orbitals

(3) in the averaged field case, how it could compensate for orbital deficiencies

(4) how well it could describe the excited states.

Utilizing the same basis set for all states is economical, in that integrals have to be calculated only once at each internuclear distance. Also, it ensures that the representation of the core orbital does not change from one state to another. The calculation of the transition moment, in addition, is considerably simplified. Since one of our primary interests was in accurately calculating the ground and first excited $^1\Sigma^+$ states, we knew that we needed a large and flexible basis set. It seemed reasonable, therefore, that with few extra functions added the basis would be sufficient for the Π states also.

The basis set used in our final calculation is listed in Table II. A subset of 21σ , 7π and 4δ STF's (all the listed functions except for those numbered 12, 19, 27) was optimized at the equilibrium internuclear distance for the $X^1\Sigma^+$ state with the 2σ shell correlated. Preliminary calculations were carried out with this reduced basis and it was found necessary to add the three additional diffuse functions (12, 19, and 27) in order to describe better the $A^1\Sigma^+$ state and the Π states. The $^3\Sigma^+$ state, however, was not recalculated. The total basis set yielded for the $X^1\Sigma^+$ state the Hartree-Fock energy of -7.987317 hartree at 3.0 bohr, essentially the Hartree-Fock limit.

CALCULATED POTENTIAL CURVES

The potential curves obtained are given in Tables III and IV and displayed in Fig. 1. Within the framework of the Hartree-Fock model the $X^1\Sigma^+$ state with configuration $1\sigma^2 2\sigma^2$ will dissociate to ions, $\text{Li}^+(^1S) +$

TABLE III. Potential curves for four states of LiH.

<i>R</i> (bohrs)	$X^1\Sigma^+$, <i>E</i> (hartrees)	$A^1\Sigma^+$, <i>E</i> (hartrees)	$B^1\Pi$, <i>E</i> (hartrees)	$^3\Pi$, <i>E</i> (hartrees)
2.00	-7.948461	-7.804494	-7.7667212	-7.7857226
2.25	-7.986659	-7.841651	-7.8048017	-7.8225261
2.50	-8.007771	-7.865183	-7.8288091	-7.8452320
2.75	-8.017994	-7.880054	-7.8438361	-7.8588998
3.00	-8.021254	-7.889358	-7.8531226	-7.8667765
3.25	-8.020163	-7.895156	-7.8587516	-7.8709706
3.50	-8.016339	-7.898690	-7.8620695	-7.8728632
4.00	-8.004649	-7.902121	-7.8649605	-7.8730600
4.50	-7.990950	-7.903239	-7.8656627	-7.8714465
5.00	-7.977741	-7.903563	-7.8656819	-7.8696445
5.50	-7.965892	-7.903427	-7.8655471	-7.8681780
6.00	-7.955901	-7.902660	-7.8654140	-7.8671223
6.50	-7.948031	-7.900999	-7.8653134	-7.8664058
7.50	-7.938476	-7.894651	-7.8651918	-7.8656261
8.50	-7.934672	-7.885984	-7.8651279	-7.8652968
10.00	-7.933082	-7.874234	-7.8650787	-7.8651187
12.00	-7.932752	-7.866665	-7.8650508	-7.8650565

H-(¹S). The ionic dissociation limit lies about 4.64 eV above the neutral atoms. [The ionization potential of Li(²S) is 5.39 eV⁸ and the electron affinity of H(²S) is taken as 0.75 eV⁹.] The neutral, ground-state atoms Li(²S) and H(²S) can give rise, however, to molecular states ¹Σ⁺ and ³Σ⁺. By the adiabatic noncrossing rule, therefore, the X¹Σ⁺ state must dissociate to Li(²S) + H(²S). Consequently the wavefunction must change character from ionic to neutral as the potential curve is traversed from small to large *R*, and this is well described by an MCSCF type wavefunction.

The A¹Σ⁺ state, with molecular configuration 1σ²2σ3σ, is predominantly Li-H⁺ for small *R*. In the region 6.0–10.0 bohr, however, this state interacts strongly with the 1/*R* ionic curve which is dominant in the ground state for small *R*. As the ground state becomes more neutral in order to dissociate correctly,

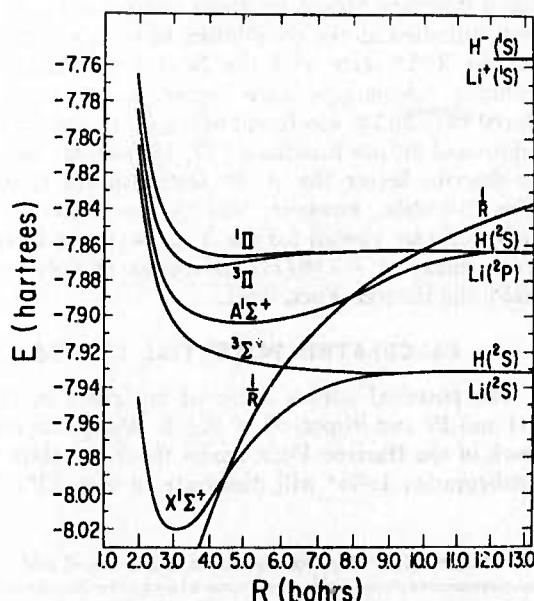


FIG. 1. Potential curves of five states of LiH. Included also is a 1/*R* curve, referred to the ionic limit Li⁺+H⁻, *E* = -7.764 hartree, at *R* = ∞.

the A¹Σ⁺ becomes ionic (Li⁺H⁻) with dominant configuration 1σ²2σ². This state would dissociate to ions if it were not for the fact that the excited atoms Li(²P) + H(²S) can also give rise to a ¹Σ⁺ state. This dissociation limit lies 1.85 eV above the ground state neutrals—almost three electron volts lower than the ionic limit. Therefore, the A¹Σ⁺ state must for large *R* become neutral and dissociate to Li(²P) + H(²S). Two avoided crossings which alter the character of the wave function occur in this A¹Σ⁺ state.

In Table V are listed the four most important configurations in the X¹Σ⁺ and A¹Σ⁺ calculation and the appropriate CI mixing coefficients for each state at three different internuclear distances. These distances, 3.0, 7.5, and 12.0 bohr were chosen to show how the

TABLE IV. Potential curve points for ³Σ⁺.^a

<i>R</i> (bohrs)	Energy (hartrees)	<i>R</i> (bohrs)	Energy (hartrees)
2.0	-7.81863	4.0	-7.91984
2.5	-7.87889	5.0	-7.92584
2.9	-7.90027	6.0	-7.92944
3.0	-7.90366	7.5	-7.93189
3.1	-7.90655	9.0	-7.93256
3.5	-7.91442	12.0	-7.93271

^a Calculated using a 21σ×7π×4δ set of STO's given in Table III eliminating basis functions 12, 19, and 27.

character of the wavefunctions for these states changes with *R*. The orbital expansion coefficients for the 2σ, 3σ, and 4σ orbitals at the three internuclear distances are presented in Tables VI, VII, and VIII, respectively. At 3.0 bohr the dominant configuration for the ground state is 1σ²2σ² with the diffuse 2σ having most weight on basis functions 17, 18, and 19 (Table VI). There is some small Li 2s-2p contribution—enough to indicate that this is a molecular orbital. The 3σ is diffuse 2s_{Li} with some 2p_{Li} and diffuse H⁻ character—also a molecular orbital. The 4σ character is difficult to pinpoint, but it has large contributions on H basis functions to correlate the 2σ and contributions arising also from Li 2s and 2p functions.

In going from 3.0 to 7.5 bohr the orbitals of course do change character slightly, but not drastically. Individual changes are difficult to identify with such a large basis merely by looking at the orbital expansion coefficients. The change in the configuration mixtures for the states is to be noted at 7.5 bohr. Now the 1σ²2σ3σ configuration is dominant in the X¹Σ⁺ state and the A¹Σ⁺ state is predominantly 1σ²2σ². The ground state has become neutral and the first excited state ionic.

TABLE V. Dominant configurations in the X¹Σ⁺ and A¹Σ⁺ states.

	Configuration mixing coefficients			
	1σ ² 2σ ²	1σ ² 2σ3σ	1σ ² 4σ ²	1σ ² 3σ4σ
<i>R</i> = 3.0 bohr				
X ¹ Σ ⁺	0.96	-0.23	-0.10	0.07
A ¹ Σ ⁺	0.24	0.94	-0.03	-0.24
<i>R</i> = 7.5 bohr				
X ¹ Σ ⁺	-0.40	0.78	0.13	-0.39
A ¹ Σ ⁺	0.84	0.44	-0.22	-0.21
<i>R</i> = 12.0 bohr				
X ¹ Σ ⁺	-0.07	0.77	0.04	-0.62
A ¹ Σ ⁺	0.84	0.06	-0.54	-0.05

TABLE VI. Comparison of 2σ orbital for X and $A\ ^1\Sigma^+$ states at three internuclear distances.

	σ Basis functions				Zeta	Orbital coefficients		
	N	L	M	K		3.0 bohr	7.5 bohr	12.0 bohr
1	1	0	0	1	4.6351	-0.00305	-0.00045	-0.00058
2	1	0	0	1	2.4730	-0.12211	-0.01359	-0.00412
3	2	0	0	1	1.0330	-0.01111	-0.14824	-0.01674
4	2	0	0	1	0.8237	0.20176	0.24952	-0.01999
5	2	0	0	1	0.5100	-0.17579	-0.12169	0.04033
6	3	0	0	1	2.6811	-0.03982	0.00632	-0.00305
7	2	1	0	1	3.9004	0.00560	0.00166	0.00103
8	2	1	0	1	2.1109	-0.00410	0.00763	0.00783
9	2	1	0	1	1.0758	0.09521	-0.03667	0.02540
10	2	1	0	1	0.7359	0.11922	0.12243	-0.03274
11	2	1	0	1	0.5100	0.03258	0.24619	0.61914
12	2	1	0	1	0.3500	-0.01408	-0.05585	-0.02548
13	3	2	0	1	1.4974	0.00919	-0.00906	-0.00143
14	3	2	0	1	0.9860	0.01120	0.02561	0.00347
15	4	3	0	1	1.7746	0.00279	0.00094	0.00013
16	1	0	0	2	1.9883	0.07231	0.07333	0.01961
17	1	0	0	2	1.0000	0.26934	0.19550	0.57531
18	1	0	0	2	0.7000	0.40755	0.39494	0.03894
19	1	0	0	2	0.4000	0.13425	0.24966	0.16892
20	2	0	0	2	2.2425	0.01403	0.02760	0.00469
21	2	1	0	2	1.0638	-0.02485	0.01042	0.00765
22	2	1	0	2	0.5480	-0.02622	-0.05529	-0.01872
23	3	2	0	2	1.5774	0.00344	0.00153	-0.00012

At 12.0 b the 2σ orbital is well represented as a linear combination of a diffuse Li $2p$ function and an H $1s$, i.e., $(2p_{Li} + 1s_H)$. The 4σ orbital is just the orthogonal component to this, $(2p_{Li} - 1s_H)$. Very atomiclike at this internuclear distance, the 3σ orbital is $2s_{Li}$ with essentially no $2p_{Li}$ character. Because the $A\ ^1\Sigma^+$ dissociates to $Li(^2P) + H(^2S)$ and has no Li $2s$ character at large R , the weights for configurations $1\sigma^2 2\sigma 3\sigma$ and $1\sigma^2 3\sigma 4\sigma$ are very small in this state. One can understand the configuration mixture for both states from a valence-bond standpoint. For the $A\ ^1\Sigma^+$ state the $2\sigma^2$ configuration is essentially $(2p_{Li} + 1s_H)^2$ while the $4\sigma^2$ configuration $(2p_{Li} - 1s_H)^2$ enters with the opposite sign. Thus valence bond components $2p_{Li}1s_H$ are enhanced, while the ionic components $2p_{Li}^2$ and $1s_H^2$ are subtracted. The $2p_{Li}1s_H$ description is necessary to be consistent with the dissociation limit.

The same sort of argument explains the equal magnitude but opposite sign mixture of $2\sigma 3\sigma$ and $3\sigma 4\sigma$ in the $X\ ^1\Sigma^+$ state. We have, in terms of atomic functions $(2p_{Li} + 1s_H)(2s_{Li}) - (2p_{Li} - 1s_H)(2s_{Li})$. The $2p_{Li}2s_{Li}$ contributions cancel, while the $2s_{Li}1s_H$ components add, giving us what we expect for dissociation to $Li(^2S) + H(^2S)$.

The remaining states arising from the $Li(^2P) + H(^2S)$ separated atom limit are $B\ ^1\Pi$, $^3\Pi$ and $^3\Sigma^+$. Of these, we performed calculations on the Π states, only, which have the dominant configuration $1\sigma^2 2\sigma 1\pi$. The $^3\Sigma^+$ state we did compute is the lowest of that par-

ticular symmetry (with configuration $1\sigma^2 2\sigma 3\sigma$) and is a repulsive state dissociating to ground state neutrals.

In order to calculate dissociation energies from the potential curves for each of the molecular states we need the energies of the separated atoms at the dissociation limits. Because we are not correlating the 1σ lithium core at all we want the energy of the separated atoms to reflect this. Therefore we choose to take for the reference energies at the dissociation limit $Li(^2S) + H(^2S)$ the calculated Hartree-Fock energy of $Li(^2S)$, $E = -7.432726$ hartree¹⁰ and the exact energy for $H(^2S)$ of $E = -0.5$ hartree. The sum of these two energies, $E = -7.932726$ hartree, gives the separated atom ground state energy with an uncorrelated $1s$ shell on lithium. The $X\ ^1\Sigma^+$ and $^3\Sigma^+$ state dissociate to these separated atoms. It can be seen from Tables III and IV that at 12.0 bohr both states are virtually at this energy limit.

The second dissociation limit of interest is $Li(^2P) + H(^2S)$, involving a $2s \rightarrow 2p$ excitation of the lithium valence electron from the ground state atom. Using the $Li(^2P)$ Hartree-Fock energy, $E = -7.365068$ hartree,¹¹ the dissociation limit energy for $Li(^2P) + H(^2S)$ is -7.865068 hartree. An estimate for this limit could also be made using the $Li(^2S)$ Hartree-Fock and the $2s \rightarrow 2p$ excitation energy.⁸ An energy about 73 cm^{-1} higher than that quoted above is obtained because this does not account for a difference in correlation in the $1s^2 2s$ versus $1s^2 2p$ configurations. It

TABLE VII. Comparison of 3σ orbital for X and $A\ ^1\Sigma^+$ states at three internuclear distances.

	σ Basis functions				Zeta	Orbital coefficients		
	N	L	M	K		3.0	7.5	12.0
1	1	0	0	1	4.6351	0.00966	0.01023	0.01039
2	1	0	0	1	2.4730	0.10867	0.15640	0.15903
3	2	0	0	1	1.0330	0.24515	0.41298	0.47360
4	2	0	0	1	0.8237	-0.70832	-1.09659	-1.19227
5	2	0	0	1	0.5100	-0.71703	-0.36182	-0.29639
6	3	0	0	1	2.5811	0.01010	0.02160	0.01323
7	2	1	0	1	3.9004	0.00135	0.00024	0.00015
8	2	1	0	1	2.1109	0.01054	0.00477	0.00077
9	2	1	0	1	1.0758	-0.01736	-0.00845	0.00595
10	2	1	0	1	0.7359	0.19866	0.02614	-0.01513
11	2	1	0	1	0.5100	0.29576	0.20617	0.03802
12	2	1	0	1	0.3500	-0.06852	-0.05162	-0.01816
13	3	2	0	1	1.4974	0.00091	-0.00326	-0.00020
14	3	2	0	1	0.9866	0.00420	0.00895	0.00050
15	4	3	0	1	1.7748	0.00012	0.00025	0.00002
16	1	0	0	2	1.9883	0.01686	0.00356	-0.00255
17	1	0	0	2	1.0000	-0.05517	0.00899	0.02582
18	1	0	0	2	0.7000	-0.02557	-0.06606	-0.04177
19	1	0	0	2	0.4000	0.44309	0.16701	0.03730
20	2	0	0	2	2.2425	0.00412	0.00049	-0.00183
21	2	1	0	2	1.0638	0.00393	-0.00130	-0.00176
22	2	1	0	2	0.5480	-0.03627	-0.02082	-0.00494
23	3	2	0	2	1.5774	0.00062	0.00062	0.00022

may be seen from Table III that the $^3\Pi$ and $B\ ^1\Pi$ states have converged to this limit at 12.0 bohr and that the $A\ ^1\Sigma^+$ state is still slightly below this limit.

The energy minima of the potential curves for the four bound states were obtained by polynomial interpolation between the calculated points and are listed in Table IX. Also listed in this table are the internuclear distance at the energy minimum (R_{min}), the dissociation energies calculated from E_{min} and the dissociation limits discussed here, and the experimental values. The calculated D_e 's are all less than the experimental quantities which is to be expected in a variational type calculation where the exact energy eigenvalue has not yet been reached.

The experimental D_e 's are thought to be relatively accurate—to within ± 0.0002 eV. The bands observed by Velasco⁶ for the $B\ ^1\Pi-X\ ^1\Sigma^+$ system showed clear breaking off of the rotational structure. This was attributed to rotational predissociation of the upper state. Extrapolation of the limiting curve of dissociation yields a dissociation limit for the $B\ ^1\Pi$ state which is felt to be accurate to within several wavenumbers. Using the $2s \rightarrow 2p$ excitation energy, the dissociation limit for the ground state was obtained by Velasco also.

The largest difference between our calculated and the experimental D_e is in the $X\ ^1\Sigma^+$ state. The calculated D_e is about 845 cm^{-1} smaller than experiment would indicate. Thus the minimum of our potential curve for

this state lies 845 cm^{-1} too high. This discrepancy in the ground state is not surprising for several reasons. One factor is the use of the averaged field. At 3.0 bohr, using the same set of configurations as in the averaged field calculation, the energy for the $X\ ^1\Sigma^+$ state was obtained alone. This energy, $E = -8.021974$ hartree, is 143 cm^{-1} below the averaged field $X\ ^1\Sigma^+$ minimum. Another source of error is neglecting to account for the change in the intershell correlation. As the potential curve is traversed from small to large R , the $2\sigma^2$ pair breaks apart, leaving at the separated atom limit only two $1\sigma-2\sigma$ (or $1s-2s$) pairs instead of four. At the potential minimum, therefore, we have twice as much correlation error due to $1\sigma-2\sigma$ pairs as at the separated limit. This is estimated, from calculations on the $K-L$ shell correlation energy of the united atom Be,¹² to be not more than 500 cm^{-1} . The largest error, however, is probably due to incomplete correlation of the 2σ shell. We estimate, from calculations of comparable accuracy using the MCSCF method for two- and four-electron atomic systems,¹² that 90%–95% of the correlation energy of the 2σ pair was obtained. Therefore somewhere between 400 and 800 cm^{-1} of correlation energy is still unaccounted for. Our error of 845 cm^{-1} is thus easily attributed to a combination of the three factors just discussed.

The other two states for which experimental D_e 's are known, the $B\ ^1\Pi$ and $A\ ^1\Sigma^+$, are shown to be too shallow by 143 and 232 cm^{-1} , respectively. Although we have

TABLE VIII. Comparison of 4σ orbital for X and $A\ ^1\Sigma^+$ states at three internuclear distances.

	σ Basis functions				Zeta	Orbital coefficients		
	N	L	M	K		3.0	7.5	12.0
1	1	0	0	1	4.6351	0.00654	-0.00154	-0.00061
2	1	0	0	1	2.4730	-0.14538	-0.02034	-0.00513
3	2	0	0	1	1.0330	0.14033	-0.29442	0.02668
4	2	0	0	1	0.8237	0.14749	0.48290	-0.03019
5	2	0	0	1	0.5100	-0.45533	-0.24050	0.05143
6	3	0	0	1	2.6811	-0.07510	0.01469	-0.00504
7	2	1	0	1	3.9004	-0.00510	-0.00577	0.00365
8	2	1	0	1	2.1109	0.01181	0.03837	0.00348
9	2	1	0	1	1.0758	0.11971	-0.13880	0.04712
10	2	1	0	1	0.7359	0.39131	0.34243	-0.06016
11	2	1	0	1	0.5100	-0.04435	0.38885	0.78293
12	2	1	0	1	0.3500	0.02392	-0.07891	-0.03383
13	3	2	0	1	1.4974	0.01238	-0.01748	-0.00105
14	3	2	0	1	0.9866	-0.00931	0.04821	0.00263
15	4	3	0	1	1.7748	-0.00335	0.00154	0.00009
16	1	0	0	2	1.9383	-0.01101	0.09821	0.02109
17	1	0	0	2	1.0000	-2.65779	-1.80925	-0.88332
18	1	0	0	2	0.7000	2.35030	0.89112	0.05627
19	1	0	0	2	0.4000	0.21902	0.44637	0.20362
20	2	0	0	2	2.2425	-0.16867	0.00603	0.00403
21	2	1	0	2	1.0638	-0.24561	0.00745	0.01779
22	2	1	0	2	0.5480	-0.07226	-0.11000	-0.02214
23	3	2	0	2	1.5774	0.01260	0.00286	-0.00078

made the least absolute error in calculating the $B\ ^1\Pi$ state, the 143 cm^{-1} represents about half the binding energy for this state and thus will greatly affect subsequent calculations of spectroscopic quantities. The correlation energy in these two states is very small compared to that in the $X\ ^1\Sigma^+$ state—less than 10%. The remaining correlation energy between the valence electrons unaccounted for is felt to be less than 50 cm^{-1} . The amount by which our dissociation energies differ from experiment probably reflects the neglect of the change in correlation of two 1σ - 2σ pairs as the potential curve is traversed.

The calculated T_e values evidence, also, the fact that the error in the ground state is much larger than the error in either excited state:

$$T_e(A\ ^1\Sigma^+ - X\ ^1\Sigma^+) = 25\,842\text{ cm}^{-1} \quad (\text{exptl } 26\,510)$$

$$T_e(B\ ^1\Pi - X\ ^1\Sigma^+) = 34\,153\text{ cm}^{-1} \quad (\text{exptl } 34\,912)$$

$$T_e(A\ ^1\Sigma^+ - B\ ^1\Pi) = 8\,310\text{ cm}^{-1} \quad (\text{exptl } 8\,402)$$

The R_{\min} for the $X\ ^1\Sigma^+$ state agrees reasonably well with experiment; however, the agreement for the $A\ ^1\Sigma^+$ and $B\ ^1\Pi$ states appears exceptionally poor. The reason for this may be seen in the fact that both of these po-

TABLE IX. Energy minima, dissociation energies, and R_e 's for four states of LiH.

State	E_{\min} (hartrees) ^a	D_e (calc, eV)	D_e (exptl, eV) ^b	R_{\min} (bohrs) ^a	R_e (exptl, bohrs)
$X\ ^1\Sigma^+$	-8.021321	2.411 ^a	2.5154	3.05	3.015 ^d
$A\ ^1\Sigma^+$	-7.903574	1.048 ^a	1.0765	5.12	4.9064 ^d
$B\ ^1\Pi$	-7.865709	0.017 ^a	0.035	4.75	4.494 ^b
$^3\Pi$	-7.873358	0.226 ^a		3.76	

^a Minimum of electronic potential curve obtained by fifth order polynomial interpolation.

^b See Ref. 6.

^c Dissociation limit energy of $\text{Li}(^3S) + \text{H}(^3S)$, $E = -7.932726$ hartree.

^d See Ref. 9, p. 546.

^e Dissociation limit energy of $\text{Li}(^3P) + \text{H}(^3S)$, $E = -7.865068$ hartree.

tential curves are very flat around their minima. It will be seen, however, in a following paper presenting a spectroscopic analysis of the potential curves, that the discrepancy is also due to the fact that R_e values obtained by an extrapolation of the B_v 's do not correspond to the minima of these potential curves.

DISCUSSION AND COMPARISON WITH OTHER THEORETICAL RESULTS

Lithium hydride has been the testing ground for almost every *ab initio* method proposed for extending calculations beyond the Hartree-Fock level in molecules; and although a plethora of theoretical calculations on LiH exist, there are very few for which a comparison with ours is instructive. This is due to the fact that most calculations are for the ground state at its potential minimum ($R_e = 3.015$ bohr), only, and most attempt correlation of both core and valence electrons. A brief review of several of these calculations follows. For comparison, Cade and Huo's calculation ($E = -7.987313$ hartree) for the $X^1\Sigma^+$ state is probably close to the true Hartree-Fock energy for the system. The experimental energy at the $X^1\Sigma^+$ potential minimum is -8.0703 .¹⁸ Although not an upper bound, the lowest energy obtained to date for the ground state is that of Boys and Handy¹⁴ ($E = -8.063$ hartree) using a transcorrelated wavefunction containing terms explicitly depending on r_{ij} . The best variational calculation was done by Bender and Davidson,¹⁵ using a natural orbital approach and a set of elliptic basis functions. They obtained an energy minimum of -8.0606 hartree. Many other results using various techniques could be mentioned¹⁸⁻²⁷; however, we will compare our work only with those calculations which correlate the valence shell.

Our MCSCF method, correlating the valence shell alone is akin to Wahl's OVC method.²⁸ Mukherjee and McWeeny,²⁹ using a similar approach with a frozen K shell, chose nine configurations to correlate the 2σ valence shell in the ground state, obtaining an energy of -8.01488 hartree at R_e . As our basis set was almost three times as large as theirs, we expect to do significantly better for the $X^1\Sigma^+$ state; hence our value of $E = -8.02121$ hartree is not surprising.

To date, the most comprehensive study of all the potential curves which we investigated is that of Bender and Davidson,³⁰ who used a frozen 1σ core and limited configuration interaction to obtain nineteen states at nine different internuclear distances. Their work represents the only other calculation of the $B^1\Pi$ and $^3\Pi$ potential curves besides our present results, and Bender and Davidson do not obtain a bound $B^1\Pi$. At $R_e = 3.0156$ they obtain an energy of -8.0036 hartree for the $X^1\Sigma^+$ state. Our value lies almost 3900 cm^{-1} lower. The main difference here is thought to be our optimization of the correlating orbitals. In preliminary calculations, using the Bender-Davidson basis set

of 13σ , 4π , and 1δ STF's, we obtained for the $X^1\Sigma^+$ state with four MCSCF configurations $1\sigma^2(2\sigma^2+3\sigma^2+4\sigma^2+1\pi^2)$ an energy of $E = -8.0173$ hartree; 3000 cm^{-1} lower than their fifty configuration result. To investigate whether our energy improvement might be due to changes in the K shell upon correlation of the valence shell, we froze our 1σ orbital to the Hartree-Fock value and carried out the same calculation. The energy change was only 6 cm^{-1} , showing that the K shell is affected very little by correlation of the valence shell. Thus the 3000 cm^{-1} difference between the 50 configuration CI result and our four configuration MCSCF result is due to our optimization of the valence and correlating orbitals only. Much of the remaining difference between our present calculation and that of Bender and Davidson is due to our more extensive basis set.

In the $A^1\Sigma^+$ curve, Bender and Davidson calculate the minimum to be $E = -7.8979$ hartree compared to our -7.9036 hartree—a difference of $\sim 1250\text{ cm}^{-1}$. In their calculation they obtain a repulsive $B^1\Pi$ state. The lowest energy which they obtain is at 6.0 bohr, $E = -7.8606$ hartree, compared to our minimum for this state which is at least 1000 cm^{-1} below this value, and at $R \approx 4.7$ bohr. The minimum of their $^3\Pi$ curve, $E = -7.8666$ hartree, is again higher than ours by about 1500 cm^{-1} . The fact that the $^3\Pi$ state is more poorly described than the $B^1\Pi$ in Bender and Davidson's calculation is probably due to an inadequate π basis set on H. The $^3\Pi$ state has a dipole moment Li^+H^- which indicates a small shift of charge to H occurring in the 1π orbital.

ACKNOWLEDGMENTS

The authors express their gratitude to H. Preston, who made available a carefully optimized basis set, and also to IBM Research, San Jose, where some of the computations were carried out.

* This research was supported in part by the Advanced Research Projects Agency of the Department of Defense, monitored by the U.S. Army Research Office-Durham, Box CM, Duke Station, Durham, North Carolina 27706, under Grant DA-ARO-D-31-124-72-G78, and by Grant GP-21108 of the National Science Foundation.

† Present address: Harvard College Observatory, Cambridge, Mass. 02138.

- ¹ F. H. Crawford and T. Jorgensen, *Phys. Rev.* **47**, 358 (1935).
- ² F. H. Crawford and T. Jorgensen, *Phys. Rev.* **47**, 932 (1935).
- ³ F. H. Crawford and T. Jorgensen, *Phys. Rev.* **49**, 745 (1936).
- ⁴ R. S. Mulliken, *Phys. Rev.* **50**, 1028 (1936).
- ⁵ F. Jenč, *J. Mol. Spectry.* **19**, 63 (1966).
- ⁶ R. Velasco, *Can. J. Phys.* **35**, 1204 (1957).
- ⁷ J. Hinze, *J. Chem. Phys.* (to be published).
- ⁸ C. E. Moore, *Natl. Bur. Std. (U.S.) Circ. No. 467*, Vol. 1.
- ⁹ G. Herzberg, *Spectra of Diatomic Molecules* (D. Van Nostrand, Princeton, N.J., 1950), 2nd ed.
- ¹⁰ Accurate basis set calculation from E. Clementi, *IBM J. Res. Develop.* **9**, 2 (1965).
- ¹¹ A. Weiss, *Astrophys. J.* **138**, 1262 (1963).
- ¹² N. Sabelli and J. Hinze, *J. Chem. Phys.* **50**, 684 (1969).
- ¹³ B. Ransil, *Rev. Mod. Phys.* **32**, 239 (1960).
- ¹⁴ S. F. Boys and N. C. Handy, *Proc. Roy. Soc. (London)* **A311**, 309 (1969).
- ¹⁵ C. F. Bender and E. R. Davidson, *J. Phys. Chem.* **70**, 2675 (1966).

- ¹⁶ J. C. Browne and F. A. Matsen, *Phys. Rev.* **135**, A1227 (1964).
- ¹⁷ R. E. Brown and H. Shull, *Intern. J. Quantum Chem.* **2**, 663 (1968).
- ¹⁸ F. E. Harris and H. S. Taylor, *Physica* **30**, 105 (1964).
- ¹⁹ H. S. Taylor, *J. Chem. Phys.* **39**, 3382 (1963).
- ²⁰ W. E. Palke and W. A. Goddard, *J. Chem. Phys.* **50**, 4524 (1969).
- ²¹ D. D. Ebbing and R. C. Henderson, *J. Chem. Phys.* **42**, 2225 (1965).
- ²² S. L. Kahalas and R. K. Nesbet, *J. Chem. Phys.* **39**, 529 (1963).
- ²³ A. M. Karo and A. R. Olson, *J. Chem. Phys.* **30**, 1232 (1959).
- ²⁴ A. M. Karo, *J. Chem. Phys.* **30**, 1241 (1959).
- ²⁵ I. G. Csizmadia, B. T. Sutcliffe, and M. P. Barnett, *Can. J. Chem.* **42**, 1645 (1964).
- ²⁶ J. Goodisman, *J. Chem. Phys.* **51**, 3540 (1969).
- ²⁷ C. F. Melius, W. A. Goddard, and L. R. Kahn, *J. Chem. Phys.* **56**, 3342 (1972).
- ²⁸ G. Das and A. C. Wahl, *J. Chem. Phys.* **44**, 87 (1966).
- ²⁹ N. G. Mukherjee and R. McWeeny, *Intern. J. Quantum Chem.* **4**, 97 (1970).
- ³⁰ C. F. Bender and E. R. Davidson, *J. Chem. Phys.* **49**, 4222 (1968).

Reprinted from:

THE JOURNAL OF CHEMICAL PHYSICS VOLUME 57, NUMBER 11 1 DECEMBER 1972

LiH Properties, Rotation-Vibrational Analysis, and Transition Moments for $X^1\Sigma^+$, $A^1\Sigma^+$, $B^1\Pi$, $^3\Sigma^+$, and $^3\Pi^*$

KATE K. DOCKEN† AND JUERGEN HINZE

Department of Chemistry, University of Chicago, Chicago, Illinois 60637

(Received 3 August 1972)

Using accurate *ab initio* calculated potential curves and electronic wavefunctions for the states $X^1\Sigma^+$, $A^1\Sigma^+$, $B^1\Pi$, $^3\Sigma^+$, and $^3\Pi$ for LiH, various properties were calculated. These include dipole and quadrupole moment, field gradient at the nuclei, etc. Rotation-vibrational wavefunctions were obtained and a rotation-vibrational analysis was carried out. Some of the properties obtained were averaged over the appropriate rotation-vibrational wavefunctions. In addition electronic transition moments were computed and from this uv and ir line strengths were obtained. In general the agreement with experimental values, where available, is satisfactory.

In the preceding paper, hereafter referred to as Paper I,¹ we discussed the calculation of the potential curves for five states of LiH: $X^1\Sigma^+$, $A^1\Sigma^+$, $B^1\Pi$, $^3\Pi$, and $^3\Sigma^+$. In computing electronic energies and wavefunctions, essentially one-half of the Born-Oppenheimer problem has been solved. Now, not only can we solve the second half of the Born-Oppenheimer problem for the motion of the nuclei in each bound state, but we can also obtain information about stationary state properties and transition probabilities. The following sections describe the calculation of various molecular properties using the multiconfiguration self-consistent field (MCSCF) wavefunctions and potential curves of Paper I and present the results. These properties are of three types and will be discussed separately: (1) spectroscopic quantities obtained by solution of the one-dimensional radial Schrödinger equation for the nuclear motion; (2) the expectation values of certain one-electron operators evaluated over the electronic wavefunctions of each state; (3) transition moments between different electronic states.

I. VIBRATION-ROTATION ANALYSIS

In the Born-Oppenheimer approximation, it is assumed that the total wavefunction of a diatomic molecule can be expressed as a product of nuclear and electronic wavefunctions, which are solutions of separate equations. The electronic energies and wavefunctions are usually obtained as in Paper I in a field

of fixed nuclei and thus depend parametrically on the internuclear distance R . With the electronic energy $U(R)$ playing the role of the potential energy, the Schrödinger equation for the nuclear motion of a diatomic molecule, regarded as a symmetric top, can be separated into angular and radial parts. The solution has the following form:

$$\Psi = R^{-1} P_{v,J}(R) Y_{J\Lambda M}(\theta, \varphi, \chi), \quad (1)$$

where the $Y_{J\Lambda M}$'s are the eigenfunctions of the symmetric top.

In the above expression, θ is the angle of the figure axis of the top with a fixed z axis; φ is the azimuthal angle about the z axis; χ is the azimuthal angle measuring rotation about the figure axis (z axis). The quantum number M is the projection of the total angular momentum along an arbitrary axis in space. The quantum numbers J and Λ differ in meaning according to the particular coupling case and will be discussed below. $P_{v,J}(R)$, the vibrational wavefunction, is the solution of the one-dimensional radial Schrödinger equation (in atomic units):

$$\left(\frac{d^2}{dR^2} \right) P_{v,J}(R) - 2\mu \{ U(R) + [J(J+1) - \Lambda^2] / 2\mu R^2 - E_{v,J} \} P_{v,J}(R) = 0, \quad (2)$$

where μ is the reduced mass of the nuclei; $U(R)$ is the electronic energy for fixed internuclear distance R (including the Coulomb repulsion of the nuclei), and v is the vibrational quantum number. $U(R)$ together with the centrifugal potential term gives an effective

TABLE I. Spectroscopic constants for the states $X^1\Sigma^+$, $A^1\Sigma^+$, $B^1\Pi$, and $^3\Pi$ of LiH and LiD.^a

	$X^1\Sigma^+$		$A^1\Sigma^+$		$B^1\Pi$		$^3\Pi$	
	LiH	LiD	LiH	LiD	LiH	LiD	LiH	LiD
Be (calc)	7.35	4.14	2.74	1.54	3.11	1.74	5.01	2.84
(exptl)	7.51	4.28	2.82	1.61	3.38	1.91
α_e (calc)	0.20	0.09	-0.05	-0.02	1.36	0.59	0.64	0.28
(exptl)	0.21	0.09	-0.08	-0.01	0.99	0.43
γ_e (calc)	-0.004	-0.001
(exptl)	-0.025	-0.002
ω_e (calc)	1387.47	1026.85	290.70	195.15	171.13 ^b	133.12 ^b	620.89	466.52
(exptl)	1405.65	1055.12	234.41	183.12	215.50	177.28
$\omega_e x_e$ (calc)	22.24	11.66	-11.37	-7.40	54.10 ^b	34.15 ^b	52.38	29.71
(exptl)	23.20	13.23	-28.95	-12.74	42.40	29.13
$\omega_e y_e$ (calc)	-0.35	-0.18
(exptl)	0.16	...	-4.18	-0.88
D_e (calc)	2.411	...	1.048	...	0.017	...	0.226	...
(exptl)	2.515	...	1.076	...	0.035
R_e (calc)	3.049	...	4.996	...	4.688	...	3.693	...
(exptl)	3.015	...	4.906	...	4.494
R_{\min} (calc)	3.05	...	5.12	...	4.75	...	3.76	...

^a All units are cm^{-1} , except D_e is in eV and R in bohr. Conversion factors used are: 1 hartree = 27.210 eV = $2.194762 \times 10^{-8} \text{ cm}^{-1}$, 1 bohr = $0.529167 \times 10^{-8} \text{ cm}$. The experimental values for $X^1\Sigma^+$ and $A^1\Sigma^+$ are from Ref. 5; D_e 's and constants for the $B^1\Pi$ state are from Ref. 7.

^b Determined using $G(1)$, $G(0)$ and the zero point energy from R_{\min} .

potential governing the vibration of the nuclei. For each J a spectrum of vibrational eigenvalues $E_{v,J}$ and corresponding wavefunctions $P_{v,J}$ is obtained. In systems such as ours, where we have included no relativistic effects in the electronic energy calculation, we can really consider only Hund's coupling case b. In this instance, the quantum number J is the total angular momentum excluding spin, and Λ is the projection of the electronic orbital angular momentum along the internuclear axis. If spin-orbit coupling had been accounted for in the electronic energy calculation, then the Λ quantum number in the radial Schrödinger equation should be Ω , and J should be the total angular momentum.

As the potential $U(R)$ is usually obtained at a few selected points R it is more convenient to solve Eq. (2) by numerical integration. Since the number of calculated $U(R)$ points are too sparse for a direct numerical integration we have used a fifth order polynomial interpolation to get the required intermediate points. For $R < 2.0$ bohr and $R > 12.0$ bohr an analytic extrapolation was used to extend the potential curves. Equation (2) was numerically integrated using Numerov's method as described by Cooley² with certain modifications due to Blatt.³ From the calculated vibration-rotation eigenvalues spectroscopic information was obtained by taking the appropriate energy differences. The resulting eigenfunctions $P_{v,J}(R)$ can be used to vibrationally average certain electronic properties, to give more realistic observables.

For the same electronic and vibrational state, the

energy difference between adjacent rotational levels can be expressed using Herzberg's⁴ notation as

$$F_v(J+1) - F_v(J) = 2(J+1)B_v - 4(J+1)^2 D_v. \quad (3)$$

The D_v contribution is often three orders of magnitude smaller than B_v , and can usually be neglected. If, however,

$$[F_v(J+1) - F_v(J)]/2(J+1)$$

is not constant for a range of J values for a particular v , the D_v term cannot be neglected. Consequently a linear least squares fit to $(J+1)^2$ must be performed to obtain B_v and D_v . The spectroscopic constants B_v and α_e can then be obtained by a linear least squares fit of B_v to $(v+1/2)$ according to the equation

$$B_v = B_e - \alpha_e(v+1/2). \quad (4)$$

The $\Delta G_{v+1/2}$ values [where $\Delta G_{v+1/2} = G(v+1) - G(v)$] are the primary spectroscopic information of interest for the vibrational levels. For Σ states, the $\Delta G_{v+1/2}$'s are obtained directly from the $J=0$ level by taking energy differences between adjacent vibrational states. For electronic states of higher symmetry, where there is no $J=0$ level, the appropriate rotational terms are subtracted out. Although the spectroscopic constants ω_e , $\omega_e x_e$, and $\omega_e y_e$ can be obtained via least squares fits to the $G(v)$ values, the most satisfactory comparison between theory and experiment is not made with these constants, but with the $\Delta G_{v+1/2}$ values themselves. We present the computed and experimental spectroscopic constants for all four states of LiH in Table I, while

TABLE II. Vibrational energy level differences^a: $X^1\Sigma^+$.

v	LiH		LiD	
	$\Delta G_{v+1/2}$ (calc)	$\Delta G_{v+1/2}$ (exptl) ^b	$\Delta G_{v+1/2}$ (calc)	$\Delta G_{v+1/2}$ (exptl) ^b
0	1330.95	1359.77	1007.39	1029.08
1	1284.93	1314.85	981.59	1003.59
2	1241.47	1270.90	955.52	978.56
3	1201.34		931.60	953.84
4	1160.82		909.14	
5	1118.47		886.59	
6	1076.77		862.92	
7	1035.58		839.33	
8	995.71		815.48	
9	955.75		792.19	
10	915.42		769.32	
11	874.21		746.78	
12	831.58		724.32	
13	786.66		701.60	
14	738.67		678.69	
15	686.25		655.45	
16	627.82		631.59	
17	561.77		606.88	
18	485.54		581.09	

^a In cm^{-1} , $\Delta G_{v+1/2} = G(v+1) - G(v)$.^b See Ref. 5.

the $\Delta G_{v+1/2}$ and B_v values for LiH and LiD are given together with the experimentally known quantities in Tables II and III for the $X^1\Sigma^+$ state, Tables IV and V for the $A^1\Sigma^+$ state, Tables VI and VII for the $B^1\Pi$, and Tables VIII and IX for the $^3\Pi$.

In cases where the theoretical potential curve is shallower than the true curve, the energy level spacing will be smaller, making the $\Delta G_{v+1/2}$'s smaller than the experimental quantities. As we calculate a dissociation energy that is smaller than the true D_0 in every case, the calculated $\Delta G_{v+1/2}$'s err to a greater or lesser extent in the expected direction.

TABLE III. Rotational constants^a: $X^1\Sigma^+$.

v	LiH		LiD	
	B_v (calc)	B_v (exptl) ^b	B_v (calc)	B_v (exptl) ^b
0	7.26	7.4067	4.10	4.1882
1	7.05	7.1950	4.01	4.0970
2	6.83	6.9848	3.92	4.0082
3	6.63	6.7782	3.83	3.9204
4	6.44		3.75	3.833
5	6.24		3.67	
6	6.04		3.58	
7	5.84		3.50	

^a In cm^{-1} .^b See Ref. 5.

In general, the deviation of the B_v 's from the experimental values is on the order of 0.2 cm^{-1} , while for the $\Delta G_{v+1/2}$'s the difference is from 2 to 30 cm^{-1} . Although the errors are approximately 1%–2% of the quantities themselves, the difference in the magnitudes is probably due to a different cancellation of error in the two cases. Adjacent rotational levels with identical v 's, the difference of which determines B_v , lie very close together. They essentially sample the same region of the potential curve—each with a slightly different centrifugal contribution. The energy difference between the calculated and the true potential curve is almost the same for these two levels. Thus the error in the computed levels is approximately the same and cancels out in the subtraction process provided $\langle 1/R^2 \rangle$ is

TABLE IV. Vibrational energy level differences^a: $A^1\Sigma^+$.

v	LiH		LiD	
	$\Delta G_{v+1/2}$ (calc)	$\Delta G_{v+1/2}$ (exptl) ^b	$\Delta G_{v+1/2}$ (calc)	$\Delta G_{v+1/2}$ (exptl) ^b
0	274.91	280.96	199.12	
1	309.47	312.96	221.30	224.6
2	333.52	335.73	237.95	239.92
3	350.80	352.80	250.68	252.19
4	363.29	365.85	260.53	262.03
5	372.55	375.60	268.36	270.14
6	379.38	382.68	274.58	276.69
7	383.99	387.55	279.82	282.00
8	386.73	390.37	283.79	286.13
9	388.04	391.59	286.69	289.28
10	387.76	391.05	288.81	291.60
11	385.99	389.19	290.30	293.08
12	382.86	385.94	291.18	293.78
13	378.17	381.32	291.28	293.30
14	371.86		290.78	293.34
15	363.81		289.71	292.11
16	353.70		288.00	290.41
17	341.17		285.71	288.0
18	325.67		282.76	285.2

^a In cm^{-1} ; $\Delta G_{v+1/2} = G(v+1) - G(v)$.^b Averaged from several band origins; see Ref. 5.

correct. The $\Delta G_{v+1/2}$'s, however, are the differences between adjacent vibrational levels for $J=0$ where the energy spacing is ~ 100 times greater than for the rotational levels. Neighboring vibrational levels sample different regions of the potential curve and thus have different intrinsic error which will not completely cancel out in taking the difference.

Because the calculated B_v 's agree very closely with the corresponding experimental values, the R_v 's calculated from these B_v 's [$R_v = 1/(2\mu B_v)^{1/2}$] also agree well with experiment. These R_v 's do not agree, in most cases, with the R_v 's obtained by interpolating the calculated potential curve points to obtain the min-

imum. The R value at the minimum of the electronic potential curve will be denoted R_{\min} . Thus the spectroscopic R_e is not always the minimum of the electronic potential energy curve, except for the potential curves very harmonic near the minimum. In comparing the theoretical results to experiment, then, the R_e calculated from B_e , rather than the R_{\min} , should be compared with the spectroscopic R_e values.

Using the electronic potential curve for each bound state, we computed vibration-rotation levels for both LiH and LiD using the atomic masses $^7\text{Li}=7.01600$, $^1\text{H}=1.007825$, $^6\text{D}=2.0140$. Most of the discussion in the following sections will center on LiH to avoid repetition, as most of the trends observed in LiH are seen in LiD also.

TABLE V. Rotational constants^a: $A \ ^1\Sigma^+$.

v	LiH		LiD	
	B_e (calc)	B_e (exptl) ^b	B_e (calc)	B_e (exptl) ^b
0	2.70	2.8536	1.52	
1	2.81	2.8897	1.57	1.6238
2	2.83	2.9044	1.59	1.6316
3	2.84	2.9083	1.59	1.6365
4	2.85	2.9057	1.60	1.6383
5	2.84	2.8959	1.60	1.6382
6	2.83	2.8804	1.60	1.6358
7	2.81	2.8589	1.60	1.6310
8	2.78	2.8333	1.59	1.6243
9	2.75	2.8022	1.59	1.6162
10	2.72	2.7707	1.58	1.6057
11	2.68	2.7322	1.56	1.5955
12	2.64	2.6895	1.55	1.5824
13	2.60	2.6442	1.54	1.5678
14	2.55	2.5942	1.52	1.5534
15			1.51	1.5361
16			1.49	1.5197
17			1.48	1.5002

^a In cm^{-1} .

^b See Ref. 5.

A. $X \ ^1\Sigma^+$

The $\Delta G_{v+1/2}$ values for this state appear in Table II. While we stopped our calculations at 20 vibrational levels, only four have been observed spectroscopically.^{5,6} The 20th vibrational level for $J=0$ lies at $E=-7.9366$ hartree, at $\sim 96\%$ of the well depth. The calculated $\Delta G_{v+1/2}$'s are smaller than the experimental ones for LiH in each case by $\sim 30 \text{ cm}^{-1}$. This is to be expected, as the calculated potential curve is too shallow by approximately 845 cm^{-1} due to incomplete correlation of the 2σ shell and neglect of the intershell $1\sigma-2\sigma$ correlation. By including all 19 $\Delta G_{v+1/2}$'s in a linear least squares fit, the spectroscopic constants $\omega_e=1387.5 \text{ cm}^{-1}$ and $\omega_e x_e=22.2 \text{ cm}^{-1}$ (see Table I) were obtained.

TABLE VI. Vibrational energy level differences^a: $B \ ^1\Pi$.

v	LiH		LiD	
	$\Delta G_{v+1/2}$ (calc)	$\Delta G_{v+1/2}$ (exptl) ^b	$\Delta G_{v+1/2}$ (calc)	$\Delta G_{v+1/2}$ (exptl) ^b
0	66.45	130.73	67.11	119.00
1	...	45.90	...	60.82

^a In cm^{-1} ; $\Delta G_{v+1/2} = E(v+1, J) - E(v, J) - (B_{v+1} - B_v)J(J+1) + (D_{v+1} - D_v)J^2(J+1)^2 = G(v+1) - G(v)$, here for $J=1$.

^b See Ref. 7.

By eliminating the first three calculated $\Delta G_{v+1/2}$'s from this fit, the values became 1402.1 and 22.8 cm^{-1} , respectively, while the experimental numbers are 1405.6 and 23.2 cm^{-1} . This does not necessarily mean that the calculated $\Delta G_{v+1/2}$'s will agree more closely with experiment for higher v . It does indicate the sensitivity of the fit to the number of $\Delta G_{v+1/2}$'s used, suggesting the inadequacy of the fit. Also, the experimental spectroscopic constants would probably be quite different from the present ones if 20 vibrational levels had been observed. Thus it seems of little value to compare the ω_e and $\omega_e x_e$'s.

The B_v values for this state are given in Table III, and in each case are less than the experimental quantities by $\sim 0.15 \text{ cm}^{-1}$. From the calculated B_v for LiH (fitted to the B_v 's), $R_e=3.049 \text{ b}$ was obtained. Within the limit of our interpolation, this is exactly equal to R_{\min} ($R_{\min}=3.05 \text{ bohr}$). The deviation from experiment ($R_e=3.015 \text{ bohr}$) is approximately 1% .

B. $A \ ^1\Sigma^+$

Twenty vibrational levels were calculated for this state, while 14 vibrational levels have been observed spectroscopically for LiH. The highest vibrational state computed here lies about 86% up the potential well from the minimum.

The $\Delta G_{v+1/2}$'s for this state, shown in Table IV, exhibit anomalous behavior, increasing with v initially until a maximum and then decreasing. The maximum $\Delta G_{v+1/2}$ for LiH is reached at $v=9$, while for LiD v_{\max} is larger, at $v=13$. This is to be expected from the

TABLE VII. Rotational constants^a: $B \ ^1\Pi$.

v	LiH		LiD	
	B_e (calc)	B_e (exptl) ^b	B_e (calc)	B_e (exptl) ^b
0	2.43	2.88	1.44	1.69
1	1.07	1.80	0.85	1.25

^a In cm^{-1} .

^b See Ref. 7.

TABLE VIII. Vibrational energy level differences*: $^2\Pi$.

v	$\Delta G_{v+1/2}$ (LiH)	$\Delta G_{v+1/2}$ (LiD)
0	513.83	403.57
1	413.83	348.38
2	308.69	290.92
3	199.71	231.32
4	92.68	169.96
5		108.19
6		49.37

* In cm^{-1} ; see Footnote (a) of Table VI.

ratio $\omega_e x_e/\omega_e y_e$, which is larger for LiD than for LiH. The calculated $\Delta G_{v+1/2}$'s for this state are smaller than the experimental ones by approximately 2 to 3 cm^{-1} on the average. This small difference between experimental and calculated values, in contrast to the situation in the $X^1\Sigma^+$ state, reflects the fact that there is very little correlation remaining unaccounted for in this state. The calculated $\Delta G_{v+1/2}$'s follow the experimental trend exactly, peaking at the same v 's as do the spectroscopic quantities. Because of this anomalous behavior, however, a polynomial representation in $(v+1/2)$ to obtain the spectroscopic constants ω_e , $\omega_e x_e$, etc., is practically meaningless, as Crawford and Jorgensen observed.⁵

The B_v 's in Table V show the same sort of anomalous behavior as the $\Delta G_{v+1/2}$'s. The calculated values are on the whole ~ 0.05 cm^{-1} less than the experimental quantities, and increase to a maximum at around $v=5$, and then decrease. Again, a polynomial fit to the B_v 's to obtain B_e and α_e is not very satisfying. The calculated B_e does yield an $R_e=4.996$ bohr which is closer to the experimental $R_e=4.906$ bohr than R_{min} , which is at 5.12 bohr. Thus we were able to reproduce the anomalous spectroscopic behavior of the $A^1\Sigma^+$ state very accurately within the framework of the Born-Oppenheimer approximation, demonstrating that Jenč's⁴ explanation for the anomalies in this state as due to a break-down of the Born-Oppenheimer approximation is incorrect.

Rydberg-Klein-Rees (RKR) potential curves were generated for the $X^1\Sigma^+$ and $A^1\Sigma^+$ states using the spectroscopic constants of Crawford and Jorgensen⁵ and are illustrated along with our calculated curves in Fig. 1. For this figure the minima of the RKR curves were obtained using the experimental D_v 's and the Hartree-Fock atomic dissociation limits, which are at -8.0252 and -7.9046 hartree respectively. The experimental vibrational levels associated with the RKR curves are the solid lines, whereas our calculated vibrational levels for $J=0$ are the dashed lines.

RKR potential curves are only accurate insofar as the energy can be expressed in a power series of $(v+1/2)$ and $J(J+1)$. In addition, the accuracy of the curves is limited to the range of v from which the

experimental spectroscopic constants were derived. For this latter reason, it is not surprising that the $X^1\Sigma^+$ RKR curve does not dissociate correctly. Only the four lowest vibrational levels have been observed for this state. The $X^1\Sigma^+$ RKR vibrational levels are below our calculated ones in every instance through $v=15$. At $v=19$, however, the two curves deviate substantially from one another and the RKR vibrational level lies above ours. This just indicates that the spectroscopic constants derived for the levels $v=0-3$ are not adequate for describing the higher part of the potential curve.

In the $A^1\Sigma^+$ state, due to the odd shape of the potential curve, the energy cannot be represented well in a Dunham-type expansion. The spectroscopic constants used in generating the RKR curve are such that for energies higher than -7.885 hartree (see Fig. 1) the R values of the left hand turning point either stay the same or become larger. The result of this would be a non-single-valued function of the energy with internuclear distance. Since this is physically unreasonable, we have drawn the $A^1\Sigma^+$ RKR curve only in the regions where the curve is well-behaved, i.e., from 3.0 to 8.5 bohr.

C. $B^1\Pi$

The calculation of the vibration-rotation levels for this state was greatly affected by the fact that only $\sim 50\%$ of the experimental binding energy was obtained. Whereas three vibrational states were observed spectroscopically,⁷ we were able to calculate only two. The highest level, for $J=2$, $v=1$ lay at -7.865042 hartree, several wavenumbers above the dissociation limit for the rotationless state. The $\Delta G_{1/2}$, as shown in Table VI, for this state is smaller by 64 cm^{-1} than the corresponding experimental $\Delta G_{1/2}$. The B_v 's agreed more closely with experiment, but the B_e is only a two point fit. It is not surprising then that R_e calculated from B_e is 5.688 bohr, whereas the experimental R_e is 4.494 bohr.

D. $^2\Pi$

Although this state has not yet been observed experimentally, the spectroscopic quantities of interest

TABLE IX. Rotational constants*: $^2\Pi$.

v	B_v (LiH)	B_v (LiD)
0	4.60	2.62
1	4.08	2.41
2	3.50	2.18
3	2.83	1.93
4	2.03	1.65
5	1.07	1.33
6		0.95
7		0.50

are given in Tables VIII and IX. The behavior of the B_v 's and $\Delta G_{v+1/2}$'s is fairly normal. The highest calculated state, $J=3$, $v=5$ at $E = -7.865032$ hartree lies several wavenumbers above the dissociation limit for the rotationless state. The R_e ($=3.69$ bohr) calculated from the B_v for LiH is 0.076 smaller than the R_{\min} due to the anharmonicity of this state. As the experimental B_v 's are expected to be slightly larger than our calculated ones, judging from our experience with the other states, the experimental R_e should be somewhat less than 3.69 bohr.

II. ONE-ELECTRON EXPECTATION VALUES

As it is important to look beyond the energy as the sole criterion for judging the accuracy of a calculated wavefunction, the degree to which an approximate wavefunction approaches the exact description of an electronic system can be deduced by comparing theoretical and experimental values for certain properties. This affords insight into the accuracy of the wavefunction description in various regions of space, since different operators are sensitive to different regions of the electronic density distribution. The calculation of such properties as the dipole moment is also of great predictive value in the case of excited states where no measurements have been made.

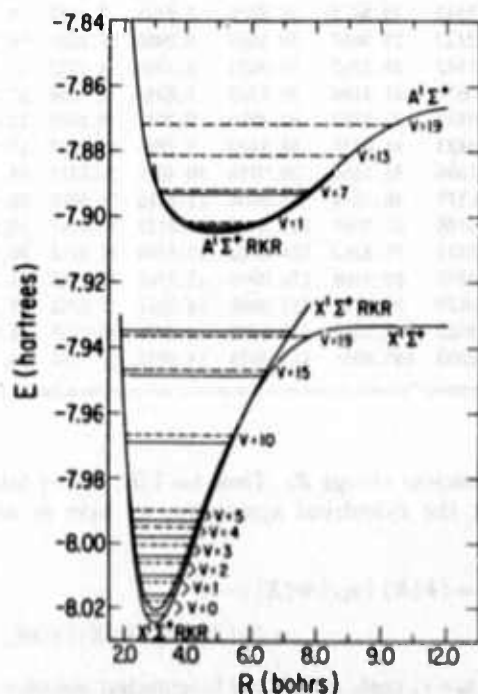


FIG. 1. RKR and computed potential curves and vibrational levels. The RKR curves are below our calculated curves for both states. The RKR curves are referred to minima obtained from the atomic Hartree-Fock dissociation limits using the experimental dissociation energies. The minima are: -8.0252 hartree for $X' \Sigma^+$ and -7.9046 hartree for $A' \Sigma^+$. The solid horizontal lines indicate vibrational levels of the RKR curves, while the dashed lines are our calculated vibrational levels for $J=0$.

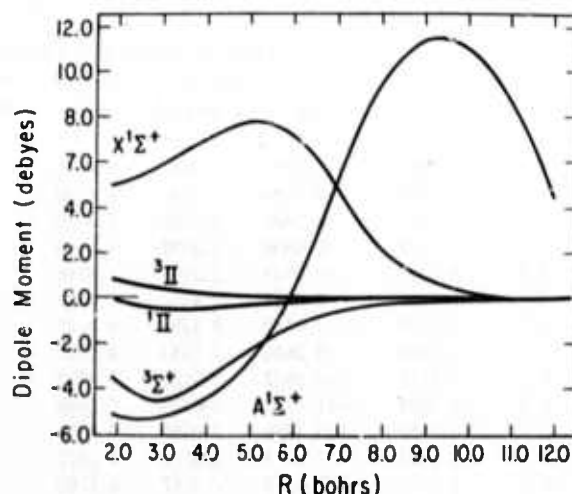


FIG. 2. Dipole moments of five states of LiH versus R . The positive sign refers to Li^+H^- .

With a normalized MCSCF wavefunction Ψ , represented in Paper I as a linear combination of configuration state functions (CSF's) Φ_I , we can write the expectation value of an arbitrary one-electron operator $Q = \sum_i q_i$ (where the summation is over all n electrons in the system) as

$$\langle \Psi | Q | \Psi \rangle = \sum_{I,J} C_I C_J \langle \Phi_I | Q | \Phi_J \rangle. \quad (5)$$

Each CSF is, in general, a linear combination of Slater determinant(s) (SD's) which are constructed from a set of orthonormal orbitals φ_i . The orbital orthogonality greatly reduces the number of terms in (5). Indeed, if configurations Φ_I and Φ_J differ by more than one spin-orbital, the matrix elements of Q between these two configurations is zero. In terms of the individual orbitals (5) can be rewritten

$$\begin{aligned} \langle \Psi | Q | \Psi \rangle &= \sum_{I,J} C_I C_J \sum_{i,j} a_{IJ,ij} \langle \varphi_i | q(1) | \varphi_j \rangle \\ &= \sum_{i,j} a_{ij} \langle \varphi_i | q(1) | \varphi_j \rangle. \end{aligned} \quad (6)$$

The one electron coupling coefficient $a_{IJ,ij}$ is determined by the orbitals occupied in each configuration, the coupling of the Slater determinants within each CSF, and the symmetry of the operator. The effective coefficients a_{ij} are defined as

$$a_{ij} = \sum_{I,J} C_I C_J a_{IJ,ij} \quad (7)$$

and are in the case of totally symmetric operators the elements of the first order reduced density matrix in the space spanned by the orbitals. The operator q which we used has the general form $r_s^k \sin^2 \theta_s \cos^2 \theta_s \times P_{lm}(\cos \theta_s) \exp(im\varphi_s)$ where k is the nuclear center which is used as the origin for the coordinates (r, θ, φ) , and P_{lm} is a normalized associated Legendre polynomial. The expectation values for seventeen different operators at the R points of the calculated potential

TABLE X. Expectation values of one-electron operators for $X^1\Sigma^+$.

R	$\langle z_{Li} \rangle$	$\langle z_H \rangle$	$\mu(e\text{-bohrs})$	$\mu(D)$	$P_1(\cos\theta_{Li})/r_{Li}^2$	$P_1(\cos\theta_H)/r_H^2$	$\cos\theta_{Li}/r_{Li}^2$	$\cos\theta_H/r_H^2$
2.0	3.9687	-4.0313	1.9687	5.0036	0.1297	0.2287	0.2382	-0.5527
2.25	4.2840	-4.7160	2.0340	5.1696	0.1050	0.1699	0.2054	-0.4811
2.5	4.6159	-5.3841	2.1159	5.3778	0.0847	0.1310	0.1839	-0.4208
2.75	4.9592	-6.0408	2.2092	5.6149	0.0692	0.1040	0.1655	-0.3706
3.0	5.3102	-6.6898	2.3102	5.8716	0.0572	0.0844	0.1500	-0.3282
3.25	5.6653	-7.3347	2.4153	6.1387	0.0470	0.0699	0.1399	-0.2943
3.5	6.0238	-7.9762	2.5238	6.4145	0.0394	0.0588	0.1280	-0.2632
4.0	6.7353	-9.2646	2.7353	6.9520	0.0289	0.0426	0.1054	-0.2111
4.5	7.4128	-10.5872	2.9128	7.4032	0.0214	0.0321	0.0893	-0.1720
5.0	8.0236	-11.9763	3.0236	7.6848	0.0156	0.0250	0.0788	-0.1419
5.5	8.5150	-13.4850	3.0150	7.6629	0.0119	0.0195	0.0650	-0.1173
6.0	8.8182	-15.1818	2.8182	7.1627	0.0087	0.0156	0.0548	-0.0978
6.5	8.9117	-17.0883	2.4117	6.1296	0.0062	0.0124	0.0459	-0.0815
7.5	8.7911	-21.2088	1.2911	3.2814	0.0032	0.0081	0.0277	-0.0581
8.5	9.0156	-24.9844	0.5156	1.3104	0.0017	0.0053	0.0173	-0.0434
10.0	10.1130	-29.8870	0.1130	0.2872	0.0007	0.0031	0.0107	-0.0307
12.0	12.0166	-35.9834	0.0166	0.0422	0.0001	0.0017	0.0073	-0.0211

R	$\sin^2\theta_{Li}/r_{Li}$	$\sin^2\theta_H/r_H$	$\cos^2\theta_{Li}/r_{Li}$	$\cos^2\theta_H/r_H$	$1/r_{Li}$	$1/r_H$	r_{Li}^2	r_H^2	$r^2 \sin^2\theta$	r_{Li}	r_H
2.0	3.9320	1.2638	2.3705	1.4736	6.3025	2.7375	17.8764	18.0015	7.2140	6.5433	7.7744
2.25	3.8963	1.2038	2.3423	1.3815	6.2386	2.5853	19.5040	20.4761	7.3578	6.8335	8.3336
2.5	3.8651	1.1493	2.3148	1.3018	6.1799	2.4511	21.4206	23.3410	7.5714	7.1513	8.9193
2.75	3.8385	1.1015	2.2892	1.2328	6.1277	2.3343	23.5812	26.5556	7.8181	7.4872	9.5206
3.0	3.8160	1.0598	2.2654	1.1725	6.0814	2.2322	25.9657	30.1047	8.0902	7.8361	10.1327
3.25	3.7967	1.0246	2.2436	1.1196	6.0403	2.1442	28.5363	33.9621	8.3664	8.1922	10.7488
3.5	3.7806	0.9942	2.2235	1.0735	6.0051	2.0677	31.3186	38.1520	8.6544	8.5564	11.3719
4.0	3.7559	0.9462	2.1878	0.9970	5.9437	1.9432	37.3763	47.4936	9.2041	9.2909	12.6279
4.5	3.7400	0.9075	2.1569	0.9349	5.8969	1.8423	44.0257	58.3102	9.7845	10.0215	13.9175
5.0	3.7315	0.8762	2.1297	0.8844	5.8612	1.7606	51.1384	70.9018	10.4275	10.7325	15.2617
5.5	3.7303	0.8462	2.1058	0.8415	5.8361	1.6877	58.3518	85.6866	11.0816	11.3882	16.6930
6.0	3.7371	0.8148	2.0846	0.8041	5.8218	1.6188	65.2567	103.4384	11.8125	11.9547	18.2696
6.5	3.7506	0.7827	2.0664	0.7708	5.8170	1.5535	71.5282	124.6762	12.5384	12.4112	20.0111
7.5	3.7828	0.7259	2.0387	0.7135	5.8216	1.4395	82.9468	176.0796	13.7348	13.1068	23.7698
8.5	3.8021	0.6963	2.0210	0.6696	5.8231	1.3659	96.2728	232.0080	14.2831	13.8382	27.3006
10.0	3.8105	0.6806	2.0035	0.6216	5.8140	1.3022	122.3312	320.0710	14.4808	15.1725	32.0266
12.0	3.8116	0.6741	1.9873	0.5762	5.7989	1.2503	165.8058	453.4078	14.5053	17.1134	38.0059

* All quantities except for dipole moment in powers of bohrs.

curves are given for the $X^1\Sigma^+$, $A^1\Sigma^+$, $B^1\Pi$, and $^3\Pi$ states of LiH in Tables X through XIII. For the $^3\Sigma^+$ state only the $\langle z_{Li} \rangle$ expectation value was obtained for certain internuclear distances in order to calculate the dipole moments. These are given in Table XIV.

The property which is probably of greatest interest is the dipole moment, which gives information on the over-all arrangement of charges in the particular state of the system. The electric dipole moment is invariant to the placement of the origin for neutral systems as long as one evaluates the expectation value of

$$\mu = e \sum_i r_i - e \sum_i Z_i R_i \quad (8)$$

where the latter term contains nuclear coordinates R_i

and nuclear charge Z_i . Thus for LiH, taking into account the cylindrical symmetry, we have in atomic units

$$\begin{aligned} \mu(R) &= \langle \Psi(R) | z_{Li} | \Psi(R) \rangle - R \\ &= \langle \Psi(R) | z_H | \Psi(R) \rangle + 3R, \quad (9) \end{aligned}$$

with $z_i = r_i \cos\theta_i$ and R the internuclear distance. The sign of the dipole moment is defined such that positive indicates Li^+H^- and negative, Li^-H^+ . We expect the dipole moment to approach zero for both large and small R (at the separated and united atom limits). The variation of the dipole moment with R for all the states of LiH is displayed graphically in Fig. 2. The correct behavior is observed for all states at

TABLE XI. Expectation values of one-electron operators for $A^1\Sigma^+$.

R	z_{Li}	z_H	μ (e·bohrs)	μ (D)	$P_z(\cos\theta_{Li})/r_{Li}^3$	$P_z(\cos\theta_H)/r_H^3$	$\cos\theta_{Li}/r_{Li}^2$	$\cos\theta_H/r_H^2$
2.0	-0.0371	-8.0371	-2.0371	-5.1775	0.1195	0.2526	0.1423	-0.5604
2.25	0.1745	-8.8255	-2.0755	-5.2751	0.0976	0.1859	0.1063	-0.4765
2.5	0.4117	-9.5883	-2.0883	-5.3076	0.0790	0.1407	0.0860	-0.4067
2.75	0.6726	-10.3274	-2.0774	-5.2799	0.0653	0.1095	0.0700	-0.3508
3.0	0.9528	-11.0472	-2.0472	-5.2031	0.0546	0.0867	0.0572	-0.3051
3.25	1.2556	-11.7444	-1.9944	-5.0690	0.0452	0.0702	0.0496	-0.2708
3.5	1.5740	-12.4260	-1.9260	-4.8951	0.0387	0.0577	0.0405	-0.2392
4.0	2.2672	-13.7328	-1.7328	-4.4041	0.0299	0.0397	0.0254	-0.1874
4.5	3.0303	-14.9697	-1.4697	-3.7354	0.0235	0.0283	0.0164	-0.1513
5.0	3.8979	-16.1021	-1.1021	-2.8011	0.0186	0.0215	0.0107	-0.1250
5.5	4.9001	-17.0999	-0.5999	-1.5247	0.0159	0.0162	0.0079	-0.1045
6.0	6.0867	-17.9133	0.0867	0.2204	0.0137	0.0128	0.0070	-0.0894
6.5	7.4695	-18.5305	0.9695	2.4641	0.0122	0.0103	0.0076	-0.0777
7.5	10.4172	-19.5828	2.9172	7.4143	0.0109	0.0076	0.0124	-0.0613
8.5	12.7077	-21.2922	4.2077	10.6943	0.0104	0.0057	0.0140	-0.0485
10.0	14.2924	-25.7075	4.2924	10.9095	0.0126	0.0037	0.0116	-0.0341
12.0	13.8196	-34.1804	1.8196	4.6247	0.0194	0.0020	0.0072	-0.0217

R	$\sin^2\theta_{Li}/r_{Li}$	$\sin^2\theta_H/r_H$	$\cos^2\theta_{Li}/r_{Li}$	$\cos^2\theta_H/r_H$	$1/r_{Li}$	$1/r_H$	r_{Li}^2	r_H^2	$r^2 \sin^2\theta$	r_{Li}	r_H
2.0	3.8758	0.9289	2.2970	1.4412	6.1728	2.3701	27.4379	43.5863	13.4908	7.6210	10.7765
2.25	3.8555	0.8793	2.2726	1.3437	6.1281	2.2230	28.8142	48.2788	13.7703	7.8531	11.5034
2.5	3.8376	0.8401	2.2502	1.2611	6.0878	2.1012	30.1885	53.1360	13.9439	8.0827	12.2188
2.75	3.8226	0.8097	2.2302	1.1905	6.0527	2.0002	31.6077	58.1583	14.0410	8.3129	12.9224
3.0	3.8101	0.7864	2.2121	1.1298	6.0221	1.9162	33.1032	63.3862	14.0716	8.5454	13.6149
3.25	3.7994	0.7694	2.1955	1.0768	5.9949	1.8461	34.7120	68.8007	14.0735	8.7831	14.2946
3.5	3.7907	0.7574	2.1805	1.0313	5.9713	1.7887	36.4685	74.4516	14.0365	9.0270	14.9647
4.0	3.7770	0.7456	2.1542	0.9570	5.9312	1.7026	40.5083	86.3710	13.9233	9.5376	16.2671
4.5	3.7659	0.7432	2.1319	0.8981	5.8978	1.6413	45.3880	99.1151	13.7631	10.0867	17.5219
5.0	3.7558	0.7480	2.1131	0.8516	5.8689	1.5996	51.2115	112.2327	13.5083	10.6777	18.6987
5.5	3.7440	0.7581	2.0972	0.8136	5.8412	1.5717	58.3281	125.4268	13.2313	11.3372	19.7747
6.0	3.7284	0.7734	2.0837	0.7830	5.8121	1.5563	67.0740	138.0340	12.8919	12.0904	20.7087
6.5	3.7085	0.7931	2.0719	0.7585	5.7804	1.5516	77.7314	149.6282	12.5535	12.9538	21.4849
7.5	3.6685	0.8244	2.0506	0.7200	5.7191	1.5444	103.5987	172.3413	12.1768	14.8644	22.8598
8.5	3.6467	0.8273	2.0319	0.6871	5.6786	1.5143	130.8756	203.8438	12.5238	16.6112	24.7102
10.0	3.6457	0.7884	2.0156	0.6412	5.6613	1.4296	165.7453	279.8965	13.6036	18.3886	28.9180
12.0	3.6712	0.7093	2.0178	0.5859	5.6890	1.2952	193.2305	437.5602	14.1631	19.1119	36.6128

* All quantities except for dipole moment in powers of bohrs.

large $R=12.0$ bohr. At $R=2.0$ bohr, however, the $^3\Pi$ dipole moment is tending away from zero, and the moments for the other states, although tending in the right direction are still far from zero. This indicates that at $R=2.0$ bohr we are still far from the united atom limit.

The dipole moment of the ground state is large even at 2.0 bohr in the direction Li^+H^- , increasing to a maximum at 5.25 bohr, the region in which the $X^1\Sigma^+$ potential curve has maximum interaction with the ionic curve. For large R , the dipole moment approaches zero in a smooth fashion reflecting the fact that the state dissociates to neutral species. Bender and Davidson⁸ have calculated dipole moments at various points of R , obtaining values close to ours for $R<3.0$ bohr.

For the region 3.0–6.0 bohr, their values are smaller, sometimes by as much as 0.3 bohr, indicating possibly that their basis set on H was inadequate to describe the diffuse H^- orbital.

For the $A^1\Sigma^+$, the dipole moment shows very clearly the large changes in character of the wavefunction with R . For small R the sign of the dipole moment indicates a charge distribution $Li-H^+$, due to the 3σ orbital being strongly polarized behind Li. The slope is steepest in the curve-crossing region from 5.0 to 7.0 bohr. Here the wavefunction is becoming rapidly ionic in the direction Li^+H^- , with a maximum reached at ~ 10.25 bohr. Dissociation to neutrals forces the rapid drop-off of the dipole moment at 12.0 bohr. Bender and Davidson's dipole moments for this state are again

TABLE XII. Expectation values of one-electron operators for $B^1\Pi$.

R	z_{Li}	z_H	μ (e bohrs)	μ (D)	$P_2(\cos\theta_{Li})/r_{Li}^2$	$P_2(\cos\theta_H)/r_H^2$	$\cos\theta_{Li}/r_{Li}^2$	$\cos\theta_H/r_H^2$
2.0	1.9490	-6.0509	-0.1510	-0.1296	0.0901	0.2463	0.1877	-0.5608
2.25	2.1503	-6.8497	-0.0997	-0.2534	0.0672	0.1795	0.1575	-0.4738
2.5	2.3631	-7.6369	-0.1369	-0.3479	0.0507	0.1358	0.1345	-0.4060
2.75	2.5853	-8.4147	-0.1647	-0.4186	0.0383	0.1056	0.1162	-0.3515
3.0	2.8169	-9.1831	-0.1831	-0.4654	0.0288	0.0840	0.1012	-0.3066
3.25	3.0576	-9.9424	-0.1924	-0.4890	0.0213	0.0680	0.0887	-0.2691
3.5	3.3052	-10.6948	-0.1948	-0.4951	0.0154	0.0558	0.0782	-0.2374
4.0	3.8191	-12.1809	-0.1809	-0.4598	0.0070	0.0389	0.0615	-0.1874
4.5	4.3478	-13.6522	-0.1522	-0.3868	0.0015	0.0283	0.0492	-0.1504
5.0	4.8802	-15.1198	-0.1198	-0.3045	-0.0020	0.0212	0.0401	-0.1226
5.5	5.4096	-16.5904	-0.0904	-0.2298	-0.0044	0.0163	0.0332	-0.1016
6.0	5.9334	-18.0666	-0.0666	-0.1693	-0.0060	0.0128	0.0279	-0.0853
6.5	6.4513	-19.5486	-0.0487	-0.1238	-0.0071	0.0102	0.0237	-0.0726
7.5	7.4736	-22.5263	-0.0264	-0.0671	-0.0085	0.0068	0.0178	-0.0543
8.5	8.4849	-25.5150	-0.0151	-0.0384	-0.0093	0.0047	0.0138	-0.0421
10.0	9.9925	-30.9974	-0.0075	-0.0191	-0.0099	0.0029	0.0100	-0.0303
12.0	11.9965	-36.0035	-0.0035	-0.0089	-0.0104	0.0017	0.0069	-0.0210

R	$\sin^2\theta_{Li}/r_{Li}$	$\sin^2\theta_H/r_H$	$\cos^2\theta_{Li}/r_{Li}$	$\cos^2\theta_H/r_H$	$1/r_{Li}$	$1/r_H$	r_{Li}^2	r_H^2	$r^2 \sin^2\theta$	r_{Li}	r_H
2.0	3.9261	0.9924	2.2051	1.3705	6.1312	2.3629	35.7093	43.9131	24.9883	8.3688	10.7228
2.25	3.9027	0.9383	2.1817	1.2774	6.0844	2.2157	37.2302	47.8039	25.5151	8.6041	11.3849
2.5	3.8830	0.8946	2.1605	1.1992	6.0434	2.0937	38.7309	51.9152	25.9076	8.8371	12.0458
2.75	3.8667	0.8594	2.1412	1.1329	6.0079	1.9923	40.2082	56.2390	26.1648	9.0661	12.7026
3.0	3.8534	0.8314	2.1237	1.0764	5.9771	1.9078	41.6882	60.7869	26.3023	9.2920	13.3549
3.25	3.8425	0.8091	2.1079	1.0280	5.9504	1.8371	43.1987	65.5743	26.3378	9.5162	14.0030
3.5	3.8337	0.7914	2.0934	0.9862	5.9272	1.7776	44.7662	70.6299	26.2951	9.7398	14.6486
4.0	3.8209	0.7660	2.0682	0.9180	5.8892	1.6840	48.1797	81.6271	26.0550	10.1895	15.9374
4.5	3.8126	0.7488	2.0471	0.8647	5.8598	1.6135	52.1123	93.9824	25.7499	10.6490	17.2356
5.0	3.8072	0.7364	2.0294	0.8217	5.8365	1.5583	56.6402	107.8385	25.4774	11.1197	18.5527
5.5	3.8035	0.7266	2.0143	0.7860	5.8178	1.5126	61.7475	123.2416	25.2565	11.5983	19.8909
6.0	3.8008	0.7185	2.0014	0.7556	5.8022	1.4742	67.4456	140.2449	25.1145	12.0846	21.2517
6.5	3.7989	0.7116	1.9902	0.7294	5.7892	1.4410	73.6893	158.8218	25.0230	12.5749	22.6313
7.5	3.7964	0.7007	1.9719	0.6859	5.7684	1.3865	87.7313	200.6263	24.9299	13.5612	25.4344
8.5	3.7950	0.6926	1.9576	0.6511	5.7526	1.3437	103.7879	248.5441	24.8953	14.5509	28.2802
10.0	3.7937	0.6843	1.9411	0.6100	5.7348	1.2943	131.6037	331.7528	24.8786	16.0382	32.6022
12.0	3.7929	0.6778	1.9252	0.5689	5.7182	1.2467	175.6518	463.7358	24.8692	18.0243	38.4285

* All quantities except for dipole moment in powers of bohrs.

smaller than ours in magnitude, indicating a less flexible basis for describing the charge distribution.

The Π states have very little charge transfer and are essentially neutral. The dipole moments, though small, do differ in sign—positive for the $^3\Pi$ and negative for the $^1\Pi$. For the $^3\Sigma^+$ state there is a substantial polarization of charge onto the Li, yielding a negative dipole moment which approaches zero at large R . Bender and Davidson's results for these states are very similar to ours.

Another property of interest is the field gradient say at nucleus A , which in a diatomic molecule may be expressed as

$$q_A(R) = 2\langle\P(R) | P_2(\cos\theta_A)/r_A^3 | \Psi(R)\rangle + 2Z_B/R^3. \quad (10)$$

The interaction of the field gradient q_A with the nuclear quadrupole moment Q_A causes a shift in the hyperfine structure splitting which is proportional to $eq_A Q_A$. In the case of ^7Li , where the nuclear quadrupole moment is not known, it can be obtained from the experimentally measured nuclear quadrupole coupling constant $e \cdot q_{Li} \cdot Q_{Li}/h$ of ^7Li in LiH and the calculated field gradient q_{Li} .

Several other molecular properties may be obtained from the expectation values listed in Tables X–XIII. Among these are:

(a) the diamagnetic contribution to the magnetic susceptibility

$$\chi(R) = -1/6 \alpha^2 \langle\P(R) | r^2 | \Psi(R)\rangle, \quad (11)$$

TABLE XIII. Expectation values of one-electron operators for ²II.*

R	z_{Li}	z_H	μ (e-bohrs)	μ (D)	$P_2(\cos\theta_{Li})/r_{Li}^3$	$P_2(\cos\theta_H)/r_H^3$	$\cos\theta_{Li}/r_{Li}^3$	$\cos\theta_H/r_H^3$
2.0	2.2934	-5.7066	0.2934	0.7457	0.0820	0.2386	0.1895	-0.5656
2.25	2.5000	-6.5000	0.2500	0.6354	0.0613	0.1731	0.1593	-0.4787
2.5	2.7130	-7.2870	0.2130	0.5414	0.0464	0.1305	0.1363	-0.4111
2.75	2.9308	-8.0692	0.1808	0.4595	0.0352	0.1014	0.1181	-0.3568
3.0	3.1526	-8.8474	0.1526	0.3878	0.0266	0.0806	0.1032	-0.3120
3.25	3.3779	-9.6221	0.1279	0.3251	0.0199	0.0652	0.0907	-0.2745
3.5	3.6063	-10.3936	0.1063	0.2702	0.0146	0.0536	0.0801	-0.2427
4.0	4.0717	-11.9282	0.0717	0.1822	0.0068	0.0376	0.0632	-0.1920
4.5	4.5469	-13.4530	0.0469	0.1192	0.0017	0.0274	0.0506	-0.1541
5.0	5.0295	-14.9704	0.0295	0.0750	-0.0017	0.0206	0.0410	-0.1254
5.5	5.5171	-16.4829	0.0171	0.0435	-0.0041	0.0159	0.0338	-0.1036
6.0	6.0085	-17.9915	0.0085	0.0216	-0.0057	0.0126	0.0283	-0.0867
6.5	6.5027	-19.4973	0.0027	0.0069	-0.0069	0.0101	0.0240	-0.0735
7.5	7.4966	-27.5033	-0.0034	-0.0086	-0.0084	0.0068	0.0179	-0.0547
8.5	8.4948	-25.5051	-0.0052	-0.0132	-0.0092	0.0047	0.0139	-0.0423
10.0	9.9953	-30.0047	-0.0047	-0.0119	-0.0099	0.0029	0.0100	-0.0303
12.0	11.9969	-36.0030	-0.0031	-0.0079	-0.0104	0.0017	0.0069	-0.0210

R	$\sin^2\theta_{Li}/r_{Li}$	$\sin^2\theta_H/r_H$	$\cos^2\theta_{Li}/r_{Li}$	$\cos^2\theta_H/r_H$	$1/r_{Li}$	$1/r_H$	r_{Li}^2	r_H^2	$r^2 \sin^2\theta$	r_{Li}	r_H
2.0	3.9586	1.0052	2.2080	1.3635	6.1666	2.3687	29.0991	35.9155	19.4615	7.7749	10.0333
2.25	3.9313	0.9487	2.1857	1.2710	6.1170	2.2197	30.8864	39.8862	20.1786	8.0434	10.7191
2.5	3.9078	0.9025	2.1651	1.1931	6.0730	2.0955	32.7715	44.2065	20.8566	8.3177	11.4136
2.75	3.8878	0.8648	2.1462	1.1269	6.0340	1.9918	34.7443	48.8750	21.4937	8.5959	12.1133
3.0	3.8709	0.8344	2.1289	1.0705	5.9998	1.9048	36.8052	53.8898	22.0871	8.8765	12.8160
3.25	3.8566	0.8099	2.1130	1.0221	5.9696	1.8320	38.9445	59.2382	22.6264	9.1578	13.5192
3.5	3.8446	0.7904	2.0984	0.9803	5.9430	1.7707	41.1570	64.9125	23.1059	9.4385	14.2218
4.0	3.8266	0.7627	2.0724	0.9124	5.8990	1.6751	45.7883	77.2144	23.8722	9.9936	15.6218
4.5	3.8146	0.7449	2.0504	0.8597	5.8650	1.6047	50.7023	90.7797	24.3962	10.5366	17.0155
5.0	3.8070	0.7328	2.0317	0.8177	5.8387	1.5505	55.9085	105.6132	24.7101	11.0643	18.4052
5.5	3.8024	0.7238	2.0158	0.7829	5.8182	1.5068	61.4640	121.7761	24.8858	11.5796	19.7966
6.0	3.7995	0.7165	2.0023	0.7534	5.8018	1.4699	67.4042	139.3022	24.9690	12.0852	21.1924
6.5	3.7976	0.7102	1.9908	0.7278	5.7884	1.4381	73.7685	158.2331	24.9999	12.5844	22.5947
7.5	3.7956	0.7001	1.9721	0.6852	5.7677	1.3852	87.8669	200.4170	24.9889	13.5736	25.4212
8.5	3.7945	0.6924	1.9576	0.6508	5.7521	1.3431	103.8926	248.4800	24.9519	14.5598	28.2758
10.0	3.7936	0.6843	1.9411	0.6099	5.7347	1.2942	131.6532	331.7475	24.9078	16.0421	32.6014
12.0	3.7928	0.6778	1.9252	0.5689	5.7181	1.2467	175.6710	463.7439	24.8822	18.0257	38.4286

* All quantities except for dipole moment in powers of bohrs.

where α is the fine structure constant and r has the center of the electronic charge as origin,

(b) the diamagnetic contribution to the nuclear shielding factor at nucleus A

$$\sigma_A(R) = 1/3 \alpha^2 \langle \Psi(R) | 1/r_A | \Psi(R) \rangle, \quad (12)$$

(c) the molecular quadrupole moment

$$\theta(R) = \sum_k Z_k d_k^2 - \langle \Psi(R) | z^2 - 1/2 \rho^2 | \Psi(R) \rangle, \quad (13)$$

where d_k is the distance of nucleus k with charge Z_k from the center of mass, z has the center of mass as origin and $\rho^2 = x^2 + y^2 = r^2 \sin^2\theta$, the distance squared from the nuclear axis, is origin independent.

Many more properties could be obtained, in particular if the computed expectation values are com-

bined with experimentally measured results. These include the parallel and perpendicular part of the diamagnetic susceptibility as well as its high frequency part, and the molecular g factor. This is discussed in detail elsewhere.⁹

When comparing computed properties, such as dipole or quadrupole moments and the like, with experimentally observed quantities, it is important to realize that the experimental values are obtained for specific rotation-vibrational states. It is therefore necessary to average the computed properties, which vary with the internuclear distance, over the rotation-vibrational wavefunctions. We have performed such rotation-vibrational averaging for some of the properties using the rotation-vibrational wavefunctions obtained from the computed potential curves. In

TABLE XIV. Expectation value of z and dipole moment for $^2\Sigma^+$.

R	z_{Li} (bohrs)	μ (e-bohrs)	μ (D)
2.0	0.3447	-1.4474	-3.6787
2.5	0.7499	-1.7501	-4.4480
3.0	1.2317	-1.7683	-4.4943
3.5	1.8730	-1.6270	-4.1352
4.0	2.5965	-1.4035	-3.5671
5.0	4.0847	-0.9153	-2.3263
6.0	5.5128	-0.4872	-1.2383
7.5	7.3248	-0.1752	-0.4453
12.0	11.9922	-0.0078	-0.0198

Table XV are presented a selected set of these rotation-vibration averaged properties, which are obtained generally as

$$Q(v, J; v'J') = \langle P_{v,J}(R) | Q(R) | P_{v',J'}(R) \rangle, \quad (14)$$

with $Q(R)$ the property as a function of the internuclear distance and $P_{v,J}(R)$ the rotation-vibrational wavefunction for vibrational state v and rotational state J .

Since practically no measurements or calculations of excited state properties were found to exist, we concentrate on comparisons for the ground $X^1\Sigma^+$ state alone. In Table XVI various expectation values (at 3.0 bohr unless otherwise noted) as well as rotation-vibration averaged values are presented and compared with other computed values and with experiment. Our values always appear in the first row, with any existing experimental values directly beneath them.

The dipole moment of LiH has been measured¹⁸ for $J=1$ of the three vibrational states, $v=0, 1$ and 2. The computed values are found to be consistently too large by about 0.1 D, a quite gratifying agreement. However, were we to compare the value obtained for μ_0 (5.886 D) with the experimental value for μ_0 (5.882 D) the agreement would appear to be even better. Another experimental parameter, related to the dipole moment and its derivative

$$\theta_v = \frac{\mu_v/R_v}{(\partial\mu/\partial R)_R}, \quad (15)$$

which is obtained from relative line intensities in the infrared spectrum¹⁹ agrees exceptionally well with our computed value.

Using the quadrupole coupling constant for ^7Li in LiH measured by Wharton *et al.*,¹⁸ and the computed field gradient at the Li nucleus in the $v=0$ state, we obtain a nuclear quadrupole moment for ^7Li somewhat smaller in magnitude than many of those calculated previously. However, our value is close, though somewhat larger than the one obtained recently by Green,²¹ using the Cade and Huo basis set in a 200 configuration CI calculation. It should be noted here that the field gradient operator, going as $P_2(\cos\theta)/r^3$, for Li will depend strongly on the description of the $1s$ or K shell

orbital. In particular it will depend critically on the $d\sigma$ basis function used to polarize this orbital. A careful study of this²² has led recently to the best value for Q_{Li} of about $-4.1 \times 10^{-26} \text{ cm}^2$, somewhat larger than our value.

Working in the other direction and using the field gradient on hydrogen together with the known nuclear quadrupole moment of deuterium ($Q_D = 2.738 \times 10^{-27} \text{ cm}^2$) we obtain a quadrupole coupling constant for LiD in excellent agreement with the experimental value.¹⁸

III. TRANSITION MOMENTS

The literature does not lack for calculations and discussions of atomic transition probabilities. Much less is known, however, about molecular transition probabilities, even though Mulliken and Rieke,²³ in 1941, published a comprehensive review of the research on the subject. Since then, with the availability of large computers, much more accurate molecular wavefunctions can be calculated, and thus theoretical transition probabilities should become more accessible. Several recent theoretical studies have appeared in which transition moments were calculated using molecular Hartree-Fock functions. The systems calculated were $\text{NH}(A-X, c-a, c-b)$ and $\text{CH}(A-X, B-X, C-X)$ by Huo²⁴ and the $A-X$ band systems in OH, BeH, MgH, and SH by Henneker and Popkie.²⁵ Huo has concluded that oscillator strengths computed in this manner have order of magnitude accuracy only. On the other hand, Wolniewicz²⁶ has obtained excellent theoretical results for the $B-X, C-X$ and $E, F-B$ transitions in the hydrogen molecule using the very accurate electronic wavefunctions calculated by Kolos and Wolniewicz.²⁷⁻²⁹

TABLE XV. Selected properties (μ is the dipole moment, θ is the quadrupole moment, q is the field gradient) vibrationally averaged, $Q(v, J; vJ) = \langle P_{v,J}(R) | Q(R) | P_{v,J}(R) \rangle$ $J=0$ for Σ states and $J=1$ for Π states. All values in atomic units.

	v	$\mu(v)$	$\theta(v)$	$q_{Li}(v)$	$q_H(v)$
$X^1\Sigma^+$	0	2.350	-3.236	-0.0383	0.0488
	5	2.559	-4.210	-0.0304	0.0429
	10	2.711	-5.244	-0.0232	0.0356
$A^1\Sigma^+$	0	-0.941	-7.931	-0.0216	0.0055
	5	-0.011	-11.741	-0.0220	0.0078
	10	0.882	-15.812	-0.0217	0.0086
	15	1.650	-19.880	-0.0216	0.0086
	20	2.228	-23.676	-0.0240	0.0069
$B^1\Pi$	0	-0.096	6.285	0.0204	0.0046
	1	-0.024	5.329	0.0197	0.0010
$^2\Pi$	0	0.080	6.019	0.0178	0.0226
	2	0.050	6.056	0.0193	0.0149
	4	0.016	5.923	0.0208	0.0060

TABLE XVI. Expectation values and properties of $X^1\Sigma^+$ state at $R=3.0$ b.^a

$(q/2e)_H$	$(q/2e)_{Li}$	$1/r_H$	$1/r_{Li}$	r_{Li}	r_H	$P_1(\cos\theta_{Li})/r_{Li}^2$	$P_1(\cos\theta_H)/r_H^2$
0.0267	-0.0202	2.2322	6.0814	7.8361	10.1327	0.1500	-0.3282
0.0263 ^b	-0.0174 ^b	2.2376 ^b	6.0820 ^b	7.8288 ^b	10.1412 ^b	0.1144 ^b	-0.3260 ^b
0.0230 ^c	-0.0187 ^c	2.2404 ^c	6.0748 ^c	7.8292 ^c	10.1008 ^c	0.1148 ^c	-0.3312 ^c
0.0292 ^d	-0.0202 ^d	2.2239 ^d	6.0848 ^d				
0.0256 ^e	-0.0173 ^e						
0.0274 ^f	-0.0166 ^f						
	-0.0195 ^g						
r_H^2	r_{Li}^2	$P_2(\cos\theta_{Li})/r_{Li}^3$	$P_2(\cos\theta_H)/r_H^3$	$\sigma_H^{(d)} \times 10^4$	$\sigma_{Li}^{(d)} \times 10^4$	$\chi^{(d)} \times 10^4$	
30.1047	25.9657	0.0572	0.0844	0.3953	1.0790	-1.6788	
30.2240 ^b	25.9296 ^b	0.0536 ^b	0.0832 ^b				
30.615 ^c	25.827 ^c	0.0548 ^c	0.0854 ^c	0.3922 ^c	1.0775 ^c		
		0.0521 ^c	0.0777 ^c				
$\mu_0(D)$	$\mu_{v=0}(D)$	$\mu_{v=1}(D)$	$\mu_{v=2}(D)$	$\theta_0 = \frac{\mu_0/R_0}{(\partial\mu/\partial R)R_0}$	$Q_{Li}(10^{-26} \text{ cm}^2)$	$(eqQ/h)_{DKC}$	
5.886 ^b	5.974 ^d	6.083 ⁱ	6.193 ⁱ	1.86	-3.75 ^b	34.4 ^a	
5.828 ⁱ	5.882 \pm 0.003 ^m	5.990 \pm 0.003 ^m	6.098 \pm 0.003 ^m	1.8 \pm 0.3 ^a	-3.96 ^c	31.4 ^c	
5.853 ^b							
5.645 ^d	5.93 ^e	6.00 ^e	6.05 ^e	1.74 ^e	-4.44 ^f	33 \pm 1 ^m	
6.002 ^j				2.5 ^g	-4.3 ^f	33.3 ^f	
5.965 ^g				4.5 ^g			
5.93 ^g				1.75 ^h			
5.888 ^f							
5.89 ^k							

^a All our values appear first in each column; they are at $R=3.0$ bohr and in atomic units unless specified differently.

^b At $R=3.015$. See Ref. 10.

^c At $R=3.015$. See Ref. 11.

^d At $R=3.015$. See Ref. 12.

^e At $R=3.046$. See Ref. 13.

^f At $R=3.042$. See Ref. 14.

^g At $R=3.046$. See Ref. 15.

^h Obtained at $R=3.015$ bohr by interpolation of our calculated values.

ⁱ Obtained by linear fit to $(v+1/2)$ of μ_0 and μ_1 experimental values.

^j At $R=3.015$ bohr. See Ref. 16.

^k At $R=3.060$ bohr. See Ref. 17.

^l Our vibrationally averaged value is for $J=1$ state.

^m See Ref. 18.

ⁿ See Ref. 19.

^o See Ref. 8.

^p See Ref. 20.

^q Calculated using $(q/2e)_H$ and $Q_D=2.738 \times 10^{-27} \text{ cm}^2$.

^r Using the vibrationally averaged values $q(v=1)$; see Table XV.

Several factors can be said to account for the dearth of transition probability calculations for molecular systems. The first is that molecular wavefunctions even of Hartree-Fock quality are relatively scarce for excited states of molecules. Because, in general, the transition moment varies with the internuclear distance R , one should also have ground and excited state electronic wavefunctions at various R values, in order to calculate band intensities or line strengths. The

Hartree-Fock potential curves, especially for large R , can be notoriously poor, leading to incorrect dissociation products. In addition, the effects of electron correlation, unaccounted for in the HF wavefunction, on the transition moment are difficult to predict. Thus, indications are that molecular wavefunctions to be used in transition probability calculations should go beyond the Hartree-Fock model, both in flexibility and in correcting for electron correlation. In order to

obtain results which can be compared with experiment, the nuclear motion must also be considered. Since the electronic energies, wavefunctions, and transition moments are obtained within the framework of the Born-Oppenheimer approximation, these quantities depend parametrically on R . The dependence of the square of the transition moment on R is not directly observed experimentally. Therefore, an average over the nuclear coordinate using vibrational wavefunctions is necessary.

The length form of the general transition moment operator is defined just as the dipole moment operator was in Sec. II.

$$m = e \sum_i r_i' - e \sum_i Z_i R_i', \quad (16)$$

except that the coordinates are with respect to the laboratory fixed frame of reference. The transition moment between two states, A and B , represented by orthogonal wavefunctions, is independent of the second term, since the matrix element over the second term above vanishes for all R . With the total wavefunction defined as

$$\Psi_{A,\text{total}} = \Psi_{A,\text{el}}(r_i', R') (1/R') P_{v,J,A}(R') Y_{J,A,M}(\theta, \varphi, \chi) \quad (17)$$

(with the quantum numbers and notation of the previous section), the transition moment can be written

$$M_{A v', J', \Lambda', M', B v'', J'', \Lambda'', M''} = \langle \Psi_{A,\text{total}} | e \sum_i r_i' | \Psi_{B,\text{total}} \rangle. \quad (18)$$

Transforming coordinates r_i' to r_i in the molecule fixed system, and integrating over the electronic coordinates r_i with the electronic transition moment defined as

$$M_e^{AB}(R) = \langle \Psi_{A,\text{el}}(r_i, R) | e \sum_i r_i | \Psi_{B,\text{el}}(r_i, R) \rangle, \quad (19)$$

we can write

$$\begin{aligned} M_{A v', J', \Lambda', M', B v'', J'', \Lambda'', M''} &= \langle P_{v', J', \Lambda'}(R) | M_e^{AB}(R) | P_{v'', J'', \Lambda''}(R) \rangle \\ &\times \langle Y_{J', \Lambda', M'} | D(\theta, \varphi, \chi) | Y_{J'', \Lambda'', M''} \rangle. \end{aligned} \quad (20)$$

The $D(\theta, \varphi, \chi)$ in the last matrix element relates the molecule-fixed coordinate system to the laboratory-fixed axes. In order to obtain the line strength for an electronic transition between vibrational and rotational states $v''J'' \rightarrow v'J'$ we must square the quantity $M_{A v', J', \Lambda', M', B v'', J'', \Lambda'', M''}$ and sum over the degenerate quantum numbers M' and M'' . This gives

$$M_{A v', J', \Lambda', B v'', J'', \Lambda''} = S_{J', \Lambda', J'', \Lambda''} p_{v', v'', J', J''}, \quad (21)$$

where $S_{J', \Lambda', J'', \Lambda''}$ is the Honl-London factor⁴ and

$$p_{v', v'', J', J''} = | \langle P_{v', J', \Lambda'}(R) | M_e^{AB}(R) | P_{v'', J'', \Lambda''}(R) \rangle |^2. \quad (22)$$

In this work, only the length form of the dipole operator was used, as the integrals program was not adapted to compute the velocity operator. The procedure we followed to obtain individual line strengths was to calculate $M_e^{AB}(R)$ using the electronic wavefunctions determined at the various R values given in Paper I. Then $p_{v', v'', J', J''}$ was obtained by averaging over the particular vibration-rotation wavefunctions. The actual sign of $M_e^{AB}(R)$ is insignificant, depending only on the relative phases of the two wavefunctions involved. A polynomial interpolation of the calculated $M_e^{AB}(R)$ points is necessary in order to obtain the electronic transition moment at each point on the numerical integration grid for which we have vibration-rotation wavefunctions.

If the electronic wavefunctions Ψ_A and Ψ_B are constructed from a common set of orthonormal orbitals, $M_e^{AB}(R)$ can be computed using Eqs. (5) and (6) in Sec. II of this paper. This is the case for the two $^1\Sigma^+$ states computed using the "averaged field" described in Paper I. The calculation of the transition moment between two states with nonorthogonal orbitals will be discussed below.

Whether or not the molecular orbitals for the two states are orthogonal, when both states are calculated with the same basis set, the computation of the one-electron integrals of the transition moment over the basis functions is greatly simplified. This was the case for four of the states of LiH. Since the basis for the $^3\Sigma^+$ differed by only three functions, the transition moment integrals for the $^3\Sigma^+ - ^3\Pi$ were obtained with the larger basis. In the $^3\Sigma^+$ wavefunction, orbital coefficients of zero were then inserted for these basis functions. The $^3\Sigma^+$ wavefunction was also not available at all the R values of the $^3\Pi$, and thus transition moments were only computed for the nine R values which matched in each state.

The treatment for nonorthogonal orbitals is very similar to that in Sec. II. For clarity, we rewrite Eq. (5) of that section as

$$M_e^{AB}(R) = \sum_{I \in A} \sum_{J \in B} C_I^A C_J^B \langle \Phi_I^A(R) | \sum_i r_i | \Phi_J^B(R) \rangle, \quad (23)$$

where the sums are over the CSF's of states A and B . The configuration state functions Φ_I may themselves be linear combinations of Slater determinants Ψ_k , enabling us to write

$$\Phi_I = \sum_{K \in I} B_K \Psi_K, \quad (24)$$

where the summation is over all SD's in CSF I . Then defining $A_{IK} = C_I^A B_K$, we can write

$$M_e^{AB}(R) = \sum_{I \in A} \sum_{J \in B} \sum_{K \in I} \sum_{L \in J} A_{IK}^A A_{JL}^B \langle \Psi_K^A | \sum_i r_i | \Psi_L^B \rangle. \quad (25)$$

Because of the nonorthogonality of orbitals belonging

to states A and B , we have an orbital overlap matrix between SD's Ψ_K^A and Ψ_L^B denoted S^{KL} with elements

$$s_{ij} = \langle \varphi_i^A | \varphi_j^B \rangle \quad i \in K \text{ and } j \in L. \quad (26)$$

Thus we can write

$$\langle \Psi_K^A | \sum_i r_i | \Psi_L^B \rangle = \sum_{i \in K} \sum_{j \in L} \langle \varphi_i^A | r(1) | \varphi_j^B \rangle D_{ij}^{KL}, \quad (27)$$

where D_{ij}^{KL} is the cofactor of the overlap matrix S^{KL} formed by omitting row i and column j and taking the determinant of the remaining matrix.

If we use spin-orbitals, S^{KL} will be a square matrix, which can be blocked into an α and a β -spin submatrix. Since our operators are spin-independent, no matrix elements over orbitals of different spins will appear, and the cofactor D_{ij}^{KL} reduces to a product of the cofactor within a particular spin block and the determinant of the other spin block. The actual calculation of cofactors was accomplished utilizing a method suggested by Prosser and Hagstrom.³⁰ Details of the over-all procedure have been presented more fully elsewhere.³¹

Transition moments were calculated for the following four systems of LiH: $X^1\Sigma^+-A^1\Sigma^+$, $X^1\Sigma^+-B^1\Pi$, $A^1\Sigma^+-B^1\Pi$, and $^3\Sigma^+-^3\Pi$. Since the $X^1\Sigma^+$ and $A^1\Sigma^+$ states were calculated using the "averaged field" their orbitals were mutually orthonormal and the first transition moment above could be obtained using Eq. (6) in Sec. II. For the other transition moments, the procedure for nonorthogonal orbitals just outlined was used. The actual values are listed in Table XVII

TABLE XVII. Electronic transition moments.^a

R	$X^1\Sigma^+-A^1\Sigma^+$	$X^1\Sigma^+-B^1\Pi$	$A^1\Sigma^+-B^1\Pi$	$^3\Sigma^+-^3\Pi^b$
2.0	0.6247	1.8222	-2.5837	2.8811
2.25	0.7034	1.8321	-2.6048	
2.5	0.7855	1.8570	-2.6096	2.9578
2.75	0.8714	1.8874	-2.6032	
3.0	0.9599	1.9223	-2.5870	3.0057
3.25	1.0530	1.9586	-2.5696	
3.5	1.1516	1.9960	-2.5445	3.0696
4.0	1.3739	2.0697	-2.4936	3.1314
4.5	1.6323	2.1612	-2.4269	
5.0	1.9448	2.2846	-2.3298	3.2203
5.5	2.3100	2.4342	-2.1949	
6.0	2.6956	2.6213	-1.9912	3.2881
6.5	3.0202	2.8221	-1.7220	
7.5	3.1453	3.1556	-1.0597	3.3230
8.5	2.7686	3.3051	-0.5209	
10.0	2.3613	3.3610	-0.1020	
12.0	2.3425	3.3715	0.0434	3.3589

^a In atomic units, i.e., e-bohrs.

^b The $^3\Sigma^+$ state was calculated at a slightly different set of R values from the others. The transition moment $^3\Sigma^+-^3\Pi$ was calculated only at identical R 's in each set.

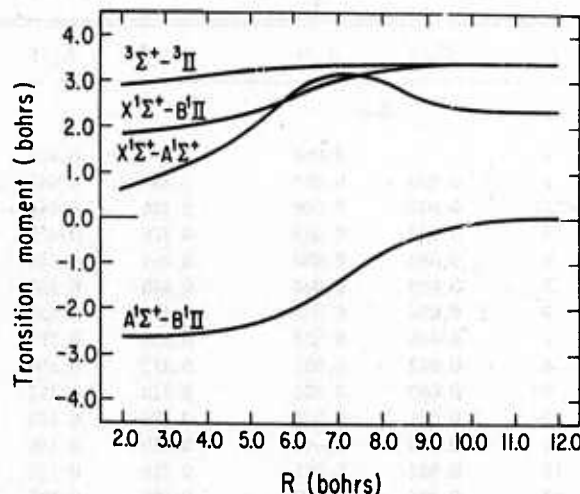
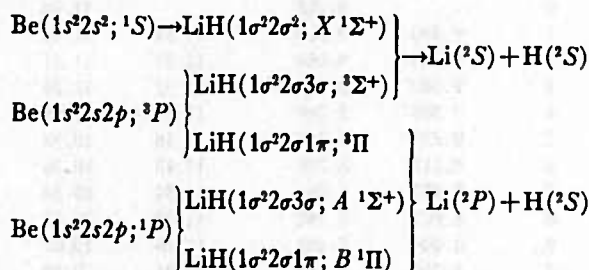


FIG. 3. Transition moments of four systems in LiH versus R .

and presented graphically in Fig. 3. In order to understand how these transition moments should behave theoretically as a function of R , it is instructive to look at the states in the united atom ($R=0$) and separated atom ($R=\infty$) limits. This can be represented schematically as



Thus for $R=0$, since the $A^1\Sigma^+$ and $B^1\Pi$ as well as the $^3\Pi$ and $^3\Sigma^+$ states become degenerate, the transition moments of $A^1\Sigma^+-B^1\Pi$ and $^3\Sigma^+-^3\Pi$ should approach zero. As can be seen from Fig. 2, this is not yet the case in our calculated values at $R=2.0$ bohr. We might expect also that the sum of the oscillator strengths for $X^1\Sigma^+-B^1\Pi$ and $X^1\Sigma^+-A^1\Sigma^+$ approaches that of the $\text{Be } 1S \rightarrow ^1P$ transition. This is definitely not the case, as the oscillator strength [defined in atomic units as $f_{AB} = 2/3(E_A - E_B)S_{AB}$] of the atomic transition is 1.36,³² whereas ours sum to 0.44. At 2.0 bohr, therefore, we are still quite far from the united atom limit.

At large R we observe exactly what we would expect from the separated atom point of view. The transition moment of $A^1\Sigma^+-B^1\Pi$ has reached zero by 12.0 bohr, since these states dissociate to the same atomic limit. The $X^1\Sigma^+-B^1\Pi$ and $X^1\Sigma^+-A^1\Sigma^+$ transitions have attained constant values at this distance. The square of the transition moment for the $X^1\Sigma^+-B^1\Pi$ transition is just 2.07 times the square of the $X^1\Sigma^+-A^1\Sigma^+$ moment of $R=12.0$ bohr. This is very good agreement considering that purely theoretically we expect a factor

TABLE XVIII. Line strengths $P_{v'v''J'J''}$ for selected bands in the $X^1\Sigma^+-A^1\Sigma^+$ transition (in $10^{-2} e^2 \cdot \text{bohrs}^2$).

J	$P(J)$	$R(J)$	$P(J)$	$R(J)$	J	$P(J)$	$R(J)$	$P(J)$	$R(J)$
0-0					1-0				
0		0.068		0.477	9	12.49	11.80	12.57	12.33
1	0.070	0.065	0.489	0.462	10	12.44	11.63	12.64	12.32
2	0.069	0.060	0.486	0.441	11	12.37	11.43	12.70	12.28
3	0.067	0.055	0.476	0.415	12	12.27	11.20	12.75	12.21
4	0.064	0.050	0.461	0.386	13	12.15	10.93	12.78	12.12
5	0.059	0.044	0.440	0.353	14	11.99	10.63	12.79	11.99
6	0.054	0.038	0.414	0.320	15	11.80	10.29	12.78	11.82
7	0.048	0.032	0.384	0.285	16	11.58	9.92	12.74	11.61
8	0.042	0.027	0.352	0.250	17	11.32	9.52	12.66	11.35
9	0.037	0.022	0.318	0.217	18	11.02	9.09	12.54	11.06
10	0.031	0.018	0.284	0.185	19	10.68		12.38	
11	0.026	0.014	0.250	0.156	9-0				
12	0.021	0.011	0.216	0.130	11-0				
13	0.017	0.009	0.185	0.107	0		10.88		7.04
14	0.014	0.007	0.157	0.087	1	10.86	10.92	6.99	7.11
15	0.011	0.005	0.131	0.070	2	10.88	10.98	7.00	7.20
16	0.009	0.004	0.108	0.056	3	10.92	11.06	7.04	7.32
17	0.007	0.003	0.089	0.044	4	10.98	11.15	7.11	7.47
18	0.005	0.002	0.072	0.035	5	11.06	11.26	7.20	7.63
19	0.004		0.058		6	11.16	11.37	7.32	7.83
5-0					7	11.28	11.50	7.46	8.04
0		9.288		11.46	8	11.41	11.62	7.64	8.27
1	9.380	9.200	11.54	11.40	9	11.56	11.75	7.83	8.53
2	9.384	9.084	11.55	11.31	10	11.72	11.87	8.06	8.80
3	9.360	8.940	11.55	11.21	11	11.88	11.99	8.30	9.08
4	9.308	8.768	11.52	11.08	12	12.05	12.08	8.57	9.38
5	9.227	8.567	11.48	10.93	13	12.21	12.16	8.86	9.68
6	9.117	8.338	11.42	10.76	14	12.37	12.22	9.16	9.98
7	8.977	8.081	11.34	10.56	15	12.52	12.24	9.48	10.28
8	8.807	7.798	11.23	10.33	16	12.65	12.22	9.81	10.58
9	8.608	7.488	11.10	10.07	17	12.76	12.17	10.15	10.86
10	8.379	7.156	10.93	9.79	18	12.84	12.07	10.49	11.12
11	8.120	6.803	10.74	9.47	19	12.89		10.84	
12	7.834	6.431	10.52	9.12	12-0				
13	7.522	6.046	10.27	8.75	0		5.19		
14	7.187	5.651	9.98	8.35	1	5.14	5.25		
15	6.831	5.250	9.66	7.93	2	5.14	5.34		
16	6.458	4.848	9.32	7.49	3	5.17	5.45		
17	6.073	4.451	8.94	7.03	4	5.23	5.59		
18	5.679	4.061	8.54	6.57	5	5.31	5.75		
19	5.281		8.12		6	5.42	5.94		
7-0					7	5.55	6.14		
0		12.44		12.14	8	5.71	6.38		
1	12.48	12.41	12.15	12.15	9	5.89	6.63		
2	12.50	12.38	12.17	12.17	10	6.10	6.91		
3	12.52	12.34	12.21	12.20	11	6.33	7.21		
4	12.53	12.29	12.25	12.23	12	6.59	7.53		
5	12.54	12.22	12.30	12.26	13	6.87	7.86		
6	12.54	12.15	12.36	12.29	14	7.18	8.20		
7	12.54	12.05	12.43	12.31	15	7.50	8.56		
8	12.52	11.94	12.50	12.33	16	7.85	8.92		
8-0					17	8.22	9.28		
0					18	8.59	9.64		
1					19	8.98			

of 2 due to the doubly degenerate $2p\pi$ versus the non-degenerate $2p\sigma$ arising from $\text{Li}(1s^2 2p)$. The $^3\Sigma^+-^3\Pi$ transition moment becomes equal to the $X^1\Sigma^+-B^1\Pi$ moment, which is just what we would anticipate for analogous terms within the singlet and triplet sequences.

The sum of the oscillator strengths of the $X^1\Sigma^+-A^1\Sigma^+$ and $X^1\Sigma^+-B^1\Pi$ transitions is 0.763 if we use the experimental energy splitting of $\text{Li}(^3P)\rightarrow\text{Li}(^3S)$ and our calculated transition moments. Weiss,²² using a 45-configuration wavefunction calculated the oscillator strength of the $\text{Li}(^3S)\rightarrow\text{Li}(^3P)$ transition to be 0.753. The Hartree-Fock f value is 0.768, also calculated by Weiss²² using the dipole length operator and the experimental splitting. It is reasonable that the Hartree-Fock model predicts too large a transition moment, because lack of electron correlation tends to create a more diffuse charge distribution than is actually the case. Since, at the dissociation limit, our calculated molecular states dissociate to Hartree-Fock atoms, we expect to approach the Hartree-Fock value for the $\text{Li}(^3S)\rightarrow\text{Li}(^3P)$ transition, and our value of 0.763 attests to this. If we had calculated the oscillator strength using our calculated energy splitting we would have obtained a value of 0.755—very close to the most accurate value. This is due to a fortuitous cancellation of errors: the larger Hartree-Fock transition moment is multiplied by the Hartree-Fock energy splitting, which is smaller (due to more correlation in the 3S than the 3P states of Li) than the experimental value.

TABLE XIX. Line strengths $P_{v',v''J''J'}$ for two bands in ground state infrared spectrum (in $10^{-2} \text{ e}^2 \cdot \text{bohr}^2$).

J	0-1		1-2	
	$P(J)$	$R(J)$	$P(J)$	$R(J)$
0		0.813		1.653
1	0.952	0.749	1.936	1.520
2	1.026	0.687	2.088	1.395
3	1.103	0.629	2.246	1.275
4	1.184	0.573	2.411	1.162
5	1.268	0.521	2.582	1.055
6	1.355	0.472	2.761	0.953
7	1.446	0.425	2.946	0.858
8	1.540	0.381	3.138	0.768
9	1.638	0.340	3.336	0.684
10	1.739	0.302	3.542	0.605
11	1.843	0.266	3.755	0.532
12	1.951	0.233	3.974	0.464
13	2.062	0.202	4.200	0.401
14	2.177	0.174	4.433	0.343
15	2.295	0.148	4.673	0.290
16	2.417	0.124	4.920	0.241
17	2.542	0.103	5.173	0.198
18	2.671	0.084	5.432	0.159
19	2.803		5.698	

Another feature of the $X^1\Sigma^+-A^1\Sigma^+$ transition moment curve which can be observed is the maximum in the region 5.0 to 9.0 bohr. This is the region of greatest interaction between the two states; the wavefunctions are changing character from ionic to neutral or neutral to ionic.

Bender and Davidson⁸ have calculated the absolute oscillator strengths for the four transitions at various R values. Since the oscillator strength contains both the energy splitting and the square of the transition moment, we have to divide by their calculated energy splittings to obtain the behavior of the transition moments. All their calculations are carried out at $R < 6.0$ bohr. For the $X-A$ transition, their transition moment is uniformly larger than ours by ~ 0.1 bohr. This is not surprising, as our wavefunctions were better correlated than theirs. For the $X^1\Sigma^+-B^1\Pi$, $A^1\Sigma^+-B^1\Pi$, and $^3\Sigma^+-^3\Pi$ transitions, however, Bender and Davidson obtain moments smaller in magnitude than ours, on the average by 0.5, 0.8, and 1.0 bohr, respectively. The $B^1\Pi$ is very poorly determined in their case—not even bound. Although they obtain a bound $^3\Pi$, the charge distribution for this state may be poor also due to the lack of diffuse $2p\pi$ functions on H in their basis set. It is this lack of diffuse basis functions which presumably yields their smaller transition moments for the $\Sigma-\Pi$ systems.

IV. LINE STRENGTHS

We have computed the transition matrix elements between various vibration-rotation states for the transitions $X^1\Sigma^+-A^1\Sigma^+$, $X^1\Sigma^+-B^1\Pi$, $A^1\Sigma^+-B^1\Pi$, and the infrared vibration-rotation transitions in the ground state. Selected values are given in Tables XVIII and XIX. Since the $^3\Sigma^+$ state is repulsive and no continuum wavefunctions were calculated, no transition matrix elements were obtained from the electronic transition moments for $^3\Sigma^+-^3\Pi$. The signs of the computed matrix elements are unimportant, as the square of the transition matrix element is the only measurable quantity.

The line strengths, $p_{v',v''J''J'}$, without the Honl-London factors, are presented for several selected bands of the $X^1\Sigma^+-A^1\Sigma^+$ transition in Table XVIII. As can be seen, the $v'=7 \rightarrow v''=0$ band would be that of maximum intensity within the $v''=0$ progression, however in cases where the Boltzmann factor weights high J'' values heavily (i.e., high rotational temperature) the 8-0 band should be most intense. From a study of Fig. 2 in which the vibrational levels of the X and $A^1\Sigma^+$ potential curves are depicted, we could have anticipated this behavior by a straightforward application of the Franck-Condon principle. Halmann and Laulicht,²⁴ computing Franck-Condon factors and r centroids for this progression using RKR potentials predicted an intensity maximum in the absorption

spectrum for the 8-0 band of the $X^1\Sigma^+-A^1\Sigma^+$ transition.

Absolute intensity measurements in absorption have been carried out for the $v''=0$ progression of the $X^1\Sigma^+-A^1\Sigma^+$ transition. Velasco and Fernandez-Florez²⁴ obtain a maximum in the intensity distribution at 8-0 and a second maximum of almost the same relative intensity at 12-0. Comparing the $p_{v',v''J',J''}$ for the 11-0 and 12-0 bands it is evident that in our calculations the intensity distribution for the 12-0 band will definitely be less than in the 11-0 band, and both are less than in the 7-0 and 8-0 bands. Using the equation relating the integrated absorption coefficient to the line strengths,

$$f_{k,l} = (8\pi^2\nu_{lm}/3hc)N_m |R_{lm}|^2, \quad (28)$$

Velasco and Fernandez-Florez have also presented the values of $|R|^2$ for the various lines in the P and R branches of the 6-0 band. The $|R|^2$ values vary greatly—by a factor of 16—from P_1 to P_{10} and R_0 to R_{10} with the largest values for P_1 and R_0 . In the 11-0 and 12-0 bands they observe several maxima and minima in the region $J'=4$ to $J'=19$ when $|R|_{J',J''}^2 + |R|_{J',J''}^2$ is calculated.

Since we were unable to determine what the factor N_m in Velasco's article contains, it is not clear to us what their $|R|^2$ represents. Our $p_{v',v''J',J''}$'s do not behave at all like the experimental $|R|^2$ values presented by Velasco and Fernandez-Florez. Even regarding their measurements as relative intensities does not help to resolve the discrepancy. Because we were able to reproduce very well the anomalous behavior in the spectroscopic constants of the $A^1\Sigma^+$ state, we would expect to be able to pick up the trends in the line strengths.

Recently, Velasco²⁴ has indicated that absolute intensity measurements in absorption are in progress for the $X^1\Sigma^+-B^1\Pi$ transition. It will be interesting to compare our results for this system with experiment to see if perhaps theory and experiment can become less inconsistent.

For the infrared transitions in the ground state, we present the $p_{v',v''J',J''}$ values for two bands: 0-1 and 1-2 in Table XIX. Because these two bands arise from different vibrational states, their intensity relative to each other in absorption will be wholly determined by the population of the $v=0$ and $v=1$ vibrational states. Although relative intensity measurements have been carried out for these bands by James, Norris and Klemperer,¹⁹ the line strengths calculated by these authors contain an unknown Boltzmann factor which

makes comparison of our absolute values with their relative values impossible.

* This research was supported in part by the Advanced Research Projects Agency of the Department of Defense, monitored by the U.S. Army Research Office-Durham, Box CM, Duke Station, Durham, North Carolina 27706, under Grant DA-ARO-D-31-124-72-G78, and by Grant GP-21108 of the National Science Foundation.

† Present address: Harvard College Observatory, Cambridge, Mass. 02138.

¹ K. K. Docken and J. Hinze, *J. Chem. Phys.* **57**, 4928 (1972), preceding article.

² J. W. Cooley, *Math. Computation* **15**, 363 (1961).

³ J. M. Blatt, *J. Computational Phys.* **1**, 382 (1967).

⁴ G. Herzberg, *Spectra of Diatomic Molecules* (Van Nostrand, Princeton, 1950), 2nd ed.

⁵ F. H. Crawford and T. Jorgensen, *Phys. Rev.* **47**, 358, 932 (1935).

⁶ F. Jenč, *J. Mol. Spectry.* **19**, 63 (1966).

⁷ R. Velasco, *Can. J. Phys.* **35**, 1204 (1957).

⁸ C. F. Bender and E. R. Davidson, *J. Chem. Phys.* **49**, 4222 (1968).

⁹ A. D. McLean and M. Yoshimine, *J. Chem. Phys.* **45**, 3676 (1966), and **47**, 3256 (1967).

¹⁰ C. F. Bender and E. R. Davidson, *Phys. Rev.* **183**, 23 (1969).

¹¹ C. F. Bender and E. R. Davidson, *J. Phys. Chem.* **70**, 2675 (1966).

¹² W. E. Palke and W. A. Goddard, *J. Chem. Phys.* **50**, 4524 (1969).

¹³ J. C. Brown and F. A. Matsen, *Phys. Rev.* **135**, A1227 (1964).

¹⁴ S. L. Kahalas and R. K. Nesbet, *J. Chem. Phys.* **39**, 529 (1963).

¹⁵ D. P. Chong and W. B. Brown, *J. Chem. Phys.* **45**, 392 (1966).

¹⁶ P. Cade and W. Huo, *J. Chem. Phys.* **47**, 614 (1967).

¹⁷ R. E. Brown and H. Shull, *Intern. J. Quantum Chem.* **2**, 663 (1968).

¹⁸ L. Wharton, L. P. Gold, and W. Klemperer, *J. Chem. Phys.* **37**, 2149 (1962).

¹⁹ T. C. James, W. G. Norris, and W. Klemperer, *J. Chem. Phys.* **32**, 728 (1960).

²⁰ A. M. Karo and A. R. Olson, *J. Chem. Phys.* **30**, 1232 (1959).

²¹ S. Green, *Phys. Rev.* **4**, 251 (1971).

²² H. Preston and M. Yoshimine, private communication.

²³ R. S. Mulliken and C. A. Rieke, *Rept. Progr. Phys.* **8**, 231 (1941).

²⁴ W. M. Huo, *J. Chem. Phys.* **49**, 1482 (1968).

²⁵ W. H. Henneker and H. E. Popkie, *J. Chem. Phys.* **54**, 1763 (1971); H. E. Popkie, *ibid.* **54**, 4597 (1971).

²⁶ L. Wolniewicz, *J. Chem. Phys.* **51**, 5002 (1969).

²⁷ W. Kolos and L. Wolniewicz, *J. Chem. Phys.* **50**, 3228 (1969).

²⁸ W. Kolos and L. Wolniewicz, *J. Chem. Phys.* **45**, 509 (1966).

²⁹ W. Kolos and L. Wolniewicz, *J. Chem. Phys.* **43**, 2429 (1965).

³⁰ F. Prosser and S. Hagstrom, *Intern. J. Quantum Chem.* **2**, 89 (1968).

³¹ K. Docken, Ph.D. dissertation, University of Chicago, 1972.

³² W. L. Wiese, M. W. Smith, and B. M. Glennon, *Natl. Std. Ref. Data Ser. Natl. Bur. Std. (U.S.)* **4**, Vol. 1.

³³ A. Weiss, *Astrophys. J.* **138**, 1262 (1963).

³⁴ M. Halmann and I. Laufer, *J. Chem. Phys.* **46**, 2684 (1967).

³⁵ J. Fernandez-Florez and R. Velasco, *Opt. Pura Appl.* **2**, 123 (1969).

³⁶ R. Velasco, private communication.

Calculated $a^1\Sigma^-$, $A^1\Delta$, $B^1\Sigma^-$ States of CH^*

GEORGE C. LIU AND JUERGEN HINZE

Department of Chemistry, The University of Chicago, Chicago, Illinois 60637

AND

BOWEN LIU

IBM Research Laboratory, San Jose, California 95114

(Received 17 March 1972)

Ab initio CI calculations have been performed over a wide range of internuclear distances to obtain the potential curves for three low-lying excited electronic states, $a^1\Sigma^-$, $A^1\Delta$, $B^1\Sigma^-$, of CH . With the computed potential curves, vibration-rotational levels are obtained by numerical integration of the radial Schrödinger equations for the motion of the nuclei. The term values are analyzed to yield the conventional spectroscopic constants. Results, with known experimental values in parentheses, are $R_e(A^1\Delta) = 2.074(2.082)$ a.u., $R_e(B^1\Sigma^-) = 2.208(2.200)$ a.u., $R_e(a^1\Sigma^-) = 2.047$ a.u.; $D_0(A^1\Delta) = 1.89(2.01)$ eV, $D_0(B^1\Sigma^-) = 0.17(\sim 0.40)$ eV, and $D_0(a^1\Sigma^-) = 2.85$ eV. The computed spectroscopic constants are found to be within 4% of known experimental values. A potential maximum of height 1600 cm^{-1} occurs in the computed potential curve of the $B^1\Sigma^-$ state. The $a^1\Sigma^-$ state, not known experimentally, is estimated to lie between 0.52 eV and 0.75 eV above the $X^1\Pi$ ground state.

I. INTRODUCTION

The CH radical has been found to be one of the more abundant molecules in comets, stellar atmospheres, and interstellar space.¹ It may play a significant role in the formation of larger molecules in interstellar space. It is also of importance in flames. Consequently, considerable effort has gone into the experimental determination and classification of its spectrum. Several electronic states have been identified and characterized using high resolution uv spectroscopy²; most notably the low-lying $A^1\Delta$, $B^1\Sigma^-$, and $C^1\Sigma^+$, as well as the $X^1\Pi$ ground state. However, one low-lying state, the $a^1\Sigma^-$, which is expected to be below the $A^1\Delta$ state in energy, has not been observed to date. This is because transitions between this and the other low-lying states are strongly forbidden. Also, no properties, other than the spectroscopic properties, have been determined experimentally for the various low-lying states of CH . Molecular properties such as dipole and quadrupole moments are difficult to obtain experimentally for reactive radicals and for excited states. However, these properties are easily calculated once approximate wave functions for the molecule are determined by *a priori* calculations.

It is also difficult to obtain, experimentally, the long range behavior of the potential curves. This long range behavior is of importance in elastic and reactive scattering, and of potential significance in interstellar molecule formation. Here again, *a priori* calculations can supply the needed information, if the calculations are carried beyond the Hartree-Fock limit to include the necessary electron correlation.

Several calculations on CH have been reported in the literature.³⁻⁶ Most of these are limited to either the $X^1\Pi$ ground state or the Hartree-Fock approximation. Exceptions are a minimal basis set, limited CI calculation by Higushi³ for six lowest-lying states

in CH and a recent calculation by Liu and Verhaegen⁴ for the same six states. In the latter calculation the Hartree-Fock results obtained are corrected semiempirically for the correlation error. In both of these calculations the agreements between computed and experimental R_e , ω_e , and term splittings are rather good. The dissociation energies obtained by Higushi are poor, whereas those obtained by the semiempirical method are very good. In this paper we report the results of an extensive and accurate *ab initio* wave mechanical calculation on three excited states, $A^1\Delta$, $B^1\Sigma^-$, and $a^1\Sigma^-$ of CH , all arising from the configuration $1\sigma^2 2\sigma^2 3\sigma 1\pi^2$. Potential curves for these states are determined for a wide range of internuclear separations, considerably beyond the scope of previous calculations.

The agreement between computed quantities and experimental results, where known, is in general satisfactory. An outline of the method used in these computations is depicted in Sec. II. The results are discussed in Sec. III.

Since all calculations with accuracy beyond Hartree-Fock indicate that the yet unobserved $a^1\Sigma^-$ state is above the experimentally observed ground state $X^1\Pi$, we shall follow the spectroscopic convention in the following and denote the state with the prefix *a*, i.e., $a^1\Sigma^-$. As a matter of fact, from the observation of the lines of lowest *J* in the three 0-0 bands of A-X , B-X , and C-X in interstellar absorption, Hersberg and Johns⁵ have concluded that the predicted low-lying $a^1\Sigma^-$ state must lie above the $X^1\Pi$ state.

II. METHOD

In the calculation of the wavefunctions for the molecule, the nonrelativistic Born-Oppenheimer approximation is used. That is, the wavefunction for the molecule is separated into a product of the electronic and the nuclear wavefunctions; by neglecting

TABLE I. Slater-type basis set used in the configuration interaction calculations.

Symmetry	Center	<i>n</i> l value	Exponents used
σ	C	1s	5.2309, 7.969
		2s	1.1678, 2.300, 10.0
		3s	1.1505, 2.8193
		2p	1.2557, 2.7263, 10.0
		3p	2.75
		3d	1.25, 2.5
		4f	2.75
	H	1s	0.70, 1.30, 2.90
		2s	1.2, 2.50
		2p	2.0
π	C	2p	1.2557, 2.7263, 10.0
		3p	1.6095, 3.5
		3d	1.25, 2.5
		4f	2.75
	H	2p	1.25, 2.5
		3p	2.5
		3d	2.5
δ	C	3d	1.5, 2.5, 3.5, 14.0
	H	3d	1.0, 3.0

small terms in the Hamiltonian, two uncoupled wave-equations are obtained and solved separately. The first equation is for the motion of the electrons in the field of the fixed nuclei; the eigenvalues and eigenfunctions are therefore dependent parametrically on the internuclear distance. The second equation is for the motion of the two nuclei in the potential determined by the electrons. The assumption of separability here, again neglecting small coupling terms in the Hamiltonian, leads to the independent nuclear vibrational and rotational motions, and the solutions for them give rise to vibration-rotational states characterized by the vibrational quantum number v and the rotational quantum numbers K and M . (Hund's coupling b is assumed.)

To solve the electronic wave equation, the usual Hartree-Fock-Roothaan self-consistent method is used first, which is followed by a large scale configuration interaction³ calculation in order to introduce the necessary electron correlation. An extended set of Slater type functions is used for the expansion of the orbitals. Some exponents of the σ and π type functions were optimized within the Hartree-Fock approximation for the $X^3\Pi$ ground state at the experimental equilibrium distance. It was found that, with the extensive set used, exponent optimization lowered the energy only little, less than 0.0005 a.u. Therefore, it appeared reasonable to use the same set of basis functions, given in Table I, throughout for all states and internuclear separations. Using the set given in Table I, the SCF result for the $X^3\Pi$ state

is 0.00008 a.u. lower than the result of Cade and Huo.⁴ The computed energies for the three excited states reported here are all found to satisfy the virial theorem to within 0.04% at the computed equilibrium internuclear distance, indicating that the basis set used was satisfactory.

Initial SCF calculations were carried out at each internuclear separation with the single restricted configuration $1\sigma^2 2\sigma^2 3\sigma^1 \pi^2$, properly coupled to yield the appropriate $^3\Delta$, $^3\Sigma^-$, and $^1\Sigma^-$ configuration state functions. It should be noted that the restricted Hartree-Fock functions for the states considered here dissociate properly; $^3\Delta \rightarrow C(^1D) + H(^3S)$, $^3\Sigma^-$, and $^1\Sigma^- \rightarrow C(^1P) + H(^1S)$. This is not so for the $^3\Pi$ ground state, which arises from the configuration $1\sigma^2 2\sigma^2 3\sigma^2 \pi^1$ at the equilibrium distance, but would need, for proper dissociation at large distances, also the configurations $1\sigma^2 2\sigma^2 3\sigma^1 4\sigma^1 \pi^1$ and $1\sigma^2 2\sigma^2 4\sigma^1 \pi^1$.

The orbitals, occupied and empty, resulting from the initial SCF calculations, are used in the following CI calculations. In these CI calculations the 1σ orbital, representing the carbon K shell, is held fixed and always doubly occupied. This is done in order to reduce the number of configurations needed, and since it appears reasonable that the K -shell correlation will not change significantly in molecule formation, a conjecture which we intend to test in future calculations. Three types of configurations are included in the CI calculations:

(a) All configuration state functions of proper symmetry arising from the distribution of five electrons in the orbitals 2σ , 3σ , 4σ , and 1π ;

(b) any possible single replacements from configurations of type (a);

(c) any possible double replacements from configurations of type (a), provided the matrix element between such a configuration and the reference state, i.e., the Hartree-Fock configuration, is nonzero.

This last restriction significantly reduces the number of configuration states used and, furthermore, is justified from a perturbation theory point of view. The actual number of configuration state functions used are 2466, 2558, and 2159 for $A^3\Delta$, $B^3\Sigma^-$, and $a^1\Sigma^-$, respectively.

Once the electronic wavefunctions and potential curves are obtained, the equations for the nuclear motion can be solved. The solutions for the angular part of the nuclear motion, i.e., the molecular rotation, can be obtained analytically as the "generalized" spherical harmonic function,⁴ with the quantum numbers A , K , and M . The total angular momentum J is not needed at this stage since the three states considered here follow Hund's coupling case b. This is obvious for the two Σ^- states; for the $^3\Delta$ state Herzberg and Johns⁵ found from experimental data that it is close to case b also. The centrifugal corrections for given K values are added to the computed elec-

TABLE II. Potential curve for CH $A^1\Delta$ state.^a

R	E_{Cv}	E_{Cl}	$E_{\text{Cv}} - E_{\text{Cl}}$	Dipole ^b (C-II ⁺)
1.55	-38.102022	-38.208910	0.1069	0.429
1.65	-38.136048	-38.243161	0.1071	0.490
1.80	-38.165790	-38.273596	0.1078	0.587
1.90	-38.175525	-38.284011	0.1085	0.656
2.00	-38.179572	-38.288894	0.1093	0.724
2.10	-38.179435	-38.289729	0.1103	0.795
2.20	-38.176275	-38.287656	0.1114	0.866
2.30	-38.171006	-38.283561	0.1126	0.933
2.40	-38.164370	-38.278143	0.1138	0.994
2.60	-38.149559	-38.265450	0.1159	1.090
2.80	-38.137666	-38.252539	0.1149	1.100
3.00	-38.131984	-38.241809	0.1098	1.029
3.20	-38.129633	-38.234168	0.1045	0.907
3.50	-38.128715	-38.227239	0.0985	0.689
3.80	-38.128970	-38.223797	0.0948	0.490
5.00	-38.130697	-38.220756	0.0901	0.102
6.00	-38.131085	-38.220437	0.0894	0.0268
8.00	-38.131165	-38.220273	0.0891	0.00185
10.00	-38.131165	-38.220254	0.0891	0.000333
12.00	-38.131164	-38.220255	0.0891	0.000280
15.00	-38.131164	-38.220254	0.0891	0.000160
20.00	-38.131163	-38.220253	0.0891	0.000052

^a R and E are in atomic units (1 bohr = 0.529177 Å, 1 hartree = 27.211652 eV), dipole in debye.

^b Calculated from CI wavefunctions.

TABLE III. Potential curve for CH $B^1\Sigma^-$ state.^a

R	E_{Cv}	E_{Cl}	$E_{\text{Cv}} - E_{\text{Cl}}$	Dipole ^b (C-II ⁺)
1.80	-38.138311	-38.256403	0.1181	0.882
1.90	-38.149862	-38.269194	0.1193	0.983
2.00	-38.156026	-38.276693	0.1207	1.082
2.10	-38.156447	-38.280419	0.1220	1.176
2.20	-38.158528	-38.281539	0.1230	1.260
2.30	-38.157588	-38.280934	0.1233	1.326
2.40	-38.156846	-38.279246	0.1224	1.370
2.60	-38.157888	-38.274785	0.1169	1.370
2.80	-38.161217	-38.271042	0.1098	1.273
3.00	-38.165337	-38.268831	0.1035	1.110
3.20	-38.169461	-38.268059	0.0986	0.915
3.50	-38.174903	-38.268665	0.0938	0.630
3.80	-38.179140	-38.270165	0.0910	0.457
4.20	-38.183037	-38.272178	0.0891	(0.263) ^c
5.00	-38.186905	-38.274505	0.0877	(0.0945) ^c
6.00	-38.188142	-38.275294	0.0872	0.0262
8.00	-38.188472	-38.275379	0.0869	0.00246
10.00	-38.188482	-38.275356	0.0869	0.000757
12.00	-38.188482	-38.275349	0.0869	0.000389
15.00	-38.188481	-38.275347	0.0869	0.000158
20.00	-38.188481	-38.275346	0.0869	0.000050

^a R and E are in atomic units (1 bohr = 0.529177 Å, 1 hartree = 27.211652 eV), dipole in debye.

^b Calculated from CI wavefunctions.

^c Interpolated, with $R = a \log(\text{dipole}) + b$, from T = 3.20, 3.50, 3.80, and 6.00 a.u.

TABLE IV. Potential curve for CH $a^1\Sigma^-$ state.^a

R	E_{Cv}	E_{Cl}	$E_{\text{Cv}} - E_{\text{Cl}}$	Dipole ^b (C-II ⁺)
1.45	-38.166370	-38.254642	0.0883	0.363
1.60	-38.233835	-38.322389	0.0886	0.429
1.80	-38.277399	-38.366860	0.0895	0.521
1.90	-38.286394	-38.376517	0.0901	0.569
2.00	-38.289669	-38.380585	0.0909	0.620
2.10	-38.288693	-38.380534	0.0918	0.668
2.20	-38.284590	-38.377486	0.0929	0.719
2.40	-38.270247	-38.365664	0.0954	0.821
2.60	-38.251458	-38.349975	0.0985	0.915
2.80	-38.231240	-38.333454	0.1022	0.983
3.00	-38.211953	-38.318224	0.1063	1.014
3.20	-38.199827	-38.305495	0.1057	0.892
3.50	-38.193398	-38.292225	0.0988	0.714
3.80	-38.190813	-38.284691	0.0939	0.531
4.20	-38.189442	-38.279778	0.0903	0.330
5.00	-38.188723	-38.276628	0.0879	0.117
6.00	-38.188547	-38.275721	0.0872	0.0318
8.00	-38.188488	-38.275395	0.0869	0.00283
10.00	-38.188483	-38.275357	0.0869	0.000775
12.00	-38.188482	-38.275349	0.0869	0.000389
15.00	-38.188481	-38.275347	0.0869	0.000158
20.00	-38.188481	-38.275346	0.0869	0.000050

^a R and E are in atomic units (1 bohr = 0.529177 Å, 1 hartree = 27.211652 eV), dipole in debye.

^b Calculated from CI wavefunctions.

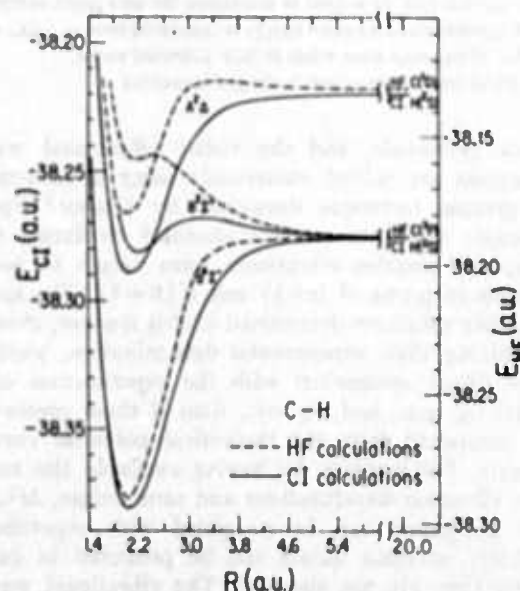


FIG. 1. Potential curves for the states $a^1\Sigma^-$, $A^1\Delta$, and $B^1\Sigma^-$ of CH as obtained from Hartree-Fock and configuration interaction calculations. The energy scale in hartree on the right is for the Hartree-Fock results; that on the left is for the configuration interaction results. The common energy point for both scales is chosen as the energy of separated atoms, H(2S) and C(3P).

TABLE V. Properties of low-lying electronic states of CH.

		$A^1\Delta$	$B^1\Sigma^-$	$a^1\Sigma^-$
R_e (a.u.)	SCF	2.045	2.152	2.022
	CI	2.074	2.208	2.047
	Exptl	2.082 ^a	2.200 ^a	
E (a.u.)	SCF	-38.179949	-38.158697	-38.289763
	CI	-38.289856	-38.281540	-38.380998
	Exptl	-38.383 ^b	(-38.3717) ^{b,c}	
D_e^d (eV)	SCF	1.33	-0.81	2.76
	CI	1.894	0.169	2.875
	Exptl	2.01 ^d	(0.407) ^e	
D_0^d (eV)	SCF	1.14	^e	2.55
	CI	1.708	0.042	2.681
	Exptl	1.83	0.26	
Dipole (debye) C-II ⁺	SCF	0.812	1.367	0.562
	CI	0.778	1.267	0.643
	Exptl			
Quadrupole with respect to center of mass (a.u.)	CI	1.70	1.92	1.52
Total Hellman-Feynman force (a.u.) ^f	CI	-0.02	0.01	-0.02
Gradient of electric field at carbon nucleus (a.u.)	CI	0.22	0.51	0.23
Gradient of electric field at hydrogen nucleus (a.u.)	CI	0.31	0.23	0.31

^a From Ref. 2.^b Total experimental energy is taken to be the sum of experimental atomic energy and spectroscopically determined D_0^d . Atomic energies are taken from Ref. 4 and from C. E. Moore, Natl. Bur. Std. (U.S.), Circ. 467, Vol. 1 (1949). For D_0^d , see Footnotes c and d.^c The spectroscopic constants ω_e and $\omega_e x_e$ for $B^1\Sigma^-$ state are not well determined experimentally; therefore only the known approximate ω_e (see Ref. 2) is used to determine the zero point energy.^d Experimental zero-point energy is calculated from ω_e , $\omega_e x_e$, and Dunham correction. (Spectroscopic constants are taken from Ref. 2.)^e No vibrational state exists in SCF potential curve.^f Attractive force towards hydrogen is positive.

tronic potentials, and the radial vibrational wave equations are solved numerically using a numerical integration technique developed by Cooley.⁷ Spectroscopic constants are now obtained by fitting the computed rotation-vibrational term values to polynomials in terms of $(v+\frac{1}{2})$ and $K(K+1)$. The spectroscopic constants determined in this manner, closely resembling their experimental determination, yield a more direct comparison with the experimental constants ω_e , $\omega_e x_e$, and B_e , etc., than if these constants are computed from the theoretical potential curves directly. Furthermore, by having available the rotation-vibration wavefunctions and term values, $\Delta G_{v+1/2}$ and B_v values can be compared with experiment directly, or these values can be predicted in cases where they are not observed. The vibrational wavefunctions, which depend only implicitly, due to the centrifugal correction, on K , are used in addition to compute some typical rotation-vibration transition matrix elements $\langle v(R, K) | D(R) | v'(R, K') \rangle$ by in-

TABLE VI. Constants obtained from rotational analysis. (Experimental values are taken from Ref. 2 and given in parentheses.)

State	v	$\Delta G_{v+1/2}$ ^a (cm ⁻¹)	B_v (cm ⁻¹)	D_v (10 ⁻³ cm ⁻¹)
$A^1\Delta$	0	2807.7(2737.4)	14.665(14.577)	1.50(1.56)
	1	2616.3(2544.1)	14.022(13.907)	1.54(1.58)
	2	2400.7	13.321(13.182)	1.62(1.65)
	3	2119.7	12.503	
	4		11.423	
$B^1\Sigma^-$	0	1658.8(1794.9)	12.628(12.645)	2.31(2.22)
	1		10.75(11.160)	10.2(3.28)
$a^1\Sigma^-$	0	30(9.3)	15.091	1.44
	1	2878.2	14.558	1.43
	2	2729.8	14.014	1.44
	3	2567.4	13.435	1.47
	4	2383.8	12.808	1.52

^a 1 a.u. = 219 474.55 cm⁻¹.

TABLE VII. Derived spectroscopic constants. (Experimental values are taken from Ref. 2 and given in parentheses.)

State	Zero-point energy (cm ⁻¹)	ν_{00} (cm ⁻¹)	ω_e (cm ⁻¹)	$\omega_e x_e$ (cm ⁻¹)	B_e (cm ⁻¹)	α_e (cm ⁻¹)
$B^2\Sigma^-$	1024.4 (~1125) ^b	21 286.1	2173.6 ^d (~2250)	249.7 ^d	13.57 (13.39)	1.88 (1.49)
$A^2\Delta$	1503.9 (1418.1) ^c	19 940.6	2991.2 (2930.7)	95.71 (96.65)	15.011 (14.934)	0.672 (0.697)
$a^4\Sigma^-$	1566.8	0	3160.4	70.54	15.36	0.538

^a Refer to $v=0$ vibrational state of $a^4\Sigma^-$.

^b Since only ω_e is approximately known experimentally, zero-point energy is taken to be $\sim \frac{1}{4}\omega_e$.

^c Calculated from experimental spectroscopic constants with Dunham correction.

^d Since only two vibrational levels are obtained in CI calculations, these constants are derived from $\Delta G_{1/2}$ and computed zero-point energy.

^e Three computed vibrational levels are used in deriving spectroscopic constants, ω_e , $\omega_e x_e$, B_e , and α_e .

tegrating over the internuclear distance dependence of the molecular dipole moment.

III. RESULTS AND DISCUSSION

The calculated SCF and CI energy values at different internuclear distances are given in Tables II–IV. The calculated dipole moments are also given in these tables. The direction of dipole, $C-H^+$, is rather surprising since from the ionization energy of C and H one would expect the direction to be the other way (in accord with what is observed in almost all hydrocarbon compounds⁸). The reason for this reversal is as follows. The ground states of the $C^+(1s^2 2s^2 2p^2 P)$ and $H^-(1S)$ ions cannot give rise to $^2\Delta$, $^2\Sigma^-$, or $^4\Sigma^-$ states. The lowest excited states of the ions C^+ and H^- , which can form $^2\Delta$, $^2\Sigma^-$, or $^4\Sigma^-$ states, lie higher than the energy of $C^-(1s^2 2s^2 2p^3 ^4S \text{ or } ^3D) + H^+$.

A similar behavior is expected for the $X^2\Pi$ state, although the situation is complicated by the fact that the ground states of C^+ and H^- do combine to give a $^2\Pi$ state. The difference in the direction of dipole moment in the CH radical and in hydrocarbons therefore indicates the importance of the valence structure $C^-(^4S \text{ or } ^3D) + H^+$ in the CH radical, but not in the formation of hydrocarbon compounds.

The calculated CI potential curves for the three states are presented in Fig. 1, together with the corresponding SCF curves. Five points around the computed energy minimum of each state were fitted to a fourth order polynomial, and the resulting analytical curve was used to determine the potential minimum and the equilibrium internuclear distance. The results, together with the known experimental values, are given in Table V.

The computed SCF equilibrium internuclear distances (Table V) for $A^2\Delta$ and $B^2\Sigma^-$ are, respectively, 0.037 and 0.048 a.u. shorter than the experimental values, whereas the CI results give $R_e(A^2\Delta) = 2.074$

a.u. and $R_e(B^2\Sigma^-) = 2.208$ a.u., in excellent agreements with the experimental values. A similar CI calculation for CH^+ by Green *et al.*⁹ gives even better agreements. We conclude that a large CI calculation of this type should be able to determine R_e to within 0.01 a.u. The computed R_e for experimentally yet unobserved $a^4\Sigma^-$ state is 2.047 a.u.

As can be seen from Table V, the SCF calculation does not give rise to a stable $B^2\Sigma^-$ state; the SCF potential curve lies entirely above the SCF energy of the separated atoms. This is another manifestation of the deficiency of the conventional Hartree-Fock method. One of the methods used to overcome this deficiency is of course the configuration interaction method used here. The CI dissociation energy for $B^2\Sigma^-$ is 0.169 eV, still too low compared with the experimental value of 0.40 eV.

The computed dissociation energies for $A^2\Delta$ and $a^4\Sigma^-$ states are 1.894 eV (experimental value 2.01 eV) and 2.875 eV, respectively. A similar calculation for the $X^2\Pi$ ground state would be desirable in order to predict more accurately the location of the unobserved $a^4\Sigma^-$ state. However, calculations of similar accuracy could not be carried out presently for the following reasons. The $X^2\Pi$ state requires three configurations, as indicated above, in order to dissociate correctly. This in turn makes it necessary to carry out a three configuration MC-SCF calculation, rather than a single configuration SCF, in order to obtain an adequate reference state. Such a reference state, containing several configurations, would yield a CI expansion with more than 7000 configuration state functions, if they are selected by the same rules as outlined above. Nevertheless, it is possible to make a reasonable prediction for the location of the $^4\Sigma^-$ state from available data. The potential curves for the $X^2\Pi$, $a^4\Sigma^-$, and $B^2\Sigma^-$ states all dissociate to the same separated atom limit. The calculated D_0 for the $B^2\Sigma^-$ is 0.23 eV too low compared to experiment.

TABLE VIII. Transition dipole matrix elements $\langle vK | D(R) | v'K' \rangle$ of the $A^2\Delta$ state in atomic units (e-bohr).

$v \setminus v'$	0	1	2	3	4
A. For $K=2$ and $K'=2$					
0	0.316				
1	0.040	0.335			
2	-0.006	0.053	0.351		
3	0.000	-0.014	0.056	0.360	
4	0.000	0.001	-0.025	0.048	0.360
B. For $K=2$ and $K'=3$					
0	0.316	0.038	-0.006	0.000	0.000
1	0.041	0.335	0.051	-0.014	0.001
2	-0.006	0.055	0.351	0.054	-0.025
3	0.000	-0.014	0.059	0.360	0.044
4	0.000	0.001	-0.025	0.052	0.360

If we assume that similar error exists in the calculated $a^4\Sigma^-$ curve, one can expect the true value for $D_e(a^4\Sigma^-)$ to lie between the computed value of 2.88 eV and 3.11 eV. Since the dissociation energy for the $X^2\Pi$ state is known experimentally to be 3.63 eV, we predict $T_e = 0.63 \pm 0.12$ eV.

As indicated above, the 1σ shell, corresponding to the carbon K shell, has been kept doubly occupied in all configuration state functions used in the CI expansion. Therefore, changes in the intra- K -shell correlation with R , as well as changes in the correlation of other electrons with the K -shell electrons, have been neglected. The constancy of the former and the smallness of the latter have been established, in the case of LiH, for example, by comparing atomic correlation energies with the partitioned molecular correlation energy of LiH.¹⁰ Therefore we expect that the neglect of K -shell correlation introduces only a small relative error into our computed potential curves.

The computed properties, such as dipole moment and quadrupole moments with respect to center of mass, given for R_e in Table V, are obtained by quadratic interpolation to R_e from the values computed

TABLE IX. Transition dipole matrix elements $\langle vK | D(R) | v'K' \rangle$ of the $B^2\Sigma^-$ state in atomic units (e-bohr).

$v \setminus v'$	0	1
For $K=0$ and $K'=1$		
0	0.503	0.021
1	0.023	0.471

directly. The dipole moments at R_e for $A^2\Delta$, $B^2\Sigma^-$, and $a^4\Sigma^-$ are, respectively, 0.778, 1.267, and 0.643 D. As discussed previously, all these dipole moments are $C-H^+$, indicating the importance of the valence structure $C-H^+$ in the CH radical. Of importance here is the dipole moment of the $B^2\Sigma^-$ state, which is twice that of the other two states. This is connected with the occurrence and interpretation of the potential maximum in the $B^2\Sigma^-$ state (see Fig. 1). This potential maximum has also been found experimentally by Herzberg and Johns,² who found the maximum at about 2.0 Å with a height greater than 500 cm^{-1} . Our calculations give the position of the maximum at 1.73 Å with a height of 1600 cm^{-1} above the dissociation limit. According to Herzberg and Johns, this maximum is of van der Waals origin. However, since the atoms forming the $B^2\Sigma^-$ state are in their ground states and different, and one of them, H, is in an S state, there cannot be any first order perturbation, which would cause a van der Waals maximum. It ap-

TABLE X. Transition dipole matrix elements $\langle vK | D(R) | v'K' \rangle$ of the $a^4\Sigma^-$ state in atomic units (e-bohr).

$v \setminus v'$	0	1	2	3	4
For $K=0$ and $K'=1$					
0	0.260	0.028	-0.003	0.000	0.000
1	0.029	0.273	0.040	-0.006	0.000
2	-0.003	0.041	0.287	0.048	-0.010
3	0.000	-0.006	0.049	0.300	0.053
4	0.000	0	-0.010	0.054	0.313

pears more likely that this maximum,¹¹ appearing at a relatively small internuclear distance, is caused by an avoided curve crossing. The most likely zeroth order curve responsible for this avoided curve crossing is the $^2\Sigma^-$ state arising from the 2D_u state of $C^-(1s^2s^2p^3)$ with the 1S state of H^+ (the bare proton). Since C^- and H^+ attract each other by a Coulomb force, and since H^+ is just a "bare" proton, we expect this potential curve to follow a $1/R$ behavior down to a small R value, i.e., to $R \approx 3$ bohr, at which time a large (0.1 hartree) interaction matrix element becomes reasonable. The ionic curve crossing proposed here for the $^2\Sigma^-$ state is also in accord with the large dipole moment of the $B^2\Sigma^-$ state, which continues to increase down to $R=2.2$ bohr.

The long range behavior of the computed potential curves has been fitted to a c/R^6 van der Waals term, supplemented for the $^2\Sigma^-$ and $^4\Sigma^-$ states by $\pm Be^{-AR}$ to account for the splitting of the two multiplets. A rough fit (the computed accuracy permits only a rough fit) yielded the following formulas for $U(\infty) -$

$U(R)$ in atomic units:

$$a^4\Sigma^-: 8/R^6 + 4.06 \exp(-1.64R),$$

$$B^2\Sigma^-: 8/R^6 - 4.06 \exp(-1.64R),$$

$$A^2\Delta: 8/R^6.$$

These formulas fit the computed potential curves down to $R=6$ bohr with a deviation of 3 cm^{-1} or less.

The $\Delta G_{v+1/2}$ and constants derived from rotational analysis are given in Table VI, together with known experimental results in parentheses. The errors in $\Delta G_{v+1/2}$ for the $A^2\Delta$ state are 70.3 cm^{-1} (2.5%) for $v=0$, and 52.2 cm^{-1} (2.0%) for $v=1$. The error for $B^2\Sigma^-$, $v=0$ is much larger, being -136.1 cm^{-1} (7.6%), and in the opposite direction compared with $A^2\Delta$. This means the calculated potential curve for the $B^2\Sigma^-$ state is too wide as well as too shallow. However, due to the narrow spacing for the rotational levels, it is seen from the table that the rotational constants B_v , and even D_v (which is 10^{-4} times B_v), are all in very good agreement with experimental values. In deriving B_v and D_v in Table VI, the 10 lowest rotational levels are used for $A^2\Delta$, $a^4\Sigma^-$ and $v=0$ of $B^2\Sigma^-$, whereas only six levels are used for $v=1$ of $B^2\Sigma^-$ since only these six levels exist in the potential well.

In Table VII we give the computed zero-point energy and the derived equilibrium spectroscopic constants. The term splittings v_{00} are also given, relative to $a^4\Sigma^-$. The known experimental v_{00} for $B^2\Sigma^- - A^2\Delta$ is 2480.7 cm^{-1} , our computed value is only 1345.5 cm^{-1} , or 1135.2 cm^{-1} too small, indicating that the error in the potential curve spacings for the various states is about 0.15 eV.

In deriving the equilibrium spectroscopic constants we have used the same number of v levels as are observed and used by experimentalists for their determination. Three v levels are used for the $a^4\Sigma^-$ state. While experimentalists do not have enough information to derive ω_e and $\omega_e x_e$ for the $B^2\Sigma^-$ state (since only two levels for this state are observed), we can derive the constants by combining $\Delta G_{1/2}$ and the computed zero-point energy. The ω_e and $\omega_e x_e$ calculated for the $B^2\Sigma^-$ state are 2173.6 cm^{-1} and 249.7 cm^{-1} , respectively. Except for α_e for $B^2\Sigma^-$, the agreements between computed and experimental equilibrium spectroscopic constants are all within 4%.

The transition matrix elements, apart from the explicit rotational quantum number dependent factors, are evaluated using the computed dipole moments from Tables II-IV, together with the rotation-vibration wavefunctions computed. The resulting transition matrix elements are fairly constant within each branch, therefore only the values for the first members of each branch are given in Tables VIII-X.

ACKNOWLEDGMENTS

The authors wish to thank Dr. P. S. Bagus, Dr. A. D. McLean, and Dr. M. Yoshimine for helpful discussions. George Lie and Juergen Hinze gratefully acknowledge hospitality extended to them by the IBM Research Laboratory in San Jose.

* This research was carried out under a Joint Study Agreement between the University of Chicago and the IBM Corporation. Lie and Hinze were supported in part by the Advanced Research Projects Agency of the Department of Defense, monitored by U.S. Army Research Office—Durham, Box CM, Duke Station, Durham, N.C. 27706, under Contract No. DA-31-124-ARO-D-447, and by Grant GP-21108 of the National Science Foundation.

¹ G. Herzberg, *Spectra of Diatomic Molecules* (Van Nostrand, N.J., 1950), 2nd ed.; D. McNally, *Advan. Astron. Astrophys.* **6**, 173 (1968).

² G. Herzberg and J. W. C. Johns, *Astrophys. J.* **158**, 399 (1969).

³ For example, H. P. D. Liu and G. Verhaegen, *J. Chem. Phys.* **53**, 735 (1970); C. F. Bender and E. R. Davidson, *Phys. Rev.* **183**, 23 (1969); W. M. Huo, *J. Chem. Phys.* **49**, 1482 (1968); A. C. Hurley, *Proc. Roy. Soc. (London)* **A249**, 402 (1959); M. Krauss, *J. Chem. Phys.* **28**, 1021 (1958); J. Higuchi, *ibid.* **22**, 1339 (1953).

⁴ P. E. Cade and W. M. Huo, *J. Chem. Phys.* **47**, 614 (1967).

⁵ The computer programs used for this calculation were written by P. S. Bagus, B. Liu, A. D. McLean, and M. Yoshimine of the Theoretical Chemistry Group at IBM Research in San Jose, Calif. Preliminary descriptions of the program are given by A. D. McLean, in "Potential Energy Surfaces from *ab initio* Computation: Current and Projected Capabilities of the ALCHEMY Computer Program," Proceedings of the Conference on Potential Energy Surfaces in Chemistry, University of California, Santa Cruz, August 1970.

⁶ See, e.g., L. D. Landau and E. M. Lifshitz, *Quantum Mechanics* (Addison-Wesley, Reading, Mass., 1958).

⁷ J. W. Cooley, *Math. Computation* **15**, 363 (1961).

⁸ The dipole moment of C-H bond in saturated systems has been estimated to be about 0.4 D (C^+H^-); theoretical calculations for polyatomic molecules containing C-H bond also indicate C^+H^- bond moment. V. W. Laurie and J. S. Muentner, *J. Am. Chem. Soc.* **88**, 2883 (1966); M. D. Newton, E. Switkes, and W. N. Lipscomb, *J. Chem. Phys.* **53**, 2645 (1970), and references therein.

⁹ S. Green, P. S. Bagus, B. Liu, A. D. McLean, and M. Yoshimine *Phys. Rev. A* **5**, 1614 (1972).

¹⁰ D. D. Ebbing, *J. Chem. Phys.* **36**, 1361 (1962).

¹¹ J. K. Knipp, *Phys. Rev.* **53**, 734 (1938).

VALENCE EXCITED STATES OF CH
I. POTENTIAL CURVES*

by

George C. Lie[†]
Juergen Hinze

Department of Chemistry
The University of Chicago
Chicago, Illinois 60637

and

Bowen Liu

IBM Research Laboratory
San Jose, California 95114

ABSTRACT: Ab initio CI calculations have been performed over a wide range of internuclear distances (1.00 bohr to 20.00 bohr) to obtain the potential curves for the first five valence excited states of CH; $X^2\Pi$, $a^4\Sigma^-$, $A^2\Delta$, $B^2\Sigma^-$, and $C^2\Sigma^+$. Results, with known experimental values in parentheses, are $R_e(X^2\Pi) = 2.113$ (2.116) bohr, $R_e(a^4\Sigma^-) = 2.053$ bohr, $R_e(A^2\Delta) = 2.083$ (2.083) bohr, $R_e(B^2\Sigma^-) = 2.216$ (2.20) bohr, $R_e(C^2\Sigma^+) = 2.100$ (2.105) bohr; $D_e(X^2\Pi) = 3.51$ (3.63) eV, $D_e(a^4\Sigma^-) = 2.84$ eV, $D_e(A^2\Delta) = 1.90$ (2.01) eV, $D_e(B^2\Sigma^-) = 0.23$ (0.40) eV, and $D_e(C^2\Sigma^+) = 0.78$ (0.94) eV. Potential maxima of heights 1284 and 3228 cm^{-1} are calculated for the $B^2\Sigma^-$ and $C^2\Sigma^+$ states, respectively. These maxima are attributed to avoided curve crossings. The $a^4\Sigma^-$ state, not observed experimentally, is estimated to lie between 0.62 eV and 0.76 eV above the $X^2\Pi$ state.

*This research was carried out under a Joint Study Agreement between the University of Chicago and the IBM Corporation. Lie and Hinze were supported in part by the Advanced Research Agency of the Department of Defense, monitored by U.S. Army Research Office--Durham, Box CM, Duke Station, Durham, N.C. 27706, under Grant DA-ARO-D-31-124-72-G78 and by Grant GP-33892X of the National Science Foundation.

[†]Present address: IBM Research Laboratory, San Jose, California 95114.

I. INTRODUCTION

The emission spectra of CH in the visible and near-ultraviolet consists of three band systems near 4300Å, 3900Å and 3140Å corresponding to the electronic transitions $A^2\Delta \rightarrow X^2\Pi$, $B^2\Sigma^- \rightarrow X^2\Pi$, and $C^2\Sigma^+ \rightarrow X^2\Pi$, respectively. Analyses of these spectra¹ in the early days of quantum mechanics played an important part in the development of our understanding of the doublet spectra of diatomic molecules. These analyses were later refined or extended by Shidei,² Gerö,³ and Kiess and Broida.⁴

While absorption spectra of CH in stars have been known for a long time, no absorption spectra in the terrestrial laboratory had been found until 1952.⁵ By 1969 strong absorption spectra were obtained in the flash photolysis of diazomethane and analyzed by Herzberg and Johns.⁶ With this a considerable number of new absorption bands were found, including a Rydberg series in the vacuum ultraviolet, which supplied an accurate value for the ionization potential. In addition, the number of observed vibrational levels in the $X^2\Pi$, $B^2\Sigma^-$ and $C^2\Sigma^+$ states was increased and effects of predissociation in the $B^2\Sigma^-$ and $C^2\Sigma^+$ states were discovered, leading to an improved value for the dissociation energy of the $X^2\Pi$ state. However, the number of observed vibrational levels in each electronic state was still inadequate to yield reliable experimental potential curves over a wide range of internuclear distances.

The experimental study of other properties of the CH radical is considerably hindered by its high reactivity. Only recently has the dipole moment of the ground electronic state been determined successfully from simultaneous observation of the Stark splittings in the $J = 1/2$, $^2\Pi$ states

of CH and OH.⁷ It is in this area that a theoretical study can be most useful, as a source of otherwise unavailable information.

Based on the then known spectra of O₂ and CH and some qualitative quantum mechanical arguments, Mulliken,⁸ in a discussion of the correlation rules for the united atom, diatomic hydride, and separate atoms, predicted the $^4\Sigma^-$ state of CH to lie closely above, or even below the $^2\Pi$ state. Since all the known stable states of CH to date are doublets, the absence of transitions connected with the $^4\Sigma^-$ state is to be expected on account of the different spin multiplicities. Porter⁹ argued that since CH lines, ($^2\Delta + ^2\Pi$) and ($^2\Sigma^- + ^2\Pi$), were observed in interstellar absorption and since most molecules in interstellar space should be in their lowest energy state, $^2\Pi$ should be the ground state. Herzberg and Johns⁶ reached the same conclusion by a similar argument. Recent ab initio calculations of the $^4\Sigma^-$ state by Lie, Hinze and Liu¹⁰ showed that the $^4\Sigma^-$ state lies above the $^2\Pi$ state. Hence, in the following, these states will be designated a $^4\Sigma^-$ and X $^2\Pi$, respectively.

Near Hartree-Fock (HF) potential curves have been reported by Cade and Huo¹¹ for the X $^2\Pi$ state and by Lie et al.¹⁰ for the a $^4\Sigma^-$, A $^2\Delta$ and B $^2\Sigma^-$ states. Cade and Huo found that spectroscopic constants calculated from the HF results for first row hydrides are generally in good agreement with experiment. This conclusion is also upheld in the excited A $^2\Delta$ state of CH. However, the HF model does not predict a stable B $^2\Sigma^-$ state, in the sense that there exists at least one vibrational level in the potential well. Also, there are other well-known systematic errors in the conventional HF approximation: calculated dissociation energies are often too low by

1 - 2 eV; results for states of lower multiplicities are generally less accurate than those for states of higher multiplicities, and incorrect dissociation to excited atomic states is often predicted.

Both Heitler-London and full valence-shell configuration interaction (CI) methods were employed by Higuchi¹² to obtain potential curves, in the range of 0.9 to 1.3 Å, for the $X^2\Pi$, $a^4\Sigma^-$, $A^2\Delta$, $B^2\Sigma^-$ and $C^2\Sigma^+$ states (energy values were given relative to the ground states of C and H of unspecified source). However, only a minimum basis set of Slater-type-functions (STF) was used.

The only accurate potential curves reported so far are those of Lie et al.¹⁰ for the $a^4\Sigma^-$, $A^2\Delta$ and $B^2\Sigma^-$ states. In their calculations, all valence electrons were explicitly correlated by using large scale CI expansions. Dissociation energies, equilibrium internuclear distances and spectroscopic constants were in quantitative agreement with the known experimental values. The $a^4\Sigma^-$ state was predicted to lie between 0.52 and 0.75 eV above the $X^2\Pi$ state.

Liu and Verhaegen¹³ used self-consistent-field (SCF) calculations, empirically corrected for electron correlation, to obtain potential curves for the first six electronic states of CH in the range of 2 to 3.5 bohrs (no total energy values were given). Close agreement with experiment was found for a number of molecular properties such as equilibrium internuclear distances, vibrational frequencies, term values and dissociation energies. The $a^4\Sigma^-$ state was calculated to lie 0.93 eV above the $X^2\Pi$ state, much too high compared with the ab initio estimate of Lie et al.¹⁰ Liu and Verhaegen found maxima in their calculated potential curves for the $X^2\Pi$, $B^2\Sigma^-$, $C^2\Sigma^+$ and $D^2\Pi_1$ states. Experimentally, Herzberg and Johns⁶ did find a

maximum for the $B^2\Sigma^-$ state, and were able to deduce the existence of humps in the potential curves for the $C^2\Sigma^+$ and $D^2\Pi_1$ states. However, Liu and Verhaegen's conclusion about the maximum in the $X^2\Pi$ state is almost certain to be in error.

The slight maximum in the $B^2\Sigma^-$ state had been overlooked until stronger absorption spectra of CH and CD were obtained and analyzed by Herzberg and Johns.⁶ Theoretically, this maximum was found only recently in the calculations of Liu and Verhaegen,¹³ Lie et al.,¹⁰ and Julienne and Krauss.¹⁴ According to Herzberg and Johns, this maximum occurs at $\sim 2\text{\AA}$ with a height greater than or equal to 500 cm^{-1} . The semi-empirical calculation of Liu and Verhaegen¹³ placed the maximum, $\sim 900\text{ cm}^{-1}$ in height, at 1.6\AA . The CI result of Lie et al.¹⁰ gave a barrier 1600 cm^{-1} high at 1.73\AA . Julienne and Krauss,¹⁴ using the optimized valence configuration method,¹⁵ estimated the barrier to be $\sim 1000\text{ cm}^{-1}$ in height around 2\AA .

In this work we have endeavored to improve the results of Lie et al.¹⁰ for the $a^4\Sigma^-$, $A^2\Delta$ and $B^2\Sigma^-$ states, and to include also calculations for the $X^2\Pi$ and $C^2\Sigma^+$ states of CH. Potential curves were calculated for all five states for a wide range of internuclear distances, from 1.00 bohr to 20.00 bohr, using the CI method. A number of frequently used computational models are examined in these calculations, in an effort to compare and establish the extent of their usefulness. The most accurate model yielded potential curves, taken relative to the separated ground state atom limit, believed to be within 0.3 eV of the exact curves.

Table I gives the electronic configurations of the five lowest electronic states of CH and their respective dissociation limits. The method

used in this work is described in Sec. II. A discussion of the resulting potential curves is given in Sec. III.

Expectation values of various one-particle operators and molecular properties, calculated at various internuclear distances from the resulting wavefunctions, as well as the calculation of vibration-rotational wavefunctions, energies, and spectroscopic analysis from the resulting potential curves, will be presented in paper II.¹⁶

II. METHOD

In the Born-Oppenheimer approximation the total wavefunction of a diatomic molecule is written as a product of electronic and nuclear wavefunctions. The electronic wavefunction, neglecting relativistic effects, are eigenfunctions of the clamped-nuclei Hamiltonian operator

$$H = -\frac{1}{2} \sum_i \nabla_i^2 + V(R, \hat{x}) , \quad (1)$$

where ∇_i^2 is the Laplacian operator for the i -th electron, R is the internuclear distance, \hat{x} is the collection of all electronic spatial coordinates. In Eq. (1) the first terms correspond to the electronic kinetic energy, and the second term to all the electrostatic interactions between electrons and nuclei of the molecule. Atomic units are used in Eq. (1) and throughout this paper, unless otherwise specified. Eigenfunctions of this Hamiltonian, which does not contain magnetic interactions, are also eigenfunctions of the total electronic spin angular momentum S^2 (quantum number S), its component along the internuclear axis S_z

(quantum number M_S), and the axial component of the total electronic orbital angular momentum L_z (quantum number Λ). These eigenfunctions are $(2 - \delta_{\Lambda 0})(2S + 1)$ -fold degenerate; namely eigenstates with common $|\Lambda|$ ($2 - \delta_{\Lambda 0}$ possibilities) and S ($2S + 1$ possibilities) have the same energy. Thus the electronic Schrödinger equation to be solved can be written

$$H \Psi^{\Lambda M_S}(R, \hat{r}, \hat{\sigma}) = E^{\Lambda|S}(R) \Psi^{\Lambda M_S}(R, \hat{r}, \hat{\sigma}) \quad (2)$$

where $\Psi^{\Lambda M_S}(R, \hat{r}, \hat{\sigma})$ is the electronic wavefunction, $E^{\Lambda|S}(R)$ is the total electronic energy including nuclear-nuclear repulsion, as a function of R . The variable $\hat{\sigma}$ is the collection of all electronic spin coordinates. In Eq. (2), the electronic wavefunction is given as a function of $\hat{\sigma}$, in addition to R and \hat{r} , because the spin coordinates affect the electronic spatial distribution and give rise to different electronic states for the same electronic configuration (see Table 1).

The method of configuration interaction (CI) is used here to obtain approximate solutions to Eq. (2). That is, the electronic wavefunction is approximated by an expansion in an orthonormal set of configuration state functions (CSF),

$$\Psi^{\Lambda M_S}(R, \hat{r}, \hat{\sigma}) = \sum_I C_I^{\Lambda M_S}(R) \Phi_I^{\Lambda M_S}(R, \hat{r}, \hat{\sigma}), \quad (3)$$

where the coefficients $C_I^{\Lambda M_S}(R)$ are determined using the variational principle. Each CSF, $\Phi_I^{\Lambda M_S}$, given as a specific linear combination of Slater determinants, is by definition an eigenfunction of L_z , S^2 and S_z .

with the corresponding quantum numbers λ , S and M_S given in superscripts. A Slater determinant is a normalized and antisymmetrized product of one-electron functions called spin orbitals (SO). The SOs are symmetry constrained in the sense that each SO is an eigenfunction of the axial component of the electronic orbital angular momentum l_z (quantum number λ), the electronic spin angular momentum s^2 (quantum number $s = 1/2$), and the axial component of the electronic spin angular momentum s_z (quantum number $m_s = \pm 1/2$). The i -th SO with quantum numbers λ and m_s is denoted $\psi_{i\lambda m_s}(x_j, q_j)$, where x_j and q_j are the spatial and spin coordinates of the j -th electron, respectively. It is constructed as a product of a spatial function and a spin function. The spatial function is again a product of two functions; one that does not depend on the azimuthal angle φ_j about the internuclear axis, and one that depends only on φ_j . Thus,

$$\begin{aligned}\psi_{i\lambda m_s}(x_j, q_j) &= \phi_{i\lambda}(x_j) s_{m_s}(q_j) \\ &= n_{i|\lambda|}(\rho_j, z_j) e^{i\lambda\varphi_j} \zeta_{m_s}(q_j)\end{aligned}\quad (4)$$

where ρ_j , z_j and φ_j are the cylindrical coordinates of the j -th electron. The functions $\phi_{i\lambda}(x_j)$ are called molecular orbitals (MO). The MOs are equivalence-constrained; i.e., they are independent of m_s and MOs with common i and $|\lambda|$ differ only in their φ_j dependence. The MOs form an orthonormal set; namely

$$\phi_{i\lambda}(x_j) \phi_{i'\lambda'}(x_j) dx_j = \delta_{ii'} \delta_{\lambda\lambda'} \quad (5)$$

These orthogonal MOs are expanded in terms of a basic set of elementary functions $\{\chi_{\lambda p}\}$.

$$\phi_{i\lambda}(r_j) = \sum_p C_{i|\lambda|p} \chi_{\lambda p}(r_j) \quad (6)$$

The elementary functions $\{\chi_{\lambda p}\}$ used here are Slater-type functions (STF) centered on the nuclei of the molecule.

From the preceding description, it is seen that our calculation begins with the choice of an elementary basis set. This choice is of great importance since the elementary basis set determines the space spanned by the orbitals, the CSFs and ultimately the accuracy of any molecular calculation. A complete linear transformation on the elementary functions, Eq. (6), leads to a set of MOs of the same dimension, spanning the same space as the starting elementary functions. If it is feasible to include in the CI expansion, Eq. (3), a complete set of CSFs derivable from the full MO set, "complete CI", then the same result would be obtained independent of the transformation coefficients $C_{i|\lambda|p}$. This is however beyond current computing capabilities, for any system involving more than four electrons and MOs must be near optimally chosen in order to achieve the best possible result with a severely truncated CI expansion. In the following we discuss in detail the choice of the elementary basis set, the construction of the MO set and the selection of CSFs to be included in the CI expansion in our study of the Cl radical.

The basis set of elementary functions used here consists of six s, four p, two d and two f type STFs on carbon, and four s, three p and two d type STFs on hydrogen. The s and p type functions on carbon

were taken from Clementi's SCF calculation¹⁷ for the $3P$ state of carbon. They differ little from the functions obtained by Clementi for the $1D$ state. The polarization functions on carbon, $3d$, $4d$, $4f$ and $5f$, were selected¹⁸ such that they are localized mainly in the L shell of carbon. The STF functions on hydrogen were taken from Liu's CI calculation for the potential curve of H_2 and the potential surface of H_3 .¹⁹ Details of the CH basis set are given in Table II.

The basis set described above yields SCF energies comparable to those obtained by Cade and Huo¹¹ with a much more compact, but carefully optimized basis set. The choice of a large basis set for the current calculation was motivated by the desirability of describing all the electronic states under consideration with a common basis set, the need of additional one-particle functions describing correlating orbitals, and the desire to avoid extensive exponent optimization. Selective changes of the s and p STF exponents lead to improvements of the SCF energies by less than 0.0001 hartree. SCF energies were virtually unaffected by changes in the exponents of d functions on carbon. Since the basis set was to be used in a CI calculation, some test CI calculations were carried out with changed exponents for the d functions on carbon. In all cases tested, the maximum energy improvement was again only of the order 0.0001 hartree; an indication that the selected basis set is reasonable.

Comparing the current basis set with that used by Lie et al.¹⁰ we see that, besides a slight increase in the number of basis functions, all functions with large exponents ($\zeta = 10.0, 14.0$) in the latter have been replaced by more diffuse d and f functions. This was done because functions with large exponents represent very contracted orbitals, which

are not likely to contribute heavily in molecule formation. Examination of the SCF 1π orbitals of Lie et al. shows that the π basis set used by them was not adequate (large orbital expansion coefficients with opposite signs). This inadequacy is absent from the current basis set.

The SCF energies obtained from the basis set given in Table II range from 0.0004 to 0.0009 hartree better than those obtained by Cade and Huo¹¹ for the $X^2\Pi$ state and Lie et al.¹⁰ for the $a^4\Sigma^-$, $A^2\Delta$ and $B^2\Sigma^-$ states.

In the HF approximation the electronic wavefunction is represented by a single CSF. The HF CSFs for the five lowest electronic states are

$$\begin{aligned}
 X^2\Pi : & \quad 1\sigma^2 2\sigma^2 3\sigma^2 1\pi, \\
 a^4\Sigma^- : & \quad 1\sigma^2 2\sigma^2 3\sigma(1\pi^2, {}^3\Sigma^-), \\
 A^2\Delta : & \quad 1\sigma^2 2\sigma^2 3\sigma(1\pi^2, {}^1\Delta), \\
 B^2\Sigma^- : & \quad 1\sigma^2 2\sigma^2 3\sigma(1\pi^2, {}^3\Sigma^-), \\
 C^2\Sigma^+ : & \quad 1\sigma^2 2\sigma^2 3\sigma(1\pi^2, {}^1\Sigma^+).
 \end{aligned} \tag{7}$$

The occupied MOs in these CSFs, or in our case the expansion coefficients $C_{i\lambda p}$, are determined using the SCF technique. The HF model for molecules has two basic deficiencies. First, the HF wavefunction often does not dissociate formally to the correct separated-atom wavefunctions. This is the case for two of the five states in (7). For the $X^2\Pi$ state of CH, the HF CSF corresponds, at $R = \infty$, to a mixture of neutral carbon and hydrogen atoms in ground and excited states, and also (C^+, H^-) and (C^-, H^+) ion pairs. For the $C^2\Sigma^+$ state of CH the HF CSF dissociates to the ground state of hydrogen atom and a mixture of the 1D and 1S states of carbon. In these cases, HF results for large R are expected to be in considerable

error. This difficulty may be overcome by a multiconfiguration self-consistent-field (MCSCF) calculation,²⁰ including the CSFs necessary to give a correct description of the separated atom limit. These CSFs are,

$$\begin{aligned}
 X^2\Pi: & \quad 1\sigma^2 2\sigma^2 3\sigma^2 1\pi \\
 & \quad 1\sigma^2 2\sigma^2 4\sigma^2 1\pi \\
 & \quad 1\sigma^2 2\sigma^2 (3\sigma 4\sigma, {}^1\Sigma^+) 1\pi \\
 & \quad 1\sigma^2 2\sigma^2 (3\sigma 4\sigma, {}^3\Sigma^+) 1\pi \\
 C^2\Sigma^+: & \quad 1\sigma^2 2\sigma^2 3\sigma (1\pi^2, {}^1\Sigma^+) \\
 & \quad 1\sigma^2 2\sigma^2 3\sigma 4\sigma^2 .
 \end{aligned} \tag{8}$$

Here the occupied MOs are determined by the MCSCF technique.

The second deficiency of the HF model is that it does not include electron correlation effects, which play an important role in the electronic structure of molecules. Neglect of electron correlation often leads to erroneous dissociation energies and term energies. For example, in the HF model of CH, the $B^2\Sigma^-$ state is unstable relative to the separated ground state atoms, and the $a^4\Sigma^-$ state lies below the $X^2\Pi$ state. In this study, electron correlation effects are introduced through CI. The CSFs included in the CI expansion are selected on the basis of their relation to a MCSCF (or SCF) wavefunction which dissociates properly to the separated atom limit. This is different from the customary approach to CI of beginning with a SCF wavefunction.

An examination of (8) shows that a proper description of the $X^2\Pi$ and $C^2\Sigma^+$ states, at large R , requires a 4σ orbital which is not occupied in the HF CSFs. This is simply because a proper description of the separated

atoms requires four σ and one π -type orbital: $(1s\sigma, H)$, $(1s\sigma, C)$, $(2s\sigma, C)$, $(2p\sigma, C)$ and $(2p\pi, C)$. To determine the MOs that correlate with these separated atom orbitals, MCSCF calculations were carried out for the following CSFs:

$$\begin{array}{lll}
 X^2\Pi & 1\sigma^2 2\sigma^2 3\sigma^2 1\pi & 1\sigma^2 3\sigma^2 1\pi^3 \\
 & 1\sigma^2 2\sigma^2 4\sigma^2 1\pi & 1\sigma^2 4\sigma^2 1\pi^3 \\
 & 1\sigma^2 2\sigma^2 (3\sigma 4\sigma, {}^1\Sigma^+) 1\pi & 1\sigma^2 (3\sigma 4\sigma, {}^1\Sigma^+) 1\pi^3 \\
 & 1\sigma^2 2\sigma^2 (3\sigma 4\sigma, {}^2\Sigma^+) 1\pi & 1\sigma^2 (3\sigma 4\sigma, {}^3\Sigma^+) 1\pi^3 \\
 a^4\Sigma^- & 1\sigma^2 2\sigma^2 3\sigma (1\pi^2, {}^3\Sigma^-) & 1\sigma^2 4\sigma^2 3\sigma (1\pi^2, {}^2\Sigma^-) \\
 A^2\Delta & 1\sigma^2 2\sigma^2 3\sigma (1\pi^2, {}^2\Delta) & 1\sigma^2 3\sigma 4\sigma^2 (1\pi^2, {}^1\Delta) \\
 B^2\Sigma^- & 1\sigma^2 2\sigma^2 3\sigma (1\pi^2, {}^3\Sigma^-) & 1\sigma^2 3\sigma 4\sigma^2 (1\pi^2, {}^3\Sigma^-) \\
 C^2\Sigma^+ & 1\sigma^2 2\sigma^2 3\sigma (1\pi^2, {}^1\Sigma^+) & 1\sigma^2 3\sigma 1\pi^4 \\
 & 1\sigma^2 2\sigma^2 3\sigma 4\sigma^2 & 1\sigma^2 4\sigma^2 3\sigma (1\pi^2, {}^1\Sigma^+)
 \end{array} \tag{9}$$

In (9), all the CSFs on the left are those needed to dissociate to the $1s^2 2s^2 2p^2$ configuration of carbon and the ground state of hydrogen. The addition of the CSFs on the right permits a two configuration description of carbon atom, $C_1 1s^2 2s^2 2p^2 + C_2 1s^2 2p^4$, at the separated atom limit.

In what follows the 2σ , 3σ , 4σ , and 1π orbitals, correlating with the $2s$ and $2p$ orbitals of carbon, and the $1s$ orbital of hydrogen will be referred to as valence orbitals. Reference will also be made to a set of external orbitals which, together with the MCSCF occupied valence orbitals,

span a subspace of the STF basis, important to an accurate description of the electronic motions.

In constructing CSFs for Eq. (3) we always keep the 1σ orbital doubly occupied. This means, no correlation effects connected with the 1σ electrons are considered. This restriction reduces significantly the number of CSFs in the final CI expansion, and is justified on the basis that correlation effects connected with the $1s$ electrons of carbon are not expected to change significantly in molecule formation. Four types of CSFs are considered in our CI calculations.

- (a) All CSFs necessary to give a HF description of the appropriate separated atom limit. These CSFs are given for the $X^2\Pi$ and $C^2\Sigma^+$ states in Eq. (8) and for the $a^4\Sigma^-$, $A^2\Delta$, and $B^2\Sigma^-$ states in Eq. (7).
- (b) All CSFs arising from distributing five electrons among the valence orbitals, that are not already included in (a).
- (c) All CSFs arising from distributing four electrons in valence orbitals and one electron in external orbitals.
- (d) All CSFs arising from distributing three electrons in valence orbitals and two electrons in external orbitals, which satisfy the condition that all CSFs of this type, and any linear combination of them, must have a non-vanishing Hamiltonian matrix element with at least one of the CSFs in (a).

A practical algorithm for constructing CSFs described in (d) has recently been developed by McLean and Liu.²¹

The additional condition placed on the type (d) CSFs, which leads to a significant reduction in the dimension of the CI problem, is justified

on the basis of Rayleigh Schrödinger perturbation theory. Consider the CI wavefunction, determined in the space spanned by the CSFs of (a), as a zeroth order approximation to the complete CI wavefunction. Then all CSFs that have vanishing Hamiltonian matrix elements with all the CSFs in (a) will make no contribution to the first order perturbative correction to the zeroth order wavefunction. These CSFs can be expected to make small contribution to the complete CI wavefunction and therefore be omitted, provided that the zeroth order wavefunction is a reasonable one. This is why the MCSCF wavefunctions, which permit proper dissociation, were chosen as the starting point for our CI calculation instead of the usual SCF wavefunctions.

From the four types of CSFs described above, three distinct CI wavefunctions are constructed. A CI in the space spanned by all the CSFs of type (a) and (b) is called a "valence CI". A CI including all CSFs of type (a), (b) and (c) is a "first order CI", following Schaefer, Klemm and Harris.²² The best wavefunctions obtained in this study, including all CSFs of the four types described above are referred to as "extended CI" functions. The "valence CI" function, constructed solely from the core and valence orbitals is clearly independent of the external orbitals. The CSFs of type (c) span a vector space invariant to an arbitrary unitary transformation among the external orbitals. The same is true for the CSFs of type (d). Thus all three types of CI functions described here are invariant to any unitary transformation among the external orbitals.

Clearly the numbers of CSFs of type (c) and (d) depends on the number of external orbitals. It is therefore desirable to compact the external

orbital set, such that the most useful part of the space spanned by the STF basis is packed into a small number of external orbitals. This permits a truncation of the external orbital set, which significantly reduces the number of CSFs of type (c) and (d) with little loss of accuracy.

The method of natural orbital (NO) transformation provides a useful approach to such a compact set of orbitals. The properties and uses of NOs have recently been reviewed by Davidson.²³ It suffices here to say that the NOs of a wavefunction are eigenfunctions of the first order reduced density matrix.²³ The eigenvalues associated with the NOs are the occupation numbers; their magnitudes to some extent reflect the importance of the associated NOs.

In what follows we shall always assume that NOs are ordered by symmetry and decreasing occupation numbers. Thus the occupation number of the i -th σ NO is greater than or equal to that of the j -th σ NO, provided that $i < j$. Also if a set of NOs is to be truncated, the NOs retained in each symmetry must always have larger occupation numbers than those omitted.

NOs extracted from four different wavefunctions were examined:

(i) the "extended CI" wavefunction, (ii) a wavefunction consisting of the same CSFs as the "extended CI", but determined by diagonalizing a Hamiltonian matrix in which all off-diagonal elements involving only type (c) and (d) CSFs were approximated by zero,²⁴ (iii) a wavefunction determined in the same manner as in (2), except that only off-diagonal matrix elements between type (d) CSFs are omitted, and (iv) the "first order CI". The CSFs in these wavefunctions were constructed from the full set of occupied and

virtual orbitals (nineteen σ , twelve π , six δ and two φ type virtual orbitals) obtained from the MCSCF calculation described earlier. The NOs extracted from these wavefunctions are referred to as NO_i , NO_{ii} , NO_{iii} , and NO_{iv} , respectively. Each of these NO sets were used with various degrees of truncation as orbital basis in a series of "extended CI" calculations. Results of some of these calculations for the $a^4\Sigma^-$ state are given in Tables III and IV. The first column of each table gives the number of leading NOs of each symmetry used in the "extended CI" calculation. The second column gives the "extended CI" energies using truncated sets of NO_i . The third column gives the difference between successive entries in the second column; namely the energy improvements resulting from the addition of a new group of NOs. The fourth and fifth columns gives results of parallel calculations using NO_{ii} . The fact that NO_i is a compact set of orbitals is evident. The last ten σ and three π orbitals contribute only ~ 0.0004 a.u. (~ 0.011 eV) to the "extended CI" energy. However, there is no real computational advantage in using NO_i , since their determination requires an "extended CI" calculation using the full set of virtual orbitals. In calculations using NO_{ii} the energy improvements do not drop off as rapidly as in calculations using NO_i . Still, the last ten σ and three π type orbitals only contribute ~ 0.0011 hartree (~ 0.03 eV) to the "extended CI" energy. More importantly, NO_{ii} are considerably easier to determine, compared to NO_i . In the "extended CI" wavefunction, using the full set of virtual orbitals, over 99% of the CSFs are of type (c) and (d). Thus to determine wavefunction (ii) it is only necessary to compute $\sim 4\%$ of the Hamiltonian matrix elements required to determine

wavefunction (i). The results of calculations using NO_{iii} and NO_{iv} are not given. It is sufficient to note that NO_{iii} , while somewhat more costly to determine than NO_{ii} , is not significantly more compact than NO_{ii} . Also, NO_{iv} , though somewhat more easily determined than NO_{ii} , is not as compact as NO_{ii} . Calculations parallel to those described above were also carried out for the $A^2\Delta$ state. The four sets of NOs examined in these calculations show essentially the same behavior as in the $a^4\Sigma^-$ case. Thus, NO_{ii} truncated to thirteen σ , ten π , six δ and two φ leading orbitals were used to construct CSFs for subsequent CI calculations. The number of CSFs in each of the three CI wavefunctions, using the truncated NO_{ii} basis, is given in Table V. The "extended CI" wavefunctions consist of 4147, 1225, 1549, 1498 and 2184 CSFs for the $X^2\Pi$, $a^4\Sigma^-$, $A^2\Delta$, $B^2\Sigma^-$ and $C^2\Sigma^+$ states, respectively. These numbers are to be compared with 9234, 2598, 2988, 3066 and 5009, respectively, which would have resulted from the full orbital set.

The NO transformation described above changes all of the MCSCF valence and virtual orbitals. For four of the five states studied here, the four leading σ and one leading π NOs are essentially unchanged from the MCSCF orbitals. That is, if the NOs are denoted by $1\sigma'$, $2\sigma'$, ..., $1\pi'$, ..., in order of decreasing occupation numbers, then we have for these four states $1\sigma \equiv 1\sigma'$, $2\sigma \approx 2\sigma'$, $3\sigma \approx 3\sigma'$, $4\sigma \approx 4\sigma'$, and $1\pi \approx 1\pi'$, where the unprimed orbitals are the MCSCF orbitals. Consequently, the space spanned by the type (a) CSFs remains essentially the same whether the CSFs are constructed from MCSCF orbitals or leading NOs. However, this is not the case for the $C^2\Sigma^+$ state. The MCSCF wavefunction for this state, which permits proper dissociation to separated HF atoms is

$$C_1 1\sigma^2 2\sigma^2 3\sigma(1\pi^2, 1\Sigma^+) + C_2 1\sigma^2 2\sigma^2 3\sigma 4\sigma^2 \quad (10)$$

where the 3σ orbital correlates with the hydrogen $1s$ orbital and the 4σ orbital with the carbon $2p\sigma$ orbital. It is easily shown that the MCSCF orbitals are also the NOs of this wavefunction, and that the occupation numbers associated with the 1σ , 2σ , 3σ and 4σ orbitals are 2, 2, 1, and $2C_2^2$, respectively. Since C_2^2 increases from 0.0001 near the equilibrium nuclear separation to $2/3$ at $R = \infty$, the ordering of the NOs is a function of R . Let the primed and unprimed orbitals again denote the NOs and MCSCF orbitals, respectively. Then, $1\sigma \equiv 1\sigma'$, $2\sigma \equiv 2\sigma'$, $1\pi \equiv 1\pi'$, $3\sigma \equiv 3\sigma'$, and $4\sigma \equiv 4\sigma'$ for small R where $C_2^2 < 1/2$. However, we have $3\sigma \equiv 4\sigma'$, and $4\sigma \equiv 3\sigma'$ for large R where $C_2^2 > 1/2$. This means, at large R the wavefunction

$$C_1' 1\sigma'^2 2\sigma'^2 3\sigma' 1\pi'^2 + C_2' 1\sigma'^2 2\sigma'^2 3\sigma' 4\sigma'^2 \quad (11)$$

is drastically different from the MCSCF wavefunction in Eq. (10) and no longer a good approximation to the true wavefunction. This invalidates the selection of type (d) CSFs, which is based on perturbation theory using the wavefunction in Eq. (10) as a zeroth order approximation. To overcome this difficulty the first four σ NOs of the $C^2\Sigma^+$ state were replaced by the MCSCF orbitals. The resulting orbital set, after Schmidt orthogonalization, was then used as the orbital basis for subsequent CI calculations.

In summary, the calculations carried out for the five lowest electronic states of CH consisted of four steps. (1) SCF calculation. (2) MCSCF calculation using the CSFs given in Eq. (9). (3) Determination of an

approximate "extended CI" wavefunction using CSFs constructed from the full set of MCSCF occupied and virtual orbitals determined in step (2). The expansion coefficients are determined by diagonalizing a Hamiltonian matrix where all off-diagonal elements involving only type (c) and type (d) CSFs are approximated by zero. The NOs extracted from this wavefunction, ordered by symmetry and decreasing occupation numbers, are then truncated to thirteen σ , ten π , six δ and two φ type orbitals. (4) Three CI calculations: (a) "extended CI", (b) "first order CI", and (c) "valence CI" within the truncated orbital set obtained in (3).

III. RESULTS AND DISCUSSIONS

The calculated SCF, "valence CI", "first order CI", and "extended CI" energies for the five lowest electronic states of CH are given in Tables VI-X. The SCF potential curves are shown in Fig. 1 and the "extended CI" curves in Fig. 2. The "valence CI" and "first order CI" curves are qualitatively similar to the "extended CI" curves, except that the $B^2\Sigma^-$ curves lies entirely above the separated atom limits. Thus, of the four computational models examined here, only "extended CI" gives a bound $B^2\Sigma^-$ state.

Five points around the computed energy minimum of each curve were fitted to a fourth degree polynomial, and the resulting analytical curve was used to determine the potential minimum and equilibrium internuclear distance, R_e . The results, together with known experimental values, are given in Table XI. The R_e 's calculated from the "extended CI" curves are in excellent agreement with known experimental values. For three of the five states studied the agreements are better than 0.01 bohr. The one

exception is the $B^2\Sigma^-$ state where the calculated value is 2.216 bohr as compared to the experimental value of 2.200 bohr. This discrepancy can be attributed to the fact that the experimental R_e is determined from the spectroscopic constant B_e using the relation $B_e = (2\mu R_e^2)^{-1/2}$. Using this relation and a theoretical value of B_e derived from the "extended CI" curve, we obtained a R_e value of 2.190 bohr for the $B^2\Sigma^-$ state. This leads us to believe the calculated value of 2.216 bohr is within 0.01 bohr of the true potential minimum. Details of the above analysis will be given in paper II. The R_e for the $a^4\Sigma^-$ state is not known experimentally; the "extended CI" result of 2.053 bohr is believed to be within 0.01 bohr of the true equilibrium nuclear distance.

The SCF R_e values are all too small compared with experiment; whereas the "valence CI" and "first order CI" results are all too large. The "valence CI" results are better than the "first order CI" results for all five electronic states studied. The R_e values obtained from the semi-empirical calculations of Liu and Verhaegen¹³ fell considerably short of the accuracy achieved by the "extended CI" calculations. Their R_e value of 2.124 bohr for the $B^2\Sigma^-$ state, is even smaller than the SCF result of 2.151 bohr.

All three CI models employed in this study have been designed to give the correct separated atom limits. However asymptotic wavefunctions, in the limit of $R = \infty$, obtained from these CI calculations are different from results of equivalent atomic calculations done in spherical symmetry. This difference is the result of relaxing atomic equivalence and symmetry constraints. In the molecular calculation the orbitals and the CSFs are constrained to belong to irreducible representation of the point group

$C_{\infty v}$, instead of the three dimensional rotation group as in the atomic case. Three constraints are relaxed in a $C_{\infty v}$ calculation. (i) Orbital equivalence constraint; degenerate atomic orbitals like $2p_x$ and $2p_y$ of carbon are not constrained to have the same radial dependence. (ii) Orbital symmetry constraint; the molecular orbitals are not constrained to be eigenfunctions of the L^2 operator. Thus the MOs corresponding to atomic s orbitals may have d components and those corresponding to atomic p orbitals may have f components. (iii) CSF symmetry constraint; the CSFs in the molecular calculation are constrained to be eigenfunctions of L_z , but not L^2 as in the spherically symmetric calculations. Thus, the CI wavefunction obtained is constrained to have the proper M_L quantum number, but may not be an eigenfunction of L^2 . The effects of relaxing these equivalence and symmetry constraints, in limited CI calculations, are lowered total energies and some apparent discrepancies in the asymptotic behavior of calculated potential curves. These effects are examined in some detail in what follows. It is appropriate here to insert the reminder that the difference between a $C_{\infty v}$ atom and a spherically symmetric one is an artifact of the method employed in the wavefunction calculation, which has no real physical significance. In the limit of a complete CI calculation, including a complete set of n-particle functions derivable from a given one-particle basis, the same result is obtained regardless of the equivalence and symmetry constraints imposed.

To begin with we examine the asymptotic results of MCSCF calculations using the CSFs given in (9). These results are of interest because the MCSCF occupied orbitals play an important role in subsequent CI calculations.

At $R = \infty$, the CSFs in Eq. (9) go over to the following carbon atom CSFs:

$$\begin{aligned}
 X^2\Pi(^3P, M_L = 1): & \sigma_{1s}^2 \sigma_{2s}^2 \sigma_{2p} \pi_{2p} + \sigma_{1s}^2 \sigma_{2p}^3 \pi_{2p} \\
 a^4\Sigma^-(^3P, M_L = 0): & \sigma_{1s}^2 \sigma_{2s}^2 \pi_{2p}^2 + \sigma_{1s}^2 \sigma_{2p}^2 \pi_{2p}^2 \\
 B^2\Sigma^-(^3P, M_L = 0): & \sigma_{1s}^2 \sigma_{2s}^2 \pi_{2p}^2 + \sigma_{1s}^2 \sigma_{2p}^2 \pi_{2p}^2 \\
 \Lambda^1\Delta(^1D, M_L = 2): & \sigma_{1s}^2 \sigma_{2s}^2 \pi_{2p}^2 + \sigma_{1s}^2 \sigma_{2p}^2 \pi_{2p}^2 \\
 C^2\Sigma^+(^1D, M_L = 0): & \sigma_{1s}^2 \sigma_{2s}^2 \sigma_{2p}^2 + \sigma_{1s}^2 \sigma_{2p}^2 \pi_{2p}^2 \\
 & \sigma_{1s}^2 \sigma_{2s}^2 \pi_{2p}^2 + \sigma_{1s}^2 \pi_{2p}^4
 \end{aligned} \tag{12}$$

In Eq. (12), the corresponding separated carbon atom states are given in parentheses following the term symbol for the CH states. The orbitals in the CSFs are identified by the irreducible representation of the $C_{\infty v}$ group to which they belong, with the corresponding carbon atomic orbital given as subscripts. The part of the CH wavefunctions that goes over to the hydrogen 1s orbital, common to all CSFs in (12), is omitted. The $X^2\Pi$, $a^4\Sigma^-$ and $B^2\Sigma^-$ states of CH all dissociate into the 3P ground state of carbon. The MCSCF energies for all three states are somewhat lower than that of the corresponding two-configuration numerical MCSCF calculation for carbon reported by Bagus and Moser.²⁵ This is because in the $C_{\infty v}$ carbon atom, the σ_{1s} orbitals are permitted to have a d σ component and the σ_{2p} and π_{2p} orbitals are

permitted to have f_σ or f_π components, and also the σ_{2p} and π_{2p} orbitals are permitted to have different radial dependence. This added freedom in the wavefunction leads to a lowered total energy. The MCSCF energy of carbon from the $a^4\Sigma^-$ and $B^2\Sigma^-$ calculations are lower than the corresponding results from the $X^2\Pi$ calculations by 0.0017 hartree. An examination of Eq. (12) shows that the σ_{2p} orbitals are not occupied in the HF CSFs for the $a^4\Sigma^-$ and $B^2\Sigma^-$ states, and can be freely optimized without jeopardizing the HF CSF of $\sigma_{1s}^2\sigma_{2s}^2\pi_{2p}^2$. This is, however, not the case for the $^2\Pi$ state, where any energy lowering due to the departure of the σ_{2p} or π_{2p} orbitals from the HF results must be balanced by an increase in the energy of the HF CSF, $\sigma_{1s}^2\sigma_{2s}^2\sigma_{2p}\pi_{2p}$. The σ_{2p} and π_{2p} MCSCF orbitals are given in Table XII. It is seen that the σ_{2p} and π_{2p} orbitals are quite similar for the $X^2\Pi$ state but drastically different in the $a^4\Sigma^-$ and $B^2\Sigma^-$ states, supporting the above argument. The $\Lambda^2\Delta$ and $C^2\Sigma^+$ states of CH dissociate into the 1D state of carbon. The MCSCF energies of carbon obtained from the MCSCF calculations on these states in $C_{\infty v}$ symmetry are again lower than the numerical MCSCF results of Bagus and Moser.²⁵ Following the argument in the 3P case, we would expect the energy of the carbon atom obtained from the $\Lambda^2\Delta$ calculation to be somewhat lower than that from the $C^2\Sigma^+$ calculation. The σ_{2p} and π_{2p} MCSCF orbitals for these two states are also given in Table XII. The two orbitals in $\Lambda^2\Delta$ state are again quite different as in the $B^2\Sigma^-$ and $a^4\Sigma^-$ states, while the two orbitals of the $^2\Sigma^+$ are similar as in the $X^2\Pi$ case. However the MCSCF energy of carbon obtained from the $^2\Sigma^+$ calculation is 0.0013 hartree lower than that from the $^2\Delta$ calculation, in apparent contradiction to our earlier argument. To resolve this apparent contradiction we again examine the CSFs in (12).

To describe a HF atom in the $^1D(1s^2 2s^2 2p^2)$ state two CSFs are required,

$$C_1 \sigma_{1s}^2 \sigma_{2s}^2 \sigma_{2p}^2 + C_2 \sigma_{1s}^2 \sigma_{2s}^2 \pi_{2p}^2 \quad (13)$$

In a calculation carried out under spherical symmetry the ratio C_1/C_2 is fixed at $-2^{1/2}$ to insure a 1D wavefunction. However, under $C_{\infty v}$ symmetry, this ratio can be varied freely to achieve the lowest possible energy, as it is only necessary to insure the correct M_L quantum number. The same situation exists for the two CSFs describing the $1s^2 2p^4$ configuration of carbon. It is this new degree of freedom, in addition to the relaxation of orbital symmetry and equivalence restrictions, that results in a lower MCSCF energy for the $C^2\Sigma^+$ state, compared to the $A^2\Delta$ state. The actual ratio between the two pairs of coefficients discussed above are -1.527 and -1.199 , respectively. Further evidence for the above argument is found in the fact that the $C^2\Sigma^+$ result is 0.0040 hartree lower than the corresponding numerical MCSCF results of Bagus and Moser,²⁵ considerably larger than the lowering obtained in the $A^2\Delta$ (0.0027 hartree), $a^4\Sigma^-$ and $B^2\Sigma^-$ (0.0018 hartree), and $X^2\Pi$ (0.0001 hartree) states. The "valence CI" results, at large R , are essentially identical to the MCSCF results, and thus no further discussion is necessary.

The "first order CI" calculations reduced the discrepancies of the 3P and 1D asymptotes from 0.0017 hartree and 0.0013 , respectively, to 0.0006 hartree. The same discrepancy remained in the "extended CI" results. It seems reasonable to assume that more extended CI calculations, involving CSFs with three or more valence electrons occupying virtual orbitals, will not further reduce the remaining discrepancy. We, therefore, attribute

the discrepancy of 0.0006 hartree to the mixing of $d\sigma$ components in the 1σ orbital corresponding to the carbon $1s$ orbital. To eliminate this discrepancy, it is necessary to carry out CI calculations including core-valence and core-core correlation effects. An alternative method for avoiding this problem is to restrict the 1σ orbital to an expansion in s type STFs alone. This approach is useful for nuclear separations where no significant core polarization takes place. At any rate, a discrepancy of 0.0006 a.u. (~ 0.02 eV) is quite acceptable, considering the accuracy of the calculations reported here.

The correlation energies obtained for the two states of carbon represent approximately 95% of the L shell correlation energy.²⁶

The "extended CI" term splitting between $C(^3P)$ and $C(^1D)$ is 1.31 eV, as compared with the experimental value of 1.26 eV. This is a considerable improvement over the previous result of Lie et al.,¹⁰ where the error is 0.24 eV.

The calculated dissociation energies D_e^0 , obtained from interpolated potential minima and corresponding dissociation limits, are given in Table XI. The "extended CI" dissociation energies are, with known experimental values given in parentheses, 3.51 eV (3.63) for $X^2\Pi$, 2.84 eV for $a^4\Sigma^-$, 1.90 eV (2.01) for $A^2\Delta$, 0.23 eV (~ 0.40) for $B^2\Sigma^-$, and 0.78 eV (0.94) for $C^2\Sigma^+$. These results are in error by 0.12 eV and 0.11 eV for the $X^2\Pi$ and $A^2\Delta$ states, respectively, and by 0.17 eV and 0.16 eV, respectively for the weakly bound states $B^2\Sigma^-$ and $C^2\Sigma^+$. A significant part of these errors can be attributed to the neglect of correlation effects between the 1σ shell and the valence electrons; in particular,

the correlation between the 1σ electrons and the 3σ electron (or one of the 3σ electrons in the $X^2\Pi$ state) which does not exist when the two atoms are far apart. Bender and Davidson²⁷ obtained -0.0050 hartree for the 1σ - 3σ intershell correlation energy in the $X^2\Pi$ state. If we take half of their value as the extra molecular correlation energy and add it to our computed dissociation energy for the $X^2\Pi$ state, then the D_e^0 for the ground state becomes 3.57 eV, which is only 0.06 eV too low compared with the experimental value. The second source of error in the computed dissociation energies is the incomplete correlations of the valence shell. As has been pointed out earlier, the truncation of the internal orbital set accounts for an error of 0.03 eV in the calculated dissociation energies. The remaining error is attributed to the incomplete STF basis and the neglect of CSFs with two or more valence electrons occupying external orbitals, which only contribute to the wavefunction through second and higher order perturbation theory.

The MO energy for the 1σ orbital in the HF calculation is essentially identical with the energy of the carbon $1s$ orbital and is nearly independent of the internuclear distances. Therefore the intra-shell correlation energy of the 1σ shell should be nearly constant for all internuclear distances and its neglect should introduce only a small error into the computed dissociation energies.

The correlation energies recovered, in the "extended CI" calculations for the $X^2\Pi$, $A^2\Delta$, $B^2\Sigma^-$ and $C^2\Sigma^+$ states, represent only about 60% of the total correlation energies. The low percentages are due to the neglect of all correlation effects involving the 1σ electrons. The valence shell correlation energies recovered in these calculations are believed to be over 90%.

The dissociation energy of the $a^4\Sigma^-$ state is certain to be larger than the calculated value of 2.84 eV. Assuming a core-valence correlation correction of 0.06 eV, as was estimated for the $X^2\Pi$ case, and an orbital truncation error of 0.03 eV we arrive at an estimated lower bound of 2.93 eV for the D_e^0 of the $a^4\Sigma^-$ state. If we further assume that the error in the calculated dissociation energy of $a^4\Sigma^-$ is no more than that of the other four states, then we have $D_e^0(a^4\Sigma^-) \leq 3.01$ eV. Thus we estimate $D_e^0(a^4\Sigma^-) = 2.94 \pm 0.07$ eV. This estimate, combined with the experimental value for $D_e^0(X^2\Pi)$, places the $a^4\Sigma^-$ state above the $X^2\Pi$ state by 0.69 ± 0.07 eV. This is in excellent agreement with the previous estimate of 0.63 ± 0.12 eV by Lie et al.,¹⁰ but contradictory to the semi-empirical result of Liu and Verhaegen¹³ which placed the $a^4\Sigma^-$ state above the $X^2\Pi$ state by 0.92 eV. Their $T_e^0(a^4\Sigma^-) = 0.92$ eV leads to $D_e^0(a^4\Sigma^-) = 2.72$ eV which is smaller than the HF value of 2.78 eV. The "extended CI" term splittings between the $X^2\Pi$, $A^2\Delta$, $B^2\Sigma^-$ and $C^2\Sigma^+$ states are all within 0.06 eV of the known experimental values.

Figure 2 shows clearly the existence of potential maxima in the "extended CI" curves for the $B^2\Sigma^-$ and $C^2\Sigma^+$ states. The existence of the maximum in the $B^2\Sigma^-$ curve has been deduced experimentally by Herzberg and Johns⁶ from the breaking-off of the emission lines and the diffuseness of the absorption lines in the spectra of CH and CD. The recognition of this maximum led to a slightly different value of the D_0^0 for the $X^2\Pi$ state from the value accepted prior to 1969. From the limiting curves of dissociation for the $B^2\Sigma^-$ states of CH and CD, Herzberg and Johns estimated the height of the maximum to be greater than (or at least equal to)

500 cm^{-1} , at $R = 2\text{\AA}$. Our calculated results show that this maximum occurs at $R = 3.29$ bohr (1.74\AA), with a height of 0.1592 eV (1284 cm^{-1}). Since the minimum in the calculated potential curve for the $B^2\Sigma^-$ state is too high, relative to the calculated dissociation limit, by 0.17 eV, the calculated barrier height is likely to be too high. Assuming the difference between the calculated and exact curves is given, as a function of R , by $-(R-R_e)^2$, the calculated barrier height is too high by ~ 0.06 eV. A likely value for the barrier height is $\sim 800 \text{ cm}^{-1}$.

Other calculations which showed a maximum in the $B^2\Sigma^-$ states were discussed in the introduction. There are Liu and Verhaegen's semi-empirical calculations¹³ which gave a barrier of height $\sim 900 \text{ cm}^{-1}$, at $\sim 1.6\text{\AA}$, Lie, Hinze and Liu's ab initio CI calculations¹⁰ which gave a barrier of height 1600 cm^{-1} , at 1.73\AA , and optimum valence MCSCF calculations of Julienne and Krauss¹⁴ indicated a barrier of height $\sim 1000 \text{ cm}^{-1}$, around 2\AA .

The potential maximum in the $C^2\Sigma^+$ state had been deduced experimentally also by Herzberg and Johns.⁶ They observed that the $v = 4$ vibrational level of the $C^2\Sigma^+$ state of CD lies slightly above the dissociation limit corresponding to $C(^1D) + D(^2S)$, and concluded that the $C^2\Sigma^+$ state cannot be correlated with the $^2\Sigma^+$ state from $^1D + ^2S$ except by assuming a large potential maximum. This large potential maximum did show up in our calculations. The "extended CI" results give a potential maximum at $R = 3.33$ bohr (1.76\AA) with a height of 0.4003 eV (3228 cm^{-1}). Here, again, the calculated value is probably too high by ~ 0.06 eV, and our estimate of the true barrier height is $\sim 2300 \text{ cm}^{-1}$.

Liu and Verhaegen¹³ also deduced this maximum in their semi-empirical calculations. To explain the existence of this and several other potential

maxima found in their calculations, they asserted "...there being several potential maxima. These result from necessary changes of molecular electronic configuration of some of the states before they dissociate." This argument is incorrect since it implies that any state whose HF configuration does not dissociate correctly into its atomic limits will have a maximum in its potential curve. It is well known that the HF configuration of the ground state of LiH does not dissociate correctly into $\text{Li}(^2\text{S}) + \text{H}(^2\text{S})$ and that there is no maximum in the $\text{X}^1\Sigma^+$ state of LiH .²⁸ In fact, the results of Liu and Verhaegen¹³ did show a potential maximum in the $\text{X}^2\Pi$ curve of CH. No such maximum has been found experimentally or in our calculation.

According to Herzberg and Johns⁶ the maximum in the $\text{B}^2\Sigma^-$ state is of van der Waals origin, similar to that for the $\text{C}^1\Pi$ state of H_2 . This explanation is incorrect for the following reasons: (a) The maximum in the $\text{C}^1\Pi$ state of H_2 is due to the degeneracy at large separations corresponding to the exchange of excitation energies, $1s \leftrightarrow 2p$. In other words, there is a non-vanishing first order dipole-dipole van der Waals interaction at large separations due to the exchange degeneracy. No such degeneracy exists in the case of $\text{C}(^3\text{P})$ and $\text{H}(^2\text{S})$; (b) A van der Waals maximum in the potential curve can arise if, besides (a), there is a non-vanishing first order dipole-dipole, dipole-quadrupole, or quadrupole-quadrupole interaction. Since the ^2S state of hydrogen does not possess dipole or quadrupole moment, there is no first order van der Waals interaction between C and H. Any second order interaction leads only to attraction,²⁹ and cannot be the cause for a maximum in the potential curve.

The repulsive character of the $B^2\Sigma^-$ state, at large R , is more likely to be caused by the exchange effect which splits a Σ^- state into an attractive $4\Sigma^-$ state and a repulsive $2\Sigma^-$ state. Therefore the occurrence of the maximum in the $B^2\Sigma^-$ state must have its origin in an avoided curve crossing between the original repulsive curve and another curve of the same symmetry.

The first candidate for this other $2\Sigma^-$ curve is that arising from the $1s^2 2s 2p^3 \ ^3D$ excited state of carbon and the ground state of hydrogen atom. Since the 3D state lies ~ 8 eV above the ground state of carbon, it is unlikely that the resulting $2\Sigma^-$ curve can reach down far enough to cross the lower repulsive curve. This is also true for all other $2\Sigma^-$ curves arising from neutral carbon and hydrogen atoms, because they have even higher separated atom asymptotes. This is one of the reasons why the potential maximum in the $B^2\Sigma^-$ curve was attributed to a van der Waals origin. A few steps up the separated atom energy ladder we find that $C^-(1s^2 2s^2 2p^3 \ ^2D)$ and H^+ gives rise to a $2\Sigma^-$ curve. This ionic curve has a $1/R$ behavior which, owing to the small size of the H^+ ion, persists down to very small R values. Therefore, in spite of the fact that $C^-(1s^2 2s^2 2p^3 \ ^2D) + H^+$ lies ~ 14 eV above the ground states of C and H, this ionic curve can reach down to cross the repulsive curve of the $B^2\Sigma^-$ state. This crossing occurs near $R = 2.5$ bohr. The shift of the potential maximum to $R = 3.30$ bohr and the low barrier height of $\sim 800 \text{ cm}^{-1}$ are results of a large interaction between the zeroth order curves. We note here, before the ionic $2\Sigma^-$ curve can cross the $B^2\Sigma^-$ curve, it must first cross many $2\Sigma^-$ curves arising from various excited states of carbon and hydrogen atoms,

including that resulting from the $1s^2 2s 2p^3 \ ^3D$ state of carbon discussed earlier. In each case there results an avoided crossing followed by the resumption of an essentially $1/R$ behavior at smaller R values. However, if we use valence-bond curves as zeroth order approximation, it is the ionic curve that is responsible for the maximum in the $B^2\Sigma^-$ curve.

A similar explanation can be found for the occurrence of the potential maximum in the $C^2\Sigma^+$ curve. The second lowest $^2\Sigma^+$ curve arising from $C(^1S)$ and $H(^2S)$ is repulsive according to elementary Heitler-London theory. There are two ionic curves that can reach down and cross the lowest $^2\Sigma^+$ curve: the first one arises from $C^+(1s^2 2s^2 2p^2 \ ^2p) + H^-(^1S)$ which lies ~ 11 eV above the ground state atoms, the second from $C^-(1s^2 2s^2 2p^3 \ ^2p) + H^+$ which lies ~ 15 eV above the ground state atoms. The $^2\Sigma^+$ curve from $C^+ + H^-$, owing to the large size of the H^- ion, deviates from the $1/R$ behavior at a considerably larger R value than the curve from $C^- + H^+$. Indeed, the $C^+ + H^-$ curve appears to turn up and cross the $C^- + H^+$ near $R = 3.5$ bohr as evidenced by the sign change in the dipole moments of the $C^2\Sigma^+$ and $X^2\Pi$ states which will be discussed in paper II. Therefore it is the $^2\Sigma^+$ curve from $C^- + H^+$ which is finally responsible for the avoided crossing and the associated potential maximum in the $C^2\Sigma^+$ curve.

Finally, we compare the three computational models employed in this study. The "extended CI" model is clearly the most reliable of the three. It alone predicts, correctly, a bound $B^2\Sigma^-$ state. It consistently gave equilibrium nuclear separations, dissociation energies, and term energies to within 0.01 bohr, 0.2 eV and 0.06 eV, respectively, of the known experimental values. The "first order CI" and "valence CI" models failed

to give results of comparable accuracy; both models also failed to predict a bound $B^2\Sigma^-$ state. The "valence CI" equilibrium nuclear distances are somewhat closer to the experimental values than those of "first order CI". No definite trend can be found by comparing the dissociation energies and term energies calculated from these two models. It is somewhat surprising that the "first order CI" model does not yield significantly better results than the considerably simpler "valence CI" model.

ACKNOWLEDGMENTS

The authors wish to thank Drs. P. S. Bagus, A. D. McLean, and M. Yoshimine for helpful discussions. George Lie and Juergen Hinze gratefully acknowledge the hospitality extended to them by the IBM Research Laboratory in San Jose.

REFERENCES

1. T. Heurlinger, Diss. Lund. (1918); E. Hulthen, Z. Phys. 11, 284 (1922);
A. Kratzer, Z. Phys. 23, 298 (1924); R. S. Mulliken, Phys. Rev. 30,
785 (1928); Rev. Mod. Phys. 3, 89 (1931); T. Hori, Z. Phys. 59, 91
(1929).
2. T. Shidei, Japanese J. Phys. 11, 23 (1936).
3. L. Gerö, Z. Phys. 117, 709 (1941); *ibid.*, 118, 27 (1941).
4. N. H. Kiess and H. P. Broida, Astrophys. J. 123, 166 (1956).
5. R. G. W. Norrish, G. Porter, and B. A. Thrush, Proc. Roy. Soc. (London)
A216, 165 (1953).
6. G. Herzberg and J. W. C. Johns, Astrophys. J. 158, 399 (1969).
7. D. H. Phelps and F. W. Dalby, Phys. Rev. Letters 16, 3 (1966).
8. R. S. Mulliken, Rev. Mod. Phys. 4, 1 (1932).
9. G. Porter, Discussions Faraday Soc. 10, 108 (1951).
10. G. C. Lie, J. Hinze, and B. Liu, J. Chem. Phys. 57, 625 (1972).
11. P. E. Cade and W. M. Huo, J. Chem. Phys. 47, 614 (1967).
12. J. Higuchi, J. Chem. Phys. 22, 1339 (1953).
13. H. P. D. Liu and G. Verhaegen, J. Chem. Phys. 53, 735 (1970).
14. P. S. Julianne and M. Krauss, to be published.
15. G. Das and A. C. Wahl, J. Chem. Phys. 44, 87 (1966).
16. G. Lie, J. Hinze and B. Liu, in press.
17. E. Clementi, Tables of Atomic Functions, Supplement to Ab Initio
Computations in Atoms and Molecules, IBM Journal of Research and
Development 9, 2 (1965).
18. A. Bunge, Ph.D. Thesis, University of Florida, Gainesville, Fla.
(1968).

19. B. Liu, J. Chem. Phys. in press.
20. J. Hinze and C. C. J. Roothean, Prog. Theoret. Phys. (Kyoto) 40, 37 (1967).
21. A. D. McLean and B. Liu, J. Chem. Phys., in press.
22. H. F. Schaefer, R. A. Klemm, and F. E. Harris, Phys. Rev. 181, 137 (1969).
23. E. R. Davidson, Adv. in Quantum Chem. 6, Academic Press, N.Y. (1972).
24. Z. Garshgorn and I. Shavitt, Intl. J. Quantum Chem. 2, 751 (1968).
25. P. S. Bagus and C. M. Moser, Phys. Rev. 167, 13 (1968).
26. F. Sasaki and M. Yoshimine, Private communication.
27. C. F. Bender and E. R. Davidson, Phys. Rev. 183, 23 (1969).
28. K. Docken and J. Hinze, J. Chem. Phys. 57, 0000 (1972).
29. L. D. Landau and E. M. Lifshitz, Quantum Mechanics (Addison-Wesley, Reading, Mass., 1965), 2nd edition, p. 131.
30. C. E. Moore, "Atomic Energy Levels," N.B.S. Circular 467.

TABLE I
Electronic Configurations of the Five Lowest States
of CH and Their Dissociation Limits

Electronic Configuration	State	Dissociation Limits
$1\sigma^2 2\sigma^2 3\sigma^2 1\pi$	$X^2\Pi$	$C(^3P) + H(^2S)$
$1\sigma^2 2\sigma^2 3\sigma 1\pi^2$	$\left\{ \begin{array}{l} a^4\Sigma^- \\ A^2\Delta \\ B^2\Sigma^- \\ C^2\Sigma^+ \end{array} \right.$	$\left\{ \begin{array}{l} C(^3P) + H(^2S) \\ C(^1D) + H(^2S) \\ C(^3P) + H(^2S) \\ C(^1D) + H(^2S) \end{array} \right.$

TABLE II
Slater-Type Basis Set

Center	nl Value	Exponents
C	1s	9.29, 5.41
	2s	4.26, 2.59, 1.50, 1.03
	2p	6.34, 2.59, 1.42, 0.96
	3d	1.95
	4d	2.00
	4f	2.50
	5f	4.10
H	1s	1.00, 2.20
	2s	1.00, 2.20
	2p	1.70, 2.90
	3p	2.90
	3d	2.70
	4d	2.70

TABLE III
ANO Convergence Study I: $a^4\Sigma^-$ at $R = 2.20$ b

σ	π	δ	φ	NO_{i1}	Improvement	NO_{i1}	Improvement
4	1	0	0	-38.304738		-38.304828	
6	1	0	0	-38.314663	0.009925	-38.314075	0.009247
8	1	0	0	-38.317600	0.002937	-38.317548	0.003473
10	1	0	0	-38.318313	0.000713	-38.318316	0.000768
13	1	0	0	-38.318855	0.000542	-38.318933	0.000617
16	1	0	0	-38.318988	0.000133	-38.319087	0.000154
19	1	0	0	-38.319082	0.000094	-38.319211	0.000124
21	1	0	0	-38.319102	0.000020	-38.319376	0.000165
23	1	0	0	-38.319111	0.000009	-38.319397	0.000021
23	3	0	0	-38.356300	(0.037189)	-38.356166	(0.036769)
23	6	0	0	-38.362760	0.006460	-38.362740	0.006574
23	8	0	0	-38.363515	0.000755	-38.363498	0.000758
23	10	0	0	-38.363813	0.000298	-38.363803	0.000305
23	13	0	0	-38.363966	0.000153	-38.363965	0.000162
23	13	3	0	-38.381973	(0.018007)	-38.381767	(0.017802)
23	13	6	0	-38.382419	0.000446	-38.382404	0.000637
23	13	6	2	-38.384098	(0.001679)	-38.384084	(0.001680)

TABLE IV
ANO Convergence Study II: $a^4\Sigma^-$ at $R = 20.0$ b

σ	π	δ	φ	NO_i	Improvement	NO_{ii}	Improvement
4	1	0	0	-38.207659		-38.207737	
					0.011563		0.011437
6	1	0	0	-38.219222		-38.219174	
					0.000201		0.000199
8	1	0	0	-38.219423		-38.219373	
					0.000184		0.000201
10	1	0	0	-38.219607		-38.219574	
					0.000064		0.000091
13	1	0	0	-38.219671		-38.219665	
					0.000015		0.000018
16	1	0	0	-38.219686		-38.219683	
					0.000000		0.000000
23	1	0	0	-38.219686		-38.219683	
					(0.033671)		(0.033647)
23	3	0	0	-38.253357		-38.253330	
					0.003324		0.003371
23	6	0	0	-38.256681		-38.256701	
					0.000341		0.000352
23	8	0	0	-38.257022		-38.257053	
					0.000000		0.000000
23	13	0	0	-38.257022		-38.257053	
					(0.022668)		(0.022608)
23	13	3	0	-38.279690		-38.279661	
					0.000151		0.000216
23	13	6	0	-38.279841		-33.279877	
					(0.002375)		(0.002375)
23	13	6	2	-38.282216		-38.282252	

TABLE V

Number of Configuration State Functions Used in the
CI Calculations^a

State	Valence	CSF TYPE	
		First Order	Extended
$X^2\Pi$	18	741	4147
$a^4\Sigma$	9	252	1225
$A^2\Delta$	8	528	1549
$B^2\Sigma^-$	9	378	1498
$C^2\Sigma^+$	14	446	2184

^aTruncated approximate natural orbital set of 13σ , 10π ,
 6δ and 2φ was used.

TABLE VI
Potential Curve for the $X^2\Pi$ State of CH^a

R	E			
	HF	Valence-CI	First-Order CI	Extended CI
1.00	-37.51455	-37.54089	-37.58686	-37.64103
1.30	-38.02545	-38.04795	-38.09068	-38.15061
1.60	-38.21406	-38.24090	-38.29012	-38.34121
1.90	-38.27297	-38.30401	-38.35359	-38.40194
2.00	-38.27848	-38.31115	-38.36091	-38.40829
2.05	-38.27957	-38.31311	-38.36295	-38.40981
2.10	-38.27974	-38.31420	-38.36409	-38.41041
2.15	-38.27914	-38.31453	-38.36446	-38.41025
2.20	-38.27786	-38.31422	-38.36419	-38.40943
2.40	-38.26780	-38.30831	-38.35834	-38.40156
2.70	-38.24437	-38.29220	-38.34201	-38.38338
3.00	-38.21759	-38.27364	-38.32295	-38.36252
3.50	-38.17408	-38.24626	-38.29405	-38.33124
4.00	-38.13568	-38.22705	-38.27315	-38.30870
5.00		-38.21048	-38.25389	-38.28786
6.00		-38.20696	-38.24929	-38.28287
8.00		-38.20611	-38.24809	-38.28160
11.00		-38.20608	-38.24803	-38.28159
15.00		-38.20608	-38.24803	-38.28159
20.00	(-38.18866) ^b	-38.20608	-38.24803	-38.28159

^aAll quantities are in atomic units.

^bHF configuration state function for the $X^2\Pi$ state does not dissociate correctly to the atomic limits of $C(^3P)$ and $H(^2S)$. The value given in the parenthesis is that obtained from the $a^4\Sigma^-$ state at $R = 20.00$ b, corresponding to the SCF energy of the ground states of C and H.

TABLE VII
Potential Curve for the $a^4\Sigma^-$ State of CH^a

E				
R	HF	Valence-CI	First-Order CI	Extended CI
1.00	-37.54271	-37.55316	-37.58386	-37.63499
1.30	-38.05082	-38.05899	-38.09198	-38.14212
1.60	-38.23421	-38.24600	-38.27864	-38.32661
1.90	-38.28677	-38.30243	-38.33637	-38.38164
2.00	-38.29006	-38.30702	-38.34165	-38.38593
2.05	-38.29003	-38.30768	-38.34268	-38.38645
2.10	-38.28909	-38.30745	-38.34283	-38.38608
2.15	-38.28738	-38.30646	-38.34222	-38.38497
2.20	-38.28501	-38.30483	-38.34098	-38.38323
2.40	-38.27069	-38.29374	-38.33143	-38.37183
2.70	-38.24185	-38.27051	-38.31045	-38.34839
3.00	-38.21239	-38.24713	-38.28936	-38.32530
3.50	-38.19366	-38.22018	-38.26465	-38.29911
4.00	-38.19016	-38.21064	-38.25411	-38.28828
5.00	-38.18890	-38.20790	-38.24958	-38.28347
6.00	-38.18872	-38.20778	-38.24889	-38.28259
8.00	-38.18866	-38.20775	-38.24870	-38.28226
11.00	-38.18866	-38.20774	-38.24868	-38.28224
15.00	-38.18866	-38.20774	-38.24867	-38.28223
20.00	-38.18866	-38.20774	-38.24867	-38.28223

^aAll quantities are given in atomic units.

TABLE VIII
Potential Curve for the $\Lambda^2\Delta$ State of CH^a

E				
R	HF	Valence-CI	First-Order CI	Extended CI
1.00	-37.42364	-37.43427	-37.48522	-37.54232
1.30	-37.93532	-37.94325	-37.99542	-38.05255
1.60	-38.12142	-38.13104	-38.18467	-38.23933
1.90	-38.17632	-38.18975	-38.24498	-38.29675
2.00	-38.18042	-38.19533	-38.25110	-38.30193
2.05	-38.18082	-38.19653	-38.25255	-38.30292
2.10	-38.18033	-38.19689	-38.25314	-38.30304
2.15	-38.17909	-38.19654	-38.25299	-38.30244
2.20	-38.17722	-38.19560	-38.25223	-38.30124
2.40	-38.16539	-38.18785	-38.24502	-38.29228
2.70	-38.14382	-38.17175	-38.22904	-38.27374
3.00	-38.13282	-38.15873	-38.21430	-38.25707
3.50	-38.12936	-38.14992	-38.20021	-38.24175
4.00	-38.12984	-38.14895	-38.19557	-38.23632
5.00	-38.13111	-38.15023	-38.19403	-38.23393
6.00	-38.13147	-38.15070	-38.19389	-38.23349
8.00	-38.13154	-38.15079	-38.19380	-38.23324
11.00	-38.13154	-38.15079	-38.19378	-38.23327
15.00	-38.13154	-38.15079	-38.19378	-38.23327
20.00	-38.13154	-38.15079	-38.19378	-38.23327

^aAll quantities are given in atomic units.

TABLE IX
Potential Curve for the $B^2\Sigma^-$ State of CH^a

R	E			
	HF	Valence-CI	First-Order CI	Extended CI
1.00	-37.38604	-37.40844	-37.44759	-37.50726
1.30	-37.99086	-37.92464	-37.95884	-38.02121
1.60	-38.09067	-38.11979	-38.15493	-38.21346
1.90	-38.15032	-38.16783	-38.22135	-38.27774
2.00	-38.15647	-38.19650	-38.23023	-38.28552
2.05	-38.15806	-38.19930	-38.23328	-38.28789
2.10	-38.15889	-38.20130	-38.23559	-38.28946
2.15	-38.15913	-38.20263	-38.23729	-38.29037
2.20	-38.15895	-38.20340	-38.23850	-38.29075
2.30	-38.15799	-38.20363	-38.23978	-38.29027
2.40	-38.15721	-38.20269	-38.24008	-38.28875
2.70	-38.15970	-38.19808	-38.23808	-38.28192
3.00	-38.16563	-38.19570	-38.23683	-38.27728
3.25	-38.17071	-38.19610	-38.23781	-38.27638
3.50	-38.17515	-38.19738	-38.23951	-38.27659
4.00	-38.18153	-38.20114	-38.24328	-38.27858
5.00	-38.18699	-38.20602	-38.24739	-38.28144
6.00	-38.18832	-38.20739	-38.24846	-38.28216
8.00	-38.18865	-38.20773	-38.24868	-38.28223
11.00	-38.18866	-38.20774	-38.24867	-38.28222
15.00	-38.18866	-38.20774	-38.24866	-38.28222
20.00	-38.18866	-38.20774	-38.24866	-38.28222

^aAll quantities are given in atomic units.

TABLE X
Potential Curve for the $C^2\Sigma^+$ State of CH^a

R	E			
	HF	Valence-CI	First-Order CI	Extended CI
1.00	-37.36927	-37.39209	-37.42268	-37.49620
1.30	-37.88227	-37.90213	-37.93538	-38.00796
1.60	-38.06920	-38.09129	-38.12668	-38.19664
1.90	-38.12463	-38.15132	-38.18893	-38.25543
2.00	-38.12884	-38.15728	-38.19575	-38.26107
2.05	-38.12929	-38.15866	-38.19756	-38.26230
2.10	-38.12884	-38.15917	-38.19851	-38.26268
2.15	-38.12764	-38.15896	-38.19875	-38.26235
2.20	-38.12579	-38.15814	-38.19838	-38.26142
2.40	-38.11400	-38.15074	-38.19284	-38.25354
2.70	-38.09209	-38.13709	-38.17911	-38.23637
3.00	-38.08018	-38.13185	-38.17294	-38.22342
3.25	-38.07088	-38.12984	-38.17538	-38.21942
3.50	-38.07579	-38.13062	-38.18013	-38.22007
4.00	-38.07577	-38.13853	-38.18723	-38.22596
5.00	-38.07662	-38.14904	-38.19201	-38.23181
6.00		-38.15135	-38.19305	-38.23342
8.00		-38.15208	-38.19330	-38.23380
11.00		-38.15212	-38.19331	-38.23393
15.00		-38.15212	-38.19331	-38.23392
20.00	(38.07690) ^b	-38.15212	-38.19331	-38.23392

^aAll quantities are given in atomic units.

^bHF configuration state function for the $C^2\Sigma^+$ state does not dissociate correctly to the atomic limits of $C(^1D)$ and $H(^2S)$, instead it dissociates into a mixture of $C(^1D)$ and $C(^1S)$, besides $H(^2S)$. The HF energy of the correct atomic limits for the $C^2\Sigma^+$ state should be -38.13154 hartrees.

TABLE XI

Properties of the Calculated Potential Curves

	$\chi^2\Pi$	$a^4\Sigma^-$	$A^2\Delta$	$B^2\Sigma^-$	$C^2\Sigma^+$
R_e (bohrs)					
HF	2.085	2.023	2.046	2.151	2.049
valence-CI	2.149	2.061	2.099	2.264	2.109
first-order-CI	2.153	2.084	2.114	2.389	2.143
extended CI	2.113	2.053	2.083	2.216	2.100
expt'l ^a	2.116		2.083	2.200	2.105
E_{min} (hartree)					
HF	-38.27978	-38.29017	-38.18082	-38.15913	-38.12929
valence-CI	-38.31453	-38.30770	-38.19689	-38.20372	-38.15918
first-order-CI	-38.36447	-38.34287	-38.25316	-38.24009	-38.19875
extended	-38.41044	-38.38645	-38.30309	-38.29077	-38.26268
expt'l ^b	-38.490		-38.383	-38.371	-38.344
D_e^o (eV)					
HF	2.48	2.76	1.34	(-0.80) ^j	(-0.06) ^j
valence-CI	2.95	2.77	1.25	(-0.11) ^j	0.19
first-order-CI	3.17	2.56	1.62	(-0.23) ^j	0.15
extended	3.51	2.84	1.90	0.23	0.73
expt'l ^c	3.63		2.01	~0.40 ^d	0.94
R_{max} (bohrs) ^e					
HF				2.460	f
valence-CI				3.068	3.305
first-order-CI				2.992	3.023
extended CI				3.296	3.328
expt'l ^a				~4.	g
E_{max} (hartree) ^e					
HF				-38.15706	i
valence-CI				-38.19562	-38.12977
first-order-CI				-38.23683	-38.17291
extended CI				-38.27637	-38.21922
expt'l ^h				≥ -38.354	g
Barrier height (cm ⁻¹) ⁱ					
HF				(6928) ^j	4905
valence-CI				(2660) ^j	4476
first-order-CI				(2598) ^j	3228
extended CI				1284	
expt'l ^a				≥ 500	g

TABLE XI

Properties of the Calculated Potential Curves - Continued

- ^aTaken from Reference 6.
- ^bTotal experimental energy is taken to be the sum of experimental atomic energy and spectroscopically determined D_e^0 . Atomic energies are taken from Reference 11 and Reference 30. For D_e^0 , see footnotes c and d.
- ^cExperimental zero point energy is calculated from ω_e , $\omega_e x_e$ with Dunham correction. (Spectroscopic constants are taken from Reference 6.)
- ^dThe spectroscopic constants ω_e and $\omega_e x_e$ for the $B^2\Sigma^-$ state are not well determined experimentally, therefore the known approximate ω_e (see Reference 6) is used to determine the zero point energy.
- ^e R_{\max} and E_{\max} are the internuclear distance and energy, respectively, at the place of the maximum in the potential curve.
- ^fHF calculations predict a slight maximum in the potential curve of the $C^2\Sigma^+$ state, but fail to describe correctly the dissociation limits.
- ^gA potential barrier exists, but no information about the height and place is known experimentally.
- ^hFrom References 6 and 11.
- ⁱBarrier height is defined as the height of the potential maximum with the dissociation limits as the base line.
- ^jMetastable predicted, i.e., E_{\min} lies higher than the dissociation limits.

Reproduced from
best available copy.

TABLE XII
MCSCF 4σ and 1π Orbitals at $R = 20.0$ b

Orbital	Basis Function ^a	$X^2\Pi$	$a^4\Sigma^-, B^2\Sigma^-$	$A^2\Delta$	$C^2\Sigma^+$
$4\sigma^b$	$2p_C \zeta = 6.34$	-0.0108	-0.0039	-0.0034	-0.0101
	$\zeta = 2.59$	-0.2347	-0.1764	-0.1836	-0.2459
	$\zeta = 1.42$	-0.5689	-1.0612	-1.0595	-0.4806
	$\zeta = 0.96$	-0.2578	0.2446	0.2502	-0.3438
	$4f_C \zeta = 2.50$	-0.0004	0.0042	0.0044	0.0288
	$5f_C \zeta = 4.10$	0.0001	0.0010	0.0010	-0.0075
$1\pi^c$	$2p_C \zeta = 6.34$	0.0110	0.0108	0.0100	0.0108
	$\zeta = 2.59$	0.2303	0.2351	0.2451	0.2268
	$\zeta = 1.42$	0.6229	0.5709	0.4837	0.6051
	$\zeta = 0.96$	0.2023	0.2552	0.3414	0.2246
	$4f_C \zeta = 2.50$	0.0004	-0.0005	0.0078	0.0469
	$5f_C \zeta = 4.10$	-0.0001	0.0001	-0.0021	-0.0115

^aExpansion coefficients for the basis orbitals not listed are all zero.

^b $\sim 2p_\sigma$ of C.

^c $\sim 2p_\pi$ of C.

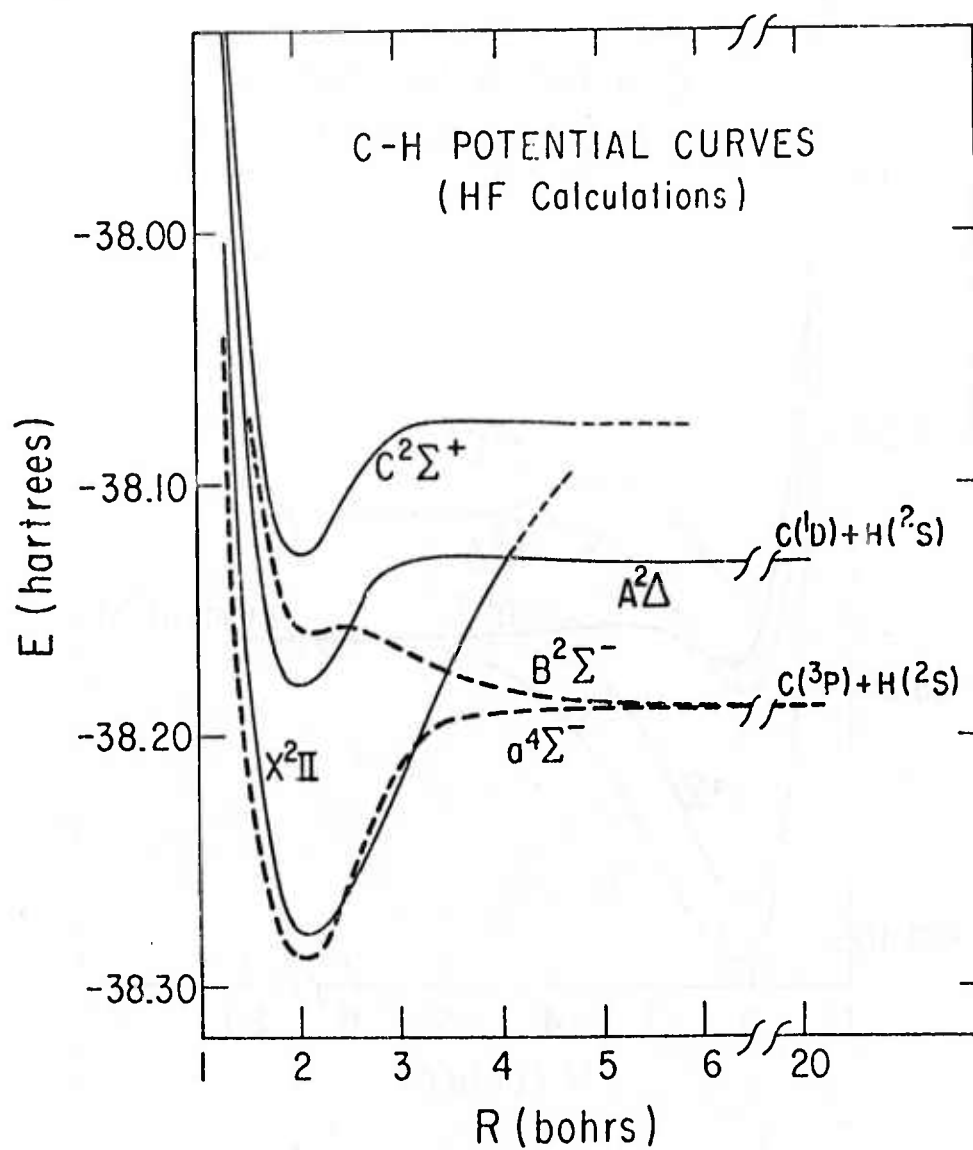


Figure 1. SCF potential curves for the five lowest electronic states of CH

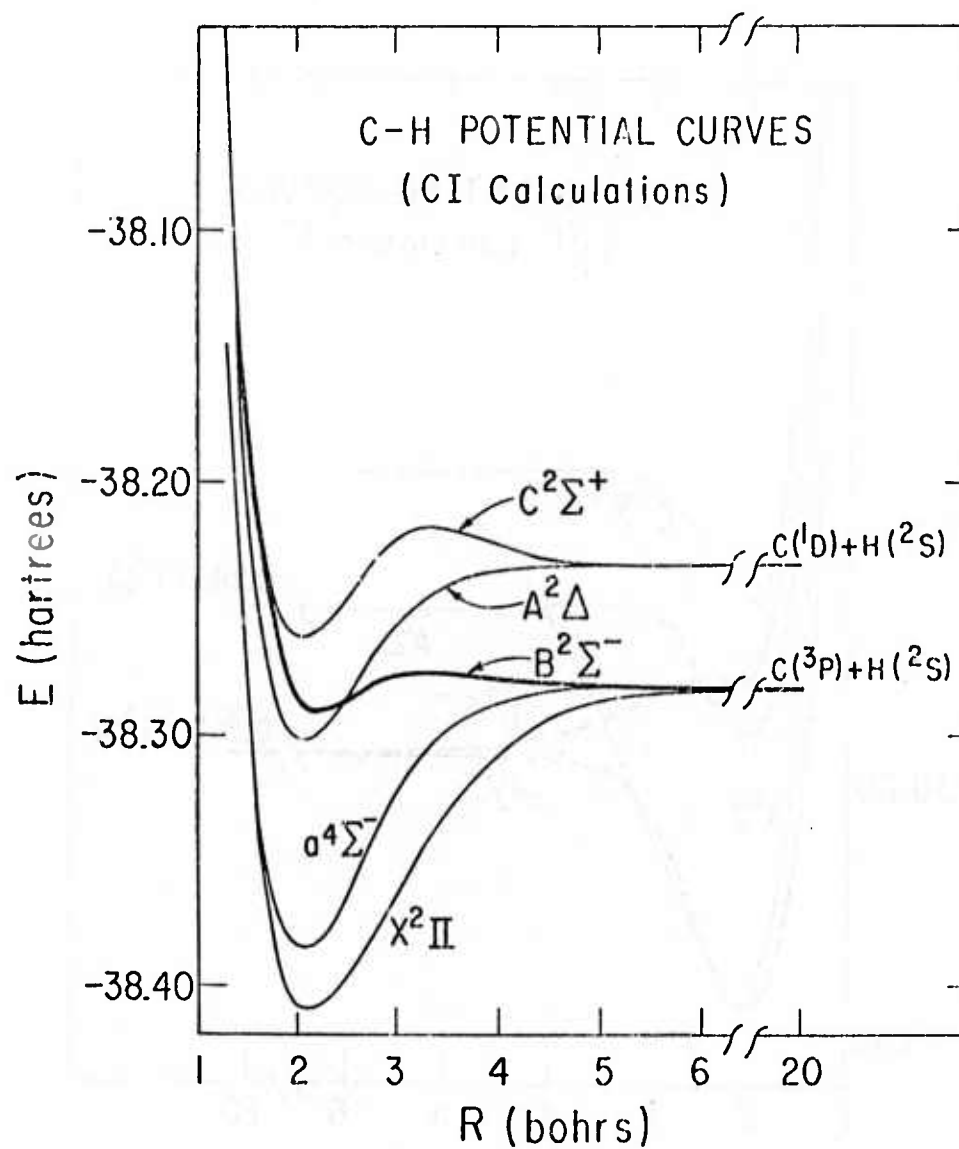


Figure 2. "Extended CI" potential curves for the five lowest electronic states of CH

VALENCE EXCITED STATES OF CH
II. PROPERTIES*

by

George C. Lie[†]
Juergen Hinze

Department of Chemistry
The University of Chicago
Chicago, Illinois

and

Bowen Liu

IBM Research Laboratory
San Jose, California

ABSTRACT: Expectation values of one-electron operators and related molecular properties were calculated for the $X^2\Pi$, $a^4\Sigma^-$, $A^2\Delta$, $B^2\Sigma^-$, and $C^2\Sigma^+$ states of CH, using accurate ab initio electronic wavefunctions and potential curves. The calculated dipole moment for the $v = 0$ vibrational level of the $X^2\Pi$ state is 1.41 debye, in excellent agreement with the experimental value of 1.46 ± 0.06 debye. Other properties studied include dipole and quadrupole moments, field gradients at the nuclei, the Langevin term of the diamagnetic susceptibility, and the Lamb term of the nuclear shielding constant. There are no known experimental values for these properties. Vibration-rotational

* This research was carried out under a Joint Study Agreement between the University of Chicago and the IBM Corporation. Lie and Hinze were supported in part by the Advanced Research Agency of the Department of Defense, monitored by U.S. Army Research Office - Durham, Box CM, Duke Station, Durham, N.C. 27706, under Grant DA-ARO-D-31-124-72-G78 and by Grant GP-33892X of the National Science Foundation.

[†] Present address: IBM Research Laboratory, San Jose, California 95193.



wavefunctions were obtained from the calculated potential curves by numerical solution of the radial Schrödinger equation for the nuclear motion. Vibration-rotational analyses were carried out to yield spectroscopic constants which are in satisfactory agreement with known experimental values.

INTRODUCTION

In the preceding paper,¹ hereafter referred to as paper I, we discussed the calculation of electronic wavefunctions and potential curves for five electronic states of CH: $X^2\Pi$, $a^4\Sigma^-$, $A^2\Delta$, $B^2\Sigma^-$ and $C^2\Sigma^+$. With these wavefunctions, it is possible to calculate expectation values of many one- and two-electron operators of physical interest. Also, from the calculated potential curves, vibration-rotational levels can be obtained by numerically integrating the one-dimensional radial Schrödinger equation.

McLean and Yoshimine² observed, in 1966, "We have reached a point, in ab initio calculations of molecular structure, where it is no longer satisfactory to discuss only energies and compare results with other calculations. A wide spectrum of expectation values must be computed and a serious effort made to compare with, and complement, experimental observations. Only by doing this can a valid assessment of the accuracy of the wavefunction be made". While their statement remains valid today, progress made in the intervening years has allowed ab initio calculations to become competitive with experiment as a tool for the determination of molecular properties. In many instances, ab initio calculation has yielded otherwise inaccessible information. The calculation of molecular properties is a minor task compared with the calculation of the electronic wavefunction. However, the very large number of parameters required to describe an accurate electronic wavefunction is difficult to communicate. It is rare that anyone, other than the original authors of the wavefunction, performs the straightforward but highly useful calculations of molecular properties. Therefore, it is desirable that authors of new wavefunctions

carry out and report molecular property calculations. After all, one of the most important purposes of wavefunction calculations is to obtain molecular properties.

In this paper we report one-electron expectation values and molecular properties obtained from the wavefunctions described in paper I. These data are not easily accessible through experimental observations, which are severely hampered by the high reactivity of the CH radical. In fact, only the dipole moment of the ground state of CH, among all the properties reported here, has been determined experimentally.³

We also report here spectroscopic constants determined from the calculated potential curves. Available spectroscopic information on CH has been summarized by Herzberg and Johns.⁴ A comparison between the theoretical and experimental results provides a valid assessment of the accuracy of the calculated potential curves, and establishes the accuracy of the calculated $^4\Sigma^-$ potential curve which is not known experimentally.

II. EXPECTATION VALUES

We restrict our discussion to expectation values of operators of the form

$$f = \sum_{i=1}^n f_i \quad (1)$$

where the summation is over all electrons of the molecule, and f_i is a one-electron operator which depends on the coordinates of the i -th electron. The one-electron operators considered in this paper have the general form

$$r_k^n \sin^i \theta_k \cos^j \theta_k P_{\ell 0}(\cos \theta_k)$$

where the subscript k refers to the nucleus of either C or H as the coordinate origin. The z -axis points from C to H, and $P_{\ell 0}(\cos \theta)$ is a normalized associated Legendre polynomial. The expectation value of f is given by

$$\begin{aligned} \langle f \rangle &= \langle \Psi, f \Psi \rangle \\ &= \sum_{I,J} C_I C_J \langle \Phi_I, f \Phi_J \rangle \\ &= \sum_{i,j} \gamma_{ij} \langle \varphi_i, f, \varphi_j \rangle . \end{aligned} \quad (2)$$

In Eq. (2), Ψ is the electron wavefunction expanded in terms of configuration state functions (CSF) Φ_I with expansion coefficients C_I , as described in paper I. The CSFs are constructed from a set of molecular orbitals $\{\varphi_i\}$. The coefficients γ_{ij} are elements of the first order reduced density matrix belonging to the wavefunction Ψ , represented in the basis $\{\varphi_i\}$.

Table I gives expectation values of one-electron operators, at the computed equilibrium internuclear distances, calculated from the "extended CI" wavefunctions of paper I. As noted in paper I, these computed R_e 's are, except for the $B^2\Sigma^-$ state, in excellent agreement with the experimental values.

III. MOLECULAR PROPERTIES

Among the molecular properties which are related to the computed expectation values, we consider the dipole moment, the quadrupole moment, the electric field gradients at the nuclei, the diamagnetic susceptibility, the nuclear shielding constant, the Hellman-Feynman forces, and the virial ratio. Strictly speaking, the last two properties are not observables; however, their values at R_e are known theoretically. How closely the computed values approach the theoretical values gives an indication of the quality of the computed wavefunction.

A. Dipole Moment

The dipole moment μ of a linear molecule is given by

$$\mu = \sum_i R_i Z_i - \langle z \rangle \quad (3)$$

In Eq. (3), the sum is over all nuclei with charge Z_i , and z -coordinate R_i in a coordinate system where the z -axis is the molecular axis. The dipole moment of a neutral molecule, such as CH, is independent of the coordinate origin.

Table II gives dipole moments computed from the "extended CI" wavefunctions of paper I for five electronic states of CH. These results are also displayed graphically in Fig. 1. All computed dipole curves have the correct asymptotic behavior at large and small R ; i.e., all dipole moments go to zero at united and separated atom limits. The dipole moments for the $a^4\Sigma^-$, $A^2\Delta$ and $B^2\Sigma^-$ states are in the direction of C^-H^+ for all internuclear distances, whereas the

dipole moments for the $X^2\Pi$ and $C^2\Sigma^+$ states are in the direction of C^+H^- for large R , and C^-H^+ for small R . The sign change in the dipole moment of the $C^2\Sigma^+$ state is consistent with the valence bond analysis, given in paper I, for the origin of a maximum in the $C^2\Sigma^+$ potential curve. The C^+H^- dipole, at large R , results from the interaction between a repulsive potential curve arising from ground state separated atoms, and an attractive curve arising from C^+H^- ($1s^2 2s^2 2p^2 P + 1s^2 {}^1S$). The C^-H^+ dipole, at small R , results from the ionic curve arising from $C^-H^+(1s^2 2s^2 2p^3 {}^2P)$. At large R , the C^+H^- curve lies ~ 2 eV below the C^-H^+ curve. However, as R decreases, the C^+H^- curve deviates from a $1/R$ behavior sooner than the C^-H^+ curve, due to the large size of H^- compared to H^+ and the small difference between the sizes of C^+ and C^- . Thus, at small R the C^-H^+ curve lies below the C^+H^- curve. As stated in paper I, this C^-H^+ curve eventually crosses the repulsive ${}^2\Sigma^+$ curve, and is responsible for the potential maximum in the $C^2\Sigma^+$ curve. The sign change in the dipole moment of the $X^2\Pi$ state can be explained in the same way. The reason why the $a^4\Sigma^-$, $A^2\Delta$ and $B^2\Sigma^-$ states have dipole moment in the sense C^-H^+ for all R , is that the lowest C^+H^- structure that can give rise to these states lies higher than the lowest C^-H^+ states of the corresponding symmetry for both large and small R .

Table III and Fig. 2 give dipole moments of CH calculated from the SCF wavefunctions of paper I. The SCF dipole moment for the $X^2\Pi$ state does not approach zero as R approaches ∞ . This results from the failure of the HF wavefunction to dissociate into the correct separated atom limit. Another difference between the SCF and "extended CI" results

is that, for the $C^2\Sigma^+$ state the SCF dipole moment remains in the direction of C^-H^+ for all internuclear distances. This reflects the failure of the HF wavefunction for the $C^2\Sigma^+$ state, $1\sigma^2 2\sigma^2 3\sigma 1\pi^2$, to properly include the contribution of the ionic structure C^+H^- , at large internuclear distances. Both of these deficiencies can be removed by going to the "valence CI" or "first order CI" wavefunctions.

The dipole moments at the computed R_e were obtained by interpolations using four calculated points around R_e . The results are given in Table IV. The "extended CI" dipole moment for the $X^2\Pi$ state at computed R_e , which is 0.003 bohr too short compared with the experimental value, is 1.45 debye. This value is in good agreement with the experimental value of 1.46 ± 0.06 debye obtained by Phelps and Dalby.³ The corresponding SCF value is 1.62 debye, in error by ~10%. The value obtained by Bender and Davidson⁵ using the iterative natural orbital approach is 1.43 debye. The "extended CI" dipole moments at R_e for $a^4\Sigma^-$, $A^2\Delta$, $B^2\Sigma^-$, and $C^2\Sigma^+$ states are 0.663, 0.904, 1.389, and 0.955 debye, respectively.

Rigorously speaking, to properly compare the calculated properties with the experimental results, the computed quantities should be averaged over the appropriate vibration-rotational wavefunctions. However, this is generally not done either for lack of vibration-rotational wavefunctions or because the average usually does not lead to significant changes in the calculated values, especially for the lowest vibrational states. For example, using the computed dipole moments as a function of R and calculating the rotation-vibration average, we obtain 1.41 debye for the $v = 0$, $K = 1$ level of the $X^2\Pi$ state as compared to 1.45 debye at

R_e . The vibrationally averaged "extended CI" dipole moments for the lowest vibration-rotational states of the $a^4\Sigma^-$, $A^2\Delta$, $B^2\Sigma^-$, and $C^2\Sigma^+$ states are 0.68, 0.93, 1.39, and 0.99 debye, respectively. Averaged dipole moments for higher vibrational states are given in Tables X-XIV. The determination of the vibrational wavefunctions will be outlined in Section IV.

B. Other Molecular Properties

The quadrupole moment Q of a diatomic molecule is given by

$$Q = \sum_i Z_i R_i^2 - \left\langle z^2 - \frac{1}{2} (x^2 + y^2) \right\rangle . \quad (4)$$

For a neutral molecule with a permanent dipole, Q depends on the coordinate origin with respect to which the variables R_i , x , y , and z are defined. To facilitate comparison with experiment, the quadrupole moment of CH were evaluated with respect to the center of mass of the molecule.⁶ Table V gives quadrupole moments as functions of R , calculated from the "extended CI" wavefunctions for the five electronic states of CH.

The field gradient of a diatomic molecule at nucleus 1, q_1 , is given by

$$q_1 = -\frac{2Z_2}{R^3} + \left\langle \frac{3 \cos^2 \theta - 1}{r_1^3} \right\rangle \quad (5)$$

where R is the internuclear distance. The first term gives the electric field gradient due to nucleus 2, and the second term the electronic contribution. The field gradient at nucleus 2 can be obtained by interchanging subscripts 1 and 2 in Eq. (5). Tables VI and VII give

field gradients at C and H, respectively, obtained from the "extended CI" wavefunctions.

The experimentally measured diamagnetic susceptibility, χ , is a rotationally averaged quantity consisting of two terms: the Langevin term and the high frequency term. The calculation of the high frequency term requires a knowledge of all the excited electronic states of the molecule. The Langevin term is given by

$$\chi^L = -\frac{1}{6} \alpha^2 \langle r^2 \rangle \quad (6)$$

where α is the fine structure constant, and the applied magnetic field is assumed to be in the direction of the internuclear axis. The diamagnetic susceptibility is invariant to a change of coordinate origin,⁷ although the Langevin and high frequency terms taken separately are not. The χ^L were evaluated at the center of electronic charge, to minimize its variation with R .

Similarly, there are two terms contributing to the nuclear shielding constant σ . The diamagnetic contribution, called the Lamb term, at nucleus k is given by⁸

$$\sigma_k^L = -\frac{1}{3} \alpha^2 \left\langle \frac{1}{r_k} \right\rangle \quad (7)$$

The Hellman-Feynman force on the carbon nucleus is given by

$$F_C = Z_H \left[-\frac{Z_C}{R^2} + \left\langle \frac{Z_C}{r_C} \right\rangle \right] \quad (8)$$

Similarly the force on the H nucleus is

$$F_H = Z_C \left[\frac{Z_H}{R^2} - \left\langle \frac{Z_H}{r_H} \right\rangle \right] \quad (9)$$

In an electronic system at equilibrium the electric field seen by a nucleus must be zero. Proper self-consistent wavefunctions should lead to vanishing electric fields at the nuclei, at the predicted equilibrium internuclear distance R_e where the energy reaches its minimum. That is

$$F_C = F_H = 0 \quad \text{at } R_e \quad (10)$$

The above theorem is one of the applications of the well-known Hellman-Feynman theorem for an exact wavefunction. It has been proven by Hurley⁹ to hold also for an exact Hartree-Fock wavefunction.

Another application of the Hellman-Feynman theorem is found in the virial theorem, which for a diatomic molecule can be written as

$$0 = 2\langle T \rangle + \langle V \rangle + R \frac{dE}{dR} = \langle T \rangle + E + R \frac{dE}{dR} \quad (11)$$

where $\langle T \rangle$ is the average electronic kinetic energy, $\langle V \rangle$ is the average potential energy including nuclear repulsion, and E is the total electronic energy equal to $\langle T \rangle + \langle V \rangle$. From the above equation we see that, when the condition $dE/dR = 0$ is satisfied

$$\frac{\langle V \rangle}{\langle T \rangle} = -2.00000 \quad (12)$$

This ratio should hold at R_e and when two nuclei are far apart. The virial theorem has also been proven to hold for exact Hartree-Fock wavefunctions by Hurley.⁹

The above two theorems can be used to test the quality of approximate wavefunctions. However, an approximate wavefunction satisfying both theorems is not necessarily a good approximation to the exact wavefunction.

In Table IV we give the properties described above, calculated from the "extended CI" wavefunctions, at the calculated R_e . Results obtained from SCF wavefunctions are also given for comparison.

Table IV shows that both the SCF and "extended CI" wavefunctions satisfy the virial theorem to within 0.0075% at the computed equilibrium internuclear distances. This is a considerable improvement over the earlier calculation by Lie et al.¹⁰ where the error is 0.04%, indicating a better choice of one-particle basis set in the current calculation. However, the Hellman-Feynman forces at R_e , calculated from the "extended CI" wavefunctions, are somewhat larger than those obtained by Lie et al.¹⁰ This may be a result of the truncation of the external orbital set used in the current calculation.

The diamagnetic contributions to the magnetic susceptibility and the nuclear magnetic shielding constants do not vary significantly from state to state. Nor do they appear sensitive to the inclusion of electron correlation.

IV. VIBRATION-ROTATIONAL ANALYSIS

In the Born-Oppenheimer approximation, it is assumed that the total wavefunction of a diatomic molecule can be expressed as a product of

electronic and nuclear wavefunctions, which are solutions of two separate equations. The first equation is for the motion of the electrons in the field of the fixed nuclei (cf. paper I); the eigenvalues and eigenfunctions are therefore dependent parametrically on the internuclear distance R . The second equation is for the motion of the two nuclei in the potential determined by the electrons, i.e., the eigenvalues of the first equation. The assumption of separability in the second equation leads to two independent equations for the nuclear vibrational and rotational motions. The solutions for the nuclear rotation, i.e., the angular part of the nuclear motion, can be obtained analytically as hypergeometric functions,¹¹ giving rise to the rotational quantum numbers K and M (Hund's coupling case b is assumed). The energy levels for a fixed internuclear distance R are given by

$$E_{\text{rot}}(R) = \frac{1}{2\mu R^2} [K(K+1) - \Lambda^2] \quad (13)$$

where μ is the nuclear reduced mass, and Λ is the electronic angular momentum along the internuclear axis. There are no general analytical solutions for the nuclear vibrational motion, the wave equation of which is

$$\left\{ \frac{1}{2\mu R^2} \frac{d}{dR} R \left(\frac{d}{dR} \right) + E_{\Lambda}(R) + E_{\text{rot}}(R) - E_{v,K} \right\} R_{v,K}(R) = 0 \quad (14)$$

where $E_{\Lambda}(R)$ is the electronic energy as a function of R determined in paper I. $E_{v,K}$ is the vibration-rotational energy, where v is the vibrational quantum number. Equation (14) was numerically integrated

using Numerov's method as described by Cooley¹² with certain modifications due to Blatt.¹³ Since the potentials $E_{\Lambda}(R)$ were obtained at a few selected points of R , we have used a fifth order polynomial interpolation to get the required intermediate points for a direct numerical integration. The integration range was from $R = 1.00$ bohr to $R = 20.00$ bohrs. No tunneling through the barriers in the potential curves of the $B^2\Sigma^-$ and $C^2\Sigma^+$ states were considered. The potential curves were leveled from the maximum on to $R = 20.00$ bohrs. From the calculated vibration-rotational eigenvalues, $E_{v,K}$, spectroscopic constants were obtained by taking the appropriate energy differences. The resulting eigenfunctions $R_{v,K}$ can be used to vibrationally average certain observable properties for a more realistic comparison with experimental values. Such vibrational averaging was carried out for the dipole moments only (see the discussion in Section IIIa).

The energy levels obtained by solving the vibrational Schrödinger equation, Eq. (14), are displayed in Fig. 3. These energy levels can be expressed as¹⁴

$$E_{v,K} = T_e + \omega_e \left(v + \frac{1}{2} \right) - \omega_e x_e \left(v + \frac{1}{2} \right)^2 + \dots + E_{\text{rot}} \quad (15)$$

where T_e is the electronic energy of the molecule at P_e , and E_{rot} is the rotational energy. The rotational energy can be written as

$$E_{\text{rot}} \equiv F_v(K) = B_v [K(K+1) - \Lambda^2] - D_v K^2(K+1)^2 \quad (16)$$

by expanding Eq. (13) about R_e . The spectroscopic constants ω_e , $\omega_e x_e$, B_v , and D_v can be determined from the computed $E_{v,K}$'s as follows.

For the same electronic and vibrational state, the energy difference between two adjacent rotational levels can be obtained from Eq. (16) as

$$F_v(K+1) - F_v(K) = 2(K+1)B_v - 4(K+1)^3D_v \quad (17)$$

For the same electronic state, the energy difference between two adjacent vibrational levels is given by Eq. (15) as

$$\begin{aligned} \Delta G_{v+1/2} &= E_{v+1,K} - F_{v+1}(K) - E_{v,K} + F_v(K) \\ &= \omega_e - 2(v+1)\omega_e x_e \end{aligned} \quad (18)$$

Equations (17) and (18), together with the computed $E_{v,K}$'s, were used to determine B_v , D_v , ω_e , and $\omega_e x_e$. A least squares fit was employed whenever there were more data points than unknowns. The results are summarized in Tables VIII and IX, together with known experimental values. Given in Table X are also the B_e and α_e 's which were obtained from the B_v 's by a least squares fit to the expression

$$B_v = B_e \left(v + \frac{1}{2} \right) - \alpha_e \left(v + \frac{1}{2} \right)^2 \quad (19)$$

While many rotational levels are known experimentally, for each vibrational state, we only carried out calculations for a few rotational levels. The reason is that spectroscopic constants B_v and D_v do not in general depend on the number of rotational levels used in carrying out a

least squares fit. This is because the primary contribution to the energy difference between different rotational levels comes from the centrifugal correction term in Eq. (20), $E_{\text{rot}} = [K(K+1) - \Lambda^2]/2\mu R^2$. Therefore the rotational energy is expected to be proportional to $[K(K+1) - \Lambda^2]$, which is used as the expansion parameter.

As can be seen from Table IX, the "extended CI" B_v 's agree quite well with the experimental values; the errors are on the order of 0.2 cm^{-1} . The only exception is $B_{v=1}$ of the $B^2\Sigma^-$ state, where the error is 0.6 cm^{-1} . This is to be expected since the $B^2\Sigma^-$ state does not have a deep potential well and our calculated dissociation energy is in error by $\sim 25\%$. The calculated B_v 's for the higher vibrational levels are less accurate than that for the lower vibrational levels, which is generally the case for calculated potential curves. Except for $B_{v=1}$ of the $B^2\Sigma^-$ state, the calculated B_v 's are all found to be within 2% of the experimental values.

The calculated D_v , which are $\sim 10^4$ smaller than B_v , are all found to be in good agreement with experimental values.

Experimentally only three vibrational levels were observed for the $X^2\Pi$, $A^2\Delta$, and $C^2\Sigma^+$ states, and two for the $B^2\Sigma^-$ state. According to the results of the "extended CI" calculations, there are only two vibrational levels for the $B^2\Sigma^-$ state, and four for the $C^2\Sigma^+$ state. We carried out spectroscopic analyses for all of them. For the $X^2\Pi$, $a^4\Sigma^-$, and $A^2\Delta$ states we only give results for $v \leq 5$.

The error in the "extended CI" $\Delta G_{v+1/2}$ is largest for the $B^2\Sigma^-$ state, $\sim 100 \text{ cm}^{-1}$, as is to be expected from the 43% error in the calculated

dissociation energy. Similarly, the errors in the calculated $\Delta G_{v+1/2}$ for the $C^2\Sigma^+$ state, 61 cm^{-1} for $v = 0$ and 90 cm^{-1} for $v = 1$, are larger than that for the $X^2\Pi$ state, 11 cm^{-1} for $v = 0$ and 49 cm^{-1} for $v = 1$, and the $A^2\Delta$ state, 36 cm^{-1} for $v = 0$ and 32 cm^{-1} for $v = 1$. The errors in the $X^2\Pi$ and $B^2\Sigma^-$ states are in the opposite direction compared with that in the $A^2\Delta$ and $C^2\Sigma^+$ states. This implies that the calculated potential curves for the $X^2\Pi$ and $B^2\Sigma^-$ states are too wide as well as too shallow, whereas they are too narrow and too shallow for the $A^2\Delta$ and $C^2\Sigma^+$ states.

In deriving the equilibrium spectroscopic constants, ω_e , $\omega_e x_e$, B_e , and α_e , we have used the same number of v levels as was observed and used in their experimental determination (three v levels were used for the $a^4\Sigma^-$ state). This is because the values obtained for the spectroscopic constants by a least squares fit depends on the number of vibrational levels used. The variation can be as much as 100 cm^{-1} in determining ω_e , and 20 cm^{-1} in determining $\omega_e x_e$; an indication that the two term expansion for the vibrational level is frequently not adequate. The variations of the B_e 's and α_e 's are not as drastic. At any rate, for a meaningful comparison between theory and experiment, the same procedure for extracting secondary data must be used.

The discrepancies between computed and experimental quantities are $\sim 50 \text{ cm}^{-1}$ (2%) or less for the ω_e 's, and $\sim 20 \text{ cm}^{-1}$ (30%) or less for the $\omega_e x_e$'s. Much better agreements are obtained for the B_e 's and α_e 's, since they are derived from B_v 's which are themselves in good agreement with the experimental values. Exceedingly good agreements between experimental and calculated results for the $A^2\Delta$ state, indicates that the shape of the

experimental RKR curve for the $A^2\Delta$ state is well reproduced by the "extended CI" calculations. This is reflected also in the nearly constant errors of the calculated $\Delta G_{v+1/2}$'s for the $A^2\Delta$ state.

The experimental R_e 's given in Table IV are all determined from the experimental B_e 's according to the relation $B_e = (2\mu R_e^2)^{-1/2}$. It was shown by Dunham¹⁵ that there are corrections of the order B_e^2/ω_e^2 to this formula. These corrections depend on the shape of the potential curve, and for a very shallow potential well they may be large. Using the relation $B_e = (2\mu R_e^2)^{-1/2}$ and the calculated B_e 's, we obtain the following R_e 's for the $X^2\Pi$, $a^4\Sigma^-$, $A^2\Delta$, $B^2\Sigma^-$, and $C^2\Sigma^+$ states: 2.114, 2.053, 2.080, 2.190, and 2.094 bohrs, respectively. Comparison with the R_e 's calculated from the energy minimum in the potential curve shows that the corrections for the $X^2\Pi$, $a^4\Sigma^-$, $A^2\Delta$, and $C^2\Sigma^+$ states are all less than 0.01 bohr, as compared to the correction of 0.026 bohr for the $B^2\Sigma^-$ state. The correction is largest for the $B^2\Sigma^-$ state since it has a very shallow potential well. The true potential curve is deeper compared with the calculated one; therefore the correction to the experimental R_e for the $B^2\Sigma^-$ state should be smaller than 0.026 bohr. This might bring the current experimental value of 2.200 bohr into agreement with the calculated value of 2.216 bohr.

Table IX also gives the calculated and experimental zero-point energy and term splitting v_{00} . The term splitting is relative to the $v = 0$ level of the "rotationless" $X^2\Pi$ state, i.e., the rotational energy has been subtracted out of the lowest vibration-rotational level. Relative to the $X^2\Pi$ state, the $A^2\Delta$, $B^2\Sigma^-$, and $C^2\Sigma^+$ states are all shifted up compared with experimental results. The errors are respectively 373,

156, and 628 cm^{-1} for the $A^2\Delta$, $B^2\Sigma^-$, and $C^2\Sigma^+$ states. The larger errors in the $A^2\Delta$ and $C^2\Sigma^+$ states may be attributed to the error in the calculated term splitting between the 3P and 1D states of carbon which is too large by 417 cm^{-1} . If we shift the $A^2\Delta$ and $C^2\Sigma^+$ states down by 417 cm^{-1} , the errors in the computed term splittings would all be less than 211 cm^{-1} . The computed zero-point energy was obtained from the energy difference between the computed energy minimum and the "rotationless" $v = 0$ level. Experimental zero-point energy was obtained from ω_e and $\omega_e x_e$ with Dunham correction.^{14,15} Zero-point energies are all found to be within 50 cm^{-1} of the experimental values. The largest error is found in the $B^2\Sigma^-$ state, where the experimental value is only known approximately.

By subtracting the computed zero-point energy from the dissociation energy D_e^0 of paper I, we obtain the spectroscopic dissociation energy D_0^0 , which is given in Table IV. Since the errors of the computed zero-point energies are all less than 50 cm^{-1} , the calculated D_0^0 's should have essentially the same accuracy as the D_e^0 's; the errors are 0.12, 0.11, 0.15, and 0.16 eV for the $X^2\Pi$, $A^2\Delta$, $B^2\Sigma^-$, and $C^2\Sigma^+$ states, respectively.

Apart from the Hönl-London factor, the vibration-rotational transition matrix element is

$$\langle R_{v',K'}(R) | \mu(R) | R_{v'',K''}(R) \rangle \quad (20)$$

where $\mu(R)$ is the dipole moment which depends on the internuclear distance and the particular electronic state considered. The integration is to be

performed over R . With the vibrational wavefunctions and the dipole moments available, the matrix elements can be obtained by numerical integration. Vibrationally averaged dipole moments are obtained by letting $v' = v''$ and $K' = K''$. The squares of the off-diagonal matrix elements are proportional to the line strengths in the infrared vibration-rotational transitions.

The vibration-rotational transition matrix elements for all five states are all found to be fairly constant within each branch, therefore only the values for the first members of each branch are given. Tables X through XIV give the matrix elements obtained from the "extended CI" curves. From a given matrix element the oscillator strength can easily be calculated. Unfortunately there are no experimental results to compare with.

We present in Table XV the $P_{v',v''}^{K',K''}$ values, the square of the transition matrix elements, for the 0 - 1 and 1 - 2 bands in the infrared transitions of the ground state for two reasons. Firstly, it is more likely to be studied experimentally, although their intensities are weak due to the small dipole moments. The second reason is to illustrate what to expect for the other states as we give only the transition matrix elements for the first member of each branch. It should be noted here that the variation of $P_{v',v''}^{K',K''}$ with K in the $X^2\Pi$ state is different from that in the other four states, because of different behavior of the dipole moments around R_e . For example, the $P(K)$ of the $a^4\Sigma^-$, $A^2\Delta$, $B^2\Sigma^-$, and $C^2\Sigma^+$ states increases with increasing K values, unlike the $P(K)$ of the $X^2\Pi$ state which decreases with increasing K as shown in Table XV.

V. CONCLUSION

The "extended CI" calculations of the potential curves and molecular properties for the valence excited states of CH are in satisfactory agreement with the available experimental results. The dissociation energies were calculated to within 0.2 eV of the experimental values. The dipole moment for the ground state was computed to well within the experimental uncertainty. Calculated $\Delta G_{v+1/2}$ were in error by less than 100 cm^{-1} ($\sim 5\%$), ω_e by less than 50 cm^{-1} ($\sim 2\%$), B_v by less than 0.2 cm^{-1} ($\sim 2\%$), term splittings by less than 630 cm^{-1} . Excellent agreement with experimental values was found in the calculated R_e 's, except for the $B^2\Sigma^-$ state where the experimental value may not correspond to the classical equilibrium internuclear distance. Large percentage errors, as high as 30% ($\sim 20 \text{ cm}^{-1}$), were found in the calculated anharmonicity corrections $\omega_e x_e$, which are two orders of magnitude smaller than ω_e . These comparisons provide a guideline for the reliability of the predictions made for the experimentally yet unobserved $a^4\Sigma^-$ state.

Many deficiencies in the SCF approximation were seen in the calculations of CH, such as the wrong dissociation limits, wrong energy level ordering, etc.

These deficiencies, leading to qualitatively incorrect results, were not found in the "valence CI" and "first order CI" wavefunctions. We have already seen, in paper I, that these simpler wavefunctions gave dissociation energies in error by as much as 0.8 eV, and equilibrium internuclear distances in error by as much as 0.15 bohr. No definite conclusion was reached concerning the relative merits of these two methods. In this

paper we did not tabulate the molecular properties calculated from the "valence CI" and "first order CI" wavefunctions, it would have doubled the number of tables. However a detailed comparison between the "valence CI", the "first order CI" and the "extended CI" results was made. The results of this comparison are summarized below.

The vibrationally averaged dipole moments, for the $v = 0$ level of the $X^2\Pi$ state, obtained from the "valence CI" and "first order CI" wavefunctions are 1.40 and 1.25 debye, respectively. These are to be contrasted to the "extended CI" result of 1.41 debye, and the experimental value of 1.46 ± 0.06 debye. No experimental result is available for the dipole moments of the remaining four electronic states. The "valence CI" and "first order CI" dipole moments for these states differ from the "extended CI" results by more than 0.01 debye and less than 0.15 debye. No correlation was found between errors in the computed dissociation energies and errors in the computed dipole moments. No conclusion was reached concerning the relative merits of these two models by comparing the calculated dipole moments. Examination of other calculated molecular properties did not yield significantly different trends. Thus, we conclude that for CH, the "valence CI" and "first order CI" wavefunctions do not consistently give results of accuracy comparable to those obtained from the "extended CI" wavefunction. It is surprising that the "first order CI" wavefunction does not consistently give results that are better than the "valence CI" wavefunction. One possible explanation is that we did not employ the iterative natural orbital method in determining the "first order CI" wavefunction, which could conceivably lead to improved results.

ACKNOWLEDGMENTS

The authors wish to thank Drs. P. S. Bagus, A. D. McLean, and M. Yoshimine for helpful discussions. George Lie and Juergen Minze gratefully acknowledge the hospitality extended to them by the IBM Research Laboratory in San Jose.

REFERENCES

1. G. C. Lie, J. Hinze and B. Liu, in press.
2. A. D. McLean and M. Yoshimine, J. Chem. Phys. 45, 3679 (1966).
3. D. H. Phelps and F. W. Dalby, Phys. Rev. Letters 16, 3 (1966).
4. G. Herzberg and J. W. C. Johns, Astrophys. J. 158, 399 (1969).
5. C. F. Bender and E. R. Davidson, Phys. Rev. 183, 23 (1969).
6. A. D. McLean and M. Yoshimine, J. Chem. Phys. 47, 3256 (1969).
7. J. H. Van Vleck, The Theory of Electric and Magnetic Susceptibility (Oxford University Press, London, 1932) p. 276.
8. D. W. Davies, The Theory of the Electric and Magnetic Properties of Molecules (John Wiley and Sons, New York, 1967).
9. A. C. Hurley, in Molecular Orbitals in Chemistry, Physics and Biology, edited by P. O. Lowdin and B. Pullman (Academic Press, New York, 1964).
10. G. C. Lie, J. Hinze and B. Liu, J. Chem. Phys. 57, 625 (1972).
11. L. Pauling and E. B. Wilson, Introduction to Quantum Mechanics (McGraw-Hill, New York, 1935) p. 275.
12. J. W. Cooley, Mathematical Computation 15, 363 (1961).
13. J. M. Blatt, J. of Computational Phys. 1, 382 (1967).
14. G. Herzberg, Spectra of Diatomic Molecules (D. Van Nostrand, Princeton, 1950), 2nd edition.
15. J. L. Dunham, Phys. Rev. 41, 721 (1932).

Table I

Expectation Values^{a,b} at R_e^c for the valence excited states of CH

	$X^2\Pi$	$a^4\Sigma^-$	$A^2\Delta$	$B^2\Sigma^-$	$C^2\Sigma^+$
Origin at C					
r^{-1}	15.1766	15.2038	15.1668	15.1533	15.1472
r	9.4539	9.2883	9.4632	9.5540	9.5694
r^2	19.8107	19.0753	19.9997	20.4280	20.5973
z	1.5428	1.7923	1.7271	1.6699	1.7246
$r \sin \theta$	6.3696	6.6879	6.8691	6.9248	6.9654
$r^{-1} \cos^2 \theta$	5.4087	5.2246	5.2067	5.1506	5.2000
$r^{-2} \cos \theta$	0.2260	0.2270	0.2186	0.1965	0.2182
$\frac{1}{2} r^{-3} (3 \cos^2 \theta - 1)$	0.5775	-0.0015	0.0064	-0.1546	0.0145
$\frac{1}{2} r^2 (3 \cos^2 \theta - 1)$	4.7942	2.5860	2.3017	2.6273	2.2021
$r^2 \cos^2 \theta$	9.7997	8.0825	8.2010	8.5608	8.3339
Origin at H					
r^{-1}	3.9170	3.9308	3.8398	3.6084	3.7980
r	16.2912	15.7778	16.1300	17.0011	16.3117
r^2	44.5496	41.2201	43.1717	47.4098	44.2269
z	-13.2496	-12.5787	-12.8525	-13.8442	-12.9761
$r \sin \theta$	6.3690	6.6874	6.8686	6.9242	6.9648
$r^{-1} \cos^2 \theta$	2.5279	2.5270	2.4806	2.3840	2.4575
$r^{-2} \cos \theta$	-1.3387	-1.4197	-1.3797	-1.2189	-1.3582
$\frac{1}{2} r^{-3} (3 \cos^2 \theta - 1)$	0.5175	0.5391	0.5169	0.4410	0.5053
$\frac{1}{2} r^2 (3 \cos^2 \theta - 1)$	29.5332	24.7309	25.4737	29.6090	25.8318

^aExpectation values calculated from the "extended C1" wavefunctions of Reference 1.^bAll quantities are given in atomic units.^cComputed equilibrium internuclear distance from Reference 1.

Table II

Variation of Dipole Moment with R ("Extended CI" Results)

R (bohrs)	Dipole (debyes) ^a				
	X ² Π	a ⁴ Σ ⁻	A ² Δ	B ² Σ ⁻	C ² Σ ⁺
1.00	1.8676	0.1516	0.1768	0.2795	0.1831
1.30	1.8914	0.2973	0.3476	0.5155	0.3588
1.60	1.8105	0.4328	0.5360	0.8009	0.5541
1.90	1.6296	0.5815	0.7569	1.1119	0.7863
2.00	1.5504	0.6343	0.8370	1.2117	0.8700
2.05	1.5072	0.6612	0.8775	1.2587	0.9122
2.10	1.4620	0.6882	0.9180	1.3026	0.9545
2.15	1.4150	0.7152	0.9581	1.3428	0.9966
2.20	1.3663	0.7423	0.9977	1.3783	1.0382
2.30				1.4312	
2.40	1.1570	0.8471	1.1443	1.4558	1.1954
2.70	0.7988	0.9793	1.2793	1.3954	1.3124
3.00	0.4550	1.0440	1.2234	1.1625	1.0792
3.25				0.9460	0.6302
3.50	0.0004	0.8037	0.8534	0.7158	0.1582
4.00	-0.2246	0.4757	0.4880	0.3880	-0.2060
5.00	-0.1766	0.1442	0.1482	0.1151	-0.1573
6.00	-0.0619	0.0474	0.0511	0.0391	-0.0517
8.00	-0.0068	0.0089	0.0101	0.0083	-0.0058
11.00	-0.0010	0.0022	0.0023	0.0022	-0.0023
15.00	-0.0003	0.0006	0.0007	0.0006	-0.0007
20.00	-0.0001	0.0002	0.0002	0.0002	-0.0002

^aPositive dipole moment is defined as C⁻H⁺.

Table III
Variation of Dipole Moment with R (SCF Results)

R (bohrs)	Dipole (debyes) ^a				
	$X^2\Pi$	$a^4\Sigma^-$	$A^2\Delta$	$B^2\Sigma^-$	$C^2\Sigma^+$
1.00	1.9904	0.1519	0.1697	0.2452	0.1694
1.30	2.0251	0.2782	0.3374	0.4718	0.3369
1.60	1.9411	0.3856	0.5214	0.7569	0.5228
1.90	1.7677	0.4949	0.7469	1.1167	0.7552
2.00	1.6914	0.5322	0.8317	1.2487	0.8437
2.05	1.6498	0.5508	0.8757	1.3151	0.8899
2.10	1.6060	0.5695	0.9207	1.3806	0.9372
2.15	1.5599	0.5882	0.9666	1.4434	0.9857
2.20	1.5117	0.6069	1.0132	1.5010	1.0350
2.30				1.5836	
2.40	1.2975	0.6809	1.2028	1.5890	1.2378
2.70	0.9205	0.7905	1.4092	1.2851	1.4724
3.00	0.4949	0.9133	1.1474	0.9289	1.2178
3.25				0.6890	0.9375
3.50	-0.2606	0.6377	0.6597	0.5063	0.7043
4.00	-1.0050	0.3600	0.3642	0.2745	0.3882
5.00	-2.3207	0.1193	0.1187	0.0907	0.1252
6.00	-3.3702	0.0455	0.0455	0.0366	
8.00		0.0100	0.0103	0.0093	
11.00		0.0024	0.0025	0.0023	
15.00		0.0007	0.0007	0.0007	(0.0007) ^b
20.00		0.0002	0.0002	0.0002	(0.0002) ^b

^aPositive dipole moment is defined as $C^{\cdot\cdot}H^+$.

^bThe HF configuration for the $C^2\Sigma^+$ state does not dissociate correctly to the atomic limits of $C(3P)$ and $H(2S)$. It dissociates to an admixture of $C(3P)$, $C(1S)$, and $H(2S)$, all of these states are electrically neutral.

Table IV
Properties of Low-lying Electronic States of CH

Property		$X^2\Pi$	$a^4\Sigma^-$	$A^2\Delta$	$B^2\Sigma^-$	$C^2\Sigma^+$
R_e (bohrs)	extended CI	2.113	2.053	2.083	2.216	2.100
	SCF	2.085	2.023	2.046	2.151	2.049
	expt'l ^a	2.116		2.082	2.200	2.105
D_o^0 (eV)	extended CI	3.33	2.64	1.72	0.11	0.61
	SCF	2.29	2.56	1.14	b	-0.26
	expt'l ^a	3.45		1.83	0.26	0.77
Dipole C^-H^+ (debyes)	extended CI	1.450	0.663	0.904	1.389	0.955
	SCF	1.619	0.541	0.872	1.444	0.889
	expt'l ^c	1.46±0.06				
$-\langle V \rangle / \langle T \rangle$	extended CI	2.00006	1.99994	1.99999	1.99987	1.99985
	SCF	1.99999	2.00001	1.99995	1.99993	1.99985
	expt'l ^d	2.00000	2.00000	2.00000	2.00000	2.00000
Total Hellman-Feynman force (a.u.) ^e	extended CI	0.02	-0.06	-0.07	-0.04	-0.05
	SCF	0.03	-0.02	-0.02	-0.02	-0.02
	expt'l ^d	0.00	0.00	0.00	0.00	0.00
Gradient of electric field at carbon nucleus (a.u.)	extended CI	0.943	-0.234	-0.209	-0.493	-0.187
	SCF	0.972	-0.187	-0.152	-0.437	-0.075
	expt'l					
Gradient of electric field at hydrogen nucleus (a.u.)	extended CI	-0.237	-0.309	-0.294	-0.220	-0.285
	SCF	-0.258	-0.331	-0.323	-0.261	-0.322
	expt'l					
Quadrupole w.r.t. the center of mass (a.u.)	extended CI	-0.693	2.079	2.584	2.820	2.806
	SCF	-0.831	1.912	2.481	2.852	2.669
	expt'l					
$-10^6 \chi^L$ (a.u.) w.r.t. the center of electronic charge	extended CI	172.8	165.2	173.7	177.8	179.0
	SCF	172.1	163.0	171.5	175.0	176.3
	expt'l					
$-10^6 \chi^L_H$ (a.u.)	extended CI	69.5	69.8	68.2	64.1	67.4
	SCF	70.2	71.0	69.2	65.2	68.9
	expt'l					
$-10^6 \chi^L_C$ (a.u.)	extended CI	269.4	269.9	269.2	269.0	268.9
	SCF	269.3	269.8	269.2	269.0	268.8
	expt'l					

Table IV - Continued

^aTaken from Reference 4.

^bNo vibrational state exists in the HF potential curve for the $B^2\Sigma^-$ state.

^cSee Reference 3.

^dTheoretical results.

^eAttractive force towards hydrogen nucleus is positive.

Table V
Variation of Quadrupole Moment^a With R^{b,c}

R	X ² _Π	a ⁴ _{Σ⁻}	A ² _Δ	B ² _{Σ⁻}	C ² _{Σ⁺}
1.00	-0.8562	0.8146	0.9959	0.8698	1.1523
1.30	-0.8590	1.0535	1.2841	1.2006	1.4420
1.60	-0.7953	1.3875	1.6849	1.6503	1.8613
1.90	-0.7358	1.8238	2.2171	2.2305	2.3937
2.00	-0.7149	1.9884	2.4149	2.4286	2.5951
2.05	-0.7049	2.0738	2.5167	2.5253	2.6992
2.10	-0.6956	2.1609	2.6200	2.6192	2.8053
2.15	-0.6869	2.2496	2.7243	2.7092	2.9131
2.20	-0.6789	2.3397	2.8292	2.7941	3.0219
2.30				2.9436	
2.40	-0.6583	2.7091	3.2419	3.0612	3.4526
2.70	-0.7022	3.2502	3.7335	3.2367	3.8477
3.00	-0.7764	3.6660	3.9055	3.1220	3.3692
3.25				2.9204	2.0342
3.50	-0.9402	3.5480	3.5853	2.7107	0.2535
4.00	-1.0720	3.0540	3.1019	2.4060	-2.0143
5.00	-1.1047	2.4053	2.5408	2.1540	-2.7150
6.00	-1.0398	2.1412	2.3126	2.0580	-2.4087
8.00	-0.9828	1.9750	2.1587	1.9679	-2.1966
11.00	-0.9661	1.9258	2.1090	1.9254	-2.1558
15.00	-0.9586	1.9114	2.0937	1.9110	-2.1392
20.00	-0.9562	1.9063	2.0882	1.9058	-2.1330

^aWith respect to the center of mass.

^bAll quantities are in atomic units.

^cCalculated from the "extended CI" wavefunctions of Reference 1.

Table VI
Electric Field Gradient at the C Nucleus^{a,b}

R	$X^2\Pi$	$a^4\Sigma^-$	$A^2\Delta$	$B^2\Sigma^-$	$C^2\Sigma^+$
1.00	1.1468	-0.4047	-0.3773	-0.6262	-0.3393
1.30	1.3721	-0.0098	0.0327	-0.1639	0.0707
1.60	1.2628	-0.0404	0.0085	-0.1702	0.0464
1.90	1.0754	-0.1609	-0.1145	-0.2989	-0.0786
2.00	1.0123	-0.2084	-0.1648	-0.3550	-0.1310
2.05	0.9813	-0.2328	-0.1910	-0.3849	-0.1586
2.10	0.9509	-0.2576	-0.2180	-0.4161	-0.1869
2.15	0.9212	-0.2827	-0.2457	-0.4484	-0.2162
2.20	0.8921	-0.3082	-0.2740	-0.4819	-0.2464
2.30				-0.5520	
2.40	0.7829	-0.4130	-0.3940	-0.6252	-0.3767
2.70	0.6432	-0.5801	-0.5949	-0.8379	-0.6183
3.00	0.5442	-0.7620	-0.8015	-1.0156	-0.7013
3.25				-1.1235	-0.4431
3.50	0.4680	-1.0546	-1.0648	-1.1948	0.0556
4.00	0.4772	-1.2115	-1.1779	-1.2624	0.8185
5.00	0.5820	-1.2908	-1.2360	-1.2964	1.2047
6.00	0.6331	-1.3015	-1.2448	-1.3020	1.2481
8.00	0.6503	-1.3032	-1.2462	-1.3032	1.2677
11.00	0.6517	-1.3032	-1.2466	-1.3032	1.2699
15.00	0.6517	-1.3032	-1.2466	-1.3032	1.2699
20.00	0.6517	-1.3032	-1.2466	-1.3032	1.2699

^aAll quantities are in atomic units.

^bCalculated from the "extended CI" wavefunctions of Reference 1.

Table VII
Electric Field Gradient at the H Nucleus^{a,b}

R	$X^2\Pi$	$a^4\Sigma^-$	$A^2\Delta$	$B^2\Sigma^-$	$C^2\Sigma^+$
1.00	-7.3467	-7.5583	-7.5843	-7.6299	-7.5869
1.30	-2.7150	-2.8227	-2.8408	-2.8699	-2.8435
1.60	-1.0885	-1.1451	-1.1599	-1.1833	-1.1656
1.90	-0.4493	-0.4807	-0.4929	-0.5128	-0.4989
2.00	-0.3336	-0.3600	-0.3717	-0.3910	-0.3770
2.05	-0.2869	-0.3112	-0.3228	-0.3418	-0.3278
2.10	-0.2463	-0.2688	-0.2803	-0.2991	-0.2850
2.15	-0.2110	-0.2319	-0.2433	-0.2620	-0.2478
2.20	-0.1803	-0.1998	-0.2112	-0.2298	-0.2156
2.30				-0.1781	
2.40	-0.0927	-0.1078	-0.1192	-0.1400	-0.1245
2.70	-0.0280	-0.0386	-0.0490	-0.0709	-0.0613
3.00	0.0000	-0.0068	-0.0300	-0.0414	-0.0359
3.25				-0.0323	-0.0235
3.50	0.0126	-0.0113	-0.0192	-0.0253	-0.0141
4.00	0.0115	-0.0101	-0.0126	-0.0150	-0.0036
5.00	0.0043	-0.0047	-0.0056	-0.0057	0.0015
6.00	0.0015	-0.0023	-0.0026	-0.0025	0.0017
8.00	0.0003	-0.0006	-0.0007	-0.0006	0.0006
11.00	0.0001	-0.0001	-0.0001	-0.0001	0.0001
15.00	0.0000	-0.0000	-0.0000	-0.0000	0.0000
20.00	0.0000	-0.0000	-0.0000	-0.0000	0.0000

^aAll quantities are in atomic units.

^bCalculated from the "extended CI" wavefunctions of Reference 1.

Table VIII
 Constants Obtained from Rotational Analysis^a
 ("extended CI" results)^b

State	v	$\Delta G_{v+1/2}(\text{cm}^{-1})$	$B_v(\text{cm}^{-1})$	$D_v(10^{-3}\text{cm}^{-1})$
$C^2\Sigma^+$	0	2673.79(2612.5)	14.349(14.2466)	1.55(1.555)
	1	2460.11(2370.5)	13.666(13.509)	1.61(1.67)
	2	2095.81	12.808(12.608)	1.99(2.0)
	3		11.317	4.57
$B^2\Sigma^-$	0	1695.40(1794.9)	12.542(12.645)	2.26(2.22)
	1		10.609(11.160)	6.47(3.28)
$A^2\Delta$	0	2773.40(2737.4)	14.618(14.577)	1.52(1.56)
	1	2576.47(2544.1)	13.951(13.907)	1.57(1.58)
	2	2349.47	13.223(13.182)	1.67(1.65)
	3	2077.97	12.387	1.88
	4	1734.02	11.366	2.33
	5		10.009	3.26
$a^4\Sigma^-$	0	3002.20	15.086	1.43
	1	2858.67	14.536	1.43
	2	2706.22	13.981	1.44
	3	2540.78	13.399	1.48
	4	2356.58	12.773	1.56
	5		12.069	1.69
$X^2\Pi$	0	2722.02(2732.50)	14.208(14.190)	1.44(1.43)
	1	2557.98(2606.46)	13.605(13.655)	1.46(1.39)
	2	2432.52	13.030(13.122)	1.40(1.39)
	3	2320.26	12.522	1.36
	4	2197.76	12.008	1.37
	5		11.481	1.36

^aExperimental values taken from Reference 4 are given in parentheses.

^bCalculated from the "extended CI" wavefunctions of Reference 1.

Table IX
Derived Spectroscopic Constants
("extended CI" results)^{a,b}

State	Zero-point energy	ν_{00}^c	ω_e	$\omega_e x_e$	B_e	α_e
$C^2\Sigma^+$	1403.1 (1381.7)	32406.7 (31778.1)	2887.5 (2840.2)	106.8 (125.9 ₆)	14.763 (14.603)	0.771 (0.7185)
$B^2\Sigma^-$	1015.1 (~1068)	25854.9 (25698.2)	2141.7 ^d (~2250) ^e	223.2 ^d (~229) ^e	13.51 (13.3 ₉)	1.933 (1.4 ₉)
$A^2\Delta$	1454.4 (1418.1)	23590.6 (23217.5)	2970.3 (2930.7)	98.5 (96.65)	14.976 (14.934)	0.697 (0.697)
$a^4\Sigma^-$	1555.4	5395.5	3145.7	71.8	15.364	0.553
$X^2\Pi$	1424.9 (1415.5)	0.0	2886.1 (2858.5)	82.0 (63.0)	14.498 (14.457)	0.589 (0.53 ₄)

^aAll quantities are given in cm^{-1} .

^bExperimental values taken from Reference 4 are given in parentheses.

^cRefer to $v = 0$ vibrational state of $X^2\Pi$.

^dSince only two vibrational levels are obtained in the CI calculations, ω_e and $\omega_e x_e$ for the $B^2\Sigma^-$ state are derived from $\Delta G_{1/2}$ and computed zero-point energy.

^eObtained from the values for CD (see Reference 4) according to the isotope relations.

Table X

Transition Dipole Matrix Elements $\langle v'K' | \mu(R) | v''K'' \rangle$ for the $X^2\Pi$ State in Atomic Units (e·bohr)^a

v'/v''	0	1	2	3	4	5
A. For $K' = 1$ and $K'' = 1$						
0	0.553 ^b					
1	-0.058	0.515 ^b				
2	0.003	-0.086	0.476 ^b			
3	0.000	0.005	-0.110	0.438 ^b		
4	0.000	0.001	0.009	-0.130	0.399 ^b	
5	0.000	0.000	0.001	0.015	-0.147	0.359 ^b
B. For $K' = 1$ and $K'' = 2$						
0	0.553	-0.059	0.003	0.000	0.000	0.000
1	-0.056	0.515	-0.089	0.006	0.001	0.000
2	0.002	-0.084	0.476	-0.112	0.011	0.008
3	0.000	0.005	-0.108	0.438	-0.132	0.016
4	0.000	0.001	0.008	-0.127	0.399	-0.150
5	0.000	0.000	0.001	0.014	-0.145	0.359

^aExtended CI results.

^bVibrationally averaged dipole moment.

Table XI

Transition Dipole Matrix Elements $\langle v'K' | \mu(R) | v''K'' \rangle$ for the
 $a^4\Sigma^-$ State in Atomic Units (e·bohr)^a

v'/v''	0	1	2	3	4	5
A. For $K' = 0$ and $K'' = 0$						
0	0.268 ^b					
1		0.282 ^b				
2			0.296 ^b			
3				0.311 ^b		
4					0.324 ^b	
5						0.332 ^b
B. For $K' = 0$ and $K'' = 1$						
0	0.268	0.030	-0.004	0.000	0.000	0.000
1	0.031	0.282	0.041	-0.007	0.001	0.000
2	-0.004	0.042	0.296	0.050	-0.010	0.002
3	0.000	-0.007	0.051	0.311	0.056	-0.015
4	0.000	0.001	-0.010	0.058	0.324	0.057
5	0.000	0.002	0.002	-0.015	0.060	0.332

^aExtended CI results.

^bVibrationally averaged dipole moment.

Table XII

Transition Dipole Matrix Elements $\langle v'K' | \mu(R) | v''K'' \rangle$ for the
 $A^2\Delta$ State in Atomic Units (e·bohr)^a

v'/v''	0	1	2	3	4	5
A. For $K' = 2$ and $K'' = 2$						
0	0.367 ^b					
1	0.046	0.390 ^b				
2	-0.008	0.061	0.409 ^b			
3	0.001	-0.016	0.065	0.420 ^b		
4	0.000	0.001	-0.029	0.056	0.421 ^b	
5	0.000	0.000	0.006	-0.040	0.032	0.401 ^b
B. For $K' = 2$ and $K'' = 3$						
0	0.367	0.044	-0.008	0.001	0.000	0.000
1	0.047	0.390	0.058	-0.016	0.002	0.000
2	-0.008	0.064	0.409	0.061	-0.028	0.006
3	0.001	-0.016	0.068	0.421	0.052	-0.040
4	0.000	0.001	-0.029	0.061	0.421	0.026
5	0.000	0.000	0.006	-0.041	0.037	0.400

^aExtended CI results.

^bVibrationally averaged dipole moment.

Table XIII

Transition Dipole Matrix Elements $\langle v'K' | \mu(R) | v''K'' \rangle$ for the $B^2\Sigma^-$ State in Atomic Units (e·bohr)^a

v'/v''	0	1
A. For $K' = 0$ and $K'' = 0$		
0	0.546 ^b	
1		0.513 ^b
B. For $K' = 0$ and $K'' = 1$		
0	0.546	0.014
1	0.017	0.513

^aExtended CI results.

^bVibrationally averaged dipole moment.

Table XIV

Transition Dipole Matrix Elements $\langle v'K' | \mu(R) | v''K'' \rangle$ for the $C^2\Sigma^+$ State in Atomic Units (e·bohr)^a

v'/v''	0	1	2	3
A. For $K' = 0$ and $K'' = 0$				
0	0.388 ^b			
1	0.048	0.412 ^b		
2	-0.009	0.062	0.428 ^b	
3	0.000	-0.022	0.052	0.416 ^b
B. For $K' = 0$ and $K'' = 1$				
0	0.388	0.048	-0.009	0.000
1	0.049	0.412	0.061	-0.022
2	-0.009	0.063	0.428	0.050
3	0.000	-0.022	0.053	0.416

^aExtended CI results.

^bVibrationally averaged dipole moment.

Table XV
 Line Strengths $P_{v'v''}^{K'K''}$ for Two Bands in Ground State
 Infrared Spectrum (in $10^{-3} e^2 \cdot \text{bohr}^2$)^a

K	0 - 1			1 - 2		
	P(K)	Q(K)	R(K)	R(K)	Q(K)	R(K)
1		3.34	3.52		7.47	7.85
2	3.16	3.34	3.63	7.12	7.49	8.05
3	3.09	3.36	3.73	6.97	7.51	8.27
4	3.01	3.37	3.84	6.82	7.54	8.49
5	2.94	3.39	3.96	6.68	7.58	8.73
6	2.88	3.41	4.08	6.56	7.63	8.98
7	2.82	3.44	4.21	6.44	7.69	9.23
8	2.77	3.47	4.35	6.33	7.75	9.50
9	2.72	3.50	4.49	6.23	7.82	9.78
10	2.67	3.54	4.63	6.15	7.91	10.06
11	2.63	3.58	4.78	6.06	8.00	10.36
12	2.59	3.63	4.94	6.00	8.09	10.67
13	2.56	3.68	5.10	5.94	8.20	10.99
14	2.53	3.74	5.27	5.89	8.31	11.31
15	2.51	3.80		5.84	8.43	

^aExtended CI results.

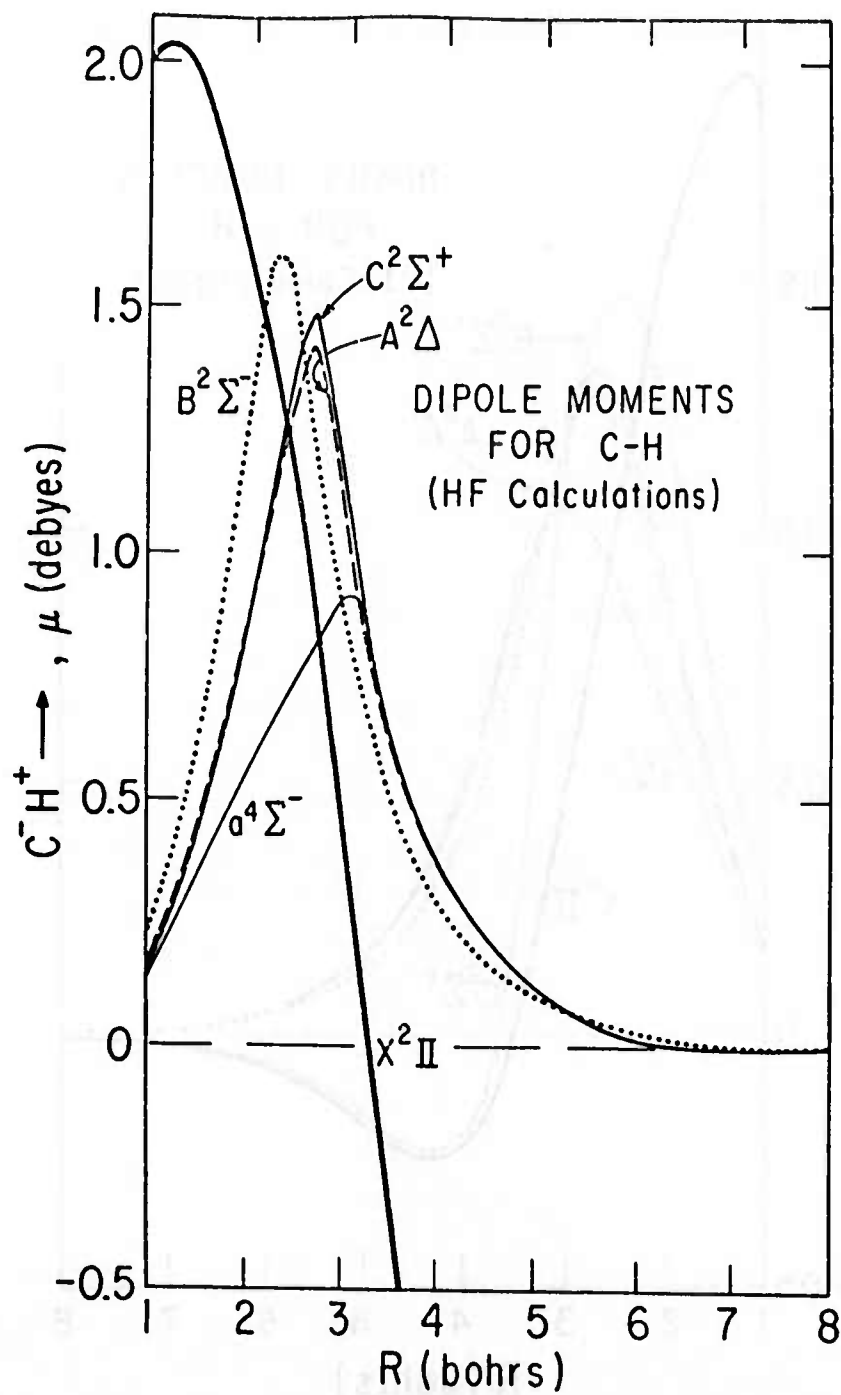
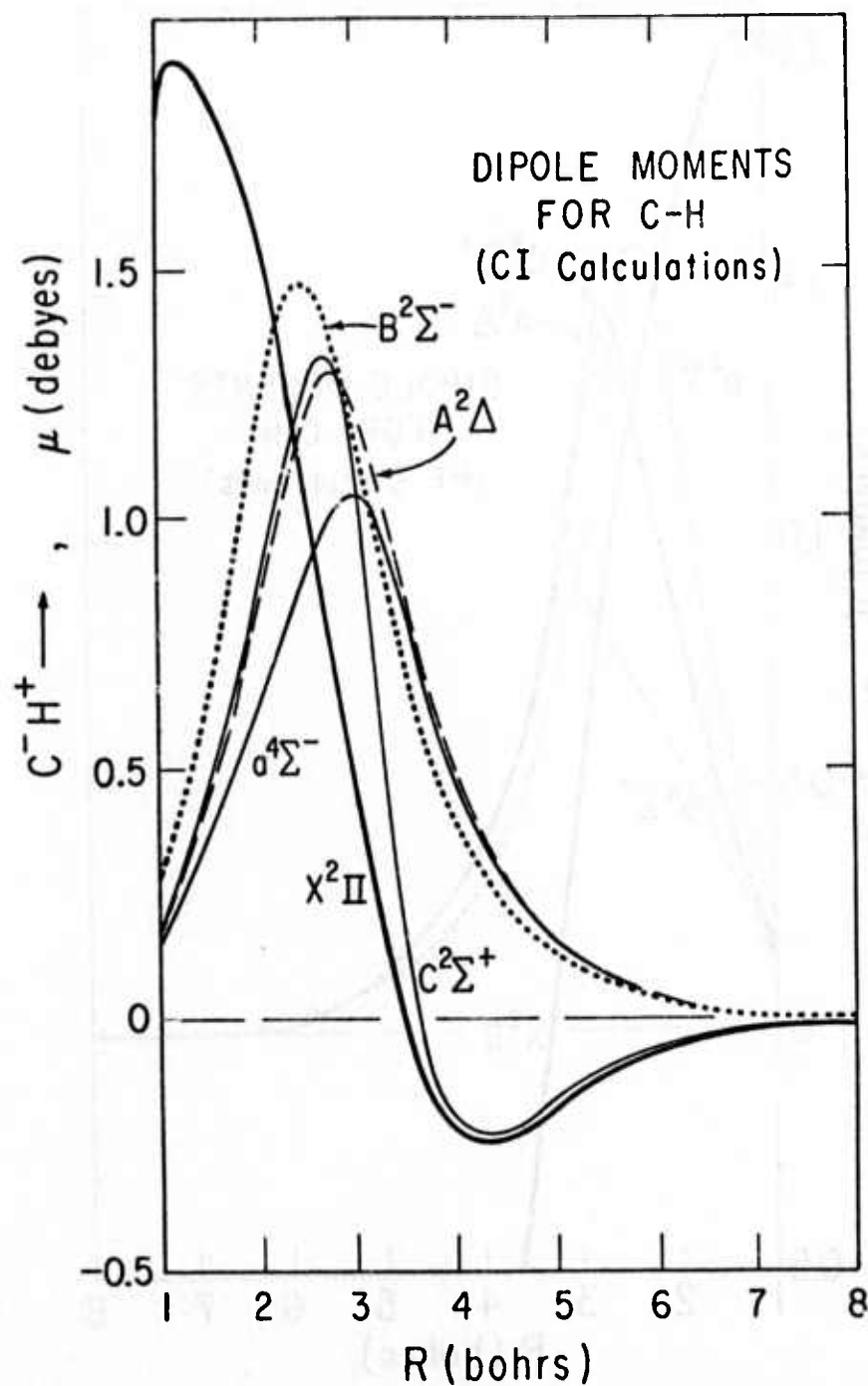


Figure 1. "Extended CI" dipole moment curves for the five lowest electronic states of CH



"Extended CI"

Figure 2. SCF dipole moment curves for the five lowest electronic states of CH

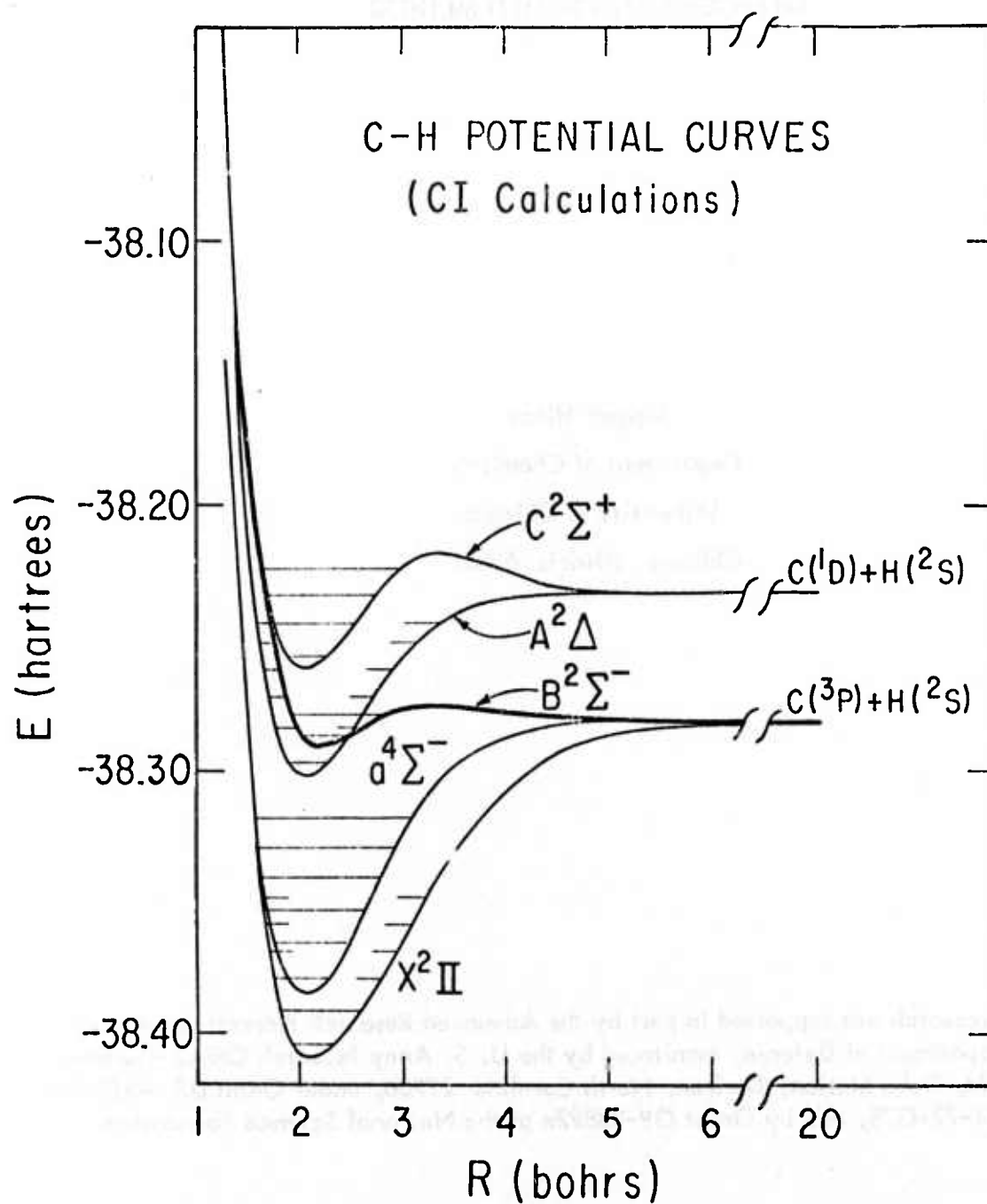


Figure 3. "Extended CI" potential curves and vibrational levels for the five lowest electronic states of CH

MC-SCF I. THE MULTI-CONFIGURATION
SELF-CONSISTENT-FIELD METHOD

Juergen Hinze
Department of Chemistry
University of Chicago
Chicago, Illinois 60637

*This research was supported in part by the Advanced Research Projects Agency of the Department of Defense, monitored by the U. S. Army Research Office-Durham, Box CM, Duke Station, Durham, North Carolina 27706, under Grant DA-ARO-D-31-124-72-G78, and by Grant GP-33892x of the National Science Foundation.

ABSTRACT

The general multi-configuration self-consistent-field (MC-SCF) method is presented with no restrictions on the types of configurations participating in the expansion of the total wave function. The general coupled Fock like equations for the "best" orbitals to be used in such a multi-configuration wave function are derived. Formally these coupled nonlinear equations are decoupled with the use of projection operators and transformed into a pseudo eigenvalue problem. Several general methods, based on orbital transformations and on the use of the generalized Brillouin theorem, are presented for solving the coupled nonlinear Fock like equations for the determination of the MC-SCF orbitals. The formalism presented is applicable not only to the ground state of a given system, but also to any excited state, yielding an upper bound to the true energy of the desired state.

Introduction

In the MC-SCF model the total wave function is determined by optimizing variationally the configuration expansion coefficients in a many configurational wave function, as well as all the one particle functions, the orbitals, which are used to construct the configurations. Clearly, the use of a many configurational function, with no restriction on the type and number of configurations, permits an arbitrarily close approximation to the exact wave function. It is well known, however, that a many configurational function frequently requires an excessively large number of configurations to obtain a reasonably accurate wave function if only the configuration expansion coefficients are optimized variationally. The idea of the MC-SCF method is to reduce the number of configurations required, by simultaneously optimizing variationally also all the single particle functions. This idea of the MC-SCF method traces back to the early years of quantum mechanics.¹ Early MC-SCF calculations for atoms were carried out by Hartree² and later by Jucys,³ who also introduced many simplifying approximations. The method was first applied to diatomic molecules by Das and Wahl⁴ and more recently has been developed and applied by many others to atoms and molecules.⁵ By now the method has been sufficiently generalized and refined, the initial numerical difficulties in solving the orbital equations have been overcome, making the routine calculations of MC-SCF wave functions only little more cumbersome than a standard Hartree-Fock calculation. It has been demonstrated that the resulting wave functions, with a reasonably small number of configurations, are of high accuracy. With this it can be expected that the MC-SCF model will enjoy renewed and growing interest.

It is the purpose of the present series of articles to (1) present the MC-SCF formalism in its fully general form, as we have developed it; (2) present methods developed for solving the orbital equations; (3) describe in detail the necessary complications in the formulae when symmetry is introduced explicitly, in order to make the actual computations more efficient; (4) explain the procedures by which excited state wave functions can be obtained, such that they give the expectation value of the energy as a true upper bound to the excited state, even though there are lower states of the same irreducible representation; (5) compare the MC-SCF method to other methods used to obtain correlated wave functions; (6) discuss several alternatives for the selection of configurations which participate in the total wave functions; (7) derive the formulae which permit the incorporation of a pseudo potential method, i.e. Frozen Core Approximation, into the MC-SCF formalism; (8) discuss the applicability of the MC-SCF approach to semi-empirical MO theories useful for large organic molecules; (9) present results of detailed molecular calculations of ground and excited states using the MC-SCF methods.^{5,6}

General MC-SCF Formalism.

The basis of an MC-SCF wave function for an N particle system⁶ is a set of m spin orbitals

$$\{\psi_1, \psi_2 \dots \psi_m\} \quad \text{with } m > N, \quad (1)$$

which may be chosen orthonormal, i.e.

$$\langle \psi_i | \psi_j \rangle = \delta_{ij}. \quad (2)$$

This orthonormality constraint represents no loss of generality, since it does not affect the total space spanned by the orbitals ψ ; it may however result in the need for more configurations in order to give a total wave function of specific quality.

From these orbitals antisymmetrized N -electron functions are constructed as Slater Determinants (SD's),

$$\Phi_I = \Phi_{(i_1, i_2 \dots i_N)} = \frac{1}{\sqrt{N!}} \det \{ \psi_{i_1}(1) \psi_{i_2}(2) \dots \psi_{i_N}(N) \} \quad (3)$$

with the restriction $i_1 < i_2 < \dots < i_N$, in order not to construct redundant SD's.

From the total m dimensional single particle space spanned by the orbitals, we obtain a total of $M = \binom{m}{N}$ linearly independent SD's, which are mutually orthonormal

$$\langle \Phi_I | \Phi_J \rangle = \delta_{IJ} \quad (4)$$

due to the orthonormality of the basis orbitals and the definition of the SD's. These

SD's span the total available M dimensional N -particle space. A linear transformation of the basis orbitals by a non singular $m \times m$ matrix A will result in a linear transformation of the N -particle basis functions, the SD's, by a non singular $M \times M$ matrix B , clearly leaving the N -particle space spanned by the SD's invariant. Thus the original choice of ortho normal orbitals represents no restriction.

In the MC-SCF model, as in a normal configuration interaction model, the total wave function of a given state K is expressed as a linear combination of these SD's,

$$\Psi_K = \sum_I \Phi_I C_{IK} \quad (5)$$

Orthonormality of the total electronic state functions demands that the configuration expansion coefficients C_{IK} form a unitary matrix, C , which is obtained variationally by solving the conventional configuration interaction eigenvalue problem

$$(H - E) C = 0 \quad (6)$$

with E the diagonal energy matrix and H defined by the elements

$$H_{IJ} = \langle \Phi_I | \mathcal{H} | \Phi_J \rangle, \quad (7)$$

where \mathcal{H} is the total Hamiltonian, which may be decomposed into sums of one and two electron operators

$$H = \sum_i^N h(i) + \sum_{i>j}^N g(i,j), \quad (8)$$

Clearly, had we used in eq. 5 for the description of the total wave function the totality of M SD's, which span the entire N -particle space available with m fixed spin orbitals, the solution of eq. 6 would yield the best possible energies E_K and Ψ_K within this restricted space.

In general, however, we do not wish to do this, because in order to get a good description of the state functions Ψ_K we will require a large number of spin orbitals, and if m is large, M and with it the computational labor to solve eq. (6) become excessive. It is therefore desirable to restrict the number of spin orbitals to a small number, and if possible to restrict the configuration expansion such that not all possible SD's are used. The idea of the MC-SCF method is to arrive at equations for the determination of the "best" orbitals to be used in the restricted expansion of the wave function, eq. (5). "Best" is used here in the sense that the "best" orbitals will yield the lowest possible eigenvalue E_K for a state K in a particular restricted expansion of the wave function into SD's. Clearly the Hartree-Fock method is a special case within the MC-SCF model, with the restriction $m = N$ and thus $M = 1$.

It is clear that the use of symmetry can reduce and simplify the configuration interaction problem, as well as the problem of determining the orbitals. However, the explicit use of symmetry would complicate the notation unnecessarily; therefore we will discuss symmetry after the general theory has been developed.

To arrive at the orbital equations of the MC-SCF model in a reasonable and compact form, it is convenient to make use of the language of second quantization.

From this we will use the creators a^+ and annihilators a , which we will define here, in order to clarify the notation to be used.

The action of the annihilator a_i , associated with the spin orbital ψ_i on an SD is defined here as

$$a_i \Phi = a_i \Phi(i_1 i_2 \dots i_N) = \begin{cases} 0 & \text{if } i \notin (i_1 i_2 \dots i_N) \\ (-1)^{N-k} \Phi(i_1 \dots i_{k-1} i_{k+1} \dots i_N) & \text{if } i = i_k \end{cases} \quad (9)$$

where $\Phi(i_1 \dots i_{k-1} i_{k+1} \dots i_N)$ is a normalized $N-1$ particle SD, which is obtained from Φ deleting row N and column k containing $\psi_{i_k} = \psi_i$.

Note here that the given definition of the annihilator acting on an SD deviates somewhat from the conventional definition in second quantization,⁷ where creators and annihilators are defined to act on state vectors specifying orbital occupation numbers, rather than of wave functions or SD's. In the definition given here the annihilator, a_i , is to be understood as an integral operator

$$a_i = \sqrt{N} \int d(N) \psi_i^*(N) \quad (10)$$

while the creator, a_i^+ , the Hermitian conjugate to a_i , acting on an $N-1$ particle SD should be presented as

$$a_i^+ \Phi(i_1, i_2, \dots, i_{N-1}) = \begin{cases} 0 & \text{if } i = (i_1, i_2, \dots, i_{N-1}) \\ (-1)^{N-k+1} \Phi(i_1, \dots, i_k, i, i_{k+1}, \dots, i_{N-1}) & \text{if } i_k < i < i_{k+1}. \end{cases} \quad (11)$$

Clearly the creators and annihilators defined in this way are linear operators and satisfy the conventional anti-commutation relations.

Using the definition of a_i in eq. (9), it can be seen readily that

$$\Phi = \frac{1}{\sqrt{N}} \sum_i^m \psi_i(N) a_i^+ \Phi \quad (12)$$

is nothing but the expansion of the SD Φ along its N 'th row.

Since creation and annihilation operators are linear, we have

$$\Psi = \frac{1}{\sqrt{N}} \sum_i^m \psi_i(N) a_i^+ \Psi. \quad (13)$$

Similarly we have

$$\Phi = \frac{1}{\sqrt{N(N-1)}} \sum_{i,j}^m \psi_i(N) \psi_j(N-1) a_i^+ a_j^+ \Phi, \quad (14)$$

and

$$\Psi = \frac{1}{\sqrt{N(N-1)}} \sum_{i,j}^m \psi_i(N) \psi_j(N-1) a_i^+ a_j^+ \Psi. \quad (15)$$

We are now in a position to write down the energy matrix elements using the Hamiltonian, eq. (8), such that the orbital dependence appears explicitly, suitable for the application of the variational principle with respect to an orbital variation.

We obtain for eq. (7)

$$\begin{aligned} \langle \Phi_I | \mathcal{H} | \Phi_J \rangle &= \sum_{ij}^m \langle \psi_i(1) | h(1) | \psi_j(1) \rangle \langle \Phi_I | a_i^\dagger a_j | \Phi_J \rangle \\ &+ \frac{1}{2} \sum_{ijkl}^m \langle \psi_i(1) \psi_k(2) | g(12) | \psi_j(1) \psi_l(2) \rangle \\ &\langle \Phi_I | a_i^\dagger a_k^\dagger a_l a_j | \Phi_J \rangle, \end{aligned} \quad (16)$$

and for the expectation value of the energy for a particular state $\Psi_K \equiv \Psi$ we get

$$\begin{aligned} \langle \Psi | \mathcal{H} | \Psi \rangle &= \sum_{ij}^m \langle \psi_i | h | \psi_j \rangle \langle \Psi | a_i^\dagger a_j | \Psi \rangle \\ &+ \frac{1}{2} \sum_{ijkl} \langle \psi_i \psi_k | g | \psi_j \psi_l \rangle \langle \Psi | a_i^\dagger a_k^\dagger a_l a_j | \Psi \rangle. \end{aligned} \quad (17)$$

In the above and following, we always focus on one particular state K only, and we have therefore dropped the state index.

In eq. (17) we can identify the first order reduced density matrix elements in the space spanned by the orbitals

$$\gamma_{ij} = \langle \Psi | a_i^\dagger a_j | \Psi \rangle, \quad (18)$$

and the second order reduced density matrix element

$$\Gamma_{ij, kl} = \langle \Psi | a_i^\dagger a_k^\dagger a_l a_j | \Psi \rangle. \quad (18a)$$

Thus eq. (17) may be rewritten as

$$\langle \Psi | \mathcal{H} | \Psi \rangle = \sum_{ij}^m \left[\langle \psi_i | h | \psi_j \rangle \gamma_{ij} + \frac{1}{2} \sum_{kl}^m \langle \psi_i \psi_k | g | \psi_j \psi_l \rangle \Gamma_{ij, kl} \right]. \quad (17a)$$

Before we proceed to apply the variational principle to eq. (18), we have to add the restrictive conditions

$$\langle \psi_i | \psi_j \rangle = \delta_{ij}$$

multiplied with as yet unknown Lagrangian multipliers to arrive at a functional, which may be varied without further constraints,

$$\delta \sum_{ij}^m \left[\langle \psi_i | h | \psi_j \rangle \gamma_{ij} + \frac{1}{2} \sum_{kl}^m \langle \psi_i \psi_k | g | \psi_j \psi_l \rangle \Gamma_{ij, kl} - \langle \psi_i | \psi_j \rangle \epsilon_{ij} \right] = 0. \quad (19)$$

The variation with respect to ψ_i yields

$$\begin{aligned}
& \sum_i^m \left[\langle \delta \psi_i | h | \psi_i \rangle \gamma_{ii} - \langle \delta \psi_i | \psi_i \rangle \epsilon_{ii} \right] \\
& \quad \frac{1}{2} \sum_{i,k,l}^m \left[\langle \delta \psi_i \psi_k | g | \psi_i \psi_l \rangle + \langle \psi_k \delta \psi_i | g | \psi_l \psi_i \rangle \right] \Gamma_{ii,kl} \\
& \quad + \text{c.c.} = 0.
\end{aligned} \tag{20}$$

Note that $\Gamma_{ii,kl} = \Gamma_{kl,ii}$.

We may now set the part which has been written out explicitly equal to zero independently of the part which is abbreviated by c.c. This has to hold for any $\delta \psi_i$; thus we get the Fock like equations for the determination of ψ 's,

$$\sum_i^m \left[h \gamma_{ii} + \sum_{k,l}^m U_{kl} \Gamma_{ii,kl} \right] \psi_i = \sum_i \psi_i \epsilon_{ii}, \tag{21}$$

with

$$U_{kl} = \int d(2) \psi_k^*(2) g(1,2) \psi_l(2). \tag{22}$$

Since $\gamma_{ij} = \gamma_{ji}^*$ and $\Gamma_{ij,kl} = \Gamma_{ji,lk}^*$ it can be shown readily that $\epsilon_{ij} = \epsilon_{ji}^*$.

The Fock like orbital equations of the MC-SCF model, in abbreviated form

$$\sum_i^m F_{ij} \psi_i = \sum_i^m \psi_i \epsilon_{ji} \tag{21a}$$

are coupled explicitly on right and left hand side. This coupling may be removed, at least formally using conventional projection operator techniques yielding a pseudo-eigenvalue equation

$$G \psi_i = \epsilon_{ii} \psi_i \quad (23)$$

with the Hermitian operator

$$G = \frac{1}{2} \sum_i (G_i + G_i^\dagger), \quad (24)$$

with

$$G_i = \left[1 - \sum_{k=1}^m |\psi_k\rangle \langle \psi_k| \right] \sum_{j=1}^m F_{ij} |\psi_j\rangle \langle \psi_j|. \quad (25)$$

The method for solving these orbital equations requires some close scrutiny. Solving the pseudo-eigenvalue equation (23) does not appear promising for two reasons:

a) the equation is of seventh order in the unknown orbitals (normal Fock equations are third order), thus it is unlikely that conventional iterative solutions of these SCF equations will converge; b) there is no unique way of assigning the solution functions of eq. (23) to the desired orbitals, except of using those with maximum overlap with the input orbitals used in constructing G .

More promising, and in practice successful, is the solution of the Fock like eq. (21) directly, based on the fact that enforcing the Hermiticity of the Lagrange multiplier matrix, i.e.

$$\epsilon_{ij} = \epsilon_{ji}^* \quad (26)$$

is a necessary and sufficient condition for eq. (21) to be satisfied. However, this method for solving the orbital equations appears to require the expansion of the orbitals into basis functions with a transformation of the relevant equations into matrix form. We will discuss this method in the next section.

Methods for Solving the Orbital Equations

In the following discussion we will restrict ourselves to the solutions of the orbital equations in the basis function expansion form, since we are not aware of a generally convergent procedure for solving the orbital equations, eq. (21) or eq. (25) in their coordinate representation. The total, available one particle space will be spanned by a set of m selected, linearly independent basis functions

$$\{x_1 \dots x_m\} \quad (27)$$

which may not be orthonormal, i.e. the matrix elements

$$\langle x_p | x_q \rangle = S_{pq} \quad (28)$$

are the elements of the overlap matrix \underline{S} , which is the matrix of this one particle space.

As indicated above, we may, without loss of generality transform this basis to an orthonormal one by the linear transformation

$$\{\psi_1 \dots \psi_m\} = \{x_1 \dots x_m\} \underline{C} \quad (29)$$

for which we have

$$\langle \psi_i | \psi_j \rangle = \delta_{ij}, \quad (30)$$

provided

$$\underline{C}^+ \underline{S} \underline{C} = \underline{1}. \quad (31)$$

These initial guess orbitals, $\psi_1 \dots \psi_m$, will in general not satisfy eq. (21). What we are looking for is a new set of orbitals, connected to the initial guessed set by a unitary transformation

$$\{\psi'_1 \dots \psi'_m\} = \{\psi_1 \dots \psi_m\} U, \quad (32)$$

such that the orbital equations for the primed set

$$\sum_i^m F_{ij}' \psi_i' = \sum_i^m \psi_i' \epsilon_{ji}' \quad (33)$$

are satisfied. Procedures of this type for solving SCF or MC-SCF equations have been described by Rossi⁹ and Levy.¹⁰ We will give a more general discussion.

A unitary transformation is all the freedom we have in the space spanned by our one particle functions, the orbitals. It should be noted, however, that this is really no restriction beyond the initial one, due to the selection of a finite set of basis functions. One may always make m sufficiently large; this does not require that we need to use more orbitals in the total wave function. In fact, generally only the first few $n < m$ orbitals will be used, be occupied, in the total wave function. However, there is no need to restrict our sums to n in eq. (33), since F_{ij}' will go to zero due to the definition of the first and second order reduced density matrix elements, eq. (18) and (19), once i or j is larger than n . Thus we may say our m dimensional one particle space is divided into an occupied $\{\psi_1 \dots \psi_n\}$ and an empty $\{\psi_{n+1} \dots \psi_m\}$ part. The unitary transformation, eq. (32), which we are to choose such that eq. (33) is satisfied, will have three

domains, transformations (1) between occupied orbitals, (2) between occupied and empty orbitals and (3) between empty orbitals. The last one will not affect the wave function.

The necessary and sufficient conditions for eq. (33) to be satisfied are

$$\epsilon_{ji}' - \epsilon_{ij}' = 0 \quad \text{with } j > i \quad (34)$$

This becomes clear once one notices that

$$\epsilon_{ji}' - \epsilon_{ij}' = \partial E / \partial u_{ij} = \langle (a_i^\dagger a_j - a_j^\dagger a_i) \Psi | \mathcal{H} | \Psi \rangle$$

must become equal to zero for a wave function built from MC-SCF orbitals. The later expression is for the generalized Brillouin theorem applicable to MC-SCF wave functions.

This leads with

$$\epsilon_{ji}' = \sum_k^m \langle \psi_i' | F_{ik}' | \psi_k' \rangle,$$

to

- (1) i and j part of the occupied set

$$\sum_k^n (\langle \psi_i' | F_{ik}' | \psi_k' \rangle - \langle \psi_j' | F_{jk}' | \psi_k' \rangle) = 0 \quad (35)$$

- (2) j part of the empty set, i part of the occupied set

$$\sum_k^n \langle \psi_i' | F_{ik}' | \psi_k' \rangle = 0 \quad (36)$$

- (3) i and j part of the empty set gives nothing, and is not required, since transformations of type (3) leave the wave function unaffected.

Eq. (35) and (36) give us just enough conditions for the determination of the independent variables of interest in the desired unitary matrix \underline{U} of eq. (32). However, it is sufficient, for ease of notation, to deal only with eq. (35), since it

contains eq. (36) as a special case provided the sum over k is extended to m and we observe $F_{ij} = 0$ if i or j is part of the empty set. One way of solving eq. (35) is to perform repeated 2×2 rotations, similar to the Jacobi procedure for matrix diagonalization. This will be described later. An alternative is to write the unitary matrix such that its independent variables are expressed explicitly, solving for these variables. This could be done using the generalized Eulerian angles,¹¹ but we will not pursue this, since it would lead to rather untractable nonlinear equations. Easier and followed here is to approximate the unitary matrix as

$$\tilde{U} = \tilde{1} + \tilde{D} \quad (37)$$

which is good to second order in terms of \tilde{D} , provided \tilde{D} is antisymmetric. Using this approximation, which requires that the guessed, unprimed set of orbitals is reasonably close, and neglecting the change of the Fock operators, F_{ij} , i.e. the potential, for the determination of \tilde{D} , we get

$$\begin{aligned} \epsilon_{jj}' - \epsilon_{ii}' &\cong \sum_k (\langle \psi_j' | F_{ik} | \psi_k' \rangle - \langle \psi_i' | F_{jk} | \psi_k' \rangle) \\ &= \sum_k \sum_{mn} (u_{mj} \langle \psi_m | F_{jk} | \psi_n \rangle - u_{mi} \langle \psi_m | F_{ik} | \psi_n \rangle) u_{nk} \\ &\cong \sum_k \{ \langle \psi_j | F_{ik} | \psi_k \rangle - \langle \psi_i | F_{jk} | \psi_k \rangle \\ &\quad + \sum_m [d_{mj} \langle \psi_m | F_{ik} | \psi_k \rangle - d_{mi} \langle \psi_m | F_{jk} | \psi_k \rangle \\ &\quad + (\langle \psi_j | F_{ik} | \psi_m \rangle - \langle \psi_i | F_{jk} | \psi_m \rangle) d_{mk}] \} \\ &\quad + O(d^2) = 0 \end{aligned} \quad (38)$$

Keeping in mind that $d_{ij} = -d_{ji}$, neglecting terms of order d^2 , and collecting terms we get a set of linear equations for the non redundant d_{ij} 's of the type

$$\sum_{mn} M_{ij,mn} d_{mn} = g_{ij} \quad (39)$$

with ij and mn as composite column and row indices of the matrix \tilde{M} , with the restrictions $i > j$; $m > n$, j and n not part of the empty set.

Defining

$$|f_i\rangle = \sum_k F_{ik} |\psi_k\rangle \quad (40)$$

we obtain

$$g_{ij} = \langle \psi_i | f_i \rangle - \langle \psi_j | f_i \rangle \quad (41)$$

and

$$\begin{aligned} M_{ij,mn} = & \delta_{mi} \langle \psi_n | f_j \rangle + \delta_{nj} \langle \psi_m | f_i \rangle - \delta_{ni} \langle \psi_m | f_j \rangle \\ & - \delta_{mj} \langle \psi_n | f_i \rangle - \langle \psi_j | F_{im} | \psi_n \rangle + \langle \psi_i | F_{jm} | \psi_n \rangle \\ & + \langle \psi_j | F_{in} | \psi_m \rangle - \langle \psi_i | F_{jn} | \psi_m \rangle. \end{aligned} \quad (42)$$

Since we have neglected the change of the Fock operators, F_{ij} , with the orbital transformation, and since we have neglected terms of second order in d in eq. (38) and (37), it will be necessary to iterate to convergence (however, see below), as in the conventional method of solving Hartree Fock equations.

Solving eq. (39) may become rather cumbersome, since there are a large number, $n(n-1)/2 + n(m-n)$, of unknowns if the number of occupied orbitals, n , and the total number of orbitals, m , becomes large. To avoid solving eq. (39) directly we may a) neglect the elements which couple the different d_{ij} 's, i.e. $M_{ij,mn} = 0$ unless $ij = mn$, or b) treat those coupling elements as small, as they should be relative to the diagonal elements of \underline{M} .

a.) Neglect of coupling between d_{ij} 's leads to

$$d_{ij} = g_{ij}/M_{ij,ij}. \quad (43)$$

This process, described by Levy¹⁰, is extremely simple, and we have used it.

However, in order to obtain convergence in solving the Fock like equations using eq. (43) it is frequently necessary to resort to sophisticated damping and extrapolation techniques, and even then many iterations will be required.

b.) Treating the off diagonal, coupling, elements of \underline{M} as small compared to the diagonal ones permits two different, simplified solutions of eq. (39). For this we split up \underline{M} into a diagonal matrix \underline{N} and an off diagonal one \underline{Q} with all diagonal elements zero, thus we have for eq. (39)

$$\underline{M} \underline{d} = (\underline{N} + \underline{Q}) \underline{d} = \underline{g} \quad (44)$$

or

$$\underline{d} = (\underline{N} + \underline{Q})^{-1} \underline{g} \cong (\underline{N}^{-1} - \underline{N}^{-1} \underline{Q} \underline{N}^{-1}) \underline{g} \quad (45)$$

Alternately we may solve eq. (44) iterative by writing

$$\tilde{N} \tilde{d}^{(n)} = \tilde{g} - \tilde{Q} \tilde{d}^{(n-1)} \quad (46)$$

where $\tilde{d}^{(n)}$ is the n'th iterate to the solution vector \tilde{d} . The process may be started with $\tilde{d}^{(0)} = 0$, and carried to convergence. A variant of this procedure has been used successfully in MCSCF calculations.¹² Clearly $\tilde{d}^{(1)}$ is the same as that obtained by eq. (43), and $\tilde{d}^{(2)}$ is the same as that obtained from eq. (45).

It should be noted that the process proposed here to solve the set of linear equations, eq. (39), which may become quite large, is the well known static Gauss-Seidel method.¹³ Clearly one could improve convergence by using the more efficient dynamic Gauss-Seidel method, where each element $\tilde{d}^{(n)}$ once found is used immediately on the right of eq. (46) for the determination of successive elements of $\tilde{d}^{(n)}$. The problem of possible nonconvergence of the Gauss-Seidel method which will occur if the diagonal element $M_{ij,ij}$ is small in magnitude relative to the off diagonal elements in row ij , may be overcome. Here we realize that $M_{ij,ij} \cong -\partial^2 E / \partial u_{ij}^2$, if this becomes small and $g_{ij} \cong \partial E / \partial u_{ij}$ is not small a 45° rotation between orbitals ψ_i and ψ_j will be required. Thus all one needs to do is carry out this rotation and recompute the F's and M continuing the SCF iterations. The realization that $M_{ij,ij} \cong -\partial^2 E / \partial u_{ij}^2$ permits one also to monitor the sign of $M_{ij,ij}$ and with it to determine whether a minimum or maximum in the energy is approached. To determine this definitely, however, would require one to ascertain that \tilde{M} is negative definite, which is clearly impractical due to the size of \tilde{M} . As long as the diagonal elements of \tilde{M} are dominant, it appears sufficient to assure that these elements are negative.

An alternate method of solving eq. (36) is obtained by writing

$$\tilde{U} = \prod_{i>j} U_{ij}$$

where U_{ij} is a unit matrix except for the elements $u_{ii} = u_{jj} = \cos \varphi$, $u_{ji} = -u_{ij} = \sin \varphi$ describing a plane rotation by the angle φ . Thus the process is quite similar to the Jacobi matrix diagonalization; however, different formulae yield $\sin \varphi \equiv s$ and $\cos \varphi \equiv c$, and the updating of the remaining matrix elements determining the angles is not quite as simple.

Using eq. (35) in order to determine the angle of rotation in the i, j plane we obtain, neglecting the dependence of the F 's on such a rotation.

$$\begin{aligned} \epsilon'_{ii} - \epsilon'_{jj} &\cong \sum_k (\langle \psi'_i | F_{ik} | \psi'_k \rangle - \langle \psi'_j | F_{jk} | \psi'_k \rangle) \\ &= c (\langle \psi_i | f_i \rangle - \langle \psi_j | f_j \rangle) + s (\langle \psi_i | f_j \rangle + \langle \psi_j | f_i \rangle) \\ &\quad + (1-c) [c (\langle \psi_i | F_{ii} | \psi_i \rangle - \langle \psi_j | F_{jj} | \psi_j \rangle + \langle \psi_i | F_{ij} | \psi_j \rangle - \langle \psi_j | F_{ji} | \psi_i \rangle) \\ &\quad + s (\langle \psi_i | F_{ij} | \psi_j \rangle + \langle \psi_j | F_{ji} | \psi_i \rangle + \langle \psi_i | F_{jj} | \psi_j \rangle + \langle \psi_j | F_{ii} | \psi_i \rangle)] \\ &\quad + s [c (\langle \psi_i | F_{ij} | \psi_j \rangle - \langle \psi_j | F_{ji} | \psi_i \rangle - \langle \psi_i | F_{jj} | \psi_j \rangle + \langle \psi_j | F_{ii} | \psi_i \rangle) \\ &\quad + s (\langle \psi_i | F_{ij} | \psi_j \rangle + \langle \psi_j | F_{ji} | \psi_i \rangle - \langle \psi_i | F_{jj} | \psi_j \rangle - \langle \psi_j | F_{ii} | \psi_i \rangle)] = 0 \end{aligned} \quad (47)$$

where we have used eq. (40) for the definition of $|f_i\rangle$.

Making the approximation

$$\cos \varphi = \sqrt{1 - \sin^2 \varphi} \cong 1 - 1/2 \sin^2 \varphi, \quad (48)$$

observing that all matrix elements are real and $F_{ij} = F_{ji}$; collecting terms in powers of $\sin \varphi$ and neglecting terms cubic in $\sin \varphi$, we obtain a quadratic equation for the determination of $\sin \varphi$

$$As^2 + Bs + C = 0 \quad (49)$$

with

$$A = \frac{1}{2} (\langle \psi_i | f_i \rangle - \langle \psi_i | f_i \rangle + 3 \langle \psi_i | F_{ii} | \psi_i \rangle - 3 \langle \psi_i | F_{ii} | \psi_i \rangle + 3 \langle \psi_i | F_{ii} | \psi_i \rangle - 3 \langle \psi_i | F_{ii} | \psi_i \rangle) \quad (50)$$

$$B = \langle \psi_i | f_i \rangle + \langle \psi_i | f_i \rangle + 2 \langle \psi_i | F_{ii} | \psi_i \rangle - \langle \psi_i | F_{ii} | \psi_i \rangle - \langle \psi_i | F_{ii} | \psi_i \rangle \quad (51)$$

and

$$C = \langle \psi_i | f_i \rangle - \langle \psi_i | f_i \rangle \quad (52)$$

The desired solution of eq. (49) is that which gives the smallest angle of rotation or

$$\sin \varphi = B/2A (-1 + \sqrt{1 - 4CA/B^2}) \quad (53)$$

It should be clear that it is possible to implement this method such that convergence is guaranteed. This would require that the formulae are derived such as to include the dependence of the F_{ij} 's on the angle of rotation and the recomputation of the F_{ij} 's after each rotation. Including the angle of rotation dependence of the F_{ij} 's appears unnecessary and undesirable, since it will require a different contraction of the basis function integrals, and we have left this dependence out of our formulae since it would unduly burden the notation. It appears to be unimportant also on physical grounds, since it is unlikely that the local potential--our F_{ij} 's contain local potentials only--will depend strongly on a small orbital change. Computational experience bears this out. Performing only one two by two rotation and then recomputing the F_{ij} 's is computationally uneconomical; thus it doesn't appear advisable to implement this form of two by two rotations such that convergence is guaranteed. The described procedure should be implemented rather in such a way that one computes the two by two rotations between all orbital pairs, then corrects the orbitals and recomputes the F_{ij} 's. Only in the case of convergence difficulty, which will be noticed readily by the appearance of large rotation angles, should one resort to performing only one or a few rotations before recomputing the F_{ij} 's, thus still taking advantage of the fact that the presented method for solving the SCF equations will guarantee convergence.

Another method for the determination of the MC-SCF orbitals is based on the extended Brillouin theorem, rather than on the Fock like equations, eq. (21).¹⁴ Using the language of second quantization introduced above, the extended

Brillouin theorem may be expressed as

$$\langle (a_i^\dagger a_i - a_i^\dagger a_j) \Psi | \mathcal{H} | \Psi \rangle = 0 \quad (54)$$

if Ψ is an MC-SCF wave function; i and j can take the values $1, 2, \dots, m$. Defining

$\Psi_{ij} \equiv (a_i^\dagger a_i - a_i^\dagger a_j) \Psi$, one needs to do a configuration interaction calculation for

$$\Psi' = A_0 \Psi + \sum_{ij} A_{ij} \Psi_{ij} \quad (55)$$

i.e. solving

$$(\underline{H} - E \underline{S}) \underline{A} = 0 \quad (56)$$

with \underline{H} defined by the elements $\langle \Psi_{ij} | \mathcal{H} | \Psi \rangle$ for the first column and else as $\langle \Psi_{ij} | \mathcal{H} | \Psi_{kl} \rangle$ and similarly \underline{S} . Note that \underline{S} will be diagonal; however it will not be a unit matrix, in general $\langle \Psi_{ij} | \Psi_{kl} \rangle = a_{ij} \delta_{ij,kl}$ with $a_{ij} \leq 1$.

The resulting expansion coefficients A_0 and A_{ij} need then to be associated with the elements of the unitary matrix \underline{U} in eq. (32) yielding the MC-SCF orbitals. This association is always possible though not simple. Using for \underline{U} the unitary matrix which diagonalizes the first order reduced density matrix of Ψ' is not always appropriate, since the first order reduced density matrix of the MC-SCF wave function Ψ need not be diagonal, depending on the configuration selection in eq. (5).

In general, eq. (56) may become quite large, and it is impractical to construct \tilde{H} fully in order to find a solution to this CI problem. It may be preferable to use a perturbation form to solve eq. (56) approximately as

$$A_{ij} \cong \langle \psi_{ij} | \mathcal{H} | \psi \rangle / (\langle \psi | \mathcal{H} | \psi \rangle \langle \psi_{ij} | \psi_{ij} \rangle - \langle \psi_{ij} | \mathcal{H} | \psi_{ij} \rangle) \quad (57)$$

This equation is quite similar to eq. (43) since A_{ij} can be identified with d_{ij} , and the numerators on the right hand side are identical; however, the denominators differ slightly. It is not appropriate to give here in detail the form of the H and S matrix elements in terms of one and two electron matrix elements over the orbitals. Their derivation in the general case discussed here in terms of spin orbitals is quite straightforward, though lengthy. This is no more true in the practical case, where one wants to include the proper spin, angular momentum or symmetry coupling.

References

1. J. Frenkel, "Wave Mechanics," Vol. 2, "Advanced General Theory," (Clarendon Press, Oxford, 1934), p. 460-462.
2. D. R. Hartree, W. Hartree and B. Swirles, Phil. Trans. Roy. Soc. (London) A238, 229 (1939).
3. A. P. Jucys, Adv. Chem. Phys. 14, 191 (1969); here much of the work on atoms done by Jucys (Yutsis, Iutsis) and others, dating back to 1950 is reviewed.
4. G. Das and A. C. Wahl, J. Chem. Phys. 44, 87 (1966).
5. For a more complete Bibliography, see T. L. Gilbert, Phys. Rev. A6, 580 (1972).
6. K. K. Docken and J. Hinze, J. Chem. Phys. 57, 4928 (1972).
7. Specifically we will discuss here n electron systems; the extension to other types of elementary particles is obvious.
8. See for example D. H. Kobe, Am. J. Phys. 34, 1150 (1966).
9. M. Rossi, J. Chem. Phys. 46, 989 (1967).
10. B. Levy, Intern. J. Quantum Chem. 4, 297 (1970).
11. R. C. Raffanetti and K. Ruedenberg, Intern. J. Quantum Chem. 35, 625 (1970); D. Hoffman, R. C. Raffanetti and K. Ruedenberg, J. Math. Phys., 13, 528 (1972).
12. G. Das and A. C. Wahl, J. Chem. Phys. 56, 1769 (1972).

13. See for example F. B. Hildebrand, "Introduction to Numerical Analysis", McGraw Hill, New York, 1956, p. 439.
14. B. Levy and G. Berthier, Intern. J. Quantum Chem. 2, 307 (1968);
corrections ibid. 3, 247 (1969).

LARGE CI VS. MC-SCF

JUERGEN HINZE*

DEPARTMENT OF CHEMISTRY

UNIVERSITY OF CHICAGO, CHICAGO, ILLINOIS 60637

*This research was supported in part by the Advanced Research Projects Agency of the Department of Defense, monitored by the U. S. Army Research Office-Durham, Box CM, Duke Station, Durham, North Carolina 27706, under Grant DA-ARO-D-31-124-72-G73, and by Grant GP-33892x of the National Science Foundation.

It is well known that the time independent, electrostatic Schroedinger equation of an n electron system

$$\mathcal{H}\Psi = E\Psi \quad (1)$$

with

$$\mathcal{H} = \sum_i^n h(i) + \sum_{i>j}^n g(ij) \quad (2)$$

may be solved to any degree of accuracy for any stationary state K by using a configuration interaction (CI) ansatz for the wave function

$$\Psi_K = \sum_I^N \Phi_I C_{IK} \quad (3)$$

provided the n electron basis spanned by the configuration state functions (CSF's) Φ_I , with $\langle \Phi_I | \Phi_J \rangle = \delta_{IJ}$ is complete or nearly so. The variational solution of (1) with ansatz (3) leads to an algebraic simple matrix equation

$$H\mathcal{C} = E\mathcal{C} \quad (4)$$

with $H_{IJ} = \langle \Phi_I | \mathcal{H} | \Phi_J \rangle$, \mathcal{C} a matrix of column eigen vectors \mathcal{C}_K and E a diagonal matrix of the eigen values E_K which are upper bounds to the true stationary state energy eigen values $E_K^{(t)}$ of (1). This is the basis of the large CI as well as the MC-SCF (multi-configuration self-consistent-field) method.¹

Solution of equation (4) and therefore (1) would be simple, were it not for the need of an exceedingly large expansion in (3), i.e. the expansion in (3) is

slowly convergent and N becomes excessively large if high accuracy is desired, unless a judicious or optimal choice of the n electron basis functions, the CSF's Φ_i is affected. It is in the approach to a judicious selection of the CSF's where the large CI and the MC-SCF method differ. In both methods the CSF's are generally constructed from antisymetrized products of orthonormal orbitals φ_i , properly coupled to yield eigen functions of S^2 , S_z and to transform as the irreducible representation of the point group of the system. Thus, the CSF's are specific linear combinations of Slater determinant (SD's). The set of orthonormal orbitals φ_i , used to construct the SD's and CSF's, span the one-electron space and they are generally expanded in terms of primitive basis functions--Slater type functions, Gaussian's or elliptical functions,

$$\varphi_i = \sum_p^m \chi_p c_{pi} \quad (5)$$

The number m and the type of basis functions χ_p used in (5) determine the size and quality of the one-electron basis. No amount of CI or other tricks can overcome the shortcoming in this basis, thus it has to be adequately large and well chosen. We will not concern ourselves here with the intricacies of the selection of these primitive basis functions, except to note that a minimal basis set for quantitative work requires at least a "double-zeta plus polarization" representation for all valence shells.²

From the m linearly independent basis functions (for simplicity they are considered to contain the spin coordinate) one can construct m orthonormal spin

orbitals, which provide the building blocks for the SD's and CSF's, the latter span the n -electron space which has a maximal dimension $N_{\max} = \binom{m}{n}$. Even though N_{\max} is reduced significantly by requiring the CSF's to be properly spin and symmetry coupled, the dimension of the remaining n -electron space NS_{\max} is still excessive for reasonable m and $n > 4$. Typically $NS_{\max} > 10^5$, preventing the solution of the full CI problem, which would mean diagonalization of the Hamiltonian in the full space spanned by all CSF's, which can be constructed from the m orbitals.

It is obvious that in the case of a full CI calculation the particular choice of orbitals is irrelevant, since the resulting wave functions and expectation values are invariant to a unitary transformation among the orbitals. However, since a full CI calculation is in general not feasible, and thus a CI calculation is performed with a truncated and judiciously selected subset of CSF types,³ the resulting wave functions and expectation values will depend critically on the choice of orbitals used. It is in this choice of the particular shape of the orbitals used, where the various large CI methods differ from the MC-SCF method.

In the MC-SCF method the CSF's used in expansion (3) are chosen judiciously with $N \ll NS_{\max}$ and all the orbitals participating in the total wave function, as well as the CI expansion coefficients are determined variationally. It is obvious that this will result in a wave function, which gives the lowest possible energy within the chosen m dimensional one-particle space and the prescribed selection of CSF's, this is merely the result of the variational principle.

The simultaneous optimization of CI coefficients and orbitals is achieved by solving iteratively, to full self-consistency equation (4) and the Fock like equations

for the orbitals

$$\sum_i (F_{ii} - \epsilon_{ii} S) c_i = 0 \quad (6)$$

which are obtained by varying the energy expectation value with respect to a change of the orbital expansion coefficient vectors c_i . In (6) we have

$$S_{pq} = \langle \chi_p | \chi_q \rangle$$

$$\epsilon_{ij} = \epsilon_{ji}^* \quad \text{Lagrangian multipliers}$$

and

$$F_{ijpq} = \gamma_{ij} \langle \chi_p | h | \chi_q \rangle + \sum_{kl} \Gamma_{ijkl} \sum_{rs} \langle \chi_p | \langle \chi_r | g | \chi_s \rangle | \chi_q \rangle c_{kr} c_{ls}$$

with γ_{ij} and Γ_{ijkl} the first and second order reduced density matrices of state K desired in the space spanned by the orbitals.

In practice an MC-SCF calculation proceeds along the steps:

- 1) Select one particle basis and an initial guess of φ_i .
- 2) Compute 1 and 2 electron integrals over the basis functions.
- 3) Select the types of CSF's to participate in the CI expansion (eq. 3).
- 4) Generate CI energy expressions.
- 5) Solve equation (4) for state K desired.
- 6) Construct γ_{ij} and Γ_{ijkl} for state K.
- 7) Solve equation (6) to convergence.

Repeat steps 5-7 until complete self-consistency is achieved.

In the large CI method, the orbitals used in constructing the CSF's are generally not fully optimized, however some optimization is obtained by performing an SCF calculation with the dominant CSF or even an MC-SCF calculation using a few of the dominant CSF's; the reference configurations. This is again followed by a judicious choice of CSF types which will participate in expansion (3) with $N < NS_{\max}$. Generally an inclusion of all single and double replacements from the reference configurations will be adequate, however even with this N becomes rapidly large, of order $n^2 m^2 / 4$. Equation (6) is then solved within this basis of CSF's for the state desired. In practice a large CI calculation proceeds along the steps:

- 1) Select one particle basis functions and initial guess of ϕ .
- 2) Compute 1 and 2 electron integrals over the basis functions.
- 3) Select the types of CSF's to participate in the CI expansion (eq. 3).
- 4) Generate CI energy expressions.
- 5) Perform SCF or limited MC-SCF calculation to obtain orbitals for the reference configurations.
- 6) Solve equation (4) for state K desired.

We are now in a position to compare the amount of computational effort required in both types of computations and indicate how much this is a function of the accuracy desired; accuracy is to be understood here as the difference between the solution obtained and that obtainable from a full CI, i.e. the best solution obtainable with the limited one-electron basis set.

Steps (1) and (2) are identical for large CI and MC-SCF. Step (3), being proportional to N is more cumbersome for large CI; however in the case of MC-SCF more care must be exercised in the selection of configurations. Step (4) being proportional to N^2 is the most time consuming step in a large CI calculation where N is of order $n^2 m^2 / 4$; in the MC-SCF method N is much smaller. Thus, this step together with the construction of the energy matrix is the limiting bottleneck for large CI calculations, while they are insignificant in the MC-SCF. However, for the MC-SCF step (7), solving equation (6) is the bottleneck. It is by no means easy to get the SCF equations to converge rapidly. There are algorithms for solving equation (6);⁴ although convergent, they require frequently 100 iterations, and in each iteration the integrals must be contracted, a process which is of order $m^4 \cdot k$, with k the number of valence orbitals. If the basis function limit is to be closely reached, k will become almost the size of m , in which case the MC-SCF method requires large amounts of computer time.

Thus, we can conclude that in cases where the basis function limit is to be approached in a calculation, the large CI method is superior to the MC-SCF method, the latter being more advantageous for more approximate calculations. This will be so, unless faster convergent algorithms can be developed for solving equation (6). However, it should be noted that in case of more approximate calculations it is possible with the MC-SCF to stay within a well defined model, for example introducing just the extra bond correlation as is done in the optimized valence configuration (OVC) variant of MC-SCF.⁵ In addition an MC-SCF function

is frequently advantageous for the construction of reference configurations for large CI methods.³

Another method of reducing the number of configurations required in a large CI calculation is the iterative natural orbital method, where in one iteration only the dominant single and double replacements from the reference configurations are used in the CI calculation. This is followed by a diagonalization of the first order reduced density matrix and corresponding orbital transformation to an approximation of the natural orbitals for the state desired. This process is repeated to convergence, and yields approximate natural orbitals and a CI expansion wave function with N between that of the MC-SCF and the large CI method.⁶ It should be understood that this is only one variant of many methods designed to obtain approximations to the natural orbitals in order to reduce the size of the required configuration interaction calculation.

References

1. For an extensive bibliography see T. L. Gilbert, Phys. Rev. A 6, 580 (1972).
2. For a more detailed discussion see P. S. Bagus et al., "Computational Methods for Large Molecules and Localized States in Solids," Edited by F. Herman and A. D. McLean, Plenum Press, New York (1973).
3. See for example A. D. McLean and B. Liu, J. Chem. Phys. 58, 0000 (1973), in press.
4. A detailed description and comparison of various algorithms will be presented in a forthcoming publication.
5. See for example G. Das and A. C. Wahl, J. Chem. Phys. 56, 3532 (1972) and earlier work by these authors.
6. See E. R. Davidson, Rev. Mod. Phys. 44, 451 (1972); H. F. Schaefer, "The Electronic Structure of Atoms and Molecules," Addison Wesley, Reading, Mass. (1972).

Multiconfiguration Self-Consistent-Field Calculations for Several States of Boron†*

Zoran Sibiñic

Laboratory of Molecular Structure and Spectra,

Department of Physics, The University of Chicago, Chicago, Illinois 60637

(Received 15 November 1971)

Multiconfiguration self-consistent-field calculations were performed on the following states of boron: $2s^2 2p$, 2P , $2s 2p^2$, 4P , 2D , 2P , $2s^2 3s$, 2S , and $2p^3$, 4S . For each state, only configurations resulting from the replacement of the valence-shell orbitals were used, and consequently only the valence-shell correlation was calculated adequately. The correlation orbital set consisted of one orbital in each of the symmetries s , p , and d (except for the $2s^2 3s$, 2S state, where there were two orbitals of p symmetry). For the ground state, the value of 0.067 hartree was obtained for the valence-shell correlation energy. From the wave functions obtained, the term energies and the oscillator strengths for the allowed transitions were calculated and found to be in general agreement with the results of more elaborate calculations and experiments.

INTRODUCTION

It is well known that Hartree-Fock (HF) calculations for atoms and molecules do not produce wave functions sufficiently accurate for calculating many atomic and molecular properties satisfactorily. What is not represented accurately in these calculations is the "correlation" between electrons,¹⁻⁴ and especially correlation between electrons of opposite spins. In order to represent the electron correlation more accurately, the method of *superposition of configurations* (SOC) was used in this work.

One of the disadvantages of the SOC approach is that usually a large number of configurations is needed to obtain a wave function of high quality. The number of configurations needed depends a great deal on the orbitals used to construct the configurations. In the *multiconfiguration self-consistent-field* (MCSCF) method, the orbitals, as well as the configuration mixing coefficients, are determined variationally, and hence the best energy possible, with a given set of configurations, is achieved. Clearly, the MCSCF method is a natural extension of the Hartree-Fock SCF model.

In any SOC approach, since the number of configurations is necessarily finite, it is possible to select the configuration set in such a way that the resulting wave function is more suitable for calculation of some properties of the system than others. Thus, for example, Sabelli and Hinze,⁵ in the earlier version of the MCSCF method, restricted the configurations to those whose shell occupation numbers have even differences, i.e., only replacements of the type $(nl)^2$ to $(n'l')^2$ were allowed. Thus, they only treated intrashell correlation accurately. In their Be wave function, for example, they had no configurations of the type $1s^2 2s 2p 3s$, and consequently they could not represent the *intershell* correlation adequately.

The MCSCF formalism presented and applied here

has no restrictions on the types of configurations that can be used in the wave function, and consequently both intershell and intrashell correlation can be calculated accurately.

In this work MCSCF calculations were performed on the ground state and several excited states of the boron atom with the aim of producing wave functions of compact form and rather high accuracy. The wave functions obtained were then used in calculations of oscillator strengths.

MCSCF PROCEDURE

The formalism for the unrestricted MCSCF method used in this work is similar to the formalism for the restricted MCSCF method presented in the paper by Hinze and Roothaan,⁶ and consequently only an outline will be given here.

A many-particle wave function is constructed from spin orbitals defined by

$$\chi_{l\lambda\alpha m_s}(r, \vartheta, \varphi) = r^{-1} P_{l\lambda}(r) Y_{l\lambda}(\vartheta, \varphi) S(m_s), \quad (1)$$

where $S(m_s)$ are the spin functions, $Y_{l\lambda}(\vartheta, \varphi)$ are the usual spherical harmonics, and $P_{l\lambda}(r)$ are the radial shell functions. A shell consists of all the spin orbitals that form a degenerate set; for example, the p shell consists of six degenerate spin orbitals. From the spin orbitals, antisymmetrized products, or *Slater determinants* (SD's), are constructed. The number of spin orbitals of a shell used for the construction of a particular SD is the *occupation number* of the shell in that SD. The set of all SD's which have the same shell occupation numbers is said to form an *electron configuration*.

When a symmetry operation is applied to a set of SD's which constitute an electron configuration, a linear transformation of the SD's among themselves is induced; this transformation is, of course, a representation of the symmetry group of the system, and is in general reducible. Linear combinations of these SD's that form irreducible represen-

tations are called *configuration state functions* (CSF's); each CSF belongs to a definite symmetry species and subspecies.

In many simple cases the CSF's are unique; in more complicated cases, such as configurations with three open shells, there may be several CSF's of the same symmetry species and subspecies arising from one configuration. In such cases the shells may be coupled together in different order, thus producing a different complete set of CSF's for that configuration. However, it is most natural to couple together, first, shells which have the largest electrostatic interaction. The CSF's obtained from different hierarchies of coupling are connected by unitary transformations, and as long as a complete set of CSF's, from any coupling scheme, is used, it does not matter which scheme is chosen. Coupling, in this context, means constructing the wave function of the combined system in such a way that it belongs to an irreducible representation of the symmetry group of the system, and is thus itself of definite symmetry species and subspecies. For example, $\Phi[(2s2p, {}^1P)3d, LSM_L M_S]$ and $\Phi[(2s2p, {}^3P)3d, LSM_L M_S]$ constitute a complete set of CSF's arising from the configuration $2s2p3d$.

Let $\Phi_{LSM_L M_S, I}$ denote a CSF where the index I is used to label CSF's arising from different configurations and/or, if necessary, from within the same configuration. The wave function for an actual state $\Psi_{LSM_L M_S}$ is now put forward as an expansion in terms of $\Phi_{LSM_L M_S, I}$. Since the spin-dependent terms in the Hamiltonian will be neglected, L , S , M_L , and M_S are good quantum numbers, so that

$$\Psi_{LSM_L M_S} = \sum_I C_I \Phi_{LSM_L M_S, I} \quad (2)$$

The good quantum numbers remain constant for a given calculation and will be omitted from now on.

The normalization chosen is such that

$$\langle \Phi_I | \Phi_J \rangle = \delta_{IJ} \quad (3)$$

and

$$\sum_I C_I^2 = 1. \quad (4)$$

Using the usual spin-free nonrelativistic Hamiltonian

$$\mathcal{H} = -\sum_i \left(\frac{1}{2} \nabla_i^2 + Z r_i^{-1} \right) + \sum_{i>j} r_{ij}^{-1}, \quad (5)$$

the expectation value of the energy of the system is given by

$$E = \langle \Psi | \mathcal{H} | \Psi \rangle = \sum_{I, J} C_I C_J \langle \Phi_I | \mathcal{H} | \Phi_J \rangle. \quad (6)$$

Each shell function $P_{\lambda i}(r)$ is now expanded into a set of (generally nonorthogonal) basis functions $R_{\lambda \rho}(r)$, namely,

$$P_{\lambda i}(r) = \sum_{\rho} R_{\lambda \rho}(r) c_{\lambda i \rho}. \quad (7)$$

The orbital expansion coefficients $c_{\lambda i \rho}$ are not to be confused with the configuration-mixing coefficients C_I introduced earlier.

In order to express the energy in a form suitable for the application of the variational principle with respect to the orbital expansion coefficients $c_{\lambda i \rho}$, the matrix elements of the Hamiltonian with respect to the CSF's are expressed in terms of integrals over the basis functions. The relevant integrals are defined by

$$S_{\lambda \rho q} = \int_0^\infty dr R_{\lambda \rho}(r) R_{\lambda q}(r), \quad (8)$$

$$H_{\lambda \rho q} = \int_0^\infty dr \left\{ \frac{1}{2} R'_{\lambda \rho}(r) R'_{\lambda q}(r) + \left[\frac{1}{2} \lambda(\lambda+1) r^{-2} - Z r^{-1} \right] R_{\lambda \rho}(r) R_{\lambda q}(r) \right\}, \quad (9)$$

$$G_{\lambda \rho \mu q, \rho' \sigma s, \nu} = \int_0^\infty dr \int_0^\infty ds U_\nu(r, s) \times R_{\lambda \rho}(r) R_{\mu q}(r) R_{\rho'}(s) R_{\sigma s}(s), \quad (10)$$

where

$$U_\nu(r, s) = \begin{cases} r^{-\nu-1} s^\nu & \text{if } r \geq s \\ r^\nu s^{-\nu-1} & \text{if } r < s. \end{cases} \quad (11)$$

For each given set of λ , μ , ρ , and σ , the allowed values of ν are from $|\lambda - \mu|$ or $|\rho - \sigma|$, whichever is larger, to $\lambda + \mu$, or $\rho + \sigma$, whichever is smaller, in steps of two; this is concisely expressed by $\nu \in V(\lambda, \mu; \rho, \sigma)$.

In the terms representing the contributions from closed shells, the special combination

$$I_{\lambda \rho q, \mu r s} = G_{\lambda \rho \lambda q, \mu r \mu s, 0} - \sum_{\nu \in V(\lambda, \mu; \lambda, \mu)} x_{\lambda \mu \nu} [G_{\lambda \rho \mu r, \lambda q \mu s, \nu} + G_{\lambda \rho \mu s, \lambda q \mu r, \nu}] \quad (12)$$

occurs, where the coefficients $x_{\lambda \mu \nu}$ are expressed in terms of Wigner 3- j symbols, namely,

$$x_{\lambda \mu \nu} = \frac{1}{4} \begin{pmatrix} \lambda & \mu & \nu \\ 0 & 0 & 0 \end{pmatrix}^2. \quad (13)$$

For the contributions from open shells, certain *interaction coefficients* occur which are constant for a given calculation; they are denoted by $a_{IJ, \lambda i j}$ and $b_{IJ, \lambda i \mu j, \rho \sigma i, \nu}$. As this notation suggests, they enter in the expression for the matrix elements $\langle \Phi_I | \mathcal{H} | \Phi_J \rangle$; they depend on the shell occupation numbers of the configurations I and J , the coupling schemes used, and the orbital and spin angular momenta of the system. The diagonal coefficients $a_{II, \lambda i j}$ are particularly simple, namely,

$$a_{II, \lambda i j} = 2(2\lambda + 1) \delta_{ij}; \quad (14)$$

the coefficients $b_{II, \lambda i \mu j, \rho \sigma i, \nu}$ can be expressed in terms of the coefficients a^b and b^b of Condon and Shortley.⁷ The off-diagonal coefficients are more complicated, but can be expressed in terms of the

coefficients of fractional parentage, 3- j and 6- j symbols, and were calculated using Racah's methods.⁸

It is also useful to define *net-interaction coefficients* $a_{\lambda ij}$ and $b_{\lambda i \mu j, \rho \kappa \sigma \tau, \nu}$ by means of

$$a_{\lambda ij} = \sum_{I, J} a_{I J, \lambda ij} C_I C_J, \quad (15)$$

$$b_{\lambda i \mu j, \rho \kappa \sigma \tau, \nu} = \sum_{I, J} b_{I J, \lambda i \mu j, \rho \kappa \sigma \tau, \nu} C_I C_J, \quad (16)$$

and the *density matrices* by

$$D_{C, \lambda \rho q} = \sum_{i \in C(\lambda)} 2(2\lambda + 1) c_{\lambda i \rho} c_{\lambda i q}, \quad (17)$$

$$D_{F, \lambda \rho q} = \sum_{i, j \in F(\lambda)} a_{\lambda i j} c_{\lambda i \rho} c_{\lambda j q}, \quad (18)$$

where $C(\lambda)$ and $F(\lambda)$ denote the sets of closed and fractionally occupied shells of symmetry λ .

Employing the integrals and coefficients just defined, the energy of the system can be written as

$$E = \sum_{\lambda \rho q} \left\{ \left(\sum_{i \in C(\lambda)} 2(2\lambda + 1) c_{\lambda i \rho} c_{\lambda i q} \right) \times \left[H_{\lambda \rho q} + \frac{1}{2} \sum_{\rho \tau s} I_{\lambda \rho q, \rho \tau s} \left(\sum_{h \in C(\rho)} 2(2\rho + 1) c_{\rho h \tau} c_{\rho h s} + 2 \sum_{h, i \in F(\rho)} a_{\rho h i} c_{\rho h \tau} c_{\rho i s} \right) \right] + H_{\lambda \rho q} \left(\sum_{i, j \in F(\lambda)} a_{\lambda i j} c_{\lambda i \rho} c_{\lambda j q} \right) \right\} + \sum_{\lambda \rho} \sum_{\mu q} \sum_{\rho \tau} \sum_{\sigma s} \sum_{\nu \in V(\lambda, \mu; \rho, \sigma)} G_{\lambda \rho \mu q, \rho \tau \sigma s, \nu} \sum_{i \in F(\lambda)} \sum_{j \in F(\mu)} \sum_{h \in F(\rho)} \sum_{i \in F(\sigma)} b_{\lambda i \mu j, \rho \kappa \sigma \tau, \nu} c_{\lambda i \rho} c_{\mu j q} c_{\rho h \tau} c_{\sigma i s}. \quad (19)$$

As was mentioned earlier, in the MCSCF method two independent variations of the energy are performed; one with respect to the orbitals, i. e., the orbital expansion coefficients $c_{\lambda i \rho}$, and the other with respect to the configuration-mixing coefficients C_I . The energy expression (6) is suitable for the variation with respect to the configuration-mixing coefficients, and expression (19) for the variation with respect to the orbitals. Performing the variation now with respect to all $c_{\lambda i \rho}$, and subject to the orthogonality conditions for the orbitals, the MCSCF equations are obtained for closed- and open-shell (fractionally occupied) orbitals, namely,

$$\sum_q F_{C, \lambda \rho q} c_{\lambda i \rho} = \sum_q S_{\lambda \rho q} (\epsilon_{\lambda i i} c_{\lambda i q} + \sum_{j \in F(\lambda)} \epsilon_{\lambda i j} c_{\lambda j q}) \quad (20)$$

for all $\lambda i \in C$, and

$$\sum_q \sum_{\mu j \in F} F_{\lambda i \rho, \mu j q} c_{\mu j q} = \sum_q S_{\lambda \rho q} \sum_{j \in C+F} \epsilon_{\lambda i j} c_{\lambda j q} \quad (21)$$

for all $\lambda i \in F$. The Fock-like matrices are

$$F_{C, \lambda \rho q} = 2(2\lambda + 1) [H_{\lambda \rho q} + 2 \sum_{\rho \tau s} I_{\lambda \rho q, \rho \tau s} (D_{C, \rho \tau s} + D_{F, \rho \tau s})], \quad (22)$$

$$F_{\lambda i \rho, \mu j q} = \delta_{\lambda \mu} a_{\lambda i j} [H_{\lambda \rho q} + \sum_{\rho \tau s} I_{\lambda \rho q, \rho \tau s} D_{C, \rho \tau s}] + 2 \sum_{\rho \tau} \sum_{\sigma s} \sum_{\nu \in V(\lambda, \mu; \rho, \sigma)} G_{\lambda \rho \mu q, \rho \tau \sigma s, \nu} \times \sum_{h \in F(\rho)} \sum_{i \in F(\sigma)} b_{\lambda i \mu j, \rho \kappa \sigma \tau, \nu} c_{\rho h \tau} c_{\sigma i s}. \quad (23)$$

The $\epsilon_{\lambda i j}$ are the Lagrange multipliers which must be introduced to fulfill the orbital orthonormality constraints. In terms of the expansion coefficients these constraints are expressed by

$$\sum_{\rho, q} c_{\lambda i \rho} S_{\lambda \rho q} c_{\lambda j q} = \delta_{ij}. \quad (24)$$

Performing the variation of the energy with respect to the configuration-mixing coefficients C_I leads to the well-known eigenvalue equation

$$\sum_J H_{IJ} C_J = E C_I \delta_{IJ}, \quad (25)$$

where

$$H_{IJ} = \langle \Phi_I | \mathcal{H} | \Phi_J \rangle. \quad (26)$$

For the MCSCF solution the orbital expansion coefficients satisfy Eqs. (20) and (21), and the configuration-mixing coefficients satisfy Eq. (25). This solution must be obtained by some iterative method, and many strategies are possible; the strategy used in this work is given by the flow diagram in Fig. 1. The pre-SCF orthonormalization, as indicated in the flow diagram, is done because it is inconvenient to supply an initial orthonormal orbital set. The post-SCF orthonormalization is desirable because the orbitals that are obtained by solving Eqs. (20) and (21) are orthonormal but not always to the desired degree of accuracy. The Schmidt orthonormalization procedure used takes the orbitals in the natural order, i. e., 1s, 2s, ...; 2p, 3p, ...; etc.

The analysis presented here does not specify the choice of the basis functions $R_{\lambda \rho}(r)$. In this work the well-known Slater-type basis functions were used; they are defined by

$$R_{\lambda \rho}(r) = [(2\xi)^{2n_{\lambda \rho}+1} / (2n_{\lambda \rho})!] | r^{n_{\lambda \rho}} e^{-\xi_{\lambda \rho} r}, \quad (27)$$

where $\xi_{\lambda \rho}$ and $n_{\lambda \rho}$ are adjustable parameters, with $n_{\lambda \rho}$ restricted to integer values and $n_{\lambda \rho} \geq \lambda + 1$. For each calculation, the program provides for the adjustment (optimization) of the exponents until the

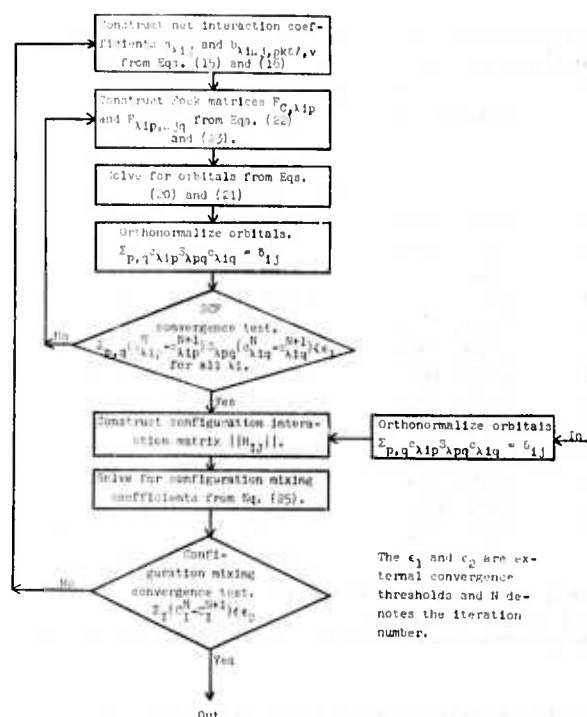


FIG. 1. Flow diagram of the MCSCF procedure.

minimum of the energy is obtained. A straightforward method for such optimization is given by Roothaan and Bagus.⁹ Their method was followed

in this work, and was often simplified to a quadratic rather than a fourth-order interpolation.

The oscillator strength (in dipole approximation) for a transition from the initial state Ψ_I to the final state Ψ_F is given by

$$f_L = \frac{2}{3} (E_I - E_F) g_I^{-1} |\langle \Psi_I | \hat{r} | \Psi_F \rangle|^2, \quad (28)$$

or, equivalently, for exact wave functions by

$$f_V = \frac{2}{3} (E_I - E_F)^{-1} g_I^{-1} |\langle \Psi_I | \nabla | \Psi_F \rangle|^2, \quad (29)$$

where g_I is the degeneracy of the initial state and the squared matrix elements are summed over the initial- and final-state degeneracies.

When approximate wave functions are used, the agreement between the two forms is a necessary but not sufficient condition for the correctness of the oscillator strength value.

Recently¹⁰ it has been shown that when HF or SOC wave functions are used, the length form f_L is more appropriate for the calculation of the oscillator strengths.

Both formulas (28) and (29) were used in this work to calculate the f values.

APPLICATION TO BORON ATOM

Calculations were performed on the following states of boron: $2s^2 2p$, $^2P^0$, $2s 2p^2$, 4P , 2D , 2P , $2s^2 3s$, 2S , and $2p^3$, $^4S^0$.¹¹ Each state considered is the lowest state of that particular symmetry for the boron atom.

As was mentioned earlier, the configuration set

TABLE I. Basis-function parameters and orbital expansion coefficients from the 28 CSF representation of the $2s^2 2p$, 2P state. (full MCSCF and frozen HF orbital calculations).

Full MCSCF					Frozen HF orbitals		
s symmetry							
n	ζ	1s	2s	3s	1s	2s	3s
1	7.3306	0.172 343	-0.047 463	-0.153 852	0.171 570	-0.054 951	-0.173 736
1	3.8999	0.913 394	-0.134 467	0.766 515	0.911 338	-0.131 943	0.816 102
2	1.7400	0.021 047	-1.193 120	-9.483 725	0.002 346	-1.418 650	-10.169 023
2	1.3370	-0.023 666	1.490 514	5.902 149	-0.000 139	1.608 475	6.141 672
3	4.7860	-0.092 969	0.075 327	0.641 943	-0.091 873	0.092 837	0.687 687
3	2.6000	-0.013 153	0.685 851	2.831 922	-0.002 837	0.777 875	3.229 055
p symmetry							
n	ζ	2p	3p		2p	3p	
2	5.4000	0.009 469	-0.165 998		0.010 075	-0.158 350	
2	2.0480	0.164 774	-0.946 628		0.200 676	-0.820 473	
2	1.2060	0.471 341	-1.447 065		0.391 755	-1.661 696	
2	0.8666	0.407 739	2.123 415		0.460 842	2.246 233	
2	3.7000	0.003 471	0.501 915		0.000 197	0.470 599	
d symmetry							
n	ζ	3d			3d		
3	1.5265	1.011 881			1.012 538		
4	4.7759	-0.025 225			-0.026 651		

TABLE II. Configuration-mixing coefficients for the 28 CSF representation of the $2s^2 2p, ^2P$ state (results from full MCSCF and frozen HF orbitals calculations).

Configuration		Coefficients		Configuration		Coefficients	
		Full MCSCF	Frozen HF			Full MCSCF	Frozen IIF
1	$2s^2 2p$	0.96209	0.96235	15	$(2s3p, ^1P)3d$	-0.02384	-0.02352
2	$2p^3$	0.20981	0.20888	16	$(2s3p, ^3P)3d$	0.01378	0.01375
3	$(2s2p, ^1P)3d$	0.10733	0.10667	17	$3s^2 3p$	0.00329	0.00399
4	$(2s2p, ^3P)3d$	-0.08210	-0.08145	18	$3p^3$	0.00356	0.00362
5	$3s^2 2p$	-0.03482	-0.03579	19	$(3s2p, ^1P)3d$	0.00338	0.00293
6	$(2s3s, ^3S)2p$	-0.01825	-0.01993	20	$(3s2p, ^3P)3d$	0.00418	0.00494
7	$2p(3d^2, ^1S)$	-0.03165	-0.03168	21	$(3s3p, ^1P)3d$	-0.00584	-0.00576
8	$2p(3d^2, ^3P)$	-0.01839	-0.01822	22	$(3s3p, ^3P)3d$	0.00144	0.00132
9	$2p(3d^2, ^1D)$	-0.01429	-0.01413	23	$3p(3d^2, ^1S)$	0.00358	0.00356
10	$2p(3p^2, ^1S)$	0.02021	0.01966	24	$3p(3d^2, ^3P)$	0.00368	0.00362
11	$2p(3p^2, ^3P)$	0.01223	0.01237	25	$3p(3d^2, ^1D)$	0.00325	0.00320
12	$2p(3p^2, ^1D)$	0.01201	0.01216	26	$(2p^2, ^1S)3p$	0.01848	0.01850
13	$(2s3s, ^1S)3p$	-0.05719	-0.05839	27	$(2p^2, ^3P)3p$	0.04547	0.04438
14	$(2s3s, ^3S)3p$	0.02139	0.02186	28	$(2p^2, ^1D)3p$	0.03593	0.03539
Total energy (full MCSCF)				Total energy (frozen HF orbitals)			
$E = -24.59597$ hartrees				$E = -24.59535$ hartrees			

for an SOC wave function can be selected in a variety of ways, depending on which properties of the system the interest is centered. This tailoring of the wave function is well known and has been used by Bagus and Moser,¹² Weiss,¹³ Schaefer, Klemm, and Harris,¹⁴ Das and Wahl,¹⁵ and others. In each instance listed, the wave-function configuration set was chosen with a different purpose in mind. Bagus and Moser wanted to represent accurately the energy level spacings, Schaefer, Klemm, and Harris the "core polarization," Das and Wahl molecular dissociation, and so on.

In this work, the interest was in the optical properties and the configuration set was chosen accordingly, i.e., the SOC wave function is composed only of configurations which result from the replacement of the 2s, 3s, and 2p orbitals, the *valence orbitals*. The *core* is represented by the doubly occupied HF-like 1s orbital, which is allowed to adjust under the influence of the correlation configurations. Since no configurations in which a core spin orbital was replaced were allowed to participate, the core correlation and the core-valence correlation are not represented accurately. But since the core electrons are energetically and spatially well separated from the valence electrons, the correlation error thus intro-

duced is nearly constant for all the states considered. This is borne out by the fact that the core orbital, which in the model is state dependent, is in practice nearly the same for all states, and only slightly changed from the ground-state HF orbital.

When, in the absence of interelectron interactions, two configurations have the same energy, they are said to be *hydrogenically degenerate*. For example, $2s^2 2p$ and $2p^3$ or $2s^2 3s$ and $2p^2 3s$ are two such pairs of configurations. (The configuration $2s2p^2$ is also hydrogenically degenerate with the first pair but is of different parity, and thus excluded from the set.) In this work a minimal set of configurations is adopted, consisting of the dominant configuration for the state, and the hydrogenically degenerate configurations obtained by replacing $2s^2$ by $2p^2$ or $2p^2$ by $2s^2$ in the dominant configuration. The orbitals that make up the configurations of the minimal set are called *dominant orbitals*. Thus, in the second of the above examples, 1s, 2s, 3s, and 2p are the dominant orbitals. All other orbitals, which are introduced to construct additional configurations, are called *correlation orbitals*. Occasionally, the dominant orbitals so defined cannot all be used for a particular state. For example, for the $1s^2 2p^4, ^4S^o$ state, replacement of $2p^2$ by $2s^2$ cannot yield a $^4S^o$ state, and

TABLE III. Valence-electron correlation energy for the ground state of Boron.

	This work 28 CSF's	Weiss (Ref. 13) $n \leq 3$ configurations	Weiss (Ref. 13) 35 CSF's	Schaefer and Harris (Ref. 19)	Nesbet (Ref. 4)
Correlation energy	0.067	0.064	0.068	0.066	0.071

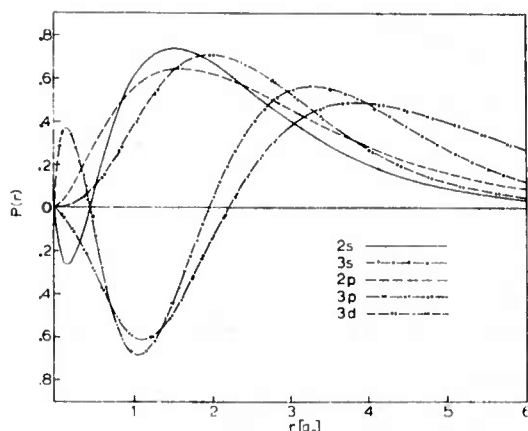


FIG. 2. Dominant orbitals $2s$ and $2p$ and the correlation orbitals $3s$, $3p$, and $3d$ for the ground state of boron.

hence the $2s$ orbital is absent from the dominant orbital set.

The calculation with dominant orbitals only serves as a starting point for more elaborate calculations, in which one correlation orbital is introduced in each of the symmetries s , p , and d .

For the CSF's the obvious notation $\Phi[1s^2(nl'n'l', S'L')n''l'', SLM_S M_L]$, with $n \leq n' \leq n''$ and $l \leq l' \leq l''$, will be used, indicating the coupling explicitly.

To determine the orbitals and configuration-mixing coefficients, the iterative procedure outlined in Fig. 1 is used. This procedure, however, does not converge unless a good basis set is chosen and a reasonable initial guess is made for the orbital expansion coefficients. The procedure used in this work, which provides good initial basis-function and orbital sets, and a method for augmenting these sets, will now be described.

For each state, the starting point for the MCSCF calculation was a single configuration SCF calculation. Guided by earlier experience a basis set appropriate for the expansion of the SCF orbitals was selected,¹⁶ and SCF calculation performed, and all exponents optimized. For the $2s^2 2p$, $^2P^o$ and $2s^2 3s$, 2S states, the hydrogenically degenerate configurations $2p^3$, 2P and $2p^2 3s$, 2S , respectively, were added, thus creating minimal configuration sets for these states. An MCSCF calculation was then performed

TABLE IV. Calculated and observed term energies for boron.

Term	HF	MCSCF	Observed
$2s^2 2p$, $^2P^o$	0	0	0
$2s 2p^2$, 2P	0.3502	0.3390	0.3305
$2s 2p^2$, 2D	0.2172	0.2271	0.2180
$2s 2p^2$, 4P	0.0784	0.1288	0.1313
$2s^2 3s$, 2S	0.1770	0.1767	0.1824
$2p^3$, $^4S^o$	0.4010	0.4424	0.4421

and all exponents reoptimized. During this re-optimization the exponents determined in the SCF calculation changed only slightly.

For one symmetry at the time, a correlation orbital was determined by performing the following three steps.

(1) The starting basis-function set was augmented by adding one basis function (two in case of d symmetry), and a new orbital generated by orthonormalizing to all previous orbitals of the same symmetry.

(2) All possible configurations, resulting from the replacement of any of the *valence* orbitals by the new (correlation) orbital, were generated, and added to the set.

(3) The MCSCF calculations were performed and the exponent(s) of the added function(s) optimized.

The exponents determined from the minimal-configuration-set calculation were not further reoptimized, since this would have yielded only a small improvement.

Since all CSF's resulting from the replacement of the valence orbitals were used in the wave function, the valence and the correlation orbitals are determined only up to a unitary transformation. Hence these orbitals are not unique, and can therefore be chosen so as to satisfy some arbitrary constraints. A particularly convenient choice, used in this work, consists of requiring that certain CSF's are absent from the wave function. As an example consider the function

$$\Phi = C_1 \Phi(1s^2) + C_2 \Phi(1s 2s, ^1S) + C_3 \Phi(2s^2), \quad (30)$$

which is composed of a complete set of CSF's that

TABLE V. Oscillator strengths.

Transition	Hartree-Fock		This work		Weiss (Ref. 13)		Experiment
	length	velocity	length	velocity	length	velocity	
$2s^2 2p$, $^2P-2s 2p^2$, 2D	0.339	0.336	0.115	0.157	0.067	0.084	0.059, ^a 0.048 ^b
$2s^2 2p$, $^2P-2s 2p^2$, 2P	1.003	0.389	0.640	0.685			
$2s^2 2p$, $^2P-2s^2 3s$, 2S	0.052	0.063	0.062	0.068	0.067	0.074	0.055 ^a
$2s 2p^2$, $^4P-2p^3$, 4S	0.266	0.146	0.214	0.216	0.213	0.225	

^aL. Bergstrom, J. Bromander, R. Buchtar, L. Lundin, and J. Martinson, Phys. Letters **28A**, 721 (1969).

^bG. M. Lawrence and B. D. Savage, Phys. Rev. **141**, 67 (1966).

TABLE VI. Basis-function parameters and orbital expansion coefficients from the 17 CSF representation of the $2s2p^2$, 2P state.

<i>s</i> symmetry				
<i>n</i>	ξ	1s	2s	3s
1	7.2867	0.161861	0.000743	-0.064722
1	4.0160	0.898495	-0.280462	0.468522
2	1.7455	0.000689	0.856251	-4.346655
2	1.1292	0.001461	0.465031	2.842027
3	4.8005	-0.065219	-0.063031	0.385078
3	2.5952	0.001504	-0.208263	1.138674
<i>p</i> symmetry				
<i>n</i>	ξ	2p	3p	
2	5.2000	0.005515	-0.050443	
2	2.0939	0.275846	0.603495	
2	1.2176	0.485508	-2.585190	
2	0.7833	0.337093	2.434843	
3	3.7000	-0.033589	-0.198903	
<i>d</i> symmetry				
<i>n</i>	ξ	3d		
3	1.4031	1.001259		
3	2.9400	-0.002013		

can be generated from the 1s and 2s orbitals for a two-electron system. Under the transformation

$$(1s) = (1s') \cos \alpha + (2s') \sin \alpha, \quad (31)$$

$$(2s) = -(1s') \sin \alpha + (2s') \cos \alpha, \quad (32)$$

where

$$\tan \alpha = 2C_2 / (C_3 - C_1), \quad (33)$$

the wave function remains invariant and can be expressed in terms of the primed orbitals as

$$\Psi = C'_1 \Phi(1s'^2) + C'_2 \Phi(2s'^2). \quad (34)$$

When similar transformations are applied to the

TABLE VII. Configuration-mixing coefficients for the 17 CSF representation of the $2s2p^2$, 2P state.

Configuration	Coefficient	Configuration	Coefficient
1 $2s2p^2$	0.89597	10 $(2p3p, ^1P)3d$	0.02552
2 $(2p^2, ^3P)3d$	0.10965	11 $(2p3p, ^3P)3d$	-0.01601
3 $(2p^2, ^1D)3d$	0.16714	12 $(2p3p, ^3D)3d$	0.01328
4 $2s3p^2$	-0.07420	13 $3s3p^2$	-0.00047
5 $2s3d^2$	0.03414	14 $3s3d^2$	0.00073
6 $(2s2p, ^1P)3p$	0.02698	15 $(3p^2, ^1D)3d$	-0.01724
7 $(2s2p, ^3P)3p$	0.37732	16 $(3p^2, ^3P)3d$	-0.00254
8 $(3s2p, ^1P)3p$	-0.03928	17 $3d^3$	0.01299
9 $(3s2p, ^3P)3p$	-0.06644		
Total energy			
$E = -24.25699$ hartrees			

TABLE VIII. Basis-function parameters and orbital expansion coefficients from the 26 CSF representation of the $2s2p^2$, 2D state.

<i>s</i> symmetry				
<i>n</i>	ξ	1s	2s	3s
1	7.2847	0.165862	-0.011129	-0.032391
1	3.9833	0.900422	-0.246106	0.430462
2	1.7463	0.000003	0.440356	-3.505518
2	1.1813	0.000117	0.650595	2.853607
3	4.7958	-0.071705	-0.031833	0.238777
3	2.9000	0.000833	-0.005983	0.319069
<i>p</i> symmetry				
<i>n</i>	ξ	2p	3p	
2	5.2500	0.005166	0.043988	
2	2.0616	0.303718	-0.916316	
2	1.2332	0.481791	-1.084907	
2	0.8172	0.309941	1.806129	
3	3.7301	-0.037733	0.305807	
<i>d</i> symmetry				
<i>n</i>	ξ	3d		
3	1.2031	0.948602		
3	2.1000	0.066017		

ground-state orbitals of boron the CSF's $\Phi[(2s3s, ^1S)2p, ^2P]$ and $\Phi[2s^23p, ^2P]$ may be omitted from the wave function. This leads to a unique set of orbitals which minimizes the energy. Aside from the advantage of a slightly shorter representation, this uniqueness is also important, for both the physical interpretability of the orbitals and for the convergence of the MCSCF procedure. Namely, if such uniqueness were not guaranteed, the iterative procedure could go from one set of equivalent orbitals to any other, and thus apparently fail to converge

TABLE IX. Configuration-mixing coefficients for the 26 CSF representation of the $2s2p^2$, 2D state.

Configuration	Coefficient	Configuration	Coefficient
1 $2s2p^2$	0.94389	14 $(2s2p, ^3P)3p$	0.16660
2 $2s3p^2$	-0.07305	15 $(3s2p, ^1P)3p$	0.00734
3 $2s3d^2$	0.04590	16 $(3s2p, ^3P)3p$	-0.06015
4 $3s2p^2$	-0.00295	17 $(2p3p, ^3S)3d$	0.00864
5 $3s3p^2$	-0.00203	18 $(2p3p, ^1P)3d$	-0.00741
6 $3s3d^2$	-0.00184	19 $(2p3p, ^3P)3d$	-0.00777
7 $(2p^2, ^1S)3d$	0.04203	20 $(2p3p, ^1D)3d$	-0.00122
8 $(2p^2, ^3P)3d$	0.13971	21 $(2p3p, ^3D)3d$	0.01246
9 $(2p^2, ^1D)3d$	-0.01004	22 $(3d^3, ^3D)$	-0.00756
10 $(3p^2, ^1S)3d$	0.00266	23 $(3d^3, ^3P)$	-0.00770
11 $(3p^2, ^3P)3d$	-0.00703	24 $(2s3s, ^4S)3d$	0.00219
12 $(3p^2, ^1D)3d$	0.00226	25 $2s^23d$	0.21944
13 $(2s2p, ^1P)3p$	-0.00661	26 $3s^23d$	-0.00896
Total energy			
$E = -24.36881$ hartrees			

TABLE X. Basis-function parameters and orbital expansion coefficients from the 12 CSF representation of the $2s2p^2$, 4P state.

s symmetry				
<i>n</i>	ζ	1s	2s	3s
1	7.2841	0.173 652	-0.007 574	0.072 826
1	3.9166	0.904 061	-0.200 056	0.270 875
2	1.7366	0.000 029	0.235 152	-0.100 672
2	1.2299	-0.001 016	1.024 672	2.065 985
3	4.7836	-0.084 853	-0.042 569	-0.208 130
3	2.4354	-0.000 208	-0.210 658	-2.178 339
p symmetry				
<i>n</i>	ζ	2p	3p	
2	5.2000	0.004 438	0.076 258	
2	2.0694	0.335 447	-1.648 509	
2	1.2285	0.539 474	-0.197 028	
2	0.8815	0.216 220	1.425 210	
3	3.5294	-0.045 283	0.434 101	
d symmetry				
<i>n</i>	ζ	3d		
3	1.5154	0.988 588		
3	2.8000	0.015 709		

under the test used.¹⁷

In order to test the effect of the correlation configurations on the HF orbitals, a variant of the full MCSCF method was employed. In this procedure the HF orbitals were taken over from a HF calculation and "frozen," i.e., not allowed to readjust, while the correlation orbitals were determined by the MCSCF method.

A detailed discussion will now be presented for the ground-state calculation only.

The Slater-type basis-function set consists of 6

TABLE XI. Configuration-mixing coefficients for the 12 CSF representation of the $2s2p^2$, 4P state.

	Configuration	Coefficient
1	$2s2p^2$	0.974 88
2	$3s2p^2$	-0.132 25
3	$(2p^2, ^3P)3d$	0.064 44
4	$2s3p^2$	-0.043 89
5	$(3p^2, ^3P)3d$	-0.003 21
6	$2s3d^2$	0.054 97
7	$3s3d^2$	-0.007 71
8	$(2s2p, ^3P)3p$	0.136 82
9	$(3s2p, ^3P)3p$	-0.063 46
10	$(2p3p, ^3P)3d$	0.001 73
11	$(2p3p, ^3D)3d$	0.013 50
12	$3d^3$	-0.002 87
Total energy		
$E = -24.467 14$ hartrees		

TABLE XII. Basis-function parameters and orbital expansion coefficients from the 24 CSF representation of the $2s^23s$, 2S state.

s symmetry					
<i>n</i>	ζ	1s	2s	3s	4s
1	7.3516	0.160 329	-0.008 106	0.002 939	0.040 332
1	3.9890	0.911 963	-0.259 869	0.067 708	-0.541 836
2	1.7422	-0.005 854	0.490 139	-0.106 168	4.737 585
2	1.3486	-0.009 731	0.599 086	-0.225 069	-4.596 339
3	4.7799	-0.074 183	-0.045 791	0.018 406	-0.076 095
3	0.5430	0.000 145	0.008 827	1.047 760	0.539 067
p symmetry					
<i>n</i>	ζ	2p	3p		
2	5.3000	-0.052 709	-0.008 223		
2	2.0672	0.892 418	-0.031 608		
2	1.2200	-0.401 842	-1.903 876		
2	0.7381	0.980 819	1.823 751		
3	3.5293	-0.348 264	0.044 579		
d symmetry					
<i>n</i>	ζ	3d			
3	1.7000	1.142 786			
3	2.8000	-0.184 575			

s-type, 5 p-type, and 2 d-type functions. This set is based on the Bagus-Gilbert 5-s, 4-p set,¹⁶ and augmented through the procedure already described. Table I contains the basis-set parameters and the expansion coefficients for all the ground-state orbitals for both the full MCSCF and the frozen HF orbitals calculations.

The MCSCF wave function consists of 28 CSF's (equivalent to 30 without constraints; see above) arising from 16 configurations. Table II shows the CSF's the configuration-mixing coefficients, and the total energy obtained for the full MCSCF and for the frozen HF orbitals wave functions. As can be seen from the size of the configuration-mixing coefficients, the most important correlation con-

TABLE XIII. Configuration-mixing coefficients for the 24 CSF representation of the $2s^23s$, 2S state.

Configuration	Coefficient	Configuration	Coefficient
1 $2s^23s$	0.951 49	13 $3s3d^2$	-0.017 17
2 $2s2p^2$	0.043 85	14 $2p^23d$	-0.006 88
3 $2s3s^2$	0.003 32	15 $3p^23d$	0.005 90
4 $3s2p^2$	0.203 88	16 $4s2p^2$	-0.002 67
5 $2s3p^2$	0.031 38	17 $4s3p^2$	-0.002 13
6 $2s3d^2$	0.007 76	18 $2s^23s$	-0.095 34
7 $(2s2p, ^1P)3p$	0.109 30	19 $3s^24s$	-0.009 11
8 $(2s2p, ^3P)3p$	-0.035 86	20 $2s4s^2$	-0.007 54
9 $(3s2p, ^1P)3p$	0.085 79	21 $3s4s^2$	-0.022 07
10 $(3s2p, ^3P)3p$	-0.148 82	22 $(4s2p, ^1P)3p$	-0.000 76
11 $(2p3p, ^3D)3d$	-0.018 43	23 $(4s2p, ^3P)3p$	-0.000 36
12 $3s3p^2$	0.076 23	24 $(2s3s, ^3S)4s$	0.013 26
Total energy			
$E = -24.419 23$ hartrees			

figuration is, of course, the hydrogenically degenerate configuration $2p^3$. The next configuration in order of importance is the $2s2p3d^{18}$ configuration, containing the CSF's $\phi[(2s2p, ^1P)3d, ^2P]$ and $\phi[(2s2p, ^3P)3d, ^2P]$. A calculation using these configurations ($2p^3$, $2s2p3d$) and the dominant configuration yields 78% of the correlation energy from all 28 CSF's. Table III shows the valence-electron correlation energy calculated by various authors and compared with the present work. Weiss,¹³ in his calculation using 35 CSF's, used s , p , d , and f symmetry orbitals, Schaefer and Harris¹⁹ used only s , p , and d symmetry orbitals but had 180 configurations (for both core and valence correlation), and Nesbet's⁴ result is obtained by adding the correlation energy of different electron pairs. The present work, as was said earlier, used s , p , and d symmetry orbitals and 16 configurations. In interpreting these results, one must keep in mind that the correlation energy of different electron pairs is not strictly additive.⁵

Weiss's calculation using only configurations with $n \leq 3$ (second entry in Table III) is analogous to the present calculation, and a comparison of the respective results should be of particular interest. In Weiss's pseudonatural orbital SOC method only 17 CSF's contribute to the lowering of the energy (his orbitals are determined so that other configurations with $n \leq 3$ contribute negligibly, and hence are omitted). In this particular case the MCSCF calculation gave 3.7% more of the correlation energy.

As can be seen from Table II, the difference be-

TABLE XIV. Basis-function parameters and orbital expansion coefficients from the 6 CSF representation of the $2p^3$, 4S state.

<i>s</i> symmetry			
<i>n</i>	ζ	1 <i>s</i>	
1	7.5061	0.101 843	
1	4.3853	0.905 392	
2	2.1010	0.006 260	
2	1.3873	-0.000 511	
3	4.8390	-0.000 800	
<i>p</i> symmetry			
<i>n</i>	ζ	2 <i>p</i>	3 <i>p</i>
2	5.3214	0.008 644	0.101 737
2	2.0795	0.241 521	-1.940 579
2	1.1307	0.582 400	0.269 296
2	0.7913	0.246 040	0.984 896
3	3.5000	-0.014 112	0.595 383
<i>d</i> symmetry			
<i>n</i>	ζ	3 <i>d</i>	
3	1.5000	0.986 369	
3	2.8000	0.018 941	

TABLE XV. Configuration-mixing coefficients for the 6 CSF representation of the $2p^3$, 4S state.

	Configuration	Coefficient
1	$2p^3$	0.990 76
2	$2p3d^2$	0.096 29
3	$2p3p^2$	-0.094 71
4	$3p^3$	-0.001 17
5	$3p3d^2$	-0.000 35
6	$2p^23p$	0.012 27
Total energy		
$E = -24.153\,54$ hartrees		

tween the energy obtained in the full MCSCF calculation and the frozen HF orbitals calculation is extremely small (0.00024*H*). This, along with the fact that the overlap integrals between the HF and the corresponding MCSCF orbitals are at least 0.999, suggests that in many MCSCF calculations one can take over the HF orbitals unchanged, and determine the correlation orbitals only.

Figure 2 shows the dominant orbitals 2*s* and 2*p* and the correlation orbitals 3*s*, 3*p*, and 3*d*. As expected, the correlation orbitals are roughly in the same region of space as the dominant orbitals, and do not resemble the hydrogenic orbitals, or even the so-called virtual SCF orbitals.²⁰

Table IV shows the HF, MCSCF and observed term energies for boron.

Table V shows the computed f values and the comparison with HF, Weiss's, and experimental values, where available. As can be seen, the greatest discrepancy occurs in the f value for the transition $2s2p^2, ^2D - 2s^22p, ^2P$. Here, there is also the largest departure from the HF value. Since the configurations involving d -symmetry correlation orbitals, mixed into the wave function of the $2s2p^2, ^2D$ state, serve to lower the oscillator strength value for the above transition,¹³ and since the present work has only one correlation orbital of d symmetry, the oscillator strength computed here is therefore too high.

All other f values agree closely with those computed by Weiss.

Tables VI-XV show the energies, basis sets, and CSF's for all other states calculated.

ACKNOWLEDGMENTS

The author would like to thank Professor C. C. J. Roothaan for sponsoring this research and for his help during the preparation of the manuscript and also Professor J. Hinze for the use of his diatomic molecules MCSCF program, which was adapted for atomic calculations by the present author.

†Research supported in part by the Advanced Research Projects Agency through the U. S. Army Research Office (Durham), under Contract No. DA-31-124-ARO-D-447 and by the National Science Foundation under Grant Nos. NSF-GP-9284, NSF-GP-15216, and NSF-GP-27138.

*Submitted in partial fulfillment of the requirements for the Ph. D., Department of Physics, University of Chicago, Chicago, Ill. 60637.

¹E. Clementi, J. Chem. Phys. **38**, 2248 (1963).

²H. P. Kelly, Phys. Rev. **144**, 39 (1966).

³V. McKoy and O. Sinanoğlu, J. Chem. Phys. **41**, 2689 (1964).

⁴R. K. Nesbet, Phys. Rev. **175**, 2 (1968).

⁵N. Sabetli and J. Hlnze, J. Chem. Phys. **50**, 684 (1969).

⁶J. Hlnze and C. C. J. Roothaan, Progr. Theoret. Phys. (Kyoto) Suppl. **40**, 37 (1967).

⁷E. U. Condon and G. H. Shortley, *The Theory of Atomic Spectra* (Cambridge U. P., Cambridge, England, 1964).

⁸G. Racah, Phys. Rev. **62**, 438 (1942); **63**, 367 (1943).

⁹C. C. J. Roothaan and P. S. Bagus, *Methods in Computational Physics* (Academic, New York, 1963), Vol. 2,

p. 47.

¹⁰A. F. Starace, Phys. Rev. A **3**, 1242 (1971).

¹¹The superscript *o* indicates states of odd parity.

¹²P. S. Bagus and C. M. Moser, Phys. Rev. **167**, 13 (1969).

¹³A. W. Weiss, Phys. Rev. **188**, 119 (1969).

¹⁴H. F. Schaefer III, R. A. Klemm, and F. E. Harris, Phys. Rev. **176**, 49 (1968).

¹⁵G. Das and A. C. Wahl, J. Chem. Phys. **44**, 87 (1966).

¹⁶P. S. Bagus and T. L. Gilbert, Table 2 in *Tables of Linear Molecule Wave Functions*, edited by A. D. McLean and M. Yoshimine, IBM J. Res. Develop. Suppl. **12** (1967).

¹⁷A more sophisticated test could have been used but the above procedure was preferred.

¹⁸This is the "spin polarization" configuration.

¹⁹H. F. Schaefer, III and F. E. Harris, Phys. Rev. **167**, 67 (1968).

²⁰These are obtained, in SCF-expansion-type calculations, as the unused (unoccupied) solutions of the SCF pseudoeigenvalue equations.

Pauli Approximation in Many-Electron Atoms^{*†}

John Detrich

Laboratory of Molecular Structure and Spectra,
Department of Physics, University of Chicago, Chicago, Illinois 60637
(Received 6 May 1971)

The Pauli approximation for many-electron atoms is derived. This yields an unambiguous expression for the fine-structure splitting and other first-order relativistic corrections to the energy, using nonrelativistic wave functions. A formalism is developed for atoms, based on these results, which is suitable for the evaluation of the fine structure using multiconfiguration wave functions. Fine-structure splittings calculated from Hartree-Fock wave functions are presented for the ground states from He through Ar; the remaining energy corrections are also presented. Multiconfiguration results are presented for the lowest ²D and ²P states of N, accounting for about 80% of the discrepancy between Hartree-Fock values and experimental values.

I. INTRODUCTION

The Pauli approximation is the basis for most attempts to deal with relativistic effects in many-electron systems. In this approach, expressions are derived, with respect to the appropriate nonrelativistic wave function, which give the first-order corrections to the energy. Such expressions were found by Breit¹ for a two-electron system and appear, with a few modifications,²⁻⁴ in their most familiar form as the terms H_1 through H_5 given by Bethe and Slapeter.⁵ These terms give the fine structure and include, among others, spin-orbit, spin-spin, and spin-other-orbit couplings. They do not account for hyperfine structure or the effects of nuclear motion. The primary reason for the popularity of the Pauli approximation lies in its ease of application in comparison to more fully relativistic treatments: Only the nonrelativistic wave function need be dealt with, rather than the more complicated relativistic wave function.

In this paper we apply the Pauli approximation to the case of atoms. The formalism we develop here is of sufficient generality to apply to wave functions which are mixtures of configurations. We present expressions for all of the terms which contribute to the first-order relativistic correction to the energy.

We begin with a derivation of the Pauli approximation in Sec. II. The relativistic formalism from which we start is not entirely satisfactory: The terms for the electron-electron interactions are not Lorentz invariant, and higher-order quantum electrodynamical effects, such as those giving rise to the Lamb shift, are not included. It does, however, contain all the first-order relativistic effects, and therefore, suffices for a derivation of the Pauli approximation. Since our relativistic formalism treats an arbitrary number of electrons

N , we obtain the Pauli approximation explicitly generalized to an N -electron system.

Along with such generality, our goal is derivation of the Pauli approximation characterized by sufficient rigor and attention to detail. In contrast to previous treatments,^{1,6-10} we do not attempt to present the first-order relativistic correction to the energy in terms of an "equivalent Hamiltonian." Consequently, we obtain an expression which is entirely unambiguous and simple to evaluate.

In Sec. III the orbital integrals arising from the first-order relativistic energy corrections in atoms are presented. We outline the construction of multiconfiguration wave functions in Sec. IV and reduce the single-configuration matrix elements to simpler forms on the basis of their assumed symmetry properties. With these results in hand, we give expressions in terms of orbital radial integrals in Sec. V.

Numerical results, obtained by application of our formalism, are given in Sec. VI. These include results from Hartree-Fock wave functions for the ground states of He through Ar. We also give multiconfiguration calculations for the lowest nitrogen ²D and ²P states. These calculations yield substantial improvement in the computed fine-structure splittings in comparison to the Hartree-Fock results.

II. DERIVATION OF THE PAULI APPROXIMATION

The many-electron Dirac Hamiltonian \mathcal{D} for an N -electron system is, in atomic units,

$$\mathcal{D} = \sum_p h_p + \frac{1}{2} \sum_p \sum_{q \neq p} 1/r_{pq}, \quad (1)$$

where the summations are from 1 to N , r_{pq} is the distance between the p th and q th electrons, and h_p is the Dirac Hamiltonian of the p th electron:

$$h_p = c^2 \beta_p + c \vec{\alpha}_p \cdot \vec{p}_p + V_p. \quad (2)$$

In Eq. (2) \vec{p} is the momentum operator, V is the potential due to the nuclear and external fields, c is the speed of light, and $\vec{\alpha}$ and β are the Dirac matrices in conventional representation, namely

$$\vec{\alpha} = \begin{pmatrix} 0 & \vec{\sigma} \\ \vec{\sigma} & 0 \end{pmatrix}, \quad \beta = \begin{pmatrix} I & 0 \\ 0 & -I \end{pmatrix}, \quad (3)$$

where $\vec{\sigma}$ has as its components the 2×2 Pauli matrices and I is the 2×2 unit matrix.

The Breit operator \mathcal{B} for an N -electron system is

$$\mathcal{B} = \frac{1}{2} \sum_p \sum_{q \neq p} b_{pq}, \quad (4)$$

where

$$b_{pq} = -\frac{1}{2} [\vec{\alpha}_p \cdot \vec{\alpha}_q / r_{pq} + (\vec{\alpha}_p \cdot \vec{r}_{pq})(\vec{\alpha}_q \cdot \vec{r}_{pq}) / r_{pq}^3], \quad (5)$$

and the summations are again from 1 to N ; we use \vec{r}_{pq} for the quantity $(\vec{r}_p - \vec{r}_q)$. Roughly speaking, b_{pq} is the correction to the interaction term $1/r_{pq}$ due to first-order magnetic and retardation effects.^{1,11}

The relativistic one-electron orbitals θ_i are four-component Dirac spinors which we take to form an orthonormal set:

$$\langle \theta_i | \theta_j \rangle = \delta_{ij}. \quad (6)$$

Note that the left-hand side of Eq. (6) involves a summation over four terms as well as integration over the space coordinates. It is also useful to write

$$\theta_i = \begin{pmatrix} \varphi_i \\ \chi_i \end{pmatrix}, \quad (7)$$

where φ_i and χ_i are two-component Pauli spinors: φ_i is the *large component* of θ_i , and χ_i is the *small component*.

From the set of orbitals θ_i we construct Slater determinants Θ_I :

$$\Theta_I = \{\theta_{i_1} \theta_{i_2} \dots \theta_{i_N}\} = (N)^{-1/2} \begin{vmatrix} \theta_{i_1}(1) & \theta_{i_2}(1) & \dots & \theta_{i_N}(1) \\ \theta_{i_1}(2) & \theta_{i_2}(2) & \dots & \theta_{i_N}(2) \\ \dots & \dots & \dots & \dots \\ \theta_{i_1}(N) & \theta_{i_2}(N) & \dots & \theta_{i_N}(N) \end{vmatrix}. \quad (8)$$

The index I indicates an *ordered* set of indices i_1, i_2, \dots, i_N :

$$I = (i_1, i_2, \dots, i_N), \quad i_1 < i_2 < \dots < i_N. \quad (9)$$

The ordering of the indices i_1, i_2, \dots, i_N avoids redundancies in the set of Slater determinants Θ_I . It follows that

$$\langle \Theta_I | \Theta_J \rangle = \delta_{IJ}. \quad (10)$$

In general, we adopt a multiconfiguration wave function Θ of the form

$$\Theta = \sum_I C_I \Theta_I; \quad (11)$$

we assume that Θ is normalized to unity, namely

$$\langle \Theta | \Theta \rangle = 1. \quad (12)$$

The many-electron generalization of the Breit equation is

$$(\mathcal{D} + \mathcal{B})\Theta = E\Theta, \quad (13)$$

where E is the total energy of the N -electron system. In view of Eq. (12), we have

$$E = \langle \Theta | \mathcal{D} + \mathcal{B} | \Theta \rangle. \quad (14)$$

The Breit equation yields unsatisfactory results,² a difficulty often circumvented by determining Θ from the equation

$$\mathcal{D}\Theta = E_D\Theta, \quad (15)$$

instead of from the generalized Breit equation.

Other modifications to the Breit equation have been proposed by Brown and Ravenhall¹² and by Salpeter.¹³ Here we shall proceed from the generalized Breit equation, pointing out the objectionable terms when we encounter them. Then the motivation for the proposal that Eq. (15) be used to determine Θ , instead of the generalized Breit equation, will be clear.

It is convenient to decompose the Dirac Hamiltonian in terms of powers of c , namely

$$\mathcal{D} = c^2 \mathcal{M} + c \mathcal{P} + \mathcal{V}, \quad (16)$$

where [see Eqs. (1), (2)]

$$\begin{aligned} \mathcal{M} &= \sum_p \beta_p, \quad \mathcal{P} = \sum_p \vec{\alpha}_p \cdot \vec{p}_p, \\ \mathcal{V} &= \sum_p V_p + \frac{1}{2} \sum_p \sum_{q \neq p} 1/r_{pq}. \end{aligned} \quad (17)$$

We introduce orbitals ω_i which satisfy the equation

$$\beta \omega_i = m_i \omega_i, \quad m_i = \pm 1. \quad (18)$$

In case $m_i = 1$, ω_i contains only a large component (the small component is zero), and in case $m_i = -1$, ω_i contains only a small component. Correspondingly, we introduce the Slater determinant Ω , where

$$\Omega = \{\omega_1 \omega_2 \dots \omega_N\}. \quad (19)$$

Then we have

$$\mathcal{M}\Omega = M\Omega, \quad (20)$$

where

$$M = \sum_i m_i = 2k - N, \quad 0 < k < N. \quad (21)$$

In Eq. (21), k is the number of orbitals with positive m_i , i.e., with large components only. We shall call M the *rest mass* of Ω . There are an infinite number of Ω 's with the same rest mass, since Eq. (20) determines nothing of the space and spin behavior of Ω . In general, a wave function with rest mass M is a linear combination of Ω 's with rest mass M .

We note that

$$[\mathfrak{M}, \mathfrak{U}] = 0, \quad (22)$$

where the brackets indicate a commutator. Hence if Ω has rest mass M , so does $\mathfrak{U}\Omega$. To deal with \mathfrak{P} and \mathfrak{B} , we introduce the matrices $\tilde{\alpha}^+$ and $\tilde{\alpha}^-$, where

$$\tilde{\alpha}^+ = \begin{pmatrix} 0 & \tilde{\sigma} \\ 0 & 0 \end{pmatrix}, \quad \tilde{\alpha}^- = \begin{pmatrix} 0 & 0 \\ \tilde{\sigma} & 0 \end{pmatrix}. \quad (23)$$

We have the relations

$$\tilde{\alpha} = \tilde{\alpha}^+ + \tilde{\alpha}^-, \quad (24)$$

$$[\beta, \tilde{\alpha}^{\pm}] = \pm 2\tilde{\alpha}^{\pm}. \quad (25)$$

In view of Eq. (24), we may write

$$\mathfrak{P} = \mathfrak{P}^+ + \mathfrak{P}^-, \quad (26)$$

$$\mathfrak{B} = \mathfrak{B}^+ + \mathfrak{B}^0 + \mathfrak{B}^-, \quad (27)$$

where

$$\mathfrak{P}^{\pm} = \sum_p \tilde{\alpha}_p^{\pm} \cdot \tilde{p}_p, \quad (28)$$

$$\mathfrak{B}^{\pm} = \frac{1}{2} \sum_p \sum_{q \neq p} b_{pq}^{\pm}, \quad (29)$$

$$\mathfrak{B}^0 = \frac{1}{2} \sum_p \sum_{q \neq p} b_{pq}^0, \quad (30)$$

with

$$b_{pq}^{\pm} = -\frac{1}{2} [(\tilde{\alpha}_p^{\pm} \cdot \tilde{\alpha}_q^{\pm} / r_{pq} + (\tilde{\alpha}_p^{\pm} \cdot \tilde{r}_{pq})(\tilde{\alpha}_q^{\pm} \cdot \tilde{r}_{pq}) / r_{pq}^3], \quad (31)$$

$$b_{pq}^0 = -\frac{1}{2} \{(\tilde{\alpha}_p^+ \cdot \tilde{\alpha}_q^- + \tilde{\alpha}_p^- \cdot \tilde{\alpha}_q^+) / r_{pq} + [(\tilde{\alpha}_p^+ \cdot \tilde{r}_{pq})(\tilde{\alpha}_q^- \cdot \tilde{r}_{pq}) + (\tilde{\alpha}_p^- \cdot \tilde{r}_{pq})(\tilde{\alpha}_q^+ \cdot \tilde{r}_{pq})] / r_{pq}^3\}. \quad (32)$$

From Eq. (25) these relations follow:

$$[\mathfrak{M}, \mathfrak{P}^{\pm}] = \pm 2\mathfrak{P}^{\pm}, \quad (33)$$

$$[\mathfrak{M}, \mathfrak{B}^{\pm}] = \pm 4\mathfrak{B}^{\pm}, \quad (34)$$

$$[\mathfrak{M}, \mathfrak{B}^0] = 0. \quad (35)$$

Hence, if Ω has rest mass M , so does $\mathfrak{B}^0\Omega$, while $\mathfrak{P}^{\pm}\Omega$ has rest mass $M \pm 2$, and $\mathfrak{B}^{\pm}\Omega$ has rest mass $M \pm 4$.

These relations suggests a partition of Θ into $N+1$ component eigenfunctions of \mathfrak{M} , each with a different rest mass, while the decomposition of \mathfrak{D} , as given by Eq. (16), suggests a perturbation expansion in c^{-1} for these components. We expect the part of Θ of order c^0 to be an eigenfunction of \mathfrak{M} with rest mass M . We anticipate that the parts of Θ of order c^{-1} will have rest masses $M \pm 2$, since \mathfrak{P}^+ and \mathfrak{P}^- occur in \mathfrak{D} multiplied by one power of c less than that multiplying \mathfrak{M} . Similarly, the parts of Θ of order c^{-2} will have rest masses M and $M \pm 4$, etc. Accordingly, we write

$$\Theta = \sum_{m=-(N+M)/2}^{(N-M)/2} \sum_{n=0}^{\infty} c^{-|m|-2n} \Theta_{mn}, \quad (36)$$

where

$$\mathfrak{M}\Theta_{mn} = (M+2m)\Theta_{mn}. \quad (37)$$

We also expand E in powers of c^{-2} :

$$E = c^2 \sum_{n=0}^{\infty} c^{-2n} E_n. \quad (38)$$

We substitute Eqs. (36) and (38) for Θ and E , respectively, in the generalized Breit equation, Eq. (13), and apply Eq. (37). $N+1$ equations result: one for each eigenvalue of \mathfrak{M} , each equation containing only functions of one particular rest mass. We equate powers of c^{-1} in these results. From the equation of order c^2 , we find

$$(M - E_0)\Theta_{00} = 0, \quad (39)$$

while the equations of order c give

$$(M - E_0 \pm 2)\Theta_{\pm 1,0} + \mathfrak{P}^{\pm}\Theta_{00} = 0, \quad (40)$$

and the equations of order unity yield

$$(M - E_0 \pm 4)\Theta_{\pm 2,0} + \mathfrak{P}^{\pm}\Theta_{\pm 1,0} + \mathfrak{P}^{\pm}\Theta_{00} = 0, \quad (41)$$

$$(M - E_0)\Theta_{01} + \mathfrak{P}^+\Theta_{-1,0} + \mathfrak{P}^-\Theta_{10} + (\mathfrak{U} + \mathfrak{B}^0 - E_1)\Theta_{00} = 0. \quad (42)$$

From these equations follow

$$M = E_0, \quad (43)$$

$$\Theta_{\pm 1,0} = \mp \frac{1}{2} \mathfrak{P}^{\pm}\Theta_{00}, \quad (44)$$

$$\Theta_{\pm 2,0} = \frac{1}{8} (\mathfrak{P}^{\pm})^2 \Theta_{00} \mp \frac{1}{4} \mathfrak{B}^{\pm}\Theta_{00}, \quad (45)$$

$$(\mathfrak{T} + \mathfrak{U} + \mathfrak{B}^0)\Theta_{00} = E_1\Theta_{00}, \quad (46)$$

where

$$\mathfrak{T} = \frac{1}{2} [\mathfrak{P}^+, \mathfrak{P}^-] = \frac{1}{2} \sum_p \beta_p \tilde{p}_p^2. \quad (47)$$

It is convenient to introduce Θ'_{01} , defined in terms of Θ_{00} and Θ_{01} by the equation

$$\Theta_{01} = -\frac{1}{8} (\mathfrak{P}^+\mathfrak{P}^- + \mathfrak{P}^-\mathfrak{P}^+) \Theta_{00} + \Theta'_{01}. \quad (48)$$

We substitute Eq. (36) for Θ in the normalization condition, Eq. (12), and equate powers of c^{-1} . The equation of order c^0 is

$$\langle \Theta_{00} | \Theta_{00} \rangle = 1, \quad (49)$$

while the equation of order c^{-2} becomes, after the substitution of Eqs. (44) and (48) for $\Theta_{\pm 1,0}$ and Θ_{01} ,

$$\langle \Theta'_{01} | \Theta_{00} \rangle + \langle \Theta_{00} | \Theta'_{01} \rangle = 0. \quad (50)$$

The substitution of Eqs. (44), (45), and (48) for $\Theta_{\pm 1,0}$, $\Theta_{\pm 2,0}$, and Θ_{01} in Eq. (36) yields a compact approximate expression for Θ , namely

$$\Theta = [1 + c^{-1}\mathfrak{K} + \frac{1}{2}c^{-2}\mathfrak{K}^2 + \frac{1}{4}c^{-2}(\mathfrak{B}^- - \mathfrak{B}^+)]\Theta_{00} + c^{-2}\Theta'_{01} + O(c^{-3}), \quad (51)$$

where

$$\mathfrak{K} = \frac{1}{2} (\mathfrak{P}^- - \mathfrak{P}^+) = \frac{1}{2} \sum_p \tilde{\alpha}_p \cdot \tilde{p}_p \beta_p. \quad (52)$$

We may evaluate E to order c^{-2} by simply using Eq. (51) to substitute for Θ in Eq. (14) and enforcing the normalization condition given by Eq. (12). We compare the resulting expression for E with that given by Eq. (38) to find

$$E_1 = \langle \Theta_{00} | \mathcal{T} + \mathcal{U} + \mathcal{B}^0 | \Theta_{00} \rangle, \quad (53)$$

which is consistent with Eqs. (46) and (49). Proceeding with the evaluation of the second-order energy, we find, after dropping the objectionable term $\frac{1}{4} \langle \Theta_{00} | [\mathcal{B}^*, \mathcal{B}^-] | \Theta_{00} \rangle$,¹⁴

$$E_2 = \langle \mathcal{T} \Theta_{00} | \frac{1}{2} \mathcal{K}^2 \Theta_{00} \rangle + \langle \frac{1}{2} \mathcal{K}^2 \Theta_{00} | \mathcal{T} \Theta_{00} \rangle - \langle \frac{1}{2} \mathcal{K}^2 \Theta_{00} | \mathcal{H} - E_0 | \frac{1}{2} \mathcal{K}^2 \Theta_{00} \rangle + \langle \Theta_{00} | \mathcal{U} + \mathcal{B} | \frac{1}{2} \mathcal{K}^2 \Theta_{00} \rangle + \langle \mathcal{K} \Theta_{00} | \mathcal{U} + \mathcal{B} | \mathcal{K} \Theta_{00} \rangle + \langle \frac{1}{2} \mathcal{K}^2 \Theta_{00} | \mathcal{U} + \mathcal{B} | \Theta_{00} \rangle. \quad (54)$$

The objectionable term does not arise in the evaluation of E_2 if Eq. (45) is replaced by the equation

$$\Theta_{2,0} = \frac{1}{8} (\mathcal{P}^*)^2 \Theta_{00}, \quad (55)$$

omitting the term $\mp \frac{1}{4} \mathcal{B}^* \Theta_{00}$ occurring in Eq. (45). Clearly, Eq. (55) results instead of Eq. (45) if we start from Eq. (15) instead of the generalized Breit equation: This is the motivation for the proposal that Eq. (15) be used to determine Θ , instead of the generalized Breit equation. We conclude that Eq. (55) is correct and abandon Eq. (45).

Now Eq. (51) is replaced by the equation

$$\Theta = [1 + c^{-1} \mathcal{K} + \frac{1}{2} c^{-2} \mathcal{K}^2] \Theta_{00} + c^{-2} \Theta'_{01} + O(c^{-3}). \quad (56)$$

This equation gives the wave function to order c^{-2} in terms of Θ_{00} and Θ'_{01} ; it is one of the central results of our treatment. Even without an evaluation of Θ'_{01} , it has application apart from the evaluation of the energy to order c^{-2} . For instance, if one supposes the large component of a relativistic orbital is given by φ_l , it follows from Eq. (56) that the small component is given, to order c^{-2} , by $\frac{1}{2} c^{-1} \vec{\sigma} \cdot \vec{p} \varphi_l$.

Since our treatment assumes relativistic effects are small, we may identify $c^2 E_0$ as the rest-mass energy. Observable electrons always have positive rest mass, hence, the rest mass of an N -electron system should be N , i.e.,

$$E_0 = N. \quad (57)$$

Combining this with Eq. (38), we give for the energy to order c^{-2}

$$E = c^2 N + E_1 + c^{-2} E_2 + \dots, \quad (58)$$

with E_1 given by Eq. (53) and E_2 given by Eq. (54).

Θ_{00} and Θ'_{01} consist only of Slater determinants which contain orbitals ω_i satisfying Eq. (18) and, in consequence of Eq. (57), only the possibility $m_i = 1$ may occur for these orbitals. Note that each term in \mathcal{B}^0 contains an operator $\vec{\alpha}_i$ which gives zero when operating on an orbital ω_i with $m_i = 1$. Hence

$\mathcal{B}^0 \Theta_{00}$ is zero, and the Breit operator does not contribute to the energy E_1 . Since each orbital ω_i has positive m_i , only the large components are different from zero. A wave function Ψ can be derived from Θ_{00} by replacing each four-component ω_i in Θ_{00} by the corresponding large component φ_i , a two-component Pauli spinor. Then Eqs. (49), (46), and (53) go over into the equations

$$\langle \Psi | \Psi \rangle = 1, \quad (59)$$

$$\mathcal{H} \Psi = E_1 \Psi, \quad (60)$$

$$E_1 = \langle \Psi | \mathcal{H} | \Psi \rangle, \quad (61)$$

respectively, where

$$\mathcal{H} = \sum_p [\frac{1}{2} \vec{p}_p^2 + V_p] + \frac{1}{2} \sum_p \sum_{q \neq p} 1/r_{pq}, \quad (62)$$

with the summations running from 1 to N . \mathcal{H} is plainly the nonrelativistic Hamiltonian, hence Ψ and E_1 must be the nonrelativistic wave function and nonrelativistic energy, respectively.

Our expression for E_2 in terms of Θ_{00} likewise goes over into an expression in terms of Ψ . We find

$$E_2 = -\frac{1}{8} \sum_p \langle \vec{p}_p^2 \Psi | \vec{p}_p^2 \Psi \rangle + \langle D_1 \Psi | \Psi \rangle + \langle \Psi | D_1 \Psi \rangle + \langle D_2 \Psi | \Psi \rangle + \langle \Psi | D_2 \Psi \rangle + \langle \Psi | F + G_0 + G_1 + G_2 | \Psi \rangle. \quad (63)$$

where

$$D_1 = -\frac{1}{8} \sum_p i \vec{\mathcal{E}}_p \cdot \vec{p}_p, \quad (64)$$

$$D_2 = \frac{1}{8} \sum_p \sum_{q \neq p} i \vec{\mathcal{E}}_{pq} \cdot \vec{p}_p, \quad (65)$$

$$F = \sum_p f_p, \quad (66)$$

$$G_0 = \frac{1}{2} \sum_p \sum_{q \neq p} g_{0,pq}, \quad (67)$$

$$G_1 = \frac{1}{2} \sum_p \sum_{q \neq p} g_{1,pq}, \quad (68)$$

$$G_2 = \frac{1}{2} \sum_p \sum_{q \neq p} g_{2,pq}, \quad (69)$$

with

$$\vec{\mathcal{E}}_p = i \vec{p}_p V_p, \quad (70)$$

$$\vec{\mathcal{E}}_{pq} = i \vec{p}_p 1/r_{pq}, \quad (71)$$

$$f_p = \frac{1}{2} (\vec{\mathcal{E}}_p \times \vec{p}_p) \cdot \vec{s}_p, \quad (72)$$

$$g_{0,pq} = -\frac{1}{2} [\gamma_{pq}^{-1} \vec{p}_p \cdot \vec{p}_q + \gamma_{pq}^{-3} \vec{r}_{pq} \cdot (\vec{r}_{pq} \times \vec{p}_p) \vec{p}_q], \quad (73)$$

$$g_{1,pq} = \frac{1}{2} (\vec{\mathcal{E}}_{pq} \times \vec{p}_p) \cdot \vec{s}_p + \frac{1}{2} (\vec{\mathcal{E}}_{qp} \times \vec{p}_q) \cdot \vec{s}_q + (\vec{\mathcal{E}}_{pq} \times \vec{p}_p) \cdot \vec{s}_q + (\vec{\mathcal{E}}_{qp} \times \vec{p}_q) \cdot \vec{s}_p, \quad (74)$$

$$g_{2,pq} = \vec{s}_p \cdot \vec{s}_q / r_{pq}^3 - 3(\vec{s}_p \cdot \vec{r}_{pq})(\vec{s}_q \cdot \vec{r}_{pq}) / r_{pq}^5. \quad (75)$$

Here we have used $\vec{s}_p = \frac{1}{2} \vec{\sigma}_p$; notice that $\vec{\mathcal{E}}_p$ and $\vec{\mathcal{E}}_{pq}$ are the electric fields acting on the p th electron due to the nuclear charge and the q th electron, respectively.

Although we have integrated by parts to express E_2 in terms of the Hermitian operators f_p , $g_{0,pq}$, $g_{1,pq}$, and $g_{2,pq}$, we have not done so in the case of the integrals

$$\langle \tilde{p}_p^2 \Psi | \tilde{p}_p^2 \Psi \rangle, \quad \langle D_1 \Psi | \Psi \rangle + \langle \Psi | D_1 \Psi \rangle, \\ \langle D_2 \Psi | \Psi \rangle + \langle \Psi | D_2 \Psi \rangle.$$

The attempt to find a general expression for the integral $\langle \tilde{p}_p^2 \Psi | \tilde{p}_p^2 \Psi \rangle$ in terms of the expectation value of an operator is unprofitable.⁴ This rules out the possibility of expressing E_2 as the expectation value of some operator. The integrals given in Eq. (63), however, are unambiguous and can be evaluated in a straightforward manner.

Integrals involving $-(\frac{8}{3}\pi)\tilde{s}_p \cdot \tilde{s}_q \delta^{(3)}(\tilde{r}_{pq})$, which occur in other treatments, have here been eliminated in favor of simpler terms. As pointed out by de-Shalit and Talmi,¹⁵ the integral involving $-(\frac{8}{3}\pi)\tilde{s}_p \cdot \tilde{s}_q \delta^{(3)}(\tilde{r}_{pq})$ is equal to the integral involving $2\pi\delta^{(3)}(\tilde{r}_{pq})$ whenever the wave function is antisymmetric with respect to the exchange of the p th and q th electrons. Accordingly we have the result

$$-\frac{1}{2} \sum_p \sum_{q \neq p} \{ \langle (i\tilde{\sigma}_{pq} \cdot \tilde{p}_p \Psi) | \tilde{s}_p \cdot \tilde{s}_q | \Psi \rangle \\ + \langle \Psi | \tilde{s}_p \cdot \tilde{s}_q | (i\tilde{\sigma}_{pq} \cdot \tilde{p}_p \Psi) \rangle \} \\ = 2[\langle D_2 \Psi | \Psi \rangle + \langle \Psi | D_2 \Psi \rangle]. \quad (76)$$

This relation was used in deriving Eq. (63).

Classically, the quantity $-\frac{1}{2}\langle \tilde{p}_p^2 \Psi | \tilde{p}_p^2 \Psi \rangle$ gives the relativistic shift in mass of the p th electron due to its speed. f is the well-known spin-orbit coupling term due to the nuclear charge, coupling the electron with its own orbital moment with respect to the nucleus. The first two terms in g_1 are similar terms, with the nuclear charge replaced by that of another electron. The last two terms in g_1 couple the spin of one electron with the orbit of another electron. g_2 gives the spin-spin coupling. The quantities $\langle D_1 \Psi | \Psi \rangle + \langle \Psi | D_1 \Psi \rangle$ and $\langle D_2 \Psi | \Psi \rangle + \langle \Psi | D_2 \Psi \rangle$ have no obvious classical interpretation.

It is worth pointing out that although we have derived Ψ starting from the relativistic Θ , the starting point of calculations using the Pauli approximation will be Ψ . From this point of view, \mathcal{H} rather than \mathcal{M} is the zeroth-order Hamiltonian, since the rest-mass energy is simply a constant. Then the relativistic effects constitute a simple perturbation on \mathcal{H} (although this perturbation is not given by a Hamiltonian operator), yielding $c^{-2}E_2$ for the first-order perturbation correction to the energy.

III. ORBITAL INTEGRALS IN TERMS OF RADIAL INTEGRALS FOR ATOMS

We shall henceforth assume that the nonrelativistic wave function Ψ is constructed from two-

component orbitals φ_i which are symmetry orbitals. In lieu of φ_i we introduce the notation $\varphi_{i\lambda\alpha}$; the orbitals are defined by

$$\varphi_{i\lambda\alpha}(r, \theta, \phi) = r^{-1} P_{\lambda i}(r) Y_{\lambda\alpha}(\theta, \phi) \eta_a. \quad (77)$$

Here $Y_{\lambda\alpha}(\theta, \phi)$ is the conventional normalized spherical harmonic, and η_a is the two-component spin function with $m_s = a$. The index i now labels orbitals not distinguishable by symmetry. We also assume that the orbitals form an orthonormal set; hence we may write

$$\int_0^\infty dr P_{\lambda i}(r) P_{\lambda j}(r) = \delta_{ij}. \quad (78)$$

Equation (77) allows us to integrate out the spin and angular dependence in the orbital integrals which arise in the evaluation of E_2 , leaving integrals only over radial functions. The orbital integrals which arise in the evaluation of the non-relativistic energy E_1 will not be treated here.

The radial integrals which emerge from the one-electron integrals are

$$\pi_{\lambda i j} = \frac{1}{2} \left\{ - \int_0^\infty dr [P_{\lambda i}'(r) - \lambda(\lambda+1)r^{-2}P_{\lambda i}(r)] \right. \\ \times [P_{\lambda j}'(r) - \lambda(\lambda+1)r^{-2}P_{\lambda j}(r)] \\ \left. + Z[r^{-2}P_{\lambda i}(r)P_{\lambda j}(r)]_{r=0} \right\}, \quad (79)$$

$$\xi_{\lambda i j} = \frac{1}{2} Z \int_0^\infty dr r^{-3} P_{\lambda i}(r) P_{\lambda j}(r). \quad (80)$$

The prime indicates differentiation with respect to r . $\xi_{\lambda i j}$ is similar to the usual notation for the single-electron spin-orbit coupling coefficient,¹⁶ but it should be noted that the factor c^{-2} is not included. All of our expressions will be presented without this factor. We express the two-electron integrals in terms of the radial integrals given by

$$R_{\lambda i, \mu j; \rho k, \sigma l; \omega} = \int_0^\infty dr \int_0^r ds (rs)^{-1} U_\omega(r, s) \\ \times P_{\lambda i}(r) P_{\mu j}(r) P_{\rho k}(s) P_{\sigma l}(s), \quad (81)$$

$$P_{\lambda i, \mu j; \rho k, \sigma l; \nu} = \int_0^\infty dr \int_0^\infty ds U_\nu(r, s) \\ \times K_{\lambda i, \mu j; \nu}(r) P_{\rho k}(s) P_{\sigma l}(s), \quad (82)$$

$$Q_{\lambda i, \mu j; \rho k, \sigma l; \nu} = \frac{1}{2} \int_0^\infty dr \int_0^\infty ds W_\nu(r, s) \\ \times K_{\lambda i, \mu j; \nu}(r) K_{\rho k, \sigma l; \nu}(s), \quad (83)$$

$$D_{\lambda i, \mu j, \rho k, \sigma l} = \frac{1}{4} \int_0^\infty dr r^{-2} P_{\lambda i}(r) P_{\mu j}(r) P_{\rho k}(r) P_{\sigma l}(r), \quad (84)$$

where

$$U_\nu(r, s) = \begin{cases} r^{-\nu-1} s^\nu, & s < r \\ s^{-\nu-1} r^\nu, & s > r \end{cases} \quad (85)$$

$$W_\nu(r, s) = rs [U_{\nu+1}(r, s)/(2\nu+3) \\ - U_{\nu-1}(r, s)/(2\nu-1)], \quad (86)$$

$$K_{\lambda, \mu; \nu}(\gamma) = k_{\lambda, \mu; \nu} P_{\lambda}(\gamma) \frac{\partial}{\partial \gamma} [\gamma^{-1} P_{\mu}(\gamma)] \\ - k_{\mu, \lambda; \nu} P_{\mu}(\gamma) \frac{\partial}{\partial \gamma} [\gamma^{-1} P_{\lambda}(\gamma)] , \quad (87)$$

with

$$k_{\lambda, \mu; \nu} = \frac{1}{2} [\nu(\nu+1) + \lambda(\lambda+1) - \mu(\mu+1)] \\ \times [\nu(\nu+1)]^{-1/2}; \quad (88)$$

it should be noted that $k_{\lambda, \lambda; 0} = 0$. Under interchange of shell indices, we have the following relations for these integrals:

$$\pi_{\lambda \lambda f} = \pi_{\lambda f \lambda} , \quad (89)$$

$$\zeta_{\lambda \lambda f} = \zeta_{\lambda f \lambda} , \quad (90)$$

$$R_{\lambda \lambda, \mu f; \rho h, \sigma l; \omega} = R_{\mu f, \lambda l; \rho h, \sigma l; \omega} = R_{\lambda \lambda, \mu f; \sigma l, \rho h; \omega} , \quad (91)$$

$$P_{\lambda \lambda, \mu f; \rho h, \sigma l; \nu} = -P_{\mu f, \lambda l; \rho h, \sigma l; \nu} = P_{\lambda \lambda, \mu f; \sigma l, \rho h; \nu} , \quad (92)$$

$$Q_{\lambda \lambda, \mu f; \rho h, \sigma l; \nu} = -Q_{\mu f, \lambda l; \rho h, \sigma l; \nu} = -Q_{\lambda \lambda, \mu f; \sigma l, \rho h; \nu} , \quad (93)$$

$$Q_{\lambda \lambda, \mu f; \rho h, \sigma l; \nu} = Q_{\rho h, \sigma l; \lambda \lambda, \mu f; \nu} , \quad (94)$$

$$D_{\lambda \lambda, \mu f, \rho h, \sigma l} = D_{\mu f, \lambda l, \rho h, \sigma l} \\ = D_{\rho h, \mu f, \lambda l, \sigma l} = D_{\sigma l, \mu f, \rho h, \lambda l} . \quad (95)$$

Note, however, that there is in general no relation between $R_{\lambda \lambda, \mu f; \rho h, \sigma l; \omega}$ and $R_{\rho h, \sigma l; \lambda \lambda, \mu f; \omega}$, nor between $P_{\lambda \lambda, \mu f; \rho h, \sigma l; \nu}$ and $P_{\rho h, \sigma l; \lambda \lambda, \mu f; \nu}$.

$$\langle \varphi_{\lambda \alpha \sigma}(1) \varphi_{\rho \gamma \tau}(2) | g_{2,12} | \varphi_{\mu \beta \delta}(1) \varphi_{\lambda \alpha \delta}(2) \rangle = C(1, 1, 2; b-a, d-c | b | s_{b-a} | a) \langle d | s_{d-c} | c \rangle \\ \times \sum_{\omega} (-1)^{\omega} \left[\frac{1}{2} \omega(\omega+1)(2\omega-1)(2\omega+1)(2\omega+3) \right]^{1/2} [C(\omega+1, \omega-1, 2; \alpha-\beta, \beta+b+d-\alpha-a-c | \lambda \alpha | C_{\omega+1, \alpha-\beta} | \mu \beta) \\ \times \langle \rho \gamma | C_{\omega-1, \beta+b+d-\alpha-a-c} | \sigma \delta \rangle R_{\lambda \lambda, \mu f; \rho h, \sigma l; \omega} + C(\omega-1, \omega+2, 2; \alpha-\beta, \beta+b+d-\alpha-a-c | \lambda \alpha | C_{\omega-1, \alpha-\beta} | \mu \beta) \\ \times \langle \rho \gamma | C_{\omega+1, \beta+b+d-\alpha-a-c} | \sigma \delta \rangle R_{\rho h, \sigma l; \lambda \lambda, \mu f; \omega}] , \quad (101)$$

where $C(\lambda \mu \nu; \alpha, \beta)$ is the Clebsch-Gordan coefficient in Rose's notation,¹⁹ and $C_{\lambda \alpha}$ is the unnormalized spherical harmonic:

$$C_{\lambda \alpha}(\theta, \phi) = [4\pi/(2\lambda+1)]^{1/2} Y_{\lambda \alpha}(\theta, \phi) . \quad (102)$$

The summation over ω in Eq. (101) may be taken to run over all positive integers, but only terms in which the angular integrals do not vanish are different from zero. Hence, only values of ω for which both of the quantities $\lambda + \mu + \omega$ and $\rho + \sigma + \omega$ are odd integers contribute to the sum. It follows that the entire integral in Eq. (101) vanishes unless $\lambda + \mu + \rho + \sigma$ is an even integer; in other words, the matrix elements of g_2 are diagonal with respect to parity. The values of ω for which $R_{\lambda \lambda, \mu f; \rho h, \sigma l; \omega}$ occurs in Eq. (101) are further restricted by the conditions

A. One-Electron Integrals

For atoms, we have

$$V_p = -Z/r_p , \quad (96)$$

hence, recalling Eq. (70),

$$\vec{\delta}_p \cdot \vec{p}_p = -iZr_p^{-2} \frac{\partial}{\partial r_p} . \quad (97)$$

Then we easily find

$$\frac{1}{8} [- \langle \vec{p}_p^2 \varphi_{\lambda \alpha \sigma} | \vec{p}_p^2 \varphi_{\mu \beta \delta} \rangle - \langle (i\vec{\delta}_p \cdot \vec{p}_p \varphi_{\lambda \alpha \sigma}) | \varphi_{\mu \beta \delta} \rangle \\ - \langle \varphi_{\lambda \alpha \sigma} | (i\vec{\delta}_p \cdot \vec{p}_p \varphi_{\mu \beta \delta}) \rangle] \\ = \delta_{\lambda \mu} \delta_{\alpha \beta} \delta_{\sigma \delta} \pi_{\lambda \lambda f} . \quad (98)$$

For the integral over f , we find

$$\langle \varphi_{\lambda \alpha \sigma} | f | \varphi_{\mu \beta \delta} \rangle = \delta_{\lambda \mu} \langle \lambda \alpha | l_{\alpha-\beta} | \lambda \beta \rangle \langle b | s_{\alpha-\beta} | a \rangle \zeta_{\lambda \lambda f} , \quad (99)$$

where the only nonvanishing components of l_{γ} and s_{γ} are given by

$$l_0 = l_x , \quad l_{\pm 1} = \mp (2)^{-1/2} (l_x \pm i l_y) , \\ s_0 = s_x , \quad s_{\pm 1} = \mp (2)^{-1/2} (s_x \pm i s_y) . \quad (100)$$

Hence the angular part of Eq. (99) is just the expectation value of $\vec{l} \cdot \vec{s}$.

B. Two-Electron Integrals

For g_2 we have, from the results of Innes¹⁷ (or the equivalent results of Horie¹⁸),

$$\lambda + \mu \geq \omega + 1 \geq |\lambda - \mu| , \\ \rho + \sigma \geq \omega - 1 \geq |\rho - \sigma| . \quad (103)$$

The values of ω for which $R_{\rho h, \sigma l; \lambda \lambda, \mu f; \omega}$ occurs are restricted by conditions similar to those given in Eq. (103), with λ and ρ interchanged and μ and σ interchanged. Note that the range of ω for which $R_{\rho h, \sigma l; \lambda \lambda, \mu f; \omega}$ may occur can differ from the range of ω for which $R_{\lambda \lambda, \mu f; \rho h, \sigma l; \omega}$ may occur.

We write

$$g_{1,12} = g'_{1,12} + g'_{1,21} , \quad (104)$$

where

$$g'_{1,12} = -\frac{1}{2} r_{12}^{-3} (\vec{r}_{12} \times \vec{p}_1) \cdot (\vec{s}_1 + 2\vec{s}_2) . \quad (105)$$

Then the results of Blume and Watson²⁰ yield

$$\begin{aligned}
\langle \varphi_{i\lambda\alpha\sigma}(1) \varphi_{k\rho\gamma c}(2) | g'_{1,12} | \varphi_{j\mu\beta\delta}(1) \varphi_{l\sigma\delta d}(2) \rangle &= \frac{1}{2} (3)^{-1/2} (\delta_{cd} \langle b | s_{\alpha+\gamma-\beta-\delta} | a \rangle + 2\delta_{ab} \langle d | s_{\alpha+\gamma-\beta-\delta} | c \rangle) \\
&\times \sum_{\nu} (-1)^{\nu} \langle \rho\gamma | C_{\nu,\gamma-\delta} | \sigma\delta \rangle \{ (2\nu+1)^{1/2} C(\nu\nu 1; \gamma-\delta, \alpha-\beta) \langle \lambda\alpha | C_{\nu,\alpha-\beta} | \mu\beta \rangle P_{\lambda l, \mu j; \rho k, \sigma l; \nu} \\
&- \sum_{\omega=\nu+1} (2\nu+1)(2\omega+1)^{1/2} C(\nu\omega 1; \gamma-\delta, \alpha-\beta) \langle \lambda\alpha | T_{\omega, \alpha-\beta}^{\nu} | \mu\beta \rangle \\
&\times [\delta_{\omega, \nu+1} R_{\lambda l, \mu j; \rho k, \sigma l; \omega} - \delta_{\omega, \nu-1} R_{\rho k, \sigma l; \lambda l, \mu j; \omega}] \} \quad (106)
\end{aligned}$$

Here we have introduced the operator $T^{\nu}\omega\alpha$, which operates on the angular coordinates θ and ϕ ; it is given by the equation

$$T_{\omega\alpha}^{\nu} = \sum_{\beta} C(\nu 1 \omega; \alpha - \beta, \beta) C_{\nu, \alpha - \beta} l_{\beta} \quad (107)$$

hence²⁰

$$\begin{aligned}
\langle \lambda\alpha | T_{\omega\gamma}^{\nu} | \mu\beta \rangle \\
= \delta_{\alpha-\beta, \gamma} (-1)^{\nu-\omega} (2\mu+1) [(2\omega+1)\mu(\mu+1)/(2\lambda+1)]^{1/2} \\
\times \left\{ \begin{matrix} \nu & 1 & \omega \\ \mu & \lambda & \mu \end{matrix} \right\} C(\mu\nu\lambda; 00) C(\mu\omega\lambda; \beta, \alpha-\beta) \quad (108)
\end{aligned}$$

where

$$\left\{ \begin{matrix} \nu & 1 & \omega \\ \mu & \lambda & \mu \end{matrix} \right\}$$

is the 6- j symbol.²¹ Nonzero terms in the summation over ν in Eq. (106) occur only when both $\lambda + \mu + \nu$ and $\rho + \sigma + \nu$ are even integers, hence the

integral for g_1 , like the integral for g_2 , vanishes unless $\lambda + \mu + \rho + \sigma$ is an even integer. The range of nonzero terms in the summation over ν in Eq. (106) is further restricted by the conditions

$$\begin{aligned}
\lambda + \mu &\geq \nu \geq |\lambda - \mu| \quad , \\
\rho + \sigma &\geq \nu \geq |\rho - \sigma| \quad . \quad (109)
\end{aligned}$$

Note that the nonvanishing terms in $R_{\lambda l, \mu j; \rho k, \sigma l; \omega}$ occur only for values of ω satisfying Eq. (103) and that a similar situation holds for the terms in $R_{\rho k, \sigma l; \lambda l, \mu j; \omega}$.

In place of our integral $P_{\lambda l, \mu j; \rho k, \sigma l; \omega}$, Blume and Watson²⁰ use an expression which contains divergent integrals when $\nu = \lambda + \mu$ (unless $\lambda = \mu$). The integrals diverge because $P_{\lambda l}(r)$ and $P_{\mu j}(r)$ are proportional to $r^{\lambda+1}$ and $r^{\mu+1}$, respectively, in the neighborhood of $r=0$. A similar situation arises in the expressions given by Beck.²² In the integral $P_{\lambda l, \mu j; \rho k, \sigma l; \nu}$ no divergences occur.

The general expression for the integral of g_0 is

$$\begin{aligned}
\langle \varphi_{i\lambda\alpha\sigma}(1) \varphi_{k\rho\gamma c}(2) | g_{0,12} | \varphi_{j\mu\beta\delta}(1) \varphi_{l\sigma\delta d}(2) \rangle &= -\delta_{ab}\delta_{cd} \sum_{\nu} [\langle \lambda\alpha | C_{\nu, \alpha-\beta} | \mu\beta \rangle \langle \sigma\delta | C_{\nu, \alpha-\beta} | \rho\gamma \rangle Q_{\lambda l, \mu j; \rho k, \sigma l; \nu} \\
&+ (2\nu+1)(\nu+2)^{-1} \langle \lambda\alpha | T_{\nu+1, \alpha-\beta}^{\nu} | \mu\beta \rangle \langle \sigma\delta | T_{\nu+1, \alpha-\beta}^{\nu} | \rho\gamma \rangle (R_{\lambda l, \mu j; \rho k, \sigma l; \omega} + R_{\rho k, \sigma l; \lambda l, \mu j; \omega})] \quad (110)
\end{aligned}$$

the summation over ν proceeds as in Eq. (106). In case $\lambda l = \mu j = \rho k = \sigma l$, Eq. (110) gives Yanagawa's result.²³ Beck's results²² imply Eq. (110) when the divergent integrals in his expressions are eliminated.

An integration by parts yield

$$\begin{aligned}
\frac{1}{i} (\langle i\vec{\delta}_{12} \cdot \vec{p}_1 \varphi_{i\lambda\alpha\sigma}(1) \varphi_{k\rho\gamma c}(2) | \varphi_{j\mu\beta\delta}(1) \varphi_{l\sigma\delta d}(2) \rangle + \langle \varphi_{i\lambda\alpha\sigma}(1) \varphi_{k\rho\gamma c}(2) | i\vec{\delta}_{12} \cdot \vec{p}_1 \varphi_{j\mu\beta\delta}(1) \varphi_{l\sigma\delta d}(2) \rangle) \\
= \delta_{ab}\delta_{cd} D_{\lambda l, \mu j; \rho k, \sigma l} \sum_{\nu} (2\nu+1) \langle \lambda\alpha | C_{\nu, \alpha-\beta} | \mu\beta \rangle \langle \sigma\delta | C_{\nu, \alpha-\beta} | \rho\gamma \rangle \quad (111)
\end{aligned}$$

where the summation over ν proceeds as in Eq. (106).

IV. REDUCED-MATRIX ELEMENTS

Since the radial function $P_{\lambda l}(r)$ introduced in Eq. (77) is the same for all values of α and a , there are $4\lambda + 2$ orbitals $\varphi_{i\lambda\alpha\sigma}$ characterized by the same radial function $P_{\lambda l}(r)$. This set is an *electron shell*, labeled by the combination index λi .

From the available orbitals, one can construct N -electron Slater determinants (SD's); each SD is completely characterized by the particular orbitals used for its construction, which are called the *occupied orbitals* in that SD. The number of

occupied orbitals of a shell in a particular SD is called the *occupation number* of the shell in that SD. Obviously, the occupation number of the shell λi in any SD is $\leq 4\lambda + 2$; when the equality applies, the shell λi is called a *closed shell* of the SD, otherwise an open shell. An *electron configuration* is the collection of all SD's which have the same shell occupation numbers. Hence, a set of occupation numbers defines a configuration completely, although in general it only partially characterizes the SD's of a configuration.

An electron configuration can be resolved into N -electron functions which belong to definite symmetry species and subspecies. These N -electron functions are linear combinations of the SD's of a

configuration; we call them *configuration state functions* (CSF's).²⁴ We introduce for the CSF's the notation Φ_{ASLJMP} . Each CSF is an eigenfunction of $\tilde{S}^2, \tilde{L}^2, \tilde{J}^2, J_z$, and \mathcal{P} (parity). The operators \tilde{J}^2, J_z , and \mathcal{P} commute with the *relativistic* Hamiltonian \mathcal{D} (and with the Breit operator \mathcal{B}), hence J, M , and P are "good" quantum numbers. The operators \tilde{S}^2 and \tilde{L}^2 only commute with the *non-relativistic* Hamiltonian, hence S and L are, strictly speaking, not good quantum numbers. The index A labels CSF's not distinguishable by their values of S, L, J, M , and P . CSF's with the same values of S, L, J, M , and P , but from different configurations, have different values of A ; so do different CSF's arising from the same configuration with the same values of S, L, J, M , and P , when this is possible.

In many cases, a CSF arising from a particular configuration is uniquely specified by its values of S, L, J , and M (the value of P can always be deduced from the set of configuration occupation numbers). Important examples are configurations which have at most one open s and/or one open

p shell. On the other hand, for multiple open p shells and for open d or f shells this is no longer always the case. A simple example is the configuration $2p^3 3p$. All of the CSF's from this configuration have $P = -1$. The CSF's arising from this configuration are uniquely determined by the specification of S, L, J , and M for the cases where S and L indicate $^2S, ^4S, ^4P, ^4D$, or 2F . On the other hand, there are three independent 2P CSF's, with the $2p$ orbitals coupled to form a $^1S, ^1D$, or 3P function; similarly there are two independent 2D CSF's, with the $2p$ orbitals coupled to form a 3P or 1D function. In these cases the index A for the CSF Φ_{ASLJMP} not only indicates the configuration $2p^3 3p$, but also serves to distinguish between the three possible 2P CSF's, or between the two possible 2D CSF's.

The use of CSF's that are eigenfunctions of \tilde{L}^2 and \tilde{S}^2 allows an application of the Wigner-Eckart theorem.²⁵ The dependence on J of the matrix elements with respect to the SCF's may be factored out in terms of a single $6-j$ symbol,²⁶ allowing us to write, for instance,

$$\langle ASLMP | F | A'S'L'J'M'P' \rangle = \delta_{JJ'} \delta_{MM'} \delta_{PP'} (-1)^{L+S'+J} \left\{ \begin{matrix} L & S & J \\ S' & L' & 1 \end{matrix} \right\} \langle ASLP | F | A'S'L'P \rangle \quad (112)$$

The quantity $\langle ASLP | F | A'S'L'P \rangle$ is the *reduced-matrix element* of F . As our notation suggests, it is independent of the values of J and M , although it still depends on other details of the construction of the two CSF's, including the values of S and L and of S' and L' . In similar fashion, we write

$$-\frac{1}{6} \sum_p \langle \tilde{p}_p^2 \Phi_{ASLJMP} | \tilde{p}_p^2 \Phi_{A'S'L'J'M'P'} \rangle + \langle D_1 \Phi_{ASLJMP} | \Phi_{A'S'L'J'M'P'} \rangle + \langle \Phi_{ASLJMP} | D_1 \Phi_{A'S'L'J'M'P'} \rangle = \delta_{JJ'} \delta_{MM'} \delta_{PP'} \delta_{SS'} \delta_{LL'} \langle ASLP | \Pi_1 | A'SLP \rangle \quad (113)$$

$$\langle D_2 \Phi_{ASLJMP} | \Phi_{A'S'L'J'M'P'} \rangle + \langle \Phi_{ASLJMP} | D_2 \Phi_{A'S'L'J'M'P'} \rangle = \delta_{JJ'} \delta_{MM'} \delta_{PP'} \delta_{SS'} \delta_{LL'} \langle ASLP | \Pi_2 | A'SLP \rangle \quad (114)$$

$$\langle ASLJMP | G_0 | A'S'L'J'M'P' \rangle = \delta_{JJ'} \delta_{MM'} \delta_{PP'} \delta_{SS'} \delta_{LL'} \langle ASLP | G_0 | A'SLP \rangle \quad (115)$$

$$\langle ASLJMP | G_1 | A'S'L'J'M'P' \rangle = \delta_{JJ'} \delta_{MM'} \delta_{PP'} (-1)^{L+S'+J} \left\{ \begin{matrix} L & S & J \\ S' & L' & 1 \end{matrix} \right\} \langle ASLP | G_1 | A'S'L'P \rangle \quad (116)$$

$$\langle ASLJMP | G_2 | A'S'L'J'M'P' \rangle = \delta_{JJ'} \delta_{MM'} \delta_{PP'} (-1)^{L+S'+J} \left\{ \begin{matrix} L & S & J \\ S' & L' & 2 \end{matrix} \right\} \langle ASLP | G_2 | A'S'L'P \rangle \quad (117)$$

These relations constitute a considerable simplification, allowing the matrix elements to be computed for all values of J with little more effort than that required for a single value of J .

The matrix elements given in Eqs. (113)–(115) vanish unless $L = L'$ and $S = S'$. However, non-zero matrix elements of F, G_1 , and G_2 for which $L' \neq L$ and/or $S' \neq S$ do exist, hence an accurate wave function describing an atomic state is not in general an eigenfunction of \tilde{L}^2 and \tilde{S}^2 . For a large

number of cases, however, wave functions with definite L and S provide excellent approximations (Russell-Saunders coupling), and the matrix elements with $L \neq L'$ and/or $S' \neq S$ may be neglected. Then the relativistic corrections simply remove the degeneracy with respect to J of the nonrelativistic energy. This case is our primary concern in this paper.

In this case the wave function Ψ is an eigenfunction of \tilde{L}^2 and \tilde{S}^2 ; we append the quantum numbers,

S, L, J, M and P , writing Ψ_{SLJMP} . Our expansion of the wave function in terms of the CSF's may be written

$$\Psi_{SLJMP} = \sum_A \Phi_{ASLJMP} C_{ASLP} \quad (118)$$

We can always choose the CSF's such that the ex-

pansion coefficients become real; we assume this to be done. Note that the expansion coefficients C_{ASLP} do not depend on the quantum numbers J and M .

We combine our expression of Ψ_{SLJMP} in terms of the CSF's with our previous results to find

$$E_{2,SLJP} = \bar{E}_{2,SLP} + (-1)^{L+S+J} \begin{Bmatrix} L & S & J \\ S & L & 1 \end{Bmatrix} \langle \Psi_{SLP} | F | \Psi_{SLP} \rangle + \langle \Psi_{SLP} | G_1 | \Psi_{SLP} \rangle + (-1)^{L+S+J} \begin{Bmatrix} L & S & J \\ S & L & 2 \end{Bmatrix} \langle \Psi_{SLP} | G_2 | \Psi_{SLP} \rangle, \quad (119)$$

where

$$\bar{E}_{2,SLP} = \sum_{AA'} C_{ASLP} \langle ASLP | \Pi_1 | A'SLP \rangle + \langle ASLP | \Pi_2 | A'SLP \rangle + \langle ASLP | G_0 | A'SLP \rangle C_{A'SLP}, \quad (120)$$

$$\langle \Psi_{SLP} | F | \Psi_{SLP} \rangle = \sum_{AA'} C_{ASLP} \langle ASLP | F | A'SLP \rangle C_{A'SLP}, \quad (121)$$

$$\langle \Psi_{SLP} | G_1 | \Psi_{SLP} \rangle = \sum_{AA'} C_{ASLP} \langle ASLP | G_1 | A'SLP \rangle C_{A'SLP}, \quad (122)$$

$$\langle \Psi_{SLP} | G_2 | \Psi_{SLP} \rangle = \sum_{AA'} C_{ASLP} \langle ASLP | G_2 | A'SLP \rangle C_{A'SLP}. \quad (123)$$

The entire dependence of $E_{2,SLJP}$ on J is contained in the 6- j symbols in Eq. (119). Hence, from the properties of the 6- j symbols, we find the relation

$$\bar{E}_{2,SLP} = [(2S+1)(2L+1)]^{-1} \sum_J (2J+1) E_{2,SLJP}, \quad (124)$$

so $\bar{E}_{2,SLP}$ is the average first-order relativistic correction to the energy of the J multiplet, as was suggested by our notation.

In the case of Russell-Saunders coupling, where Eq. (119) holds, $E_{2,SLJP}$ would follow the Landé interval rule with respect to J if the term proportional to $\langle \Psi_{SLP} | G_2 | \Psi_{SLP} \rangle$ were absent, since for $L \neq 0$ and $S \neq 0$,

$$(-1)^{L+S+J} \begin{Bmatrix} L & S & J \\ S & L & 1 \end{Bmatrix} = \frac{1}{2} \frac{J(J+1) - L(L+1) - S(S+1)}{[L(L+1)(2L+1)S(S+1)(2S+1)]^{1/2}}.$$

As pointed out by Araki,²⁷ the terms proportional to $\langle \Psi_{SLP} | G_2 | \Psi_{SLP} \rangle$ cause a deviation from the Landé interval rule even in the case of Russell-Saunders coupling, as may be seen from the relation

$$(-1)^{L+S+J} \begin{Bmatrix} L & S & J \\ S & L & 2 \end{Bmatrix} = \frac{3[J(J+1) - L(L+1) - S(S+1)][J(J+1) - L(L+1) - S(S+1) + 1] - 4S(S+1)L(L+1)}{2[L(L+1)(2L-1)(2L+1)(2L+3)S(S+1)(2S-1)(2S+1)(2S+3)]^{1/2}}$$

for $S=1$ and $L=1$.

V. MATRIX ELEMENTS OF THE FIRST-ORDER RELATIVISTIC CORRECTIONS TO THE ENERGY IN TERMS OF RADIAL INTEGRALS

The matrix elements and reduced-matrix elements with respect to the CSF's arising from the first-order relativistic correction to the energy can be expressed in terms of the corresponding one- and two-electron orbital integrals. We have dealt with these orbital integrals in Sec. III. In accord with our results there we write

$$\langle ASLP | \Pi_1 | A'SLP \rangle = \sum_{\lambda l j} s_{ASLP, A'SLP; \lambda l j} \pi_{\lambda l j}, \quad (125)$$

$$\langle ASLP | F | A'SLP \rangle = \sum_{\lambda l j} t_{ASLP, A'SLP; \lambda l j} \zeta_{\lambda l j}, \quad (126)$$

$$\langle ASLP | \Pi_2 | A'SLP \rangle = \sum_{\lambda l} \sum_{\mu j} \sum_{\rho k} \sum_{\sigma i} d_{ASLP, A'SLP; \lambda l, \mu j, \rho k, \sigma i} D_{\lambda l, \mu j, \rho k, \sigma i}, \quad (127)$$

$$\langle ASLP | G_0 | A'SLP \rangle = \sum_{\lambda l} \sum_{\mu j} \sum_{\rho k} \sum_{\sigma l} \left(\sum_{\omega} \gamma_{0;ASLP,A'SLP;\lambda l, \mu j; \rho k, \sigma l; \omega} R_{\lambda l, \mu j; \rho k, \sigma l; \omega} + \sum_{\nu} q_{ASLP,A'SLP;\lambda l, \mu j; \rho k, \sigma l; \nu} Q_{\lambda l, \mu j; \rho k, \sigma l; \nu} \right), \quad (128)$$

$$\langle ASLP | G_1 | A'S'L'P \rangle = \sum_{\lambda l} \sum_{\mu j} \sum_{\rho k} \sum_{\sigma l} \left(\sum_{\omega} \gamma_{1;ASLP,A'S'L'P;\lambda l, \mu j; \rho k, \sigma l; \omega} R_{\lambda l, \mu j; \rho k, \sigma l; \omega} + \sum_{\nu} p_{ASLP,A'S'L'P;\lambda l, \mu j; \rho k, \sigma l; \nu} P_{\lambda l, \mu j; \rho k, \sigma l; \nu} \right), \quad (129)$$

$$\langle ASLP | G_2 | A'S'L'P \rangle = \sum_{\lambda l} \sum_{\mu j} \sum_{\rho k} \sum_{\sigma l} \sum_{\omega} \gamma_{2;ASLP,A'S'L'P;\lambda l, \mu j; \rho k, \sigma l; \omega} R_{\lambda l, \mu j; \rho k, \sigma l; \omega}. \quad (130)$$

The radial integrals appearing here are defined in Eqs. (79)–(84); the summations over ω and ν proceed as in Eqs. (101) and (106), respectively.

The coefficients $S_{ASLP,A'SLP;\lambda l, \mu j}$, $t_{ASLP,A'S'L'P;\lambda l, \mu j}$, $d_{ASLP,A'SLP;\lambda l, \mu j, \rho k, \sigma l}$, $\gamma_{0;ASLP,A'SLP;\lambda l, \mu j; \rho k, \sigma l; \omega}$, $\gamma_{1;ASLP,A'S'L'P;\lambda l, \mu j; \rho k, \sigma l; \omega}$, $\gamma_{2;ASLP,A'SLP;\lambda l, \mu j; \rho k, \sigma l; \omega}$, $q_{ASLP,A'SLP;\lambda l, \mu j; \rho k, \sigma l; \nu}$, and $p_{ASLP,A'S'L'P;\lambda l, \mu j; \rho k, \sigma l; \nu}$ characterize the angular and spin parts of the various relativistic corrections to the energy. They depend only on the details of the construction of the CSF's from Slater determinants. For simple cases, their derivation, with the help of the results given in Sec. III, is usually not a difficult matter; however, general formulas for them, particularly the coefficients originating from the two-electron integrals, can be only obtained by an elaborate analysis involving Clebsch-Gordan and/or Racah algebra, and this will not be attempted here. Note that the nonvanishing coefficients for any particular case are actually rather sparse. For example, in the case $ASLP = A'S'L'P$, $S_{ASLP,ASLP;\lambda l, \mu j}$ and $t_{ASLP,ASLP;\lambda l, \mu j}$ vanish unless $i=j$, while $d_{ASLP,ASLP;\lambda l, \mu j, \rho k, \sigma l}$, $\gamma_{n;ASLP,ASLP;\lambda l, \mu j; \rho k, \sigma l; \omega}$ ($n=0, 1, 2$), $q_{ASLP,ASLP;\lambda l, \mu j; \rho k, \sigma l; \nu}$, and $p_{ASLP,ASLP;\lambda l, \mu j; \rho k, \sigma l; \nu}$ all have nonzero values only in case $\lambda l = \mu j$, $\rho k = \sigma l$, or in the cases $\lambda l = \rho k$, $\mu j = \sigma l$, and $\lambda l = \sigma l$, $\mu j = \rho k$. Note also that $S_{ASLP,ASLP;\lambda l, \mu j}$ is simply the occupation number of the shell λl in the CSF indexed by $ASLP$.

We note also the relation

$$\gamma_{0;ASLP,A'SLP;\lambda l, \mu j; \rho k, \sigma l; \omega} = \gamma_{0;ASLP,A'SLP;\rho k, \sigma l; \lambda l, \mu j; \omega}, \quad (131)$$

which follows from Eq. (109). However, no similar relation exists in general for

$$\gamma_{1;ASLP,A'S'L'P;\lambda l, \mu j; \rho k, \sigma l; \omega} \text{ or for } \gamma_{2;ASLP,A'S'L'P;\lambda l, \mu j; \rho k, \sigma l; \omega}.$$

In practical calculations, CSF's with closed shells are a frequent occurrence.²⁸ Simplifications then apply which we give here. We suppose that there is some shell ρk for which

$$S_{ASLP,ASLP;\rho k, \rho k} = S_{A'S'L'P,A'S'L'P;\rho k, \rho k} = 4\rho + 2; \quad (132)$$

that is, that some shell ρk is a closed shell in both

the CSF labeled by $ASLP$ and the CSF labeled by $A'S'L'P$ (the case $ASLP = A'S'L'P$ is not excluded). Then we have²⁸

$$t_{ASLP,A'S'L'P;\rho k, \rho k} = 0, \quad (133)$$

and, in accord with Elliott's results,²⁹

$$\begin{aligned} \gamma_{2;ASLP,A'S'L'P;\lambda l, \mu j; \rho k, \rho k; \omega} &= 0, \\ \gamma_{2;ASLP,A'S'L'P;\rho k, \rho k; \lambda l, \mu j; \omega} &= 0, \end{aligned} \quad (134)$$

$$\gamma_{2;ASLP,A'S'L'P;\lambda l, \rho k; \mu j, \rho k; \omega} = 0,$$

for all values of λl , μj , and ω . From the results of Blume and Watson²⁰ and Beck,²² we have

$$\begin{aligned} p_{ASLP,A'S'L'P;\lambda l, \mu j; \rho k, \rho k; \nu} &= 0, \\ \gamma_{1;ASLP,A'S'L'P;\lambda l, \mu j; \rho k, \rho k; \omega} &= -\frac{1}{2} \delta_{\lambda \mu} \delta_{\omega, 1} t_{ASLP,A'S'L'P;\lambda l, \mu j} (4\rho + 2), \end{aligned} \quad (135)$$

$$\gamma_{1;ASLP,A'S'L'P;\rho k, \rho k; \lambda l, \mu j; \omega} = 0;$$

$$\begin{aligned} p_{ASLP,A'S'L'P;\lambda l, \rho k; \mu j, \rho k; \nu} &= \frac{1}{4} \delta_{\lambda \mu} t_{ASLP,A'S'L'P;\lambda l, \mu j} \\ &\times (4\rho + 2) 3[\lambda(\lambda + 1)]^{-1} k_{\lambda, \rho; \nu} x_{\lambda \rho \nu}, \end{aligned} \quad (136)$$

$$\gamma_{1;ASLP,A'SLP;\lambda l, \rho k; \omega}$$

$$= \frac{1}{4} \delta_{\lambda \mu} t_{ASLP,A'S'L'P;\lambda l, \mu j} (4\rho + 2) 3[\lambda(\lambda + 1)]^{-1} v_{\lambda \rho \omega}.$$

Here $k_{\lambda, \mu; \nu}$ is given by Eq. (88) and $x_{\lambda \mu \nu}$ is given by

$$x_{\lambda \mu \nu} = \frac{1}{2} B_{\lambda \mu \nu} B_{\lambda \mu \nu} B_{\mu \nu \lambda} / [(\lambda + \mu + \nu + 1) B_{\lambda \mu \nu}], \quad (137)$$

$$B_{20} = (2\sigma)! / (\sigma!)^2,$$

when $\lambda + \mu + \nu$ is an even integer; $x_{\lambda \mu \nu}$ vanishes if $\lambda + \mu + \nu$ is odd. Also, we have used

$$\begin{aligned} v_{\lambda \mu \omega} &= \frac{1}{4} [\omega(\omega + 1)]^{-1} (\lambda + \mu + \omega + 1)(\lambda + \mu - \omega + 1) \\ &\times (\lambda + \omega - \mu)(\mu + \omega - \lambda) x_{\lambda \mu \omega - 1}. \end{aligned} \quad (138)$$

For the orbit-orbit coupling coefficients, we find

$$\gamma_{0;ASLP,A'SLP;\lambda l, \mu j; \rho k, \rho k; \omega} = 0,$$

$$\gamma_{0;ASLP,A'SLP;\lambda l, \rho k; \mu j, \rho k; \omega}$$

$$= -\frac{1}{4} \delta_{\lambda \mu} S_{ASLP,A'SLP;\lambda l, \mu j} (4\rho + 2) v_{\lambda \rho \omega},$$

TABLE I. Fine-structure splittings in cm^{-1} .

	Blume and Watson ^a	Maili ^b	This work, Hartree-Fock	Experiment
$B(^2P_{3/2} - ^2P_{1/2})$	14.6		15.16	16
$C(^2P_1 - ^2P_0)$	15.8	16.17	16.18	16.4
$C(^2P_2 - ^2P_1)$	25.8	28.59	26.56	27.1
$N(^2D_{3/2} - ^2D_{1/2})$	-13.6		-12.97	-8
$N(^2P_{3/2} - ^2P_{1/2})$	-5.5		-5.09	0
$O(^2P_1 - ^2P_0)$	-72.7	-73.69	-73.62	-68.0
$O(^2P_2 - ^2P_1)$	-162	-163.94	-163.83	-158.5
$F(^2P_{3/2} - ^2P_{1/2})$	-397		-402.2	-404.0
$Al(^2P_{3/2} - ^2P_{1/2})$	90.8		92.72	112.04
$Si(^2P_1 - ^2P_0)$	64.5	66.17	65.10	77.15
$Si(^2P_2 - ^2P_1)$	128	129.03	128.95	146.16
$S(^2P_1 - ^2P_0)$	-183	-181.89	-181.61	-176.8
$S(^2P_2 - ^2P_1)$	-369	-366.95	-366.35	-396.8
$Cl(^2P_{3/2} - ^2P_{1/2})$	-818		-822.9	-881

^aSee Ref. 32.^bSee Ref. 33.

$$q_{ASLP, A' SLP; \lambda i, \rho k; \mu j, \rho k; \nu}$$

$$= -\frac{1}{4} \delta_{\lambda \mu} S_{ASLP, A' SLP; \lambda i j} (4\rho + 2) x_{\lambda \rho \nu}, \quad (139)$$

except in case $\lambda i = \mu j = \rho k$; in that case we find

$$r_{0; ASLP, A' SLP; \rho k, \rho k; \rho k, \rho k; \omega}$$

$$= -\frac{1}{2} S_{ASLP, A' SLP; \rho k k} (4\rho + 2) v_{\rho \rho \omega}. \quad (140)$$

Equations (139) and (140) are consistent with the results of Beck.²² Note that the occurrence of the factor $\frac{1}{4}$ in Eqs. (136) and (138) compensates for the fourfold occurrence of such terms in the summations given in Eqs. (128) and (129). Finally, we have

$$d_{ASLP, A' SLP; \lambda i, \mu j, \rho k, \rho k}$$

$$= \frac{1}{2} \left[\frac{1}{8} \delta_{\lambda \mu} S_{ASLP, A' SLP; \lambda i j} (4\rho + 2) \right], \quad (141)$$

unless $\lambda i = \mu j = \rho k$, where we have

$$d_{ASLP, A' SLP; \rho k, \rho k, \rho k, \rho k} = \frac{1}{4} S_{ASLP, A' SLP; \rho k k} (4\rho + 2). \quad (142)$$

The factor $\frac{1}{8}$ in Eq. (141) compensates for the sixfold occurrence of such terms in Eq. (127).

VI. NUMERICAL APPLICATION

A. Hartree-Fock Results

We have computed the first-order relativistic corrections to the energy for the ground states of the atoms He through Ar, and for the two lowest excited states each of C, N, and O. The analytic Hartree-Fock wave functions of Cohen³⁰ were used for He through Ne and Maili's wave functions³¹ were used for Na through Ar. In Table I we present our results for the fine-structure splittings and compare them with the previous results of Blume and Watson³² and Maili,³³ and with experimental

values.³⁴ In Table II we present the parts of the relativistic corrections to the energy which do not contribute to the fine-structure splitting. These are the quantities $c^{-2}E_2$, where E_2 is defined in Eq. (120).

Essentially the same formalism was used for all of the computed results in Table I, but different wave functions were used in each case. The analytic wave functions we have used are characterized by carefully chosen basis functions and should prove quite accurate. The close agreement between our results and Maili's results, based on numerical wave functions, confirms this. [Note that Maili's results omit B, $N(^2D)$, $N(^2P)$, F, Al, and Cl.] The earlier results of Blume and Watson are based on analytic wave functions of poorer accuracy.

Our results in Tables I and II were all computed with wave functions which exactly satisfy the cusp condition.³⁵ Additional computations were made using wave functions³⁶ in which the cusp condition was relaxed, but were otherwise of comparable accuracy. These resulted in virtually the same values for the fine-structure splittings as those we have given. There is, however, a difference in the computed value of $c^{-2}E_2$ of about 2% or 3% for atoms in the first row of the periodic table; for example, for $N(^4S)$ we obtain $c^{-2}E_2 = -0.026926$, while the value from the exact cusp wave function is -0.026545 . This difference comes mainly from the different values obtained for the integrals $\pi_{\lambda i j}$

TABLE II. Average relativistic corrections to the energy in a.u.

	Nonrelativistic energy ^a	Average relativistic correction $c^{-2}E_2$
He(¹ S)	-2.861680	-0.000064842
Li(² S)	-7.432726	-0.000052552
Be(¹ S)	-14.57302	-0.0021148
B(² P)	-24.52906	-0.0058933
C(³ P)	-37.68861	-0.013343
C(¹ D)	-37.63132	-0.013359
C(¹ S)	-37.54960	-0.013369
N(⁴ S)	-54.40092	-0.026545
N(² D)	-54.29615	-0.026440
N(² P)	-54.22807	-0.026432
O(³ P)	-74.80938	-0.047540
O(¹ D)	-74.72926	-0.047576
O(¹ S)	-74.61101	-0.047534
F(² P)	-99.40934	-0.079573
Ne(¹ S)	-128.5470	-0.12567
Na(² S)	-161.85884	-0.19187
Mg(¹ S)	-199.61461	-0.28312
Al(² P)	-241.87664	-0.40340
Si(² P)	-288.85429	-0.56000
P(³ S)	-340.71871	-0.75952
S(³ P)	-397.50472	-1.00957
Cl(² P)	-459.48197	-1.31804
Ar(¹ S)	-526.81744	-1.69400

^aFrom Refs. 30 and 31.

TABLE III. Total Hartree-Fock energies in a.u.

	Relativistic Hartree-Fock ^a	This work $E_1 + c^{-2}E_2$
He	-2.8617	-2.861745
Be	-14.5752	-14.57513
Ne	-128.6753	-128.6727
Ar	-528.5513	-528.51144

^aSee Ref. 38.

[defined in Eq. (79)] for the orbitals of s symmetry, which seems to be caused by different behavior of these orbitals near $r=0$ in the two cases. It is the exact cusp wave function that gives the more accurate description near $r=0$, and hence the more accurate value of $c^{-2}E_2$.

When relativistic effects are small, there should be good agreement between our Hartree-Fock results and results from relativistic Hartree-Fock calculations of the type outlined by Kim.³⁷ In Table III we compare our results for the sum $E_1 + c^{-2}E_2$ with the total energy, including the Breit correction terms, obtained by Mann and Johnson,³⁸ for the atoms He, Be, Ne, and Ar. It should be noted that their relativistic Hartree-Fock results include energy corrections of order c^{-4} , c^{-6} , etc. which come from the Dirac Hamiltonian and the Breit operator, while our results omit such terms. Since their calculations omit other higher-order energy corrections (e.g., the Lamb-shift correction), it is not at all clear that their results actually improve on ours.

B. Multiconfiguration Results for Nitrogen

For most of the atoms in the first row of the periodic table, the Hartree-Fock results given in Table I are in good agreement with experiment. The most noticeable discrepancies occur for the nitrogen 2D and 2P states. Hence these states

provide a good testing ground for multiconfiguration results for the fine-structure splittings.

The wave functions used here were computed using a multiconfiguration self-consistent-field (MC-SCF) formalism of the type put forward by Hinze and Roothaan,²⁴ in which the orbitals and CSF expansion coefficients are simultaneously optimized. The radial functions $P_{\lambda}(r)$ are expansions in terms of normalized Slater-type basis functions, namely

$$P_{\lambda}(r) = \sum_p R_{\lambda p}(r) c_{\lambda p}, \quad (143)$$

$$R_{\lambda p}(r) = [2\zeta_{\lambda p}]^{2\lambda} \lambda p^{*1} / (2n_{\lambda p})^{1/2} r^{n_{\lambda p}} e^{-\zeta_{\lambda p} r}.$$

The basis functions were taken from the results of Bagus and Gilbert³⁶ for the nitrogen 2D and 2P states; the ζ 's were not reoptimized. The radial functions for our wave functions are given in Table IV, together with the nonrelativistic energies and the values for $c^{-2}E_2$.

The CSF expansion coefficients are given in Table V. The nitrogen 2D wave function consists of CSF's from the configurations $1s^2 2s^2 2p^3$, $1s^2 2s^2 2p^2 3p$, and $1s^2 2s^2 3p^2 2p$. The nitrogen 2P wave function contains CSF's from these configurations and also from the configurations $1s^2 2p^5$ and $1s^2 2s^2 3s^2 2p$. Note that only 2P CSF's arise from the last two configurations. Since we have required that the 2D wave function be orthogonal to the 2D function

$$1s^2 2s^2 (1/\sqrt{2}) [2p^2(^3P)3p - 2p^2(^1D)3p]$$

the five CSF expansion coefficients provide only four independent variational parameters. The substitution $2p - 2p + \epsilon 3p$ yields

$$2p^3 {}^2D \sim 2p^3 {}^2D + \sqrt{3}\epsilon (1/\sqrt{2}) \{ [2p^2(^3P)3p {}^2D] - [2p^2(^1D)3p {}^2D] \} + O(\epsilon^2),$$

hence our constraint on the 2D wave function corresponds to the exclusion of the function coming

TABLE IV. Energies and radial functions for MC-SCF $N(^2D)$ and $N(^2P)$.

Nitrogen 2D : $E_0 = -54.314\,29$, $c^{-2}\bar{E}_2 = -0.026\,914$								
n	ζ	c_{1s}	c_{2s}	n	ζ	c_{2p}	c_{3p}	
1	10.595	0.110 750	0.001 260	2	7.693	0.008 103	0.025 191	
1	6.026	0.929 642	-0.266 426	2	3.272	0.225 920	-0.682 047	
3	7.332	-0.042 260	-0.030 465	2	1.877	0.438 952	-0.774 379	
2	2.528	0.002 159	0.539 124	2	1.168	0.414 068	1.430 358	
2	1.586	-0.000 088	0.554 662					
Nitrogen 2P : $E_0 = -54.28665$, $c^{-2}\bar{E}_2 = -0.026\,943$								
n	ζ	c_{1s}	c_{2s}	c_{3s}	n	ζ	c_{2p}	c_{3p}
1	10.592	0.111 253	0.002 583	0.010 633	2	7.748	0.007 716	0.024 814
1	6.022	0.932 954	-0.255 389	-0.338 239	2	3.275	0.226 397	-0.613 019
3	7.323	-0.042 279	-0.032 453	-0.239 912	2	1.865	0.451 033	-0.825 028
2	2.527	-0.005 195	0.550 576	2.512 475	2	1.131	0.405 991	1.432 865
2	1.589	-0.007 302	0.544 268	-2.251 829				

TABLE V. CSF expansion coefficients for MC-SCF $N(^2D)$ and $N(^2P)$.

$N(^2D)$		$N(^2P)$	
$1s^2 2s^2 2p^3$	0.995 871	$1s^2 2s^2 2p^3$	0.978 718
$1s^2 2s^2 2p^2(^3P)3p$	0.014 176	$1s^2 2s^2 2p^2(^1S) 3p$	-0.028 881
$1s^2 2s^2 2p^2(^1D) 3p$	0.014 176	$1s^2 2s^2 2p^2(^3P) 3p$	-0.024 768
$1s^2 2s^2 3p^2(^3P)2p$	-0.051 748	$1s^2 2s^2 2p^2(^1D) 3p$	0.006 861
$1s^2 2s^2 3p^2(^1D)2p$	0.071 852	$1s^2 2s^2 3p^2(^1S) 2p$	-0.064 996
		$1s^2 2s^2 3p^2(^3P) 2p$	0.051 006
		$1s^2 2s^2 3p^2(^1D) 2p$	0.054 263
		$1s^2 2p$	0.174 074
		$1s^2 2s^2 3s^2 2p$	0.023 747

from the "single replacement" of a $2p$ function by a $3p$ function in $2p^3^2D$. For the same reason, we have required the 2P wave function to be orthogonal to the 2P function

$$\frac{1}{3} (1/\sqrt{2}) 1s^2 2s^2 \{ 2[2p^2(^1S)3p] - 3[2p^2(^3P)3p] - \sqrt{5}[2p^2(^1D)3p] \} ;$$

hence the nine CSF expansion coefficients provide only eight independent variational parameters.

Our wave functions for the nitrogen 2D and 2P are much too crude to be considered accurate descriptions of the electronic states to which they pertain. Accordingly, our results must be regarded as only preliminary, to be confirmed by calculations with more accurate wave functions. Still, the fine-structure splittings for the nitrogen 2D and 2P states computed with these wave functions are a substantial improvement over the Hartree-Fock results, as may be seen from Table VI. This is perhaps not unreasonable, in view of the quite good agreement with experiment already obtained with a Hartree-Fock wave function in the case of the carbon fine-structure splitting.

The situation can perhaps be made more plausible by observing that in carbon the addition of the CSF

TABLE VI. Nitrogen fine-structure splittings in cm^{-1} .

	Hartree-Fock	MC-SCF	Experiment
$^2D_{5/2} - ^2D_{3/2}$	-12.97	-9.23	-8
$^2P_{3/2} - ^2P_{1/2}$	-5.09	-0.34	0

from the configuration $(1s)^2(2s)^2 2p^3p$ does not improve the wave function, since a version of Brillouin's theorem³⁰ applies. This argument breaks down in nitrogen, since there is more than one 2D or 2P CSF which can come from the configuration $(1s)^2(2s)^2(2p)^2 3p$. The addition of such a CSF can influence the one-electron nuclear spin-orbit contribution and the contributions from the two-electron integrals containing $1s$ -shell and $2s$ -shell functions (which behave in many respects as corrections to the one-electron integral ξ_{Mj}). Ordinarily, these contributions to the fine-structure splitting are the major part, although the remainder is not negligible; for example, in the carbon Hartree-Fock calculation for the $^3P_2 - ^3P_1$ splitting these two parts amount to 32.36 and -5.80 cm^{-1} , respectively. Thus, the addition of such a CSF can have a much greater influence on the calculation of the fine-structure splitting than would be the case for most CSF's. In fact, our calculations indicate that the major part of the difference between the Hartree-Fock results and the MC-SCF results presented here may be attributed to the addition of CSF's from the configuration $1s^2 2s^2 2p^2 3p$.

ACKNOWLEDGMENTS

The author is greatly indebted to Professor C. C. J. Roothaan for suggesting this problem, and for his encouragement and helpful advice. The author would also like to thank Dr. Y. K. Kim for many useful suggestions. The availability of the MC-SCF program written by Professor J. Hinze and Z. Sibincic, and Z. Sibincic's helpful advice in the use of this program were indispensable for the successful completion of this work.

*Research supported by the Advanced Research Projects Agency of the Department of Defense and monitored by U. S. Army Research Office-Durham, Box CM, Duke Station, Durham, N. C. 27706, under Contract No. DAH0 0470 C 0037.

[†]Submitted in partial fulfillment of the requirements for the degree of Doctor of Philosophy, Department of Physics, the University of Chicago, Chicago, Ill.

¹G. Breit, Phys. Rev. **34**, 553 (1929).

²G. Breit, Phys. Rev. **36**, 383 (1930); **39**, 616 (1932).

³V. Berestetsky and L. Landau, Zh. Eksperim. i Teor. Fiz. **19**, 673 (1949).

⁴A. M. Sessler and H. M. Foley, Phys. Rev. **91**, 1321 (1953); J. Sucher and H. M. Foley, *ibid.* **95**, 966 (1954).

⁵H. A. Bethe and E. E. Salpeter, *Quantum Mechanics of One- and Two-Electron Atoms* (Springer-Verlag, Berlin, 1957), p. 181.

⁶Reference 5, pp. 178-181.

⁷Z. V. Chraplyvy, Phys. Rev. **91**, 388 (1953); **92**, 1310 (1953).

⁸W. A. Barker and F. N. Glover, Phys. Rev. **99**, 317 (1955).

⁹T. Itoh, Rev. Mod. Phys. **37**, 159 (1965).

¹⁰J. C. Slater, *Quantum Theory of Atomic Structure* (McGraw-Hill, New York, 1960), Vol. 2, Chaps. 23 and 24.

¹¹The derivation and discussion of b_{pq} from the viewpoint of S-matrix theory can be found in A. I. Akhiezer

- and V. B. Berestetsky, *Quantum Electrodynamics* (Interscience, New York, 1965).
- ¹²G. E. Brown and D. G. Ravenhall, *Proc. Roy. Soc. (London)* **A208**, 552 (1951).
- ¹³E. E. Salpeter, *Phys. Rev.* **87**, 323 (1952).
- ¹⁴For the two-electron case, this term is obtained and reduced to a large component expression in Ref. 1. See Refs. 2 and 8 for the objections to it.
- ¹⁵A. de-Shalit and I. Talmi, *Nuclear Shell Theory* (Academic, New York, 1963), p. 207.
- ¹⁶E. U. Condon and G. H. Shortley, *The Theory of Atomic Spectra* (Cambridge U.P., Cambridge, England, 1964), p. 122.
- ¹⁷F. R. Innes, *Phys. Rev.* **91**, 31 (1953).
- ¹⁸H. Horie, *Progr. Theoret. Phys. (Kyoto)* **10**, 296 (1953).
- ¹⁹M. E. Rose, *Elementary Theory of Angular Momentum* (Wiley, New York, 1957).
- ²⁰M. Blume and R. E. Watson, *Proc. Roy. Soc. (London)* **A270**, 127 (1962).
- ²¹For the definition and properties of the 6-j symbol, see, for instance, E. P. Wigner, *Group Theory and Its Application to Quantum Mechanics* (Academic, New York, 1959).
- ²²D. R. Beck, *J. Chem. Phys.* **51**, 2171 (1969).
- ²³S. Yanagawa, *J. Phys. Soc. Japan* **10**, 1029 (1955).
- ²⁴Our definitions and terminology are those of Hinze and Roothaan [J. Hinze and C. C. J. Roothaan, *Progr. Theoret. Phys. (Kyoto)* **40**, 37 (1967)].
- ²⁵Reference 21, p. 245.
- ²⁶Reference 21, p. 308.
- ²⁷G. Araki, *Progr. Theoret. Phys. (Kyoto)* **3**, 152 (1948).
- ²⁸Reference 16, p. 183.
- ²⁹I. P. Elliott, *Proc. Roy. Soc. (London)* **A218**, 345 (1953).
- ³⁰C. C. J. Roothaan (private communication).
- ³¹G. L. Malli, *Can. J. Phys.* **44**, 3121 (1966).
- ³²M. Blume and R. E. Watson, *Proc. Roy. Soc. (London)* **A271**, 565 (1963).
- ³³G. Malli, *J. Chem. Phys.* **48**, 1088 (1968); **48**, 1092 (1968).
- ³⁴C. E. Moore, *Atomic Energy Levels as Derived from Analysis of Optical Spectra*, National Bureau of Standards Circular No. 467 (U.S. GPO, Washington, D.C., 1949), Vol. 1.
- ³⁵C. C. J. Roothaan and P. S. Kelley, *Phys. Rev.* **131**, 1177 (1963).
- ³⁶A. D. McLean and M. Yoshimine, *IBM J. Res. Develop. Suppl.* **12** (1967), Table 2.
- ³⁷Y. K. Kim, *Phys. Rev.* **154**, 17 (1967).
- ³⁸J. B. Mann and W. R. Johnson, *Phys. Rev. A* **4**, 41 (1971).
- ³⁹L. Brillouin, *Actualities Sci. Ind.* **71**, (1933); C. Moller and M. S. Plesset, *Phys. Rev.* **46**, 618 (1934).

Steady States and Quasi-Energies of a Quantum-Mechanical System in an Oscillating Field^{*†}

HIDEO SAMBE

Laboratory of Molecular Structure and Spectra,
Department of Physics, University of Chicago,
Chicago, Illinois 60637

A general formalism is presented for a system whose Hamiltonian is periodic in time. The formalism is intended to deal with the interactions between bound electrons and an external electromagnetic field, which can be treated semi-classically, such as electric and magnetic polarizations, optical rotation, and transitions among discrete levels. A particular bound solution of the Schrödinger equation which belongs to an irreducible representation of the time-translation symmetry group is defined as a steady state, and the characteristic number of the irreducible representation as a quasi-energy. It is shown that the defined steady states and quasi-energies behave in a newly constructed Hilbert space like stationary states and energies of a conservative system in many respects. It is also shown that for a resonant case the unperturbed quasi-energy becomes degenerate and the transitions among discrete levels can be accounted for by the familiar degenerate perturbation procedure. Using a suitable Hilbert space, the steady states are established as firmly as the stationary states stand in the theory of a conservative system.

1. INTRODUCTION

It is well known in solid-state physics that for a spatially periodic Hamiltonian, there exist quasi-momenta and corresponding Bloch wavefunctions. Analogously, for a periodically time-dependent Hamiltonian, one expects the existence of quasi-energies and Bloch-type states. For these states Young *et al.*¹ coined the term quasi-periodic states; we prefer to use the term steady states. Such steady states have been discussed and used in the theories of susceptibilities,^{1,2} and in the theories of multiple-quantum transitions among discrete levels.³⁻⁵

In spite of the widespread utilization of steady states for the study of the semiclassical interaction between bound electrons and an external electromagnetic field, many aspects of steady states have been discussed only partially and superficially in the literature and apparently require further investigation. The essential points missed by previous workers are the introduction of a Hilbert space suitable for steady states and the uniform treatment of steady states in this space. The introduction of such a Hilbert space not only makes the formalism transparent, but also introduces new aspects of steady states. Above all, it makes possible the unification of two seemingly different theories namely, the theory of susceptibilities and the theory of transitions among discrete levels. Furthermore the approximate nature of the previous theories of transitions³⁻⁵ is removed in the new formalism. The main purpose of this paper is to show that, using a suitable

Hilbert space, the steady states of a periodically time-dependent system can be placed on a foundation equally as firm as that possessed by the stationary states of time-independent quantum mechanics.

In Sec. 2 of this paper, we shall study the properties of steady states from a more fundamental point of view than has been done before. We first construct a Hilbert space suitable for steady states, and then show that steady states and quasi-energies behave in this Hilbert space like stationary states and energies of a conservative system in many respects: Quasi-energies and steady states are eigenvalues and eigenfunctions of a Hermitian operator (which we call the "Hamiltonian" for steady states); the variational principle for steady states takes the familiar form of the Ritz variational principle; and theorems analogous to the Hellmann-Feynman theorem and to the hypervirial theorem for stationary states hold for steady states. The "Hamiltonian" for steady states, which is a sum of the periodically time-dependent Hamiltonian and the time-derivative operator $-i\hbar\partial/\partial t$, plays a central role in this formalism. Unlike energies (or like quasi-momenta), quasi-energies are only defined modulo $n\hbar\omega$, where ω is the frequency of external field and n is an integer; a zone analogous to the Brillouin zone is introduced in order to obtain only physically different steady states.

In Sec. 3, a perturbation theory for steady states is formulated analogously to the Rayleigh-Schrödinger perturbation theory for stationary (bound) states. The nonresonant cases

(e.g., linear and non-linear optical susceptibilities) can be accounted for by the non-degenerate perturbation procedure.

In a resonant case, the unperturbed quasi-energy becomes degenerate or almost-degenerate; multiple-quantum transitions and the attendant Stark shift can be accounted for by the degenerate or almost-degenerate perturbation procedure. Previously, these two cases (nonresonant and resonant cases) are treated with quite different formalisms; we treat them on an equal footing as described above. Furthermore, we do not need to restrict ourselves to a finite-dimensional Hilbert space, the use of which was essential in the previous theories of transitions.³⁻⁵ Another advantage of the present formalism is that it provides the validity conditions for the obtained formulas. These aspects are demonstrated in Sections 3 and 4.

In order to avoid the "secular divergences," Langhoff et al. write a wavefunction as a product of time-dependent regular part and phase factor; certain conditions imposed on the regular part render this partition unique.² Although these authors used the fact that for a periodic perturbation, the regular part is a periodic function of time, they did not show that the conditions imposed on the regular part go hand in hand with the periodic properties of the regular part. We shall clarify this point in Sec. 3.

In Sec. 4, we apply the formalism to two specific examples in order to demonstrate the potential of this formalism.

2. STEADY STATE AND QUASI-ENERGY

A. Definition of Steady State and Quasi-Energy

We shall study a system whose Hamiltonian $H(t)$ is periodic in time with period τ : $H(t+\tau)=H(t)$. The period τ is positive, finite, and fixed at some value. The corresponding frequency is denoted by $\omega (\equiv 2\pi/\tau)$. The Schrödinger equation for the system is given by

$$\left[H(t) - i\hbar \frac{\partial}{\partial t} \right] \psi(\vec{r}, t) = 0. \quad (2.1)$$

The vector \vec{r} in the wavefunction $\psi(\vec{r}, t)$ symbolizes all the spatial and spin coordinates of the system; we use this convention throughout.

Let us assume that there exists a solution $\psi(\vec{r}, t)$ of the form

$$\left. \begin{aligned} \psi(\vec{r}, t) &= u(\vec{r}, t) e^{-i\epsilon t/\hbar}, \\ u(\vec{r}, t+\tau) &= u(\vec{r}, t), \end{aligned} \right\} \quad (2.2)$$

$$\left[H(t) - i\hbar \frac{\partial}{\partial t} \right] u(\vec{r}, t) = \epsilon u(\vec{r}, t), \quad (2.3)$$

where $u(\vec{r}, t)$ is square-integrable and ϵ is a real number. If a state of the system is represented by such a solution, we call the state a steady bound state (or simply steady state) and the characteristic real number ϵ the quasi-energy of the state.

We define a time-translation operator $T(\Delta t)$ by means of

$$T(\Delta t)\psi(\vec{r}, t+\Delta t) = \psi(\vec{r}, t) . \quad (2.4)$$

The time-translation operators

$$T(q\tau) , \quad q = 0, \pm 1, \pm 2, \dots, \quad (2.5)$$

commute with operator $H(t) - i\hbar(\partial/\partial t)$ and form a symmetry group of the Schrödinger equation (2.1). Since the time-translation group (2.5) is Abelian, all its irreducible representations are one-dimensional. The steady state solution $\psi(\vec{r}, t)$ given by (2.2) satisfies

$$T(q\tau)\psi(\vec{r}, t) = e^{iq\mathcal{E}\tau/\hbar}\psi(\vec{r}, t) ; \quad (2.6)$$

hence it belongs to an irreducible representation given by $e^{iq\mathcal{E}\tau/\hbar}$ for $q=0, \pm 1, \pm 2, \dots$, where the quasi-energy \mathcal{E} characterizes the irreducible representation. We could define a steady state solution as a bound solution which belongs to an irreducible representation of the time-translation symmetry group (2.5).

There is a close analogy between the stationary states of a time-independent Hamiltonian and the steady states of a periodically time-dependent Hamiltonian. For a time-independent Hamiltonian, the time-translation operators,

$$T(t) , \quad -\infty < t < \infty , \quad (2.7)$$

form a symmetry group of the Schrödinger equation. A stationary

state can be defined as a state which belongs to an irreducible representation of the time-translation group (2.7); the energy eigenvalue characterizes the irreducible representation.

We shall discuss the existence of steady states in Sec. 5; for the time being we assume the existence of steady states.

B. Hilbert Space for Steady States

For the definition of terminology used here, we refer to textbooks on abstract Hilbert space.^{6,7}

It is well known that a linear space consisting of all square-integrable functions of configuration space \vec{r} [i.e., all functions $f(\vec{r})$ with finite $\int |f(\vec{r})|^2 d\vec{r}$] with the inner product $\langle f, g \rangle$ defined as $\int f^*(\vec{r})g(\vec{r})d\vec{r}$ is a Hilbert space, where the range of integration is the entire configuration space.⁶ This Hilbert space shall be denoted by \mathcal{R} , and a complete orthonormal set in \mathcal{R} by $\{f_1(\vec{r}), f_2(\vec{r}), \dots\}$, which contains countably infinite basis functions. This is the Hilbert space which plays an important role for the study of stationary bound states of conservative systems.

Let us introduce another well established Hilbert space \mathcal{T} , which consists of all possible periodic functions $a(t)$ of time t with the period τ with finite $\int_{-\tau/2}^{\tau/2} |a(t)|^2 dt$ and which is furnished with the inner product

$$(a, b) \equiv \frac{1}{\tau} \int_{-\tau/2}^{\tau/2} a^*(t)b(t)dt, \quad (2.8)$$

where τ is a fixed, finite, positive, real number.⁷ The function $e^{iq\omega t}$, for $q=0, \pm 1, \pm 2, \dots$, form a complete orthonormal set in the Hilbert space \mathcal{T} , where $\omega=2\pi/\tau$.

We construct the composite space $\mathcal{R}+\mathcal{T}$ consisting of all possible functions $u(\vec{r}, t)$ which are periodic in the time with period τ and for which

$$\int_{-\tau/2}^{\tau/2} \int |u(\vec{r}, t)|^2 d\vec{r} dt \quad (2.9)$$

is finite, where the range of integration variable \vec{r} is the entire configuration space as before. This composite space $\mathcal{R}+\mathcal{T}$ is a linear space; the inner product of the functions $u(\vec{r}, t)$ and $v(\vec{r}, t)$ in $\mathcal{R}+\mathcal{T}$ is defined by

$$\langle\langle u(\vec{r}, t), v(\vec{r}, t) \rangle\rangle \equiv \frac{1}{\tau} \int_{-\tau/2}^{\tau/2} \int u^*(\vec{r}, t) v(\vec{r}, t) d\vec{r} dt, \quad (2.10)$$

which satisfies the required conditions to be an inner product in Hilbert space. The composite space $\mathcal{R}+\mathcal{T}$ furnished with this inner product is again a Hilbert space, and the functions $u_{nq}(\vec{r}, t)$,

$$u_{nq}(\vec{r}, t) \equiv f_n(\vec{r}) e^{iq\omega t}, \quad n=1, 2, \dots; \quad q=0, \pm 1, \pm 2, \dots, \quad (2.11)$$

form a complete orthonormal set in the composite Hilbert space $\mathcal{R}+\mathcal{T}$. This is the Hilbert space which we shall use to study steady states.

Once we have defined the composite Hilbert space, we can define operators in that space according to the theory of abstract Hilbert space. The definition of a linear operator in $\mathcal{R}+\mathcal{T}$ is

apparent. A Hermitian operator \mathcal{A} in $\mathcal{R}+\mathcal{T}$ is defined as an operator which satisfies

$$\langle\langle u, \mathcal{A}v \rangle\rangle = \langle\langle \mathcal{A}u, v \rangle\rangle \quad (2.12)$$

for any functions $u(\vec{r}, t)$ and $v(\vec{r}, t)$ in $\mathcal{R}+\mathcal{T}$. A linear Hermitian operator in \mathcal{R} (or \mathcal{T}) is also one in the composite Hilbert space $\mathcal{R}+\mathcal{T}$. The time-derivation operator $-i\hbar(\partial/\partial t)$ is a linear Hermitian operator in \mathcal{T} and $\mathcal{R}+\mathcal{T}$.

We should mention here that Okuniewicz also has been using the similar Hilbert space for the study of steady states.⁸

C. Properties of Steady State and Quasi-Energy

"Hamiltonian" for steady states. Let us introduce the operator defined by

$$\mathcal{K} \equiv H(t) - i\hbar \frac{\partial}{\partial t}, \quad (2.13)$$

where $H(t)$ is the Hamiltonian of a system concerned, which is periodic in time with period τ as before. This operator \mathcal{K} is linear and Hermitian in the composite Hilbert space $\mathcal{R}+\mathcal{T}$. Using this operator \mathcal{K} , the steady state Schrödinger equation (2.3) can be written in the form

$$\mathcal{K}u(\vec{r}, t) = \epsilon u(\vec{r}, t), \quad (2.14)$$

where the solution $u(\vec{r}, t)$ is located in $\mathcal{R}+\mathcal{T}$. Clearly \mathcal{K} is

analogous to the Hamiltonian for stationary states of the time-independent Schrödinger equation; we shall call the operator the "Hamiltonian" for steady states. Quasi-energies and steady states are eigenvalues and eigenfunctions of the "Hamiltonian" \mathcal{H} . Since \mathcal{H} is Hermitian, every eigenvalue (quasi-energy) is real, and two eigenfunctions (steady states) belonging to different eigenvalues (quasi-energies) are orthogonal.

Physically equivalent steady states. If $\{\mathcal{E}, u(\vec{r}, t)\}$ is a solution of the steady state eigenvalue equation (2.14), then

$$\mathcal{E}' \equiv \mathcal{E} + q\hbar\omega; \quad u'(\vec{r}, t) \equiv u(\vec{r}, t)e^{iq\omega t}, \quad (2.15)$$

is also a solution for any integer q ; the complete wavefunctions of them are, however, the same:

$$u(\vec{r}, t)e^{-i\mathcal{E}t/\hbar} = u'(\vec{r}, t)e^{-i\mathcal{E}'t/\hbar}. \quad (2.16)$$

In other words, all solutions given by (2.15) are physically equivalent. It is evident that one can always reduce any quasi-energy \mathcal{E} to a point in a zone

$$E - \frac{1}{2}\hbar\omega < \mathcal{E} \leq E + \frac{1}{2}\hbar\omega \quad (2.17)$$

specified by a real number E ; therefore physically different steady states can be characterized (partially) by their reduced quasi-energies, which lie in the same zone. The choice of zone (i.e., the choice of E) is, however, arbitrary; we shall make use of this freedom from time to time.

If $\{\mathcal{E}_m, u_m(\vec{r}, t)\}$ and $\{\mathcal{E}_n, u_n(\vec{r}, t)\}$ are solutions of Eq. (2.14) and if the quasi-energies \mathcal{E}_m and \mathcal{E}_n lie in the same zone, then the eigenfunctions $u_m(\vec{r}, t)$ and $u_n(\vec{r}, t)$ satisfy

$$\langle u_m(\vec{r}, t), u_n(\vec{r}, t) \rangle = \langle\langle u_m(\vec{r}, t), u_n(\vec{r}, t) \rangle\rangle . \quad (2.18)$$

This relation implies that one can always choose the eigenfunctions $u_n(\vec{r}, t)$ such that $\langle u_m, u_n \rangle = \delta_{mn}$, since it is always possible to choose the eigenfunctions such that $\langle\langle u_m, u_n \rangle\rangle = \delta_{mn}$.

From now on, we assume that quasi-energies of a "Hamiltonian" lie in the same zone, so that Eq. (2.18) holds and corresponding complete wavefunctions represent different physical situations.

Variational principle. The variational form of the steady state Schrödinger equation (2.14) is given by

$$\delta \mathcal{E}[u] = 0 ; \quad \mathcal{E}[u] \equiv \langle\langle u, \mathcal{H}u \rangle\rangle / \langle\langle u, u \rangle\rangle , \quad (2.19)$$

where $u(\vec{r}, t)$ and its variation $\delta u(\vec{r}, t)$ are both in $\mathcal{R} + \mathcal{I}$. The eigenfunctions $u_n(\vec{r}, t)$ of Eq. (2.14) are given by the stationary solutions of the variational equation (2.19), and the corresponding eigenvalues \mathcal{E}_n are given by the stationary values $\mathcal{E}[u_n]$ of the functional $\mathcal{E}[u]$. We can easily show, analogously to the time-independent case, that the variational principle (2.19) is equivalent to the steady state Schrödinger equation (2.14). The variational principle plays a central role for the determination of approximate eigenfunctions and eigenvalues, as in the case of stationary states.

Hellmann-Feynman theorem. A theorem analogous to the Hellmann-Feynman theorem⁹ for stationary states in a conservative system holds also for steady state solutions in a periodically time-dependent system. If the Hamiltonian $H(t, \lambda)$ of a system depends on a time-independent parameter λ and the periodic relation $H(t+\tau, \lambda) = H(t, \lambda)$ holds for any λ , then the solution $\{\mathcal{E}(\lambda), u(\vec{r}, t, \lambda)\}$ of the steady state Schrödinger equation (2.14) satisfies the relation

$$\left. \begin{aligned} \frac{d\mathcal{E}(\lambda)}{d\lambda} &= \langle\langle u, \frac{\partial \mathcal{H}}{\partial \lambda} u \rangle\rangle / \langle\langle u, u \rangle\rangle , \\ \mathcal{E}(\lambda) &\equiv \langle\langle u, \mathcal{H} u \rangle\rangle / \langle\langle u, u \rangle\rangle . \end{aligned} \right\} \quad (2.20)$$

The proof is analogous to the corresponding proof for stationary states,¹⁰ and will be omitted.

Hypervirial theorem. The steady state solutions also satisfy a theorem analogous to the hypervirial theorem¹¹ for stationary states: If $u(\vec{r}, t)$ is a solution of Eq. (2.14) and if operator \mathcal{A} is periodic in time with period τ , this theorem states that

$$\langle\langle u, [\mathcal{H}, \mathcal{A}] u \rangle\rangle = 0 , \quad (2.21)$$

where $[\mathcal{H}, \mathcal{A}]$ is the commutator of \mathcal{H} and \mathcal{A} . This hypervirial relation (2.21) has a wide range of application depending upon the choice of the operator \mathcal{A} . For a particular choice of \mathcal{A} , namely $\mathcal{A} = \frac{1}{2} \sum_n (\vec{r}_n \cdot \vec{p}_n + \vec{p}_n \cdot \vec{r}_n)$, where \vec{r}_n and \vec{p}_n are the position and linear momentum operators of the n th particle in the system

concerned, Eq. (2.21) yields the virial theorem analogue for steady states:

$$2\langle\langle u, Tu \rangle\rangle = \langle\langle u, \left\{ \sum_n \vec{r}_n \cdot \vec{\nabla}_n V(t) \right\} u \rangle\rangle, \quad (2.22)$$

where $H(t) = T + V(t)$, T is the kinetic energy, and $V(t)$ is the potential energy, which is of course periodic.

A remark. Relations with $\langle\langle \cdot, \cdot \rangle\rangle$ for steady states have analogues of $\langle \cdot, \cdot \rangle$ relations in the stationary case, as seen before; relations with $\langle \cdot, \cdot \rangle$ for steady states, however, have no special standing and must be expected to differ from the stationary case in general.

3. STEADY STATE PERTURBATION THEORY

A. Preliminary Remarks

Let the Hamiltonian $H(t, \lambda)$ of a given system be given by

$$H(t, \lambda) = H^{(0)} + \lambda V(t), \quad (3.1)$$

where $H^{(0)}$ is a time-independent Hermitian operator, the operator $V(t)$ is also Hermitian but periodic in time with period τ , and λ is a small, real, expansion parameter.

The steady state Schrödinger equation for the system is given by

$$\left[\mathcal{H}^{(0)} + \lambda V(t) - \mathcal{E}(\lambda) \right] u(\vec{r}, t, \lambda) = 0, \quad (3.2)$$

where

$$\mathcal{H}^{(0)} \equiv H^{(0)} - i\hbar \frac{\partial}{\partial t}, \quad (3.3)$$

which is a Hermitian operator in the composite Hilbert space $\mathcal{R}+\mathcal{T}$; the solution $u(\vec{r}, t, \lambda)$ is located in $\mathcal{R}+\mathcal{T}$ for any λ . Note that the complete wavefunction $\psi(\vec{r}, t, \lambda)$ is given by

$$\left. \begin{aligned} \psi(\vec{r}, t, \lambda) &= u(\vec{r}, t, \lambda) e^{-i\mathcal{E}(\lambda)t/\hbar}, \\ u(\vec{r}, t+\tau, \lambda) &= u(\vec{r}, t, \lambda), \end{aligned} \right\} \quad (3.4)$$

where $\{\mathcal{E}(\lambda), u(\vec{r}, t, \lambda)\}$ is a solution of Eq. (3.2).

We demand, of course, that $u(\vec{r}, t, \lambda)$ varies continuously with λ , and adopt the normalization

$$\langle\langle u(\vec{r}, t, \lambda), u(\vec{r}, t, \lambda) \rangle\rangle = 1, \quad (3.5)$$

which is equivalent to $\langle u, u \rangle = 1$ so long as $u(\vec{r}, t, \lambda)$ is a solution of Eq. (3.2), and which assures, therefore, the normalization of the complete wavefunction, namely $\langle \psi, \psi \rangle = 1$. The phase factor of $u(\vec{r}, t, \lambda)$ will be fixed by the standard phase convention,¹² namely

$$\langle\langle u(\vec{r}, t, 0), u(\vec{r}, t, \lambda) \rangle\rangle = \langle\langle u(\vec{r}, t, \lambda), u(\vec{r}, t, 0) \rangle\rangle, \quad (3.6)$$

which is always possible.

The unperturbed eigenvalue equation is given by

$$\mathcal{H}^{(0)} u(\vec{r}, t, 0) = \mathcal{E}(0) u(\vec{r}, t, 0), \quad (3.7)$$

where $u(\vec{r}, t, 0)$ is located in $\mathcal{R} + \mathcal{I}$. Let E_n and $f_n(\vec{r})$ be discrete eigenvalues and eigenfunctions of the operator $H^{(0)}$, namely

$$H^{(0)} f_n(\vec{r}) = E_n f_n(\vec{r}) ; \quad (3.8)$$

then the solutions of Eq. (3.7) are given by

$$\mathcal{E}(0) = E_n + q\hbar\omega ; \quad u(\vec{r}, t, 0) = f_n(\vec{r}) e^{iq\omega t} , \quad (3.9)$$

where q is any integer. A choice of the zone (2.17) for the unperturbed quasi-energies $\mathcal{E}(0)$ determines the integers q uniquely. As mentioned before, if $\{\mathcal{E}(\lambda), u(\vec{r}, t, \lambda)\}$ is a solution of Eq. (3.2), then $\{\mathcal{E}(\lambda) + q\hbar\omega, u(\vec{r}, t, \lambda) e^{iq\omega t}\}$ is also a solution representing the same physical situation. Due to the continuity of the solutions $\{\mathcal{E}(\lambda), u(\vec{r}, t, \lambda)\}$ with respect to λ , a choice of the zone (2.17) for the unperturbed solutions $\{\mathcal{E}(0), u(\vec{r}, t, 0)\}$ fixes the time-dependent phase factors $e^{iq\omega t}$ for all λ .

Consider now an eigenvalue E_k of $H^{(0)}$ and suppose that $H^{(0)}$ has eigenvalues $E_m, E_{m'}, E_{m''}, \dots$, which satisfy

$$E_k = E_m + p\hbar\omega, E_{m'} + p'\hbar\omega, E_{m''} + p''\hbar\omega, \dots, \quad (3.10)$$

for some integers p, p', p'', \dots ; then the functions,

$$f_k(\vec{r}), f_m(\vec{r}) e^{ip\omega t}, f_{m'}(\vec{r}) e^{ip'\omega t}, f_{m''}(\vec{r}) e^{ip''\omega t}, \dots, \quad (3.11)$$

are eigenfunctions of $\mathcal{H}^{(0)}$ and belong to the eigenvalue E_k of $\mathcal{H}^{(0)}$. (Note that several E_n may be the same.) This shows that even if the eigenvalue E_k of $H^{(0)}$ is non-degenerate in \mathcal{R} , the

eigenvalue E_k of $\mathcal{H}^{(0)}$ could be degenerate in $\mathcal{R}+\mathcal{T}$. If the eigenvalue E_k of $H^{(0)}$ is degenerate in \mathcal{R} , then E_k is certainly a degenerate eigenvalue of $\mathcal{H}^{(0)}$ in $\mathcal{R}+\mathcal{T}$. Since $\mathcal{H}^{(0)}$ is linear, the $\mathcal{E}(0)$ and $u(\vec{r},t,0)$ given by

$$\left. \begin{aligned} \mathcal{E}(0) &= E_k, \\ u(\vec{r},t,0) &= c_k f_k(\vec{r}) + c_m f_m(\vec{r}) e^{ip\omega t} + c_{m'} f_{m'}(\vec{r}) e^{ip'\omega t} + \dots, \end{aligned} \right\} \quad (3.12a)$$

is also a solution of Eq. (3.7), where $c_k, c_m, c_{m'}, \dots$ are arbitrary complex numbers; the corresponding complete wavefunction $\psi(\vec{r},t,0)$ is given by

$$\begin{aligned} \psi(\vec{r},t,0) &= u(\vec{r},t,0) e^{-i\mathcal{E}(0)t/\hbar} \\ &= c_k f_k(\vec{r}) e^{-iE_k t/\hbar} + c_m f_m(\vec{r}) e^{-iE_m t/\hbar} + c_{m'} f_{m'}(\vec{r}) e^{-iE_{m'} t/\hbar} + \dots \end{aligned} \quad (3.12b)$$

Equation (3.12b) clearly shows the physical significance of the coefficients, $c_k, c_m, c_{m'}, \dots$, namely the probability amplitudes of finding in the stationary states with the energies, $E_k, E_m, E_{m'}, \dots$. One can see here the reason why degenerate perturbation theory for steady states can explain transitions among discrete levels.

B. Perturbation Theory

The Rayleigh-Schrödinger (stationary bound state) perturbation theory is formulated for an eigenvalue equation in the Hilbert space \mathcal{R} ; the analogous theory for the eigenvalue equation (3.2)

in $\mathcal{R}+\mathcal{T}$ can be formulated by simply translating the formulas for \mathcal{Q} into the corresponding ones for $\mathcal{R}+\mathcal{T}$. We shall simply write down the formulas which will be used in the following chapter.

Non-degenerate case. Expanding $\xi(\lambda)$ and $u(\vec{r}, t, \lambda)$ in Eq. (3.2) according to

$$\left. \begin{aligned} \xi(\lambda) &= \xi^{(0)} + \lambda \xi^{(1)} + \lambda^2 \xi^{(2)} + \dots, \\ u(\vec{r}, t, \lambda) &= u^{(0)}(\vec{r}, t) + \lambda u^{(1)}(\vec{r}, t) + \lambda^2 u^{(2)}(\vec{r}, t) + \dots, \\ u^{(n)}(\vec{r}, t+\tau) &= u^{(n)}(\vec{r}, t), \quad n=0, 1, 2, \dots, \end{aligned} \right\} \quad (3.13)$$

and equating the coefficients of the same powers of λ , one obtains the following sequence of equations,

$$[\mathcal{H}^{(0)} - \xi^{(0)}] u^{(0)} = 0, \quad (3.14a)$$

$$[\mathcal{H}^{(0)} - \xi^{(0)}] u^{(1)} + [V(t) - \xi^{(1)}] u^{(0)} = 0, \quad (3.14b)$$

$$[\mathcal{H}^{(0)} - \xi^{(0)}] u^{(2)} + [V(t) - \xi^{(1)}] u^{(1)} - \xi^{(2)} u^{(0)} = 0. \quad (3.14c)$$

The combination of normalization and phase conditions (3.5, 6) yields another sequence of equations,

$$\langle\langle u^{(0)}, u^{(0)} \rangle\rangle = 1, \quad (3.15a)$$

$$\langle\langle u^{(0)}, u^{(1)} \rangle\rangle = 0, \quad (3.15b)$$

$$\langle\langle u^{(0)}, u^{(2)} \rangle\rangle = -\frac{1}{2} \langle\langle u^{(1)}, u^{(1)} \rangle\rangle. \quad (3.15c)$$

Expressions for the perturbation eigenvalues are

$$\mathcal{E}^{(1)} = \langle\langle u^{(0)}, v(t)u^{(0)} \rangle\rangle, \quad (3.16a)$$

$$\mathcal{E}^{(2)} = \langle\langle u^{(0)}, v(t)u^{(1)} \rangle\rangle. \quad (3.16b)$$

Degenerate case. Suppose that the unperturbed eigenvalue $\mathcal{E}^{(0)}$ in question is degenerate and that one set of corresponding orthonormal eigenfunctions are $u_1^{(0)}(\vec{r}, t), \dots, u_N^{(0)}(\vec{r}, t)$; then the first-order eigenvalues $\mathcal{E}_a^{(1)}$ and the corresponding "correct" zeroth-order eigenfunctions $u_{a\alpha}^{(0)}(\vec{r}, t)$ are given by

$$\left. \begin{aligned} \sum_{n=1}^N \left(\langle\langle u_m^{(0)}, v(t)u_n^{(0)} \rangle\rangle - \mathcal{E}_a^{(1)} \delta_{mn} \right) c_{n,a\alpha} &= 0, \quad m=1, \dots, N, \\ u_{a\alpha}^{(0)}(\vec{r}, t) &= \sum_{n=1}^N u_n^{(0)}(\vec{r}, t) c_{n,a\alpha}, \end{aligned} \right\} \quad (3.17)$$

where the index a distinguishes between the values of eigenvalues $\mathcal{E}_a^{(1)}$ and the index α in the eigenvector $[c_{1,a\alpha}, c_{2,a\alpha}, \dots, c_{N,a\alpha}]$ distinguishes between the eigenvectors belonging to the same eigenvalue $\mathcal{E}_a^{(1)}$. We can always choose the coefficients $c_{n,a\alpha}$ to constitute a unitary matrix; then the N eigenfunctions $u_{a\alpha}^{(0)}(\vec{r}, t)$ are again orthonormal.

Almost-degenerate case.¹³ Let $\mathcal{E}_1^{(0)}$ and $\mathcal{E}_2^{(0)}$ be two non-degenerate eigenvalues of $\mathcal{H}^{(0)}$ and $u_1^{(0)}(\vec{r}, t)$ and $u_2^{(0)}(\vec{r}, t)$ be the corresponding eigenfunctions respectively. The expansion parameter λ is now considered as a fixed finite number, which is small enough so that one can still put forward the solution of Eq. (3.2) as a power series. If the unperturbed eigenvalues $\mathcal{E}_1^{(0)}$ and $\mathcal{E}_2^{(0)}$ are so close together that they satisfy the relation,

$$|(\xi_1^{(0)} - \xi_2^{(0)})/\lambda| \approx |\langle\langle u_1^{(0)}, v(t)u_2^{(0)} \rangle\rangle|, \quad (3.18)$$

then the first-order approximate solution,

$$\left. \begin{aligned} \xi(\lambda) &= \frac{1}{2}(\xi_1^{(0)} + \xi_2^{(0)}) + \lambda \xi^{(1)} + o(\lambda^2), \\ u(\vec{r}, t, \lambda) &= \{c_1 u_1^{(0)}(\vec{r}, t) + c_2 u_2^{(0)}(\vec{r}, t)\} + o(\lambda), \end{aligned} \right\} \quad (3.19)$$

is given by the secular equation,

$$\left. \begin{aligned} \begin{pmatrix} v_{11} + \Delta - \xi^{(1)}, & v_{12} \\ v_{21}, & v_{22} - \Delta - \xi^{(1)} \end{pmatrix} \begin{pmatrix} c_1 \\ c_2 \end{pmatrix} &= 0, \\ \Delta \equiv (\xi_1^{(0)} - \xi_2^{(0)})/2\lambda; & v_{mn} \equiv \langle\langle u_m^{(0)}, v(t)u_n^{(0)} \rangle\rangle. \end{aligned} \right\} \quad (3.20)$$

C. Transformed Perturbation Equations

We now transform the eigenvalue equation (3.2) by introducing a factor $\exp[i\theta(t, \lambda)/\hbar]$, where $\theta(t, \lambda)$ is a function of t and λ :

$$v(\vec{r}, t, \lambda) = e^{i\theta(t, \lambda)/\hbar} u(\vec{r}, t, \lambda), \quad (3.21)$$

$$[\mathcal{H}^{(0)} + \lambda V(t) - \partial\theta(t, \lambda)/\partial t - \xi(\lambda)] v(\vec{r}, t, \lambda) = 0. \quad (3.22)$$

The complete wavefunction $\psi(\vec{r}, t, \lambda)$ is now given by

$$\psi(\vec{r}, t, \lambda) = v(\vec{r}, t, \lambda) \exp[-i(\xi(\lambda)t + \theta(t, \lambda))/\hbar]. \quad (3.23)$$

Let us first make the transformation such that $v(\vec{r}, t, \lambda)$ satisfies the conditions

$$\left. \begin{aligned} \langle v(\vec{r}, t, \lambda), v(\vec{r}, t, \lambda) \rangle &= 1, \\ \langle v(\vec{r}, t, \lambda), \frac{\partial}{\partial t} v(\vec{r}, t, \lambda) \rangle &= \langle \frac{\partial}{\partial t} v(\vec{r}, t, \lambda), v(\vec{r}, t, \lambda) \rangle. \end{aligned} \right\} \quad (3.24)$$

The corresponding $\theta(t, \lambda)$ has to be real and satisfy

$$\frac{\partial \theta(t, \lambda)}{\partial t} = \langle u, [H^{(0)} + \lambda V(t)] u \rangle - \mathcal{E}(\lambda), \quad (3.25)$$

where we have used the fact that the operators $V(t)$ and $\exp[i\theta(t, \lambda)/\hbar]$ commute. Suppose that $\theta(t+\tau, \lambda) = \theta(t, \lambda)$; then, integrating Eq. (3.25) with respect to t over the period τ , one has

$$\mathcal{E}(\lambda) = \langle\langle u, [H^{(0)} + \lambda V(t)] u \rangle\rangle. \quad (3.26)$$

This equation, of course, does not hold in general. Hence neither $\theta(t, \lambda)$ nor $v(\vec{r}, t, \lambda)$ can be a periodic function of time with period τ . In other words, the conditions (3.24) and the periodic relation

$$v(\vec{r}, t+\tau, \lambda) = v(\vec{r}, t, \lambda) \quad (3.27)$$

do not hold simultaneously. It is important to notice the close relation between the conditions imposed on $v(\vec{r}, t, \lambda)$ and its periodic property (3.27).

As stated by Langhoff et al.,² one can avoid the "secular divergences" by imposing the conditions

$$\langle v(\vec{r}, t, \lambda), v(\vec{r}, t, \lambda) \rangle = 1, \quad (3.28a)$$

$$\langle v(\vec{r}, t, 0), v(\vec{r}, t, \lambda) \rangle = \langle v(\vec{r}, t, \lambda), v(\vec{r}, t, 0) \rangle, \quad (3.28b)$$

on $v(\vec{r}, t, \lambda)$, or by imposing another set of conditions

$$\langle \psi(\vec{r}, t, \lambda), \psi(\vec{r}, t, \lambda) \rangle = 1, \quad \langle v(\vec{r}, t, 0), v(\vec{r}, t, \lambda) \rangle = 1. \quad (3.29)$$

In the following paragraphs, we shall show that one can always choose $\theta(t, \lambda)$ so that $v(\vec{r}, t, \lambda)$ satisfies both the conditions (3.28) and the periodic relation (3.27).

In order to satisfy Eqs. (3.27) and (3.28a), the corresponding $\theta(t, \lambda)$ has to be real and periodic in time with period τ . For any given $\theta(t, \lambda)$ which is real and periodic in time with period τ , the corresponding solution $v(\vec{r}, t, \lambda)$ of Eq. (3.22) satisfies

$$\frac{\partial}{\partial t} \langle v, v \rangle = 0, \quad (3.30)$$

$$\begin{aligned} \frac{1}{2} \frac{\partial}{\partial t} \ln \left[\frac{\langle v^{(0)}, v \rangle}{\langle v, v^{(0)} \rangle} \right] &= \frac{\partial}{\partial t} [\theta(t, 0) - \theta(t, \lambda)] + [\mathcal{E}^{(0)} - \mathcal{E}(\lambda)] \\ &+ \lambda \operatorname{Re} \left[\frac{\langle v, v(t) v^{(0)} \rangle}{\langle v, v^{(0)} \rangle} \right]. \end{aligned} \quad (3.31)$$

where $\mathcal{E}^{(0)} \equiv \mathcal{E}(0)$ and $v^{(0)} \equiv v(\vec{r}, t, 0)$. Equation (3.31) is the key relation to prove the statement.

The eigenvalue $\mathcal{E}(\lambda)$ is given by

$$\mathcal{E}(\lambda) = \frac{1}{\tau} \int_{-\tau/2}^{\tau/2} \mathcal{E}(t, \lambda) dt, \quad (3.32)$$

$$\mathcal{E}(t, \lambda) = \mathcal{E}^{(0)} + \lambda \operatorname{Re} \left[\frac{\langle v, v(t) v^{(0)} \rangle}{\langle v, v^{(0)} \rangle} \right], \quad (3.33)$$

as is seen from Eq. (3.31). We choose the function $\theta(t, \lambda)$ such that

$$\frac{\partial}{\partial t} \theta(t, \lambda) = \mathcal{E}(t, \lambda) - \mathcal{E}(\lambda) , \quad \int_{-\tau/2}^{\tau/2} \theta(t, \lambda) dt = 0 , \quad (3.34)$$

where the function $v(\vec{r}, t, \lambda)$ in the $\mathcal{E}(t, \lambda)$ is the corresponding solution for this chosen $\theta(t, \lambda)$. In order to be self-consistent, the function $\theta(t, \lambda)$ defined by Eqs. (3.34) must be real and periodic in time with period τ ; using Eq. (3.32), one can easily show the self-consistency.

For this specially chosen $\theta(t, \lambda)$, the corresponding $v(\vec{r}, t, \lambda)$ satisfies

$$\left[\mathcal{H}^{(0)} + \lambda V(t) - \mathcal{E}(t, \lambda) \right] v(\vec{r}, t, \lambda) = 0 , \quad (3.35)$$

$$\frac{\partial}{\partial t} \left[\langle v^{(0)}, v \rangle / \langle v, v^{(0)} \rangle \right] = 0 , \quad (3.36)$$

where the second equation follows from Eq. (3.31). If $v(\vec{r}, t, \lambda)$ is a solution of Eq. (3.35), then $c(\lambda)v(\vec{r}, t, \lambda)$ is also a solution, where $c(\lambda)$ is an arbitrary complex function of λ . Using this freedom and Eqs. (3.30, 36), one can always make a solution $v(\vec{r}, t, \lambda)$ to satisfy the conditions (3.28a, b).

Thus we have shown that the conditions (3.28) imposed on $v(\vec{r}, t, \lambda)$ go hand in hand with the periodic relation (3.27). Similarly one can show that Eqs. (3.27, 29) hold simultaneously. For this case, however, the corresponding $\theta(t, \lambda)$ is not real, and the transformed "Hamiltonian," $\mathcal{H}^{(0)} + \lambda V(\lambda) - \partial \theta(t, \lambda) / \partial t$, is

no longer Hermitian in $\mathcal{R}+\mathcal{T}$. Because of this disadvantage, we prefer the conditions (3.28) to (3.29) in order to avoid the secular divergences.

To sum up, the equations for the desired $v(\vec{r}, t, \lambda)$ are Eqs. (3.35, 33) and Eqs. (3.28), and the solution $v(\vec{r}, t, \lambda)$ of them must be located in $\mathcal{R}+\mathcal{T}$. The eigenvalue $\mathcal{E}(\lambda)$ and the phase function $\theta(t, \lambda)$ are given by Eq. (3.32) and Eqs. (3.34), respectively, where $v(\vec{r}, t, \lambda)$ in the $\mathcal{E}(t, \lambda)$ is the solution of Eqs. (3.35, 33). The complete wavefunction $\psi(\vec{r}, t, \lambda)$ is given by (3.23). Since the solution $v(\vec{r}, t, \lambda)$ of Eq. (3.35) satisfies automatically Eqs. (3.30, 36), the conditions (3.28) are equivalent to the conditions

$$\left. \begin{aligned} \langle\langle v(\vec{r}, t, \lambda), v(\vec{r}, t, \lambda) \rangle\rangle &= 1, \\ \langle\langle v(\vec{r}, t, 0), v(\vec{r}, t, \lambda) \rangle\rangle &= \langle\langle v(\vec{r}, t, \lambda), v(\vec{r}, t, 0) \rangle\rangle, \end{aligned} \right\} (3.37)$$

so long as $v(r, t, \lambda)$ is a solution of Eq. (3.35). The solution $v(\vec{r}, t, \lambda)$ of Eqs. (3.35, 33, 28) satisfies

$$\langle\langle v^{(0)}, v(t)v \rangle\rangle = \langle\langle v, v(t)v^{(0)} \rangle\rangle. \quad (3.38)$$

Note that in general the relation $\langle v^{(0)}, v(t)v \rangle = \langle v, v(t)v^{(0)} \rangle$ cannot be expected to hold.

Expanding $\mathcal{E}(\lambda)$, $\mathcal{E}(t, \lambda)$, $\theta(t, \lambda)$ and $v(\vec{r}, t, \lambda)$ according to

$$\left. \begin{aligned} \mathcal{E}(\lambda) &= \sum_{k=0}^{\infty} \lambda^k \mathcal{E}^{(k)}, & \mathcal{E}(t, \lambda) &= \sum_{k=0}^{\infty} \lambda^k \mathcal{E}^{(k)}(t), \\ \theta(t, \lambda) &= \sum_{k=0}^{\infty} \lambda^k \theta^{(k)}(t), & v(\vec{r}, t, \lambda) &= \sum_{k=0}^{\infty} \lambda^k v^{(k)}(\vec{r}, t), \end{aligned} \right\} (3.39)$$

and substituting into Eqs. (3.35, 33, 28), one obtains

$$[\mathcal{H}^{(0)} - \mathcal{E}^{(0)}] v^{(0)} = 0, \quad \langle v^{(0)}, v^{(0)} \rangle = 1, \quad \mathcal{E}^{(0)}(t) = \mathcal{E}^{(0)}, \quad (3.40)$$

and for $n=1, 2, \dots$,

$$[\mathcal{H}^{(0)} - \mathcal{E}^{(0)}] v^{(n)} + [V(t) - \mathcal{E}^{(1)}(t)] v^{(n-1)} - \sum_{k=2}^n \mathcal{E}^{(k)}(t) v^{(n-k)} = 0, \quad (3.41a)$$

$$\mathcal{E}^{(n)}(t) = \text{Re} \langle v^{(0)}, V(t) v^{(n-1)} \rangle - \sum_{k=1}^{n-1} \mathcal{E}^{(k)}(t) \langle v^{(0)}, v^{(n-k)} \rangle, \quad (3.41b)$$

$$\langle v^{(0)}, v^{(n)} \rangle = -\frac{1}{2} \sum_{k=1}^{n-1} \langle v^{(k)}, v^{(n-k)} \rangle. \quad (3.41c)$$

One can solve the sequence of equations (3.40) and (3.41) progressively. The $\mathcal{E}^{(k)}$ and $\theta^{(k)}(t)$ are given by

$$\left. \begin{aligned} \mathcal{E}^{(k)} &= \frac{1}{\tau} \int_{-\tau/2}^{\tau/2} \mathcal{E}^{(k)}(t) dt; \\ \frac{d}{dt} \theta^{(k)}(t) &= \mathcal{E}^{(k)}(t) - \mathcal{E}^{(k)}, \quad \int_{-\tau/2}^{\tau/2} \theta^{(k)}(t) dt = 0. \end{aligned} \right\} \quad (3.42)$$

Incidentally, the variational equation for the $v^{(1)}(\vec{r}, t)$ is given by

$$\left. \begin{aligned} \delta F[u(\vec{r}, t)] &= 0, \\ F[u] &\equiv \langle\langle u, [\mathcal{H}^{(0)} - \mathcal{E}^{(0)}] u \rangle\rangle + 2\text{Re} \langle\langle v^{(0)}, [V(t) - \mathcal{E}^{(1)}(t)] v^{(0)} \rangle\rangle, \end{aligned} \right\} \quad (3.43)$$

where $u(\vec{r}, t)$ and $\delta u(\vec{r}, t)$ are in $\mathcal{R} + \mathcal{T}$.

Remarks. Let us consider an inhomogeneous equation with an auxiliary condition,

$$\left. \begin{aligned} [H^{(0)} - i\hbar(\partial/\partial t) - E_0] v(\vec{r}, t) &= w(\vec{r}, t) , \\ \langle f_0(\vec{r}), v(\vec{r}, t) \rangle &= 0 , \end{aligned} \right\} \quad (3.44)$$

where $H^{(0)} f_0(\vec{r}) = E_0 f_0(\vec{r})$ and the given function $w(\vec{r}, t)$ is periodic in time with period τ . If $v(\vec{r}, t)$ is a solution of Eqs. (3.44), then the $v'(\vec{r}, t)$ given by

$$v'(\vec{r}, t) = v(\vec{r}, t) + \sum_{n(\neq 0)} c_n f_n(\vec{r}) e^{i(E_0 - E_n)t/\hbar} \quad (3.45)$$

is also a solution of Eqs. (3.44), where E_n and $f_n(\vec{r})$ are discrete eigenvalues and eigenfunctions of $H^{(0)}$, and the coefficients c_n are arbitrary. This shows that the solution of Eqs. (3.44) is not unique and in general not periodic in time with period τ . The fact that $w(\vec{r}, t)$ is a periodic function of time does not insure that solutions $v(\vec{r}, t)$ of Eqs. (3.44) are periodic in time.¹⁴ One should establish the periodicity of the solution $v^{(n)}(\vec{r}, t)$ of Eq. (3.41a) on the basis of the steady state $u(\vec{r}, t)$, as we have done before. Finally we emphasize that the transformed equation and the original one are equivalent as long as the period τ is finite.

4. APPLICATIONS

We shall now apply the steady state perturbation theory to the case when the perturbing operator $V(t)$ is harmonic, namely

$$V(t) = 2V^{(1)} \cos \omega t, \quad (4.1)$$

where $V^{(1)}$ is a time-independent Hermitian operator, and $\omega = 2\pi/\tau \neq 0$; we shall study two examples for demonstration.

A. One-Level System

In this section we consider the case when the discrete eigenvalue E_0 of $H^{(0)}$ in question is non-degenerate in \mathcal{R} , and when there is, besides E_0 , no discrete eigenvalue of $H^{(0)}$ in the vicinity of E_0 , $E_0 \pm \hbar\omega$, $E_0 \pm 2\hbar\omega$, and $E_0 \pm 3\hbar\omega$.

Time-dependence of the perturbed wavefunction. Let us first assume that there is no discrete eigenvalue E_n of $H^{(0)}$ which satisfies $E_n = E_0 + q\hbar\omega$ for some non-zero integer q ; namely the eigenvalue E_0 of $\mathcal{H}^{(0)}$ is non-degenerate. We shall use the transformed perturbation equations (3.40,41), because of the desirable limiting behavior of the perturbed wavefunction at $\omega=0$; the same notations as the previous section C will be used in this section.

We choose the zone (2.17) such that the zeroth-order eigenfunction $v^{(0)}(\vec{r}, t)$ is time-independent:

$$\left. \begin{aligned} [H^{(0)} - E_0] f_0(\vec{r}) &= 0, & \langle f_0(\vec{r}), f_0(\vec{r}) \rangle &= 1, \\ \mathcal{E}^{(0)} &= E_0, & v^{(0)}(\vec{r}, t) &= f_0(\vec{r}). \end{aligned} \right\} \quad (4.2)$$

Knowing $v^{(0)}(\vec{r}, t)$, one can calculate $\mathcal{E}^{(1)}(t)$ from Eq. (3.14b),

namely

$$G^{(1)}(t) = 2E^{(1)} \cos \omega t, \quad E^{(1)} \equiv \langle f_0, v^{(1)} f_0 \rangle. \quad (4.3)$$

Since the first-order eigenfunction $v^{(1)}(\vec{r}, t)$ is a periodic function of t with period $2\pi/\omega$, it can be expanded in a Fourier series, namely

$$v^{(1)}(\vec{r}, t) = \sum_q f_q^{(1)}(\vec{r}) e^{iq\omega t}, \quad (4.4)$$

where functions $f_q^{(1)}(\vec{r})$ are in \mathcal{R} . Substituting (4.3,4) into the first-order equation of (3.41a,c) and using the fact that $\omega \neq 0$, one obtains

$$[H^{(0)} - E_0 \pm \hbar\omega] f_{\pm 1}^{(1)} + [V^{(1)} - E^{(1)}] f_0 = 0, \quad (4.5a)$$

$$\langle f_0, f_{\pm 1}^{(1)} \rangle = 0, \quad (4.5b)$$

$$[H^{(0)} - E_0 + q\hbar\omega] f_q^{(1)} = 0, \quad \langle f_0, f_q^{(1)} \rangle = 0, \quad \text{for } q \neq \pm 1. \quad (4.6)$$

From the assumption we made, there are no non-vanishing functions in \mathcal{R} which satisfy Eqs. (4.6); therefore, the functions $f_q^{(1)}(\vec{r})$ must vanish except for $q = \pm 1$. Thus the first-order eigenfunction $v^{(1)}(\vec{r}, t)$ is given by

$$v^{(1)}(\vec{r}, t) = f_{+1}^{(1)}(\vec{r}) e^{i\omega t} + f_{-1}^{(1)}(\vec{r}) e^{-i\omega t}, \quad (4.7)$$

where the functions $f_{\pm 1}^{(1)}(\vec{r})$ satisfy Eqs. (4.5), respectively.

Note that Eqs. (4.5a) yield Eqs. (4.5b).

From Eq. (3.41b), one has

$$\mathcal{E}^{(2)}(t) = 2E^{(2)}(1+\cos 2\omega t), \quad E^{(2)} \equiv \frac{1}{2}\langle f_0, V^{(1)}(f_{+1}^{(1)} + f_{-1}^{(1)}) \rangle; \quad (4.8)$$

it is easy to see from Eqs. (4.5a) that $\langle f_0, V^{(1)} f_{\pm 1}^{(1)} \rangle$ are real.

By similar manipulation, one obtains

$$v^{(2)}(\vec{r}, t) = f_{+2}^{(2)}(\vec{r})e^{i2\omega t} + f_{-2}^{(2)}(\vec{r})e^{-i2\omega t} + 2f_0^{(2)}(\vec{r}), \quad (4.9)$$

where the functions $f_{\pm 2}^{(2)}(\vec{r})$ and $f_0^{(2)}(\vec{r})$ satisfy

$$\left. \begin{aligned} [H^{(0)} - E_0 \pm 2\hbar\omega]f_{\pm 2}^{(2)} + [V^{(1)} - E^{(1)}]f_{\pm 1}^{(1)} - E^{(2)}f_0 &= 0, \\ [H^{(0)} - E_0]f_0^{(2)} + \frac{1}{2}[V^{(1)} - E^{(1)}](f_{+1}^{(1)} + f_{-1}^{(1)}) - E^{(2)}f_0 &= 0, \end{aligned} \right\} \quad (4.10)$$

$$\langle f_0, f_{+2}^{(2)} \rangle = \langle f_0, f_{-2}^{(2)} \rangle = -\frac{1}{2}\langle f_{+1}^{(1)}, f_{-1}^{(1)} \rangle = -\frac{1}{2}\langle f_{-1}^{(1)}, f_{+1}^{(1)} \rangle, \quad (4.11a)$$

$$\langle f_0, f_0^{(2)} \rangle = -\frac{1}{4}[\langle f_{+1}^{(1)}, f_{+1}^{(1)} \rangle + \langle f_{-1}^{(1)}, f_{-1}^{(1)} \rangle]; \quad (4.11b)$$

note that Eqs. (4.5a) and (4.10) yield Eqs. (4.11a).

From the formulas (3.42), one obtains the eigenvalues $\mathcal{E}^{(k)}$ and the phase functions $\theta^{(k)}(t)$, namely

$$\mathcal{E}^{(0)} = E_0, \quad \mathcal{E}^{(1)} = 0, \quad \mathcal{E}^{(2)} = 2E^{(2)}, \quad \mathcal{E}^{(3)} = 0, \quad (4.12)$$

$$\theta^{(0)}(t) = 0, \quad \theta^{(1)}(t) = 2E^{(1)}\frac{\sin \omega t}{\omega}, \quad \theta^{(2)}(t) = 2E^{(2)}\frac{\sin 2\omega t}{2\omega}. \quad (4.13)$$

Thus the complete wavefunction $\psi(\vec{r}, t, \lambda)$, to the second-order, is given by

$$\begin{aligned} \psi(\vec{r}, t, \lambda) = & \left[f_0 + \lambda(f_{+1}^{(1)}e^{i\omega t} + f_{-1}^{(1)}e^{-i\omega t}) \right. \\ & \left. + \lambda^2(f_{+2}^{(2)}e^{i2\omega t} + f_{-2}^{(2)}e^{-i2\omega t} + 2f_0^{(2)}) + \dots \right] e^{-i\eta(t, \lambda)/\hbar}, \end{aligned} \quad (4.14a)$$

$$\eta(t, \lambda) = E_0 t + 2\lambda E^{(1)} \frac{\sin \omega t}{\omega} + 2\lambda^2 E^{(2)} \left[t + \frac{\sin 2\omega t}{2\omega} \right] + \dots, \quad (4.14b)$$

where $f_{\pm 1}^{(1)}$ satisfy Eqs. (4.5), and $f_{\pm 2}^{(2)}$ and $f_0^{(2)}$ satisfy Eqs. (4.10, 11).

The second-order quasi-energy eigenvalue $\varepsilon^{(2)}$ is the quantity of physical interest; for example, when $v^{(1)}$ is the x component of the dipole moment operator, $-\varepsilon^{(2)}$ gives the frequency-dependent polarizability $\alpha_{xx}(\omega)$.

Applicability conditions. Suppose this time that there are functions $g_{q\alpha}(\vec{r})$ in \mathcal{Q} which satisfy

$$\left[H^{(0)} - E_0 + q\hbar\omega \right] g_{q\alpha}(\vec{r}) = 0, \quad \langle g_{q\alpha}, g_{q\beta} \rangle = \delta_{\alpha\beta}, \quad (4.15)$$

for some non-zero integer q , where the second index α in $g_{q\alpha}(\vec{r})$ distinguishes between the eigenfunctions belonging to the same eigenvalue $E_0 - q\hbar\omega$ of $H^{(0)}$; then the functions $f_0(\vec{r})$ and $g_{q\alpha}(\vec{r})e^{iq\omega t}$ belong to the eigenvalue E_0 of $\mathcal{H}^{(0)}$, and E_0 is no longer a non-degenerate eigenvalue of $\mathcal{H}^{(0)}$. For this case, one has to use the degenerate perturbation method.

If the functions $v^{(0)}(\vec{r}, t)$, $v^{(1)}(\vec{r}, t)$ and $v^{(2)}(\vec{r}, t)$ given by Eqs. (4.2, 7, 9) satisfy

$$\langle\langle g_{q\alpha} e^{iq\omega t}, \left\{ \left[v(t) - \varepsilon^{(1)}(t) \right] v^{(m-1)} - \sum_{k=2}^m \varepsilon^{(k)}(t) v^{(m-k)} \right\} \rangle\rangle = 0, \quad \text{for all } q\alpha, \quad (4.16)$$

for $m=1, \dots, (n+1)$, where $\varepsilon^{(1)}(t)$ and $\varepsilon^{(2)}(t)$ are given by Eqs. (4.3, 8), then the function $v^{(0)} + \dots + \lambda^n v^{(n)}$ satisfies the degenerate

perturbation equations up to the n th-order with the eigenvalue $\xi^{(0)} + \dots + \lambda^n \xi^{(n)}$, and $\xi^{(n+1)}$ is an eigenvalue of the $(n+1)$ th-order equation, where the eigenvalues $\xi^{(k)}$ are given by Eqs. (4.12).

We still assume that E_0 is a non-degenerate eigenvalue of $H^{(0)}$. For $m=1$, Eq. (4.16) yields

$$\langle g_{\alpha\alpha}, v^{(1)} f_0 \rangle (\delta_{q,+1} + \delta_{q,-1}) = 0, \quad \text{for all } q\alpha; \quad (4.17)$$

hence if $E_0 \pm \hbar\omega$ are not eigenvalues of $H^{(0)}$, then $\{\xi^{(1)}=0, v^{(0)}(\vec{r}, t)=f_0(\vec{r})\}$ is a solution of the first-order degenerate perturbation equation, and furthermore the solutions $f_{\pm 1}^{(1)}(\vec{r})$ of Eqs. (4.5) are unique. If there exist the eigenvalues of $H^{(0)}$ which are close to the $E_0 + \hbar\omega$ or $E_0 - \hbar\omega$, then the solution $f_{+1}^{(1)}(\vec{r})$ or $f_{-1}^{(1)}(\vec{r})$ becomes large. Therefore the applicability condition for $\{\xi^{(0)} + \lambda \xi^{(1)}, v^{(0)}\}$ is that there exists no eigenvalue of $H^{(0)}$ at the vicinity of $E_0 \pm \hbar\omega$.

For $m=2$, Eq. (4.16) yields

$$\langle g_{\alpha\alpha}, [v^{(1)} - E^{(1)}] f_{+1}^{(1)} \rangle \delta_{q,+2} + \langle g_{\alpha\alpha}, [v^{(1)} - E^{(1)}] f_{-1}^{(1)} \rangle \delta_{q,-2} = 0, \\ \text{for all } q\alpha; \quad (4.18)$$

if $E_0 \pm 2\hbar\omega$ are not eigenvalues of $H^{(0)}$, then $\{\xi^{(2)}, v^{(2)}\}$ is a solution of the second-order degenerate perturbation equation, and the solution $f_{\pm 2}^{(2)}(\vec{r})$ and $f_0^{(2)}(\vec{r})$ of Eqs. (4.10,11) are unique. If there exist the eigenvalues of $H^{(0)}$ which are close

to the $E_0 + 2\hbar\omega$, $E_0 - 2\hbar\omega$, or E_0 . then the solution $f_{+2}^{(2)}(\vec{r})$, $f_{-2}^{(2)}(\vec{r})$, or $f_0^{(2)}(\vec{r})$ again becomes large. Hence the applicability condition for $\{\epsilon^{(0)} + \lambda\epsilon^{(1)} + \lambda^2\epsilon^{(2)}, v^{(0)} + \lambda v^{(1)}\}$ is that besides E_0 , there exists no eigenvalue of $H^{(0)}$ at the vicinity of E_0 , $E_0 \pm \hbar\omega$, and $E_0 \pm 2\hbar\omega$. Similarly the applicability condition for $\{\epsilon^{(0)} + \lambda\epsilon^{(1)} + \lambda^2\epsilon^{(2)} + \lambda^3\epsilon^{(3)}, v^{(0)} + \lambda v^{(1)} + \lambda^2 v^{(2)}\}$ is that besides E_0 there exists no eigenvalue of $H^{(0)}$ at the vicinity of E_0 , $E_0 \pm \hbar\omega$, $E_0 \pm 2\hbar\omega$, and $E_0 \pm 3\hbar\omega$.

Limiting behavior at $\omega=0$. If $\hbar\omega$ is much smaller than the difference between E_0 and the closest eigenvalue of $H^{(0)}$, then there will be, besides E_0 , no eigenvalue of $H^{(0)}$ in the vicinity of E_0 , $E_0 \pm \hbar\omega$, $E_0 \pm 2\hbar\omega$, and $E_0 \pm 3\hbar\omega$; hence one may consider Eqs. (4.1-14) valid in the neighborhood of $\omega=0$.

At the limit $\omega=0$, the functions $f_{\pm 1}^{(1)}(\vec{r})$, $f_{\pm 2}^{(2)}(\vec{r})$, and $f_0^{(2)}(\vec{r})$ become

$$\left. \begin{aligned} f^{(1)}(\vec{r}) &= f_{+1}^{(1)}(\vec{r}) = f_{-1}^{(1)}(\vec{r}) , \\ f^{(2)}(\vec{r}) &= f_{+2}^{(2)}(\vec{r}) = f_{-2}^{(2)}(\vec{r}) = f_0^{(2)}(\vec{r}) , \end{aligned} \right\} \quad (4.19)$$

where $f^{(1)}(\vec{r})$ and $f^{(2)}(\vec{r})$ satisfy the stationary perturbation equations, namely

$$\left. \begin{aligned} [H^{(0)} - E_0]f_0 &= 0 , \\ [H^{(0)} - E_0]f^{(1)} + [v^{(1)} \langle f_0, v^{(1)} f_0 \rangle]f_0 &= 0 , \\ [H^{(0)} - E_0]f^{(2)} + [v^{(1)} \langle f_0, v^{(1)} f_0 \rangle]f^{(1)} - \langle f_0, v^{(1)} f^{(1)} \rangle f_0 &= 0 , \end{aligned} \right\} \quad (4.20a)$$

$$\langle f_0, f_0 \rangle = 1, \quad \langle f_0, f^{(1)} \rangle = 0, \quad \langle f_0, f^{(2)} \rangle = -\frac{1}{2} \langle f^{(1)}, f^{(1)} \rangle. \quad (4.20b)$$

When $\omega \rightarrow 0$, the complete wavefunction $\psi(\vec{r}, t, \lambda)$ smoothly joins the stationary solution of the Hamiltonian $H^{(0)} + (2\lambda)V^{(1)}$,

$$\left. \begin{aligned} \psi(\vec{r}, t, \lambda) &= [f_0 + (2\lambda)f^{(1)} + (2\lambda)^2 f^{(2)} + \dots] e^{-i\eta(t, \lambda)/\hbar}, \\ \eta(t, \lambda) &= t[E_0 + (2\lambda)\langle f_0, V^{(1)} f_0 \rangle + (2\lambda)^2 \langle f_0, V^{(1)} f^{(1)} \rangle + \dots], \end{aligned} \right\} \quad (4.21)$$

for any finite t .

This limiting behavior is due to the transformation we made; the original eigenfunction $u(\vec{r}, t, \lambda)$ does not have this limiting property. If one wishes to expand the perturbed wavefunction in powers of ω , then the limiting property we obtained is indispensable.

Variational method. The variational equations for the solutions $f_{\pm 1}^{(1)}(\vec{r})$ of Eqs. (4.5) are given by

$$\left. \begin{aligned} \delta F_+[h_+(\vec{r})] &= 0; \quad \delta F_-[h_-(\vec{r})] = 0, \\ F_{\pm}[h_{\pm}] &= \langle h_{\pm}, [H^{(0)} - E_0 \pm \hbar\omega] h_{\pm} \rangle + 2\text{Re} \langle f_0, [V^{(1)} - \langle f_0, V^{(1)} f_0 \rangle] h_{\pm} \rangle. \end{aligned} \right\} \quad (4.22)$$

These equation can be obtained from Eq. (3.43), or merely by inspection.

A remark. If one adopts another normalization and phase convention, namely $\langle \psi, \psi \rangle = 1$ and $\langle v^{(0)}, v \rangle = 1$ with complex $\theta(t, \lambda)$, then one obtains somewhat more complex equations than Eqs. (4.1-14).¹⁵

B. Two-Level System Connected with Single-Quantum Transition

We shall now study the case which obtains when two discrete non-degenerate eigenvalues E_1 and E_2 of $H^{(0)}$ satisfy $E_2 = E_1 + \hbar\omega$, and there are, besides E_1 and E_2 , no eigenvalues of $H^{(0)}$ in the vicinity of $E_1 \pm \hbar\omega$ and $E_2 \pm \hbar\omega$; the eigenvalue E_1 of $\mathcal{H}^{(0)}$ is then almost degenerate. We can treat this problem by the almost-degenerate perturbation method as developed in the previous section. In particular, the eigenfunctions and eigenvalues are determined by Eq. (3.19,20); we shall use the same notation here as was used there.

Let $f_1(\vec{r})$ and $f_2(\vec{r})$ be the eigenfunctions of $H^{(0)}$ belonging to the eigenvalues E_1 and E_2 , respectively; choosing the zone (2.17) suitably, one has the eigenvalues and eigenfunctions of $\mathcal{H}^{(0)}$ in the form,

$$\left. \begin{aligned} \epsilon_1^{(0)} &= E_1, & u_1^{(0)}(\vec{r}, t) &= f_1(\vec{r}), \\ \epsilon_2^{(0)} &= E_2 - \hbar\omega, & u_2^{(0)}(\vec{r}, t) &= f_2(\vec{r})e^{-i\omega t}. \end{aligned} \right\} \quad (4.23)$$

The eigenvalues of Eq. (3.20) are given by

$$\left. \begin{aligned} \epsilon_{\pm 1}^{(1)} &= \pm [\Delta^2 + |\langle f_1, v^{(1)} f_2 \rangle|^2]^{\frac{1}{2}}, \\ \Delta &= (E_1 - E_2 + \hbar\omega)/2\lambda; \end{aligned} \right\} \quad (4.24)$$

the corresponding eigenvectors $\{c_{1+}, c_{2+}\}$ and $\{c_{1-}, c_{2-}\}$ are

determined up to a phase factor from the equations,

$$R_{\pm} = \frac{c_{1\pm}}{c_{2\pm}} = \frac{\langle f_1, v^{(1)} f_2 \rangle}{\delta_{\pm}^{(1)} - \Delta}, \quad |c_{1\pm}|^2 + |c_{2\pm}|^2 = 1. \quad (4.25)$$

Thus the first-order solutions are given by

$$\left. \begin{aligned} \psi_{\pm}(\vec{r}, t, \lambda) &= [c_{1\pm} u_1^{(0)}(\vec{r}, t) + c_{2\pm} u_2^{(0)}(\vec{r}, t)] e^{-i(\epsilon^{(0)} + \lambda \epsilon_{\pm}^{(1)}) t / \hbar}, \\ \epsilon^{(0)} &= \frac{1}{2}(\epsilon_1^{(0)} + \epsilon_2^{(0)}) \end{aligned} \right\} \quad (4.26)$$

Suppose that the system is in the state $f_1(\vec{r})$ at $t=0$; then the wavefunction $\psi(\vec{r}, t, \lambda)$ at subsequent values of t is, in first-order, given by

$$\begin{aligned} \psi(\vec{r}, t, \lambda) &= (c_{2-} \psi_+ - c_{2+} \psi_-) / (c_{2-} c_{1+} - c_{2+} c_{1-}) \\ &= \frac{e^{-i\epsilon^{(0)} t / \hbar}}{R_+ - R_-} \left[(R_+ e^{-i\lambda \epsilon_+^{(1)} t / \hbar} - R_- e^{-i\lambda \epsilon_-^{(1)} t / \hbar}) f_1 \right. \\ &\quad \left. + e^{-i\omega t} (e^{-i\lambda \epsilon_+^{(1)} t / \hbar} - e^{-i\lambda \epsilon_-^{(1)} t / \hbar}) f_2 \right], \quad (4.27) \end{aligned}$$

since $\psi(\vec{r}, t, \lambda)$ is the first-order solution of the Schrödinger equation, and satisfies $\psi(\vec{r}, 0, \lambda) = f_1(\vec{r})$. The probability $P_2(t)$ of finding the system in the state $f_2(\vec{r})$ at the time t is given by

$$P_2(t) = |(e^{-i\lambda \epsilon_+^{(1)} t / \hbar} - e^{-i\lambda \epsilon_-^{(1)} t / \hbar}) / (R_+ - R_-)|^2; \quad (4.28)$$

substituting (4.25) into (4.28), one obtains

$$\left. \begin{aligned} P_2(t) &= \frac{\lambda^2 |\langle f_1, v^{(1)} f_2 \rangle|^2}{\hbar^2} \left[\frac{\sin(\omega^{(1)} t)}{\omega^{(1)}} \right]^2, \\ \omega^{(1)} &= \left[\frac{1}{\hbar} (E_1 - E_2 + \hbar\omega)^2 + \lambda^2 |\langle f_1, v^{(1)} f_2 \rangle|^2 \right]^{1/2} / \hbar. \end{aligned} \right\} \quad (4.29)$$

It is easy to show that the probability $P_1(t)$ finding the system in the state $f_1(\vec{r})$ at the time t is given by $P_1(t) + P_2(t) = 1$.

The formula (4.29) is nothing but the well-known Rabi formula.¹⁶

The applicability conditions for the formula (4.29) are given by Eq. (3.18), namely

$$|(E_1 - E_2 + \hbar\omega)/\lambda| \ll |\langle f_1, v^{(1)} f_2 \rangle|; \quad (4.30)$$

and by the requirement that there are, besides E_1 and E_2 , no eigenvalues of $H^{(0)}$ in the vicinity of $E_1 \pm \hbar\omega$ and $E_2 \pm \hbar\omega$. The presence of eigenvalues of $H^{(0)}$ in the vicinity of $E_1 + q\hbar\omega$ and $E_2 + q\hbar\omega$ for $|q| \geq 2$ does not change the final result (4.29).

These applicability conditions give the conditions for two-level system model to be valid in the first-order transition probability calculation.

5. DISCUSSIONS

Existence of steady state solutions. Most of Hamiltonians which one encounters in practice are of the form $H^{(0)} + \lambda V(t)$, where $H^{(0)}$ is a time-independent Hermitian operator, $V(t)$ is also Hermitian but periodic in time, and λ is a small real

parameter. If the steady state Schrödinger equation (3.2,3) for the system has a discrete eigenvalue $\mathcal{E}(\lambda)$ and its eigenfunction $u(\vec{r}, t, \lambda)$ in $\mathcal{R} + \mathcal{J}$, then we certainly have a steady state solution, since $u(\vec{r}, t, \lambda)e^{-i\mathcal{E}(\lambda)t/\hbar}$ is a bound solution of the Schrödinger equation and has the required form. Hence the question of the existence of steady states can be reduced to the question of the existence of the perturbation solutions of Eq. (3.2,3).

The unperturbed Hamiltonian $H^{(0)}$ that we are interested in has usually bound states solutions in \mathcal{R} and therefore the operator $\mathcal{H}^{(0)} (= H^{(0)} - i\hbar\partial/\partial t)$ has discrete eigenvalues and corresponding eigenfunctions in $\mathcal{R} + \mathcal{J}$, namely steady state solutions (see Eq. (3.7-9)). The solutions that we are interested in are such that the eigenvalue $\mathcal{E}(\lambda)$ approaches one of the discrete eigenvalues of $\mathcal{H}^{(0)}$, when $\lambda \rightarrow 0$. The question on the existence of such perturbation solutions can be treated analogously to the static case¹⁷; again the difference is the Hilbert spaces we use, \mathcal{R} or $\mathcal{R} + \mathcal{J}$.

By analogy, one can expect that for some $V(t)$ (including the perturbing operator for the Stark effect), there exist only asymptotic eigenvalues and eigenfunctions; in other words the perturbation equations have solutions only up to some order.¹⁷ For this case, one has asymptotic steady states, which is sufficient to explain phenomena such as the Stark effect. Young et al. have also given an argument on the existence of asymptotic steady states.¹

Switching function. In this paper, we have intentionally avoided use of a switching function, which describes how the oscillating part $V(t)$ is turned on and reaches its asymptotic form. We simply regard steady state solutions as asymptotic solutions of the Schrödinger equation which has a switching function, and expect that steady state solutions are valid at times long after the oscillating part has reached its asymptotic form, namely a periodically time-dependent form. As is well known, the static Stark effect has been treated in similar manner. In this way, we avoid tricky arguments on switching functions and hope the above statement is correct. Langhoff et al. have included a switching function in their formalism and somehow obtained essentially the same equations as ours for one-level system.²

Prospects. Just recently the multi-level theory was proposed for the simultaneous occurrence of Stark shifts and multiple-quantum transitions by Hicks et al.⁵; in essence, they solve a steady state Schrödinger equation for a perturbed system [for example, Eq. (3.2) with a finite λ] within a specially chosen subspace of the composite Hilbert space $\mathcal{R} + \mathcal{J}$, which is composed from several eigenfunctions of the unperturbed operator $H^{(0)}$ and the functions $e^{iq\omega t}$ with small integers q . As is well known for the Stark effect calculation, the unperturbed eigenfunctions of $H^{(0)}$ are not suited to expand the perturbed portion of the wavefunction, since so many unperturbed eigenfunctions, including

those belonging to the continuous spectrum, are required in order to obtain reasonably accurate susceptibilities. One avoids this difficulty by choosing the basis functions properly. We can reformulate the multi-level theory within our formalism by developing a higher-order almost-degenerate perturbation theory. Research along this line is in progress and the results will be published in the near future.

The Hellmann-Feynman theorem and the hypervirial theorem are expected to yield useful relations which can be used to check the accuracy of calculated, induced charge and current densities of an atom (or a molecule) in an external electromagnetic field. This will be considered subsequently elsewhere.

ACKNOWLEDGMENTS

I am very much indebted to Professor C. C. J. Roothaan for his valuable advice during all stages of this work. I am also grateful to Professor U. Fano for his interest in this work and for several helpful suggestions.

FOOTNOTES

* Research supported in part by the Advanced Research Projects Agency through the U. S. Army Research Office (Durham), under Contract NO. DA-31-124-ARO-D-447 and by the National Science Foundation under Grant NOS. NSF-GP-15216, and NSF-GP-27138.

† Submitted in partial fulfillment of the requirements for the Ph. D., Department of Physics, University of Chicago, Chicago, Ill.

¹ R. H. Young, W. J. Deal, Jr., and N. R. Kestner, Mol. Phys. 17, 369 (1969).

² P. W. Langhoff, S. T. Epstein, and M. Karplus, Rev. Mod. Phys. 44, 602 (1972).

³ S. H. Autler and C. H. Townes, Phys. Rev. 100, 703 (1955).

⁴ J. H. Shirley, Phys. Rev. B138, 974 (1965).

⁵ W. W. Hicks, R. A. Hess, and W. S. Cooper, Phys. Rev. A5, 490 (1972).

⁶ J. von Neumann, Mathematical Foundations of Quantum Mechanics (Princeton University Press, Princeton, 1955); translated by R. T. Beyer.

⁷ G. F. Simmons, Topology and Modern Analysis (McGraw-Hill Book Co., New York, 1963), pp. 256-258.

⁸ J. M. Okuniewicz (private communication), Ph. D. Dissertation, University of Minnesota (unpublished).

⁹ R. P. Feynman, Phys. Rev. 56, 340 (1936).

¹⁰ A. Dalgarno, in Quantum Theory (Academic Press, New York, 1961), edited by D. R. Bates, Vol. I, Chapter 5, p. 190.

¹¹ J. O. Hirschfelder, J. Chem. Phys. 33, 1462 (1960).

¹² This choice is in correspondence with the standard phase convention of stationary perturbation theory. See Footnote 45 of the paper by Langhoff et al. (Footnote 2). There is another type of normalization and phase convention which is commonly used, namely $\langle\langle u(\vec{r}, t, 0), u(\vec{r}, t, \lambda) \rangle\rangle = 1$.

¹³ G. Baym, Lectures on Quantum Mechanics (W. A. Benjamin Inc., New York, 1969), pp. 237-241.

¹⁴ The argument given by Langhoff et al. (Footnote 2, p. 618) is incorrect.

¹⁵ The corresponding equations with this normalization and phase convention are given by Langhoff et al. (Footnote 2).

¹⁶ I. I. Rabi, Phys. Rev. 51, 652 (1937).

¹⁷ See, for example, C. C. Conley and P. A. Rejto, in Perturbation Theory and its Applications in Quantum Mechanics (John Wiley & Sons Inc., New York, 1966), edited by C. H. Wilcox, p. 129, and references cited therein.

Effective Charge Tensors of Atoms in a Molecule and
Electric Dipole Shielding of Nuclei*

HIDEO SAMBE

Laboratory of Molecular Structure and Spectra
Department of Physics, University of Chicago,
Chicago, Illinois 60637

ABSTRACT

Exact formulas are derived for the electric shielding tensors of nuclei in a molecule bathed in a static, uniform, electric field. It is shown that the derived relations hold also in the coupled Hartree-Fock approximation. The resulting equations should provide useful checks on the accuracy of the first-order induced electron density, a quantity required for the calculation of the electric dipole polarizability tensor. A tensor quantity, which is a function of the electric dipole moment and its derivatives with respect to the internal coordinates, is proposed as an effective charge of an atom in a molecule.

INTRODUCTION

The dipole shielding factor β for an atom in a static uniform electric field is given by N/Z , where N is the number of electrons and Z is the nuclear charge.¹ This relation, $\beta=N/Z$, holds also in the coupled Hartree-Fock (H.F.) approximation,² which is, in essence, the H.F. formalism in the presence of a weak external field. Since the dipole shielding factor contains the first-order induced electron density, which is also required for the calculation of the electric dipole polarizability, the relation $\beta=N/Z$ has been providing a useful check on the accuracy of the given first-order induced electron density.³

In this paper, we derive the similar relations for the electric dipole shielding tensors of nuclei in a molecule, and show that the coupled H.F. approximation yields the same relations. The derived expression for the nuclear shielding tensor can be interpreted as an "effective electron number" of an atom divided by the nuclear charge, as in the atomic case. The equations obtained should provide useful checks on the accuracy of the first-order induced electron density.

SEPARATION OF RIGID BODY MOTION

Consider a molecule consisting of N_n nuclei and N_e electrons.

Let us choose the coordinate origin at the center of nuclear mass and denote the positions of the α th nucleus and the μ th electron by the radius vectors \mathbf{r}_α and \mathbf{r}_μ respectively. Relative positions and distances will be denoted by $\mathbf{r}_{\alpha\beta} = \mathbf{r}_\alpha - \mathbf{r}_\beta$, $r_{\alpha\beta} = |\mathbf{r}_\alpha - \mathbf{r}_\beta|$; we shall also use the symbols $\mathbf{r}_{\alpha\mu}$, $r_{\alpha\mu}$, $\mathbf{r}_{\mu\nu}$, and $r_{\mu\nu}$ defined in analogy to $\mathbf{r}_{\alpha\beta}$ and $r_{\alpha\beta}$. The vector $\mathbf{p}_\mu = -i\nabla_\mu$ denotes the linear momentum of the μ th electron. The charge of nucleus α is given by Z_α . We shall use atomic units throughout this paper.

We use the clamped nuclei Hamiltonian H_0 for the electronic motion of the molecule:

$$H_0 = \sum_\mu \left(\frac{1}{2} \mathbf{p}_\mu^2 - \sum_\alpha Z_\alpha r_{\mu\alpha}^{-1} \right) + \sum_{\mu < \nu} r_{\mu\nu}^{-1} + \sum_{\alpha < \beta} Z_\alpha Z_\beta r_{\alpha\beta}^{-1}; \quad (1)$$

in the presence of a uniform electric field \mathbf{F} , the total Hamiltonian H of the perturbed system is given by

$$H = H_0 - \mathbf{F} \cdot \mathbf{D}, \quad (2)$$

where the electric dipole moment \mathbf{D} of the molecule is defined with respect to the coordinate origin (i.e., the nuclear mass center):

$$\mathbf{D} = -\sum_\mu \mathbf{r}_\mu + \sum_\alpha Z_\alpha \mathbf{r}_\alpha. \quad (3)$$

Suppose that the normalized electronic wavefunction Φ of the perturbed system H satisfies the Hellmann-Feynman theorem⁴

$$\nabla_\alpha \langle \Phi | H | \Phi \rangle = \langle \Phi | \nabla_\alpha H | \Phi \rangle = -\langle \Phi | \mathbf{f}_\alpha | \Phi \rangle, \quad \alpha = 1, 2, \dots, N_n, \quad (4)$$

where ∇_α denotes the gradient with respect to the coordinates r_α , and the operator f_α , which represents the force on nucleus α , is given by

$$f_\alpha = -\nabla_\alpha H = -\sum_\mu Z_\alpha r_{\alpha\mu} r_{\alpha\mu}^{-3} + \sum_{\beta(\neq\alpha)} Z_\alpha Z_\beta r_{\alpha\beta} r_{\alpha\beta}^{-3} + Z_\alpha E. \quad (5)$$

The $3N_n$ equations (4) could be used in solving a problem of the forces on nuclei. However, it is convenient to separate the translational and rotational rigid body motion at an early stage. Moreover the quantities $\nabla_\alpha \langle \Phi | H | \Phi \rangle$ do not correspond to physically meaningful quantities in general; only some combinations of them do.

Let us introduce the operator which represents the force on the μ th electron,

$$f_\mu = -\nabla_\mu H = -\sum_\alpha Z_\alpha r_{\mu\alpha} r_{\mu\alpha}^{-3} + \sum_{\nu(\neq\mu)} r_{\mu\nu} r_{\mu\nu}^{-3} - E, \quad (6)$$

and the total charge of the molecule,

$$Q = \sum_\alpha Z_\alpha - N_e. \quad (7)$$

The operator equations concerning the total force and torque on the molecule are, respectively,

$$\sum_\mu f_\mu + \sum_\alpha f_\alpha = QE, \quad (8)$$

$$\sum_\mu r_\mu \times f_\mu + \sum_\alpha r_\alpha \times f_\alpha = P \times E. \quad (9)$$

Evaluating commutators, one can easily demonstrate the following operator equations:

$$i[H, \sum_{\mu} p_{\mu}] = \sum_{\mu} f_{\mu} , \quad (10)$$

$$i[H, \sum_{\mu} r_{\mu} \times p_{\mu}] = \sum_{\mu} r_{\mu} \times f_{\mu} . \quad (11)$$

According to the hypervirial theorems,⁵ on the other hand, we have

$$\langle \Phi | i[H, \sum_{\mu} p_{\mu}] | \Phi \rangle = 0 , \quad (12)$$

$$\langle \Phi | i[H, \sum_{\mu} r_{\mu} \times p_{\mu}] | \Phi \rangle = 0 . \quad (13)$$

From Eqs. (8-13), we obtain the equations of nuclear motion corresponding to the rigid translation and rotation, respectively,

$$\sum_{\alpha} \langle \Phi | f_{\alpha} | \Phi \rangle = QF , \quad (14)$$

$$\sum_{\alpha} r_{\alpha} \times \langle \Phi | f_{\alpha} | \Phi \rangle = \langle \Phi | p | \Phi \rangle \times F , \quad (15)$$

where the electronic wavefunction Φ of the perturbed system H is normalized to unity. The derived Eqs. (14) and (15) are satisfied by the exact wavefunction and also by the coupled H.F. wavefunction, since both wavefunctions satisfy the hypervirial theorems (12) and (13).^{5,6}

Now let q_1 be a set of suitably chosen internal coordinates of the nuclei. In general, the index 1 runs from one to $3N_n - 6$ (up to $3N_n - 5$ for linear molecules). From the Hellmann-Feynman theorem (4), we obtain the internal force relations:

$$\sum_{\alpha} \frac{\partial r_{\alpha}}{\partial q_1} \cdot \langle \Phi | f_{\alpha} | \Phi \rangle = - \frac{\partial \langle \Phi | H | \Phi \rangle}{\partial q_1} . \quad (16)$$

Note that we now have physically meaningful quantities at the right of Eq. (16). The exact⁴ and the coupled H.F.⁷ wavefunctions yield Eq. (16).

In general Eqs. (14-16) provide 3 , 3 , and $3N_n-6$ equations respectively; for linear molecules 3 , 2 , and $3N_n-5$ respectively. Equations (14-16), therefore, form a set of $3N_n$ simultaneous linear equations for the $3N_n$ unknowns $\langle \phi | f_\alpha | \phi \rangle$. All the subsequent formulas have been derived assuming that Eqs. (14-16) are satisfied.

If we expand ϕ in powers of the field strength F ,

$$\phi = \phi^{(0)} + F \cdot \phi^{(1)} + \dots, \quad (17)$$

Eqs. (14-16) yield the first-order relations

$$\left. \begin{aligned} \sum_\alpha \langle f_\alpha \rangle^{(1)} &= QF, \\ \sum_\alpha r_\alpha \times \langle f_\alpha \rangle^{(1)} &= \langle D \rangle^{(0)} \times F, \\ \sum_\alpha \frac{\partial r_\alpha}{\partial q_1} \cdot \langle f_\alpha \rangle^{(1)} &= \frac{\partial \langle D \rangle^{(0)}}{\partial q_1} \cdot F, \end{aligned} \right\} \quad (18)$$

where

$$\langle D \rangle^{(0)} = \langle \phi^{(0)} | D | \phi^{(0)} \rangle, \quad (19)$$

$$\langle f_\alpha \rangle^{(1)} = z_\alpha \left[\langle \phi^{(0)} | \sum_\mu r_{\mu\alpha} r_{\mu\alpha}^{-3} | F \cdot \phi^{(1)} \rangle + \text{c.c.} + F \right]. \quad (20)$$

The set of Eqs. (18) shows that $\langle f_\alpha \rangle^{(1)}$ can be expressed in terms of the dipole moment $\langle D \rangle^{(0)}$ and its derivatives with respect to the internal coordinates $\partial \langle D \rangle^{(0)} / \partial q_1$.

EFFECTIVE CHARGE TENSOR

We define the "effective charge tensor" \underline{Q}_α^* of atom α in the molecule such that, in dyadic notation,

$$\left. \begin{aligned} \underline{Q}_\alpha^* &= \nabla_\alpha \langle \underline{D} \rangle^{(0)} , \\ \underline{\epsilon}_1 \cdot \underline{Q}_\alpha^* \cdot \underline{\epsilon}_j &= (\underline{\epsilon}_1 \cdot \nabla_\alpha) \langle \underline{D} \rangle^{(0)} \cdot \underline{\epsilon}_j , \quad 1, j=1, 2, 3 , \end{aligned} \right\} \quad (21)$$

where $\underline{\epsilon}_1, \underline{\epsilon}_2, \underline{\epsilon}_3$ are the unit base vectors of the coordinate axes. Note that dyadic \underline{Q}_α^* is not necessarily symmetric.

If we expand ϕ in Eq. (4) according to the powers of the field strength F , the first-order equation of Eq. (4) yields

$$\langle \underline{f}_\alpha \rangle^{(1)} = -\underline{Q}_\alpha^* \cdot \underline{F} , \quad (22)$$

where $\langle \underline{f}_\alpha \rangle^{(1)}$ is defined by Eq. (20). Substituting (22) into (18), we have

$$\left. \begin{aligned} \sum_\alpha \underline{Q}_\alpha^* &= q \underline{1} , \\ \sum_\alpha \underline{r}_\alpha \times (\underline{Q}_\alpha^* \cdot \underline{\epsilon}_k) &= \langle \underline{D} \rangle^{(0)} \times \underline{\epsilon}_k , \\ \sum_\alpha \frac{\partial \underline{r}_\alpha}{\partial q_1} \cdot \underline{Q}_\alpha^* &= \frac{\partial \langle \underline{D} \rangle^{(0)}}{\partial q_1} , \end{aligned} \right\} \quad (23)$$

where $\underline{1}$ is the unit dyadic, and index k runs over $k=1, 2, 3$.

A set of Eqs. (23) provides the equations necessary and sufficient to express \underline{Q}_α^* in terms of $\langle \underline{D} \rangle^{(0)}$ and $\partial \langle \underline{D} \rangle^{(0)} / \partial q_1$.

The first equation in (23) shows that the sum of the "effective charges" of atoms is equal to the total charge Q of the molecule. According to Eq. (22), the force on an atom due to the external electric field is given simply by the "effective charge" times the electric field. Furthermore, the change $\delta\langle D \rangle^{(0)}$ in the dipole moment against the infinitesimal displacements $\delta\mathbf{r}_\alpha$ of nuclear positions \mathbf{r}_α is given by

$$\delta\langle D \rangle^{(0)} = \sum_{\alpha} \delta\mathbf{r}_\alpha \cdot \mathbf{Q}_\alpha^{\bullet}, \quad (24)$$

which is easily seen from the definition of $\mathbf{Q}_\alpha^{\bullet}$. Because of these relations (22-24), the dyadic $\mathbf{Q}_\alpha^{\bullet}$ deserves to be called "effective charge tensor." It is important to note that both Eqs. (22) and (24) are first-order relations.

DIPOLE SHIELDING TENSOR

Let us first define the electron density $\rho(\mathbf{r})$ as

$$\rho(\mathbf{r}) = N_e \int d\mathbf{r}_2 \dots d\mathbf{r}_{N_e} ds_1 \dots ds_{N_e} \phi^{\bullet}(\mathbf{r}, \mathbf{r}_2, \dots, \mathbf{r}_{N_e}; s_1, \dots, s_{N_e}) \times \phi(\mathbf{r}, \mathbf{r}_2, \dots, \mathbf{r}_{N_e}; s_1, \dots, s_{N_e}), \quad (25)$$

where s_μ is the spin coordinate of the μ th electron. Expanding ϕ in powers of the field strength F , we have the corresponding expansion for the electron density:

$$\rho(\mathbf{r}) = \rho^{(0)}(\mathbf{r}) + F \cdot \rho^{(1)}(\mathbf{r}) + \dots \quad (26)$$

Note that $\rho^{(1)}(\underline{r})$ is a vector quantity.

In dyadic notation, the dipole shielding tensor β_α of nucleus α is defined as

$$\left. \begin{aligned} \beta_\alpha &= -\int d\underline{r} \frac{(\underline{r} - \underline{r}_\alpha)}{|\underline{r} - \underline{r}_\alpha|^3} \rho^{(1)}(\underline{r}) , \\ \epsilon_i \cdot \beta_\alpha \cdot \epsilon_j &= -\int d\underline{r} \frac{\epsilon_i \cdot (\underline{r} - \underline{r}_\alpha)}{|\underline{r} - \underline{r}_\alpha|^3} \rho^{(1)}(\underline{r}) \cdot \epsilon_j , \quad i, j=1,2,3 . \end{aligned} \right\} (27)$$

With this definition, the first-order induced electric field at nucleus α is given by $-\beta_\alpha \cdot \underline{F}$.

We now relate the dipole shielding tensor β_α to the "effective charge thensor" \dot{Q}_α . Simply rewriting Eq. (20) in terms of β_α , we find

$$\langle \underline{r}_\alpha \rangle^{(1)} = Z_\alpha (\underline{1} - \beta_\alpha) \cdot \underline{F} . \quad (28)$$

Equations (28) and (22) yield the desired tensor equation

$$\beta_\alpha = (Z_\alpha \underline{1} - \dot{Q}_\alpha) / Z_\alpha . \quad (29)$$

Since $\dot{Q}_\alpha - Z_\alpha \underline{1}$ can be interpreted as the "effective charge" due to the electrons of atom α , the dipole shielding is equal to an "effective electron number" of atom α divided by the nuclear charge Z_α , as in the atomic case $\beta = N_1/Z$. The derived relation (29) is satisfied by the exact wavefunction and also by the coupled H.F. wavefunction.

If one has reliable effective charge tensor \dot{Q}_α , the relation $\beta_\alpha = (Z_\alpha \underline{1} - \dot{Q}_\alpha) / Z_\alpha$ should provide useful checks on the accuracy of

$\rho^{(1)}(\underline{r})$ near the nucleus α , because of the weight function $(\underline{r}-\underline{r}_\alpha)/|\underline{r}-\underline{r}_\alpha|^3$ in β_α . In the coupled H.F. formalism, Eq. (29) with the H.F. Q_α^* provides absolute criteria to be the exact coupled H.F. $\rho^{(1)}(\underline{r})$.

In dyadic notation, the dipole polarizability tensor α are given by

$$\left. \begin{aligned} \alpha &= -\int d\underline{r} \underline{r} \rho^{(1)}(\underline{r}) , \\ \epsilon_i \cdot \alpha \cdot \epsilon_j &= -\int d\underline{r} \epsilon_i \cdot \underline{r} \rho^{(1)}(\underline{r}) \cdot \epsilon_j , \quad i, j=1, 2, 3 . \end{aligned} \right\} \quad (30)$$

Note that β_α and α are determined by the same first-order induced electron density vector $\rho^{(1)}(\underline{r})$. This is the main reason why we are concerned with the dipole shielding tensors β_α and the relation (29).

VIRIAL RELATION

The operator equations for the virial relations are

$$\sum_\mu \underline{r}_\mu \cdot \underline{f}_\mu + \sum_\alpha \underline{r}_\alpha \cdot \underline{f}_\alpha = \underline{D} \cdot \underline{E} + H_0 - T , \quad (31)$$

$$i[H, \sum_\mu \frac{1}{2}(\underline{r}_\mu \cdot \underline{p}_\mu + \underline{p}_\mu \cdot \underline{r}_\mu)] = 2T + \sum_\mu \underline{r}_\mu \cdot \underline{f}_\mu , \quad (32)$$

where $T = \sum_\mu \frac{1}{2} \underline{p}_\mu^2$. Assuming that the wavefunction Φ satisfies the virial theorem

$$\langle \Phi | i[H, \sum_\mu \frac{1}{2}(\underline{r}_\mu \cdot \underline{p}_\mu + \underline{p}_\mu \cdot \underline{r}_\mu)] | \Phi \rangle = 0 , \quad (33)$$

we obtain

$$\sum_{\alpha} \underline{r}_{\alpha} \cdot \langle \Phi | \underline{r}_{\alpha} | \Phi \rangle = \langle \Phi | \underline{D} | \Phi \rangle \cdot \underline{E} + \langle \Phi | H_0 + T | \Phi \rangle \quad (34)$$

The first-order equation of Eq. (34) is

$$\langle \Phi^{(0)} | T | \Phi^{(1)} \rangle + \langle \Phi^{(1)} | T | \Phi^{(0)} \rangle = \sum_{\alpha} \underline{r}_{\alpha} \cdot \underline{Q}_{\alpha}^* - \langle \underline{D} \rangle^{(0)} \quad (35)$$

This virial relation also can be used to check the accuracy of the first-order induced electron density.

SPECIALIZATION FOR DIATOMIC MOLECULES

Consider a diatomic molecule consisting of nucleus a, nucleus b, and N_e electrons. The internuclear distance, the internal coordinate, is denoted by R . We use the Cartesian coordinate system centered the nuclear mass center. The z axis points toward nucleus b along the symmetry axis. The unit vectors along the x , y , z axes are denoted by \underline{i} , \underline{j} , \underline{k} , respectively. Due to the axial symmetry, the electric dipole moment $\langle \underline{D} \rangle^{(0)}$ can be written as

$$\langle \underline{D} \rangle^{(0)} = \mu \underline{k} \quad (36)$$

Note again that the origin of the dipole moment μ is the nuclear mass center, and a positive μ implies a^-b^+ .

For diatomic molecules, a set of Eqs. (23) yields the effective charge tensors of atoms a and b

$$\left. \begin{aligned} Q_a^* &= \frac{Z_a}{Z_a + Z_b} Q_1 - \frac{\mu}{R} (\underline{11} + \underline{jj}) - \frac{\partial \mu}{\partial R} \underline{kk} , \\ Q_b^* &= \frac{Z_b}{Z_a + Z_b} Q_1 + \frac{\mu}{R} (\underline{11} + \underline{jj}) + \frac{\partial \mu}{\partial R} \underline{kk} ; \end{aligned} \right\} \quad (37)$$

and the equations,

$$\left. \begin{aligned} \beta_a &= (Z_a \underline{1} - Q_a^*)/Z_a , \quad \beta_b = (Z_b \underline{1} - Q_b^*)/Z_b , \\ \langle \Phi^{(0)} | T | \Phi^{(1)} \rangle + \langle \Phi^{(1)} | T | \Phi^{(0)} \rangle &= R \left(\frac{\partial \mu}{\partial R} - \frac{\mu}{R} \right) \underline{k} , \end{aligned} \right\} \quad (38)$$

can be used to check the accuracy of the first-order induced electron density.

For neutral diatomic molecules (i.e., $Q=0$), only the quantities $\partial \mu / \partial R$ and μ / R appear in the effective charge tensors Q_a^* and Q_b^* . The quantity $\partial \mu / \partial R$ was actually used as an "effective" charge of an atom in a neutral diatomic molecules by J. H. Van Vleck⁸; the quantity μ / R was interpreted as a measure of ionic character of neutral diatomic molecules by L. Pauling.⁹

ACKNOWLEDGMENTS

The author is indebted to Professor C. C. J. Roothaan for his interest and guidance in this work.

FOOTNOTES

* This work was supported by a grant from the National Science Foundation, NSF-GP-27138 and by Advanced Research Projects Agency through the U. S. Army Research Office (Durham), under Contract No. DA-31-124-ARO-D-447.

¹ It would be very instructive to compare the derivation of the relation $\beta=N/Z$ given by R. M. Sternheimer, Phys. Rev. 96, 951 (1954); M. Cohen and G. W. F. Drake, Proc. Phys. Soc. (London) 92, 23 (1967); and references in Footnote 2.

² E. S. Chang, J. Chem. Phys. 49, 2904 (1968); S. T. Epstein and R. E. Johnson, J. Chem. Phys. 51, 188 (1969).

³ See especially references in Footnote 2 and also A. Dalgarno, Advan. Phys. 11, 281 (1962).

⁴ R. P. Feynman, Phys. Rev. 56, 340 (1936).

⁵ J. O. Hirschfelder, J. Chem. Phys. 33, 1462 (1960).

⁶ S. T. Epstein and J. O. Hirschfelder, Phys. Rev. 123, 1495 (1961).

⁷ R. E. Stanton, J. Chem. Phys. 36, 1298 (1962).

⁸ J. H. Van Vleck, The Theory of Electric and Magnetic Susceptibilities (Oxford University Press, London, 1932), pp. 45-52, 200.

⁹ L. Pauling, The Nature of the Chemical Bond (Cornell University Press, Ithaca, New York, 1948), 2nd ed., p. 46.

Induced Electron Current Density of a Molecule
under a Static Magnetic Field*

HIDEO SAMBE

Laboratory of Molecular Structure and Spectra
Department of Physics, University of Chicago,
Chicago, Illinois 60637

ABSTRACT

The induced electron current density of a polyatomic molecule under a static magnetic field is studied theoretically. It is shown that a form of the hypervirial theorem is equivalent to the continuity equation for the charge and current densities, and that the continuity equation is a necessary condition for the gauge invariance of the total energy. An alternative form of the continuity equation is used to obtain relations useful in the magnetic susceptibility and nuclear magnetic shielding calculations, and also to define the paramagnetic and diamagnetic current densities uniquely. Finally a procedure for choosing the best gauge origin in the coupled Hartree-Fock method with the expansion basis functions is discussed.

Induced Electron Current Density of a Molecule
under a Static Magnetic Field*

HIDEO SAMBE

Laboratory of Molecular Structure and Spectra
Department of Physics, University of Chicago,
Chicago, Illinois 60637

ABSTRACT

The induced electron current density of a polyatomic molecule under a static magnetic field is studied theoretically. It is shown that a form of the hypervirial theorem is equivalent to the continuity equation for the charge and current densities, and that the continuity equation is a necessary condition for the gauge invariance of the total energy. An alternative form of the continuity equation is used to obtain relations useful in the magnetic susceptibility and nuclear magnetic shielding calculations, and also to define the paramagnetic and diamagnetic current densities uniquely. Finally a procedure for choosing the best gauge origin in the coupled Hartree-Fock method with the expansion basis functions is discussed.

HYPERVIRIAL THEOREM, CONTINUITY EQUATION AND GAUGE INVARIANCE

Consider a polyatomic molecule in a static magnetic field whose vector potential is given by $\mathbf{A}(\mathbf{r})$. We use the clamped nuclei Hamiltonian for the electronic motion of the molecule; the Hamiltonian H is, in atomic units,

$$H = \sum_{\mu} \left(\frac{1}{2} \pi_{\mu}^2 - \sum_a Z_a r_{\mu a}^{-1} \right) + \sum_{\mu < \nu} r_{\mu \nu}^{-1} + \sum_{a < b} Z_a Z_b r_{ab}^{-1}, \quad (1)$$

where $\pi_{\mu} = \mathbf{p}_{\mu} + \alpha \mathbf{A}(\mathbf{r}_{\mu})$. The \mathbf{r}_{μ} and \mathbf{p}_{μ} denote the position and linear momentum of the μ th electron, respectively; Z_a is the nuclear charge of the a th nucleus, and α is the fine structure constant. The electron current density of the state Φ is given by

$$\mathbf{j}(\mathbf{r}) = -\frac{1}{2} \langle \Phi | \sum_{\mu} [\delta(\mathbf{r}_{\mu} - \mathbf{r}) \pi_{\mu} + \pi_{\mu} \delta(\mathbf{r}_{\mu} - \mathbf{r})] | \Phi \rangle. \quad (2)$$

Let us assume that the wavefunction Φ satisfies a hypervirial theorem,¹

$$\langle \Phi | i[H, \sum_{\mu} f(\mathbf{r}_{\mu})] | \Phi \rangle = 0, \quad (3)$$

for any real function $f(\mathbf{r})$ which is expandable with finite powers of the Cartesian coordinates centered on the molecule. Using commutator algebra, we find the operator equation

$$i[H, \sum_{\mu} f(\mathbf{r}_{\mu})] = \frac{1}{2} \sum_{\mu} [(\nabla f)_{\mu} \cdot \pi_{\mu} + \pi_{\mu} \cdot (\nabla f)_{\mu}], \quad (4)$$

where ∇ operates only on $f(\mathbf{r})$, while π applies to all functions

which appear to the right of it. Substituting (4) into (3) and employing the current density $\underline{J}(\underline{r})$ as given by Eq. (2), we can rewrite Eq. (3) in the form

$$\int \underline{J}(\underline{r}) \cdot \nabla f(\underline{r}) d\underline{r} = 0 . \quad (5)$$

Furthermore, we have the following relation

$$\int \underline{J}(\underline{r}) \cdot \nabla f(\underline{r}) d\underline{r} = - \int f(\underline{r}) \nabla \cdot \underline{J}(\underline{r}) d\underline{r} . \quad (6)$$

This relation is derived by integrating the well-known formula of vector analysis

$$\nabla \cdot (f \underline{J}) = \underline{J} \cdot \nabla f + f \nabla \cdot \underline{J} , \quad (7)$$

applying the divergence theorem of Gauss, and using the fact that the surface integral vanishes at infinitely far distance from the molecule due to $f \underline{J} = 0$ at infinity. Since Eqs. (5) and (6) are valid for arbitrary functions $f(\underline{r})$, we obtain the continuity equation for stationary states:

$$\nabla \cdot \underline{J}(\underline{r}) = 0 . \quad (8)$$

Conversely we can prove the hypervirial relation (3) starting from the continuity equation (8). Therefore, the hypervirial relation (3), Eq. (5), and the continuity equation (8) are equivalent. Since both the exact and the coupled Hartree-Fock wavefunctions satisfy Eq. (3),¹ the current densities given by these wavefunctions satisfy Eqs. (5) and (8).

We now relate the continuity equation to the gauge invariance of the total energy. The energy change δE resulting from a change $\delta \underline{A}(\underline{r})$ in the vector potential is given by the general expression

$$\delta E = -\alpha \int \underline{J}(\underline{r}) \cdot \delta \underline{A}(\underline{r}) d\underline{r} . \quad (9)$$

If the change $\delta \underline{A}(\underline{r})$ is due to a gauge transformation (i.e., $\delta \underline{A}(\underline{r}) = \nabla f(\underline{r})$), then the corresponding change δE in energy should be zero, since physical quantities are gauge invariant. This argument leads to Eq. (5). In other words, the continuity equation (8) is a necessary condition for the gauge invariance of total energy. Incidentally Eq. (3) is the condition proposed by S. T. Epstein² to ensure the "local" gauge invariance.

APPLICATIONS

1. Useful Relations for the Magnetic Susceptibility and Nuclear Magnetic Shielding Calculations

Consider a molecule in a static uniform magnetic field $\underline{B}(=\underline{B}_0)$. Its vector potential $\underline{A}(\underline{r})$ can be given by

$$\underline{A}(\underline{r}) = \frac{1}{2} \underline{B} \times (\underline{r} - \underline{c}) , \quad (10)$$

where \underline{c} is a constant vector and sometimes called "gauge origin." The field direction \underline{c} is fixed, and the field strength B will vary by an infinitesimally small amount from zero. The wave-

function ϕ and the current density $\underline{J}(\underline{r})$ are expanded in powers of B:

$$\phi = \phi^{(0)} + B\phi^{(1)} + \dots; \quad \underline{J} = \underline{J}^{(0)} + B\underline{J}^{(1)} + \dots. \quad (11)$$

The magnetic susceptibility χ and the nuclear magnetic shielding σ_a of the a th nucleus are given by

$$\chi = \frac{1}{2}\alpha \int (\underline{r} - \underline{c}) \times \underline{J}^{(1)}(\underline{r}) d\underline{r}, \quad (12)$$

$$\sigma_a = -\alpha \int (\underline{r} - \underline{r}_a) \times \underline{J}^{(1)}(\underline{r}) / |\underline{r} - \underline{r}_a|^3 d\underline{r}. \quad (13)$$

On the other hand, substituting $(\underline{r}-\underline{c})^2$ and $|\underline{r}-\underline{r}_a|^{-1}$ for $f(\underline{r})$ in Eq. (5) and expanding the resulting equations in powers of B, one has the first-order relations:

$$\int (\underline{r} - \underline{c}) \cdot \underline{J}^{(1)}(\underline{r}) d\underline{r} = 0, \quad (14)$$

$$\int (\underline{r} - \underline{r}_a) \cdot \underline{J}^{(1)}(\underline{r}) / |\underline{r} - \underline{r}_a|^3 d\underline{r} = 0. \quad (15)$$

Because of the similarity of the weight functions, Eqs. (14,15) may provide useful information on the accuracy of the first-order current density for the magnetic susceptibility and nuclear magnetic shielding calculations (compare (12) with (14) and (13) with (15), respectively).

Another useful relation is

$$\int \underline{J}^{(1)}(\underline{r}) d\underline{r} = 0, \quad (16)$$

which can be derived by choosing $f(\underline{r})=x, y,$ and z in (5). This

relation ensures the "local" gauge invariance against a gauge transformation $\varphi \rightarrow \varphi + \delta\varphi$.

The first-order induced current density $\underline{j}^{(1)}(\underline{r})$ should satisfy the first-order continuity relation:

$$\nabla \cdot \underline{j}^{(1)}(\underline{r}) = 0. \quad (17)$$

This nontrivial relation also can be used to check the accuracy of the given first-order current density.

2. A Definition of Paramagnetic and Diamagnetic Current Densities

A number of authors have divided the first-order induced current density $\underline{j}^{(1)}(\underline{r})$ into the paramagnetic $\underline{j}_p^{(1)}(\underline{r})$ and the diamagnetic $\underline{j}_d^{(1)}(\underline{r})$ current densities and attempted to interpret those current densities separately. The explicit expressions for those current densities are given by

$$\underline{j}_d^{(1)}(\underline{r}) = -\frac{1}{2}e\hbar\langle\phi^{(0)}|\alpha\sum_{\mu}(\underline{r}_{\mu}-\underline{r})\delta(\underline{r}_{\mu}-\underline{r})|\phi^{(0)}\rangle, \quad (18)$$

$$\underline{j}_p^{(1)}(\underline{r}) = -\frac{1}{2}(\langle\phi^{(0)}|\sum_{\mu}[\delta(\underline{r}_{\mu}-\underline{r})\underline{p}_{\mu} + \underline{p}_{\mu}\delta(\underline{r}_{\mu}-\underline{r})]|\phi^{(1)}\rangle + \text{c.c.}) \quad (19)$$

These current densities depend on the choice of the "gauge origin" \underline{r} .

Although the divided current densities are not physical quantities (only the total current density $\underline{j}^{(1)}(\underline{r})$ is physically meaningful), it would be desirable if each one behave like the

physical quantity $J^{(1)}(\underline{r})$ in some aspect. With that in mind we impose a requirement on each divided current densities:

$$\int J_d^{(1)}(\underline{r}) d\underline{r} = 0, \quad (\text{or } \int J_p^{(1)}(\underline{r}) d\underline{r} = 0) . \quad (20)$$

Note that the $J^{(1)}(\underline{r})$ satisfies the same relation (16). The condition (20) yields the electronic charge center as the "gauge origin" and renders the partition unique. In other words, the electronic charge center is proposed as the "gauge origin" in order to define the paramagnetic and diamagnetic current densities.

3. A "Best" Gauge Origin for Coupled Hartree-Fock Method

Since the exact coupled Hartree-Fock procedure is gauge invariant,^{2,3} the following argument will be applied to the coupled Hartree-Fock method with the finite expansion basis functions to calculate the second-order magnetic properties of molecules.

Let us restrict ourselves to the ground state, and assume that we have the exact unperturbed Hartree-Fock solution. Fixing the unperturbed orbitals, we have a minimal principle for the second-order energy with respect to the first-order perturbed orbitals. Suppose that two sets of trial first-order perturbed orbitals give the second-order energies $E_a^{(2)}$ and $E_b^{(2)}$ at the corresponding gauge origins \underline{c}_a and \underline{c}_b , respectively.

If $E_a^{(2)} > E_b^{(2)}$, then $E_b^{(2)}$ is a better approximation to the exact Hartree-Fock second-order energy $E_{HF}^{(2)}$ than $E_a^{(2)}$, since $E_a^{(2)} \geq E_{HF}^{(2)}$, and $E_b^{(2)} \geq E_{HF}^{(2)}$. This is not necessarily true, if approximate unperturbed orbitals are used in place of the exact ones. However this may also be applied to the wavefunctions which are believed to be very near to the Hartree-Fock solution. Under these circumstances, the criterion for the best second-order energy $E^{(2)}$ is the energy minimum regardless of the gauge origin. "Best" gauge origin is, therefore, the gauge origin that gives the smallest second-order energy. If we apply this criterion to W. N. Lipscomb and co-workers' results,^{3,4} we choose the right gauge origin in the sense that the first-order induced current density obtained with the gauge origin gives better agreement with experimental data on the magnetic susceptibility, the rotational magnetic moment, the nuclear magnetic shielding, and the spin-rotational constant without exception. If we minimize the second-order energy against the gauge origin g , the induced current density $\mathbf{j}^{(1)}(\mathbf{r})$ satisfies Eq. (16) as a consequence.

ACKNOWLEDGMENTS

I am grateful to Professor C. C. J. Roothaan for his interest in this work and for several helpful suggestions.

FOOTNOTES

This work was supported in part by the Advanced Research Projects Agency through the U. S. Army Research Office (Durham), under Contract NO. DA-31-124-ARO-D-447 and by the National Science Foundation under Grant NO. NSF-GP-27138.

¹ J. O. Hirschfelder, J. Chem. Phys. 33, 1462 (1960);
S. T. Epstein and J. O. Hirschfelder, Phys. Rev. 123, 1495 (1961).

² S. T. Epstein, J. Chem. Phys. 42, 2897 (1965).

³ R. M. Stevens, R. M. Pitzer, and W. N. Lipscomb, J. Chem. Phys. 38, 550 (1963).

⁴ R. M. Stevens and W. N. Lipscomb, J. Chem. Phys. 40, 2238 (1964); 41, 184 (1964); 41, 3710 (1964); 42, 3666 (1965); 42, 4302 (1965). R. A. Hegstrom and W. N. Lipscomb, J. Chem. Phys. 45, 2378 (1966); 48, 809 (1968). A summary of the above-mentioned papers is given by W. N. Lipscomb in Advances in Magnetic Resonance 2, 137 (1966).

SELF-CONSISTENT FIELD CALCULATIONS FOR THE ELASTIC SCATTERING
OF ELECTRONS FROM HYDROGEN-LIKE SYSTEMS^{*†}

George Andrew Soukup

Department of Physics, The University of Chicago

Chicago, Illinois 60637

ABSTRACT

A general formalism is presented for the description of elastic scattering of electrons from hydrogen-like atomic systems. The total wave function for the two-electron system is put forth as a multiconfiguration expansion in terms of suitably normalized orthogonal orbitals. These radial orbitals as well as the coefficients of the expansion are determined variationally via a system of coupled integrodifferential equations. The formalism is applied to the calculation of elastic electron-hydrogen scattering in the energy range below the first resonance for the $1S$ state of the two-electron system. Accurate phase shifts are obtained with short expansions, as the newly introduced orbitals obtained by numerically integrating the integrodifferential equations account quite adequately for short range correlation.

INTRODUCTION

Partial wave phase shift calculations for the elastic scattering of electrons from atomic systems have been carried out by many workers.¹ The approach generally taken is to calculate an approximate total wave function of definite total angular momentum, parity, and spin. Such wave functions, called partial waves, are standing wave stationary state solutions to the Schrödinger equation for a continuum state of the system consisting of the target atom and the scattering electron. The methods used in these calculations are analogous to the methods developed for the calculation of bound state atomic wave functions.

In scattering processes, the incident electron can either be scattered by the target atom without loss of energy (elastic scattering) or can give up some of its energy to the target, leaving it in an excited state, while the projectile leaves the vicinity of the target with a speed in accord with the conservation of energy (inelastic scattering). Each distinct process by which the scattered electron recedes from the target, leaving it in a definite energy state, is called an "open channel". All partial wave methods represent each open channel by a term consisting of an antisymmetrized product of an $N-1$ electron target wave function and an open channel orbital used to describe the scattered electron.

These orbitals are not square integrable and have sinusoidal behaviour for large argument. The wavelength of the oscillation is determined by the speed of the receding electron in the open channel. In addition to the open channel term(s), the solution to the Schrödinger equation must contain a "bound part" which is square integrable in all electronic coordinates in the usual way. This bound part of the partial wave is particularly important in describing interactions which take place in the vicinity of the target.

The various methods used in the partial wave description differ in the way the bound part of the wavefunction is represented and also in the way the open channel orbital is calculated. In the case of two-electron calculations where we wish to describe the scattering from a hydrogen-like system, the bound part of the partial wave can be made to depend explicitly upon the interelectronic distance in the spirit of Hylleraas and Pekeris. The eigenstates of the target used in the construction of the open channel terms are in this case exactly known. In the important case of elastic scattering of electrons from hydrogen atoms in the energy range below the first resonance, calculations of this type have been carried out for S-waves by Schwartz² and for P-waves by Armstead³. In these calculations the single open channel orbital was represented by suitably chosen analytic

functions. Very accurate phase shifts were obtained by these workers in the energy range considered.

Because of the particular way in which these calculations were carried out, the wave functions used did not have sufficient flexibility to describe resonance formation adequately. Resonances occur near an excitation threshold of the target, and it is desirable to include in the total wave function, terms which continuously go over into the required open channel functions as the scattering electrons incident energy increases to permit excitation of the target.

⁴
In the "close coupling" method, bound state wave functions for the target atom in excess of those needed to construct the open channel terms are used with square integrable "closed channel orbitals" to construct the bound part of the partial wave in the same way that the open channel orbitals are used with target wave functions to construct the open channel part. Together the open and closed channel orbitals satisfy a system of linear integro-differential equations which are solved numerically. Hence in the close coupling method the bound portion of the partial wave is constructed in complete analogy to the open channel part; the individual terms are called "closed channels".

The close coupling scheme is suited for the description of inelastic scattering and resonance formation as well as

elastic scattering. The wave function goes smoothly across an excitation threshold of the target; one or more of the closed channel terms below threshold become open channel terms above threshold as the radial orbitals make a smooth transition from square integrable form to open channel type.

The set of open and closed channel terms which make up the close coupling wave function are not a complete set of N-particle functions. This is so because there are no terms included which are formed from continuum states of the N-1 particle target. Even if wave functions were in hand for every bound target state, the close coupling expansion would still be deficient.

Burke and Taylor⁵ have overcome the deficiency of the close coupling model while retaining its advantages by appending to a suitably chosen close coupling expansion, a flexible expansion of the Hylleraas type as used by Schwartz². The phase shifts which they obtain for S-wave elastic scattering of electrons from Hydrogen atoms match in accuracy those obtained by Schwartz. This modified close coupling wave function retains the suitability of ordinary close coupling for the description of resonance formation, crossing a threshold when opening up a new scattering channel, and inelastic scattering. For many-electron situations, however, the explicit dependence of the wave function on the interelectronic distances presents a formidable obstacle to calculations.

Gailitis⁶ used an approach similar to that of Burke and Taylor for the elastic scattering of electrons from atomic hydrogen. He appended to a one term close coupling expansion, a bilinear form of known one-electron functions. His expansions had to be a good deal longer than those of Burke and Taylor to achieve similar accuracy, but the method can be extended to many-electron cases with much less difficulty. Gailitis, like Burke and Taylor, obtained his open channel orbital by numerical integration. Recently, Chung and Chen⁷ have performed calculations similar to Gailitis, except that the open channel function is obtained in analytic form.

In this paper we present a method for elastic scattering in the two-electron case similar in spirit to that of Gailitis. To the requisite open channel term we add a bound part consisting of a multiconfiguration expansion using a set of orthonormal orbitals which are determined along with the open channel orbital and the coefficients of the expansion, by a coupled set of integro-differential equations. This method removes the deficiency of close coupling through the full flexibility permitted for the newly introduced orbitals. For the two-electron case, the method is intermediate between Burke and Taylor on the one hand and Gailitis and Chung-Chen on the other. For the same accuracy in the calculated phase shifts, we require a longer expansion than the former but considerably shorter than the

latter. Moreover, the generalization of this model to many-electron cases will be especially simple because of the use of orthonormal orbitals. Resonance description is also permitted, as wave functions can be constructed which pass smoothly through an excitation threshold. To test the accuracy of the method, we solve the equations numerically for the 1S state of the e^-H system in the elastic scattering region below the first resonance. Both phase shifts and orbitals are obtained.

FORMALISM

We consider the calculation of those continuum states of a two-electron system which describe a situation where one of the two electrons remains, on the average, in the vicinity of the nucleus. Thus we want to calculate the total wave function $\Psi(x_1, x_2)$ of the space and spin coordinates of two electrons orbiting about a fixed nucleus of charge Z . The function $\Psi(x_1, x_2)$, so depicted, is to be understood as a standing wave solution to the Schrödinger equation:

$$\mathcal{H}(x_1, x_2) = E \Psi(x_1, x_2) \quad (1)$$

where E is the fixed and given total energy of the system and where \mathcal{H} is the usual nonrelativistic spin-independent Hamiltonian operator; in atomic units:

$$\mathcal{H} = -\frac{1}{2} \nabla_1^2 - \frac{1}{2} \nabla_2^2 - r_1^{-1} Z - r_2^{-1} Z + r_{12}^{-1} \quad (2)$$

Here r_1 and r_2 are, respectively, the distances of the two electrons from the nucleus, while r_{12} is the interelectronic separation. The motion of the nucleus, being slight, is neglected.

The operator \mathcal{H} is independent of the spin coordinates of the electrons, and the system under consideration contains but two electrons. These facts permit the factorization of

$\Psi(x_1, x_2)$ into a function $\psi(\vec{r}_1, \vec{r}_2)$ of the space coordinates only, multiplied by a function of the spin coordinates.

These spin functions are well known and need not be further considered in this paper.

The Hamiltonian \mathcal{H} is invariant under rotation of the coordinate system used to describe the electronic positions. The total wave function ψ is therefore required to exhibit definite angular symmetry and to be a simultaneous eigenfunction of \mathcal{H} , \vec{L}^2 , and L_z . Here \vec{L} is the operator for the total orbital angular momentum and L_z is its z component.

Additional invariances of \mathcal{H} , namely under inversion of the coordinates and particle exchange, are also reflected in symmetry properties of the wave function. The exchange symmetry of the spatial function ψ , which is a consequence of the Pauli principle, is determined by the value of S, the total spin quantum number which must be 0 or 1. Likewise, the symmetry of ψ under inversion of the particle coordinates is completely determined by the total angular momentum quantum number L. This is so because the spatial wavefunction must "dissociate" properly into a product form consisting of a hydrogen-like system in its ground state, multiplied by a continuum function describing a transiting electron with angular momentum L.

These facts are summarized in the following equations:

$$\left. \begin{aligned} \mathcal{H} \psi_{\text{LMSE}}(\vec{r}_1, \vec{r}_2) &= E \psi_{\text{LMSE}}(\vec{r}_1, \vec{r}_2) , \\ \mathcal{L}^2 \psi_{\text{LMSE}}(\vec{r}_1, \vec{r}_2) &= L(L+1) \psi_{\text{LMSE}}(\vec{r}_1, \vec{r}_2) , \\ \mathcal{L}_z \psi_{\text{LMSE}}(\vec{r}_1, \vec{r}_2) &= M \psi_{\text{LMSE}}(\vec{r}_1, \vec{r}_2), \quad -L \leq M \leq L, \end{aligned} \right\} (3)$$

$$\left. \begin{aligned} \mathcal{O} \psi_{\text{LMSE}}(\vec{r}_1, \vec{r}_2) &= \psi_{\text{LMSE}}(-\vec{r}_1, -\vec{r}_2) = (-1)^L \psi_{\text{LMSE}}(\vec{r}_1, \vec{r}_2) , \\ \mathcal{Q}_{12} \psi_{\text{LMSE}}(\vec{r}_1, \vec{r}_2) &= \psi_{\text{LMSE}}(\vec{r}_2, \vec{r}_1) = (-1)^S \psi_{\text{LMSE}}(\vec{r}_1, \vec{r}_2) , \end{aligned} \right\} (4)$$

where \mathcal{O} and \mathcal{Q}_{12} are the parity and exchange operators, respectively.

In general, one might expect to find both parities for given LMSE. The first Eq. (4) expresses the inversion behavior of the "normal" spectral terms. (These are the only ones occurring in one-electron spectra.) The "abnormal" terms, for which

$$\mathcal{O} \psi_{\text{LMSE}}(\vec{r}_1, \vec{r}_2) = (-1)^{L+1} \psi_{\text{LMSE}}(\vec{r}_1, \vec{r}_2), \quad (5)$$

are in this case ruled out by the "dissociation" requirement which must be satisfied when either of the arguments of ψ_{LMSE} becomes very large.

We introduce the two-particle angular functions defined by⁸

$$Y_{LM\ell\ell'}(\Omega_1, \Omega_2) = \sum_{m=-\ell}^{\ell} \sum_{m'=-\ell'}^{\ell'} C(\ell\ell' L; mm' M) Y_{\ell m}(\Omega_1) Y_{\ell' m'}(\Omega_2), \quad (6)$$

$-L \leq M \leq L$

They satisfy the equations

$$\langle Y_{LM\ell\ell'} | Y_{LM\ell\ell'} \rangle = \delta_{LL} \delta_{MM} \delta_{\ell\ell'} \delta_{\ell'\ell'}, \quad (7)$$

$$\rho_{Y_{LM\ell\ell'}}(\Omega_1, \Omega_2) = (-1)^{\ell+\ell'} Y_{LM\ell\ell'}(\Omega_1, \Omega_2), \quad (8)$$

$$\mathcal{L}^2 Y_{LM\ell\ell'}(\Omega_1, \Omega_2) = L(L+1) Y_{LM\ell\ell'}(\Omega_1, \Omega_2), \quad (9)$$

$$\mathcal{L}_z Y_{LM\ell\ell'}(\Omega_1, \Omega_2) = M Y_{LM\ell\ell'}(\Omega_1, \Omega_2), \quad (10)$$

$$\begin{aligned} \rho_{12} Y_{LM\ell\ell'}(\Omega_1, \Omega_2) &= Y_{LM\ell\ell'}(\Omega_2, \Omega_1) \\ &= (-1)^{\ell+\ell'-L} Y_{LM\ell\ell'}(\Omega_1, \Omega_2). \end{aligned} \quad (11)$$

In Fig. 1 we illustrate the permissible pairs (l, l') used to construct the functions $Y_{LM, l, l'}(\Omega_1, \Omega_2)$ for $L = 0, 1, 2$. The functions $Y_{LM, l, l'}(\Omega_1, \Omega_2)$ are an essential ingredient in the construction of the total wave function $\psi_{LMSE}(\vec{r}_1, \vec{r}_2)$. According to the Pauli principle, ψ_{LMSE} has a definite exchange symmetry, so that whenever the pair (l, l') is permitted, (l', l) is mandatory; hence the diagrams are symmetrical about the line $l = l'$. The permitted points (l, l') lie within and on the boundaries of the region of the l, l' plane bounded by the lines

$$\left. \begin{aligned} l + l' &= L \\ l - l' &= L \\ l' - l &= L \end{aligned} \right\} \quad (12)$$

We define the sets \mathcal{V}_L^+ and \mathcal{V}_L^- of permitted points (l, l') according to the equations:

$$\left. \begin{aligned} \mathcal{V}_L^+ &= \{(l, l') \text{ such that } l + l' \text{ is even and } |l - l'| \leq L \leq l + l'\} \\ \mathcal{V}_L^- &= \{(l, l') \text{ such that } l + l' \text{ is odd and } |l - l'| < L < l + l'\} \end{aligned} \right\} \quad (13)$$

these sets are illustrated in Fig. 1.

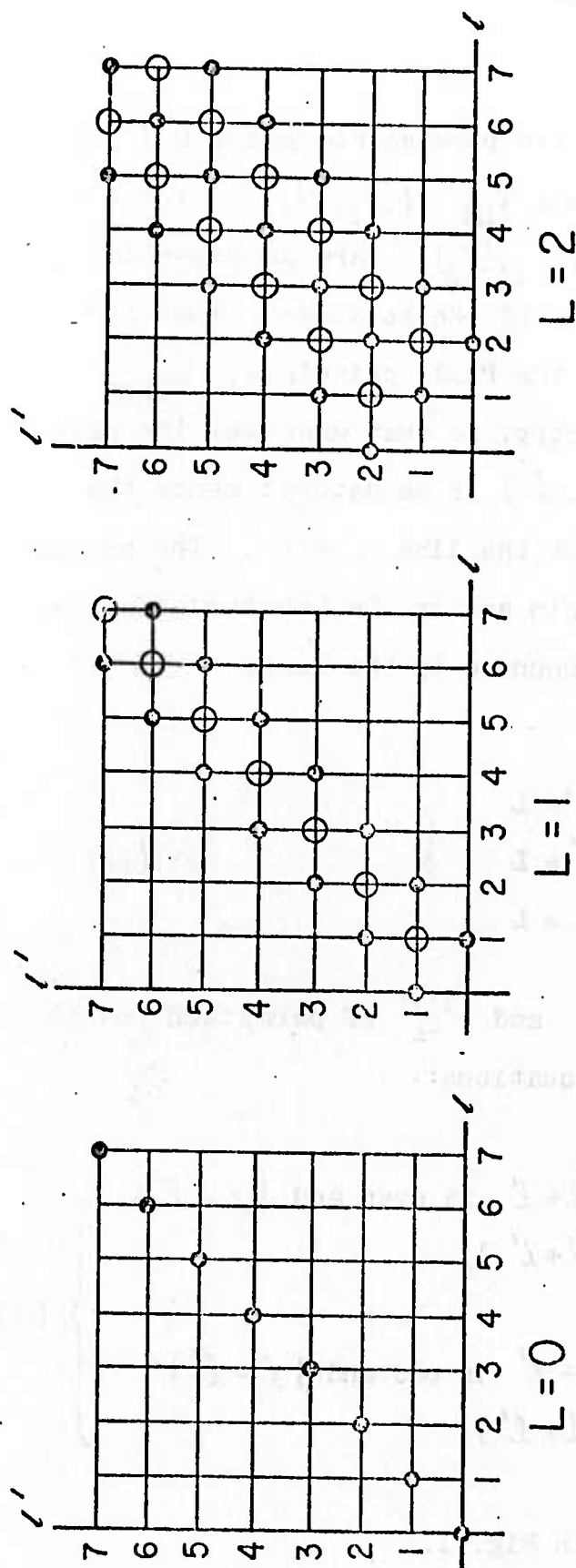


Fig. 1. Permitted pairs used in the construction of the angular two-particle functions $Y_{LM\ell\ell'}$, illustrated for $L = 0, 1, 2$.

Points indicated by • are used to represent "normal" terms for which

$$Q_{Y_{LM\ell\ell'}} = (-1)^{L_Y} Y_{LM\ell\ell'}.$$

Points indicated by ○ are used to represent "abnormal" terms for which

$$Q_{Y_{LM\ell\ell'}} = (-1)^{L+L_Y} Y_{LM\ell\ell'}.$$

For pairs $(\ell, \ell') \in \mathcal{V}_L^+$ we have, according to Eq. (11)

$$\rho_{12} Y_{\ell\ell\ell}(\Omega_1, \Omega_2) = Y_{\ell\ell\ell}(\Omega_1, \Omega_2), \quad (14)$$

while for $(\ell, \ell') \in \mathcal{V}_L^-$

$$\rho_{12} Y_{\ell\ell\ell}(\Omega_1, \Omega_2) = -Y_{\ell\ell\ell}(\Omega_1, \Omega_2). \quad (15)$$

The functions $Y_{\ell\ell\ell}(\Omega_1, \Omega_2)$ constitute a complete set of two-particle angular functions. The total wave functions may therefore be expanded according to

$$\left. \begin{aligned} \psi_{\text{LMSE}}(\vec{r}_1, \vec{r}_2) &= (r_1 r_2)^{-1} \sum_{\ell\ell'} \Phi_{\text{LSE}\ell\ell'}(r_1, r_2) Y_{\ell\ell\ell}(\Omega_1, \Omega_2), \\ \psi'_{\text{LMSE}}(\vec{r}_1, \vec{r}_2) &= (r_1 r_2)^{-1} \sum_{\ell\ell'} \Phi_{\text{LSE}\ell\ell'}(r_1, r_2) Y_{\ell\ell\ell}(\Omega_1, \Omega_2). \end{aligned} \right\} \quad (16)$$

for "normal" and "abnormal" terms, respectively. Since terms corresponding to the pairs $(0, L)$ and $(L, 0)$ must be present in the partial wave to satisfy the "dissociation" requirement, only the "normal" series is acceptable. We see also from Fig. 1 that for $L = 0$ only "normal" terms can exist; this is a well known special property of two electron spectra.

The "normal series" (16) can represent the exact wave function $\psi_{\text{LMSE}}(\vec{r}_1, \vec{r}_2)$ provided that the functions $\Phi_{\text{LSE}\ell\ell'}(r_1, r_2)$

are given by

$$\overline{\Phi}_{\text{LSE}\ell\ell}(r_1, r_2) = \int d\Omega_1 \int d\Omega_2 Y_{\ell\ell}^*(\Omega_1, \Omega_2) \psi_{\text{LMSE}}(\vec{r}_1, \vec{r}_2); \quad (17)$$

using Eq. (14), they are easily shown to satisfy

$$\overline{\Phi}_{\text{LSE}\ell\ell}(r_1, r_2) = (-1)^S \overline{\Phi}_{\text{LSE}\ell\ell}(r_2, r_1) \quad (18)$$

Suppose now that $|\vec{r}_2| = r_2$ becomes very large, indicating that one of the two electrons is far from the nucleus. In this case, ψ_{LMSE} must describe a system consisting of an electron in transit past a one electron atom or ion. Moreover, since we consider here only those values of E for which the target atom or ion must remain in its ground state, we can write

$$\psi_{\text{LMSE}}(\vec{r}_1, \vec{r}_2) \cong (r_1 r_2)^{-1} \Phi_{1s}(r_1) \Phi_{ks}(r_2) Y_{\ell\ell}(\Omega_1, \Omega_2), \quad (19)$$

$r_2 \longrightarrow \infty,$

where

$$\Phi_{1s}(r) = 2Z^{\frac{3}{2}} e^{-Zr} \quad (20)$$

is the normalized ground state orbital of the atom (or ion)

core about which the motion of the unbounded electron, described by the function $\Phi_{kL}(r)$, takes place. This continuum electron has angular momentum quantum number L . For large argument,

$$\Phi_{kL}(r) \cong A \sin(kr + k^{-1}[Z-1]\ln(r) + \eta), \quad r \longrightarrow \infty, \quad (21)$$

where A is the amplitude, usually taken to be unity, η is the phase shift, and k is the wave number, defined by

$$\left. \begin{aligned} \frac{1}{2}k^2 + \epsilon &= E, \\ \epsilon &= -\frac{1}{2}Z^2, \end{aligned} \right\} \quad (22)$$

ϵ is the energy of the atom (or ion) core in its groundstate.

The exchange symmetry of Ψ_{LMSE} requires, of course, that if $|\mathbf{r}_1| = r_1$ should become large, we must have

$$\left. \begin{aligned} \Psi_{LMSE}(\mathbf{r}_1, \mathbf{r}_2) &\cong (r_1 r_2)^{-1} \Phi_{kL}(r_1) \Phi_{1s}(r_2) Y_{LMLO}(\Omega_1, \Omega_2), \\ r_1 &\longrightarrow \infty. \end{aligned} \right\} \quad (23)$$

We shall call the function $\Phi_{kL}(r)$ an orbital, even though it is not square integrable. When it is important to distinguish it from square integrable functions, the term "continuum orbital" will be employed.

The indices LMSE, being good quantum numbers, are constant for a given calculation; hence we suppress them on both ψ_{LMSE} and \mathcal{V}_L , writing in view of Eqs. (16,18)

$$\psi(r_1, r_2) = \Phi_{\ell\ell'}(r_1, r_2) Y_{\ell\ell'}(\Omega_1, \Omega_2), \quad (24)$$

$$\Phi_{\ell\ell'}(r_1, r_2) = (-1)^S \Phi_{\ell'\ell}(r_2, r_1). \quad (25)$$

We turn now to the detailed consideration of the functions $\Phi_{\ell\ell'}(r_1, r_2)$. In practical calculations we use, instead of the infinite set \mathcal{V} , a finite subset $[\mathcal{V}] \in \mathcal{V}$, which is arbitrary, except that if (ℓ, ℓ') is included in it, so also is (ℓ', ℓ) . For this chosen subset $[\mathcal{V}]$, we propose to determine the functions $\Phi_{\ell\ell'}(r_1, r_2)$ variationally.

Since the set $[\mathcal{V}]$ contains a finite number of pairs (ℓ, ℓ') , it will be convenient to replace the pair index (ℓ, ℓ') by a running index v which is in one-one correspondence with the pairs $(\ell, \ell') \in [\mathcal{V}]$. This correspondence can be set up in many ways, and a convenient one is illustrated in Fig. 2 for $L = 4$. We adopt the convention that $v = 1$ corresponds to the "elastic scattering term" $(0, L)$. Moreover, if v corresponds to the pair (ℓ, ℓ') , we shall understand \bar{v} to mean that value of the running index which corresponds to the exchanged pair (ℓ', ℓ) . We shall write $v \rightarrow (\ell, \ell')$

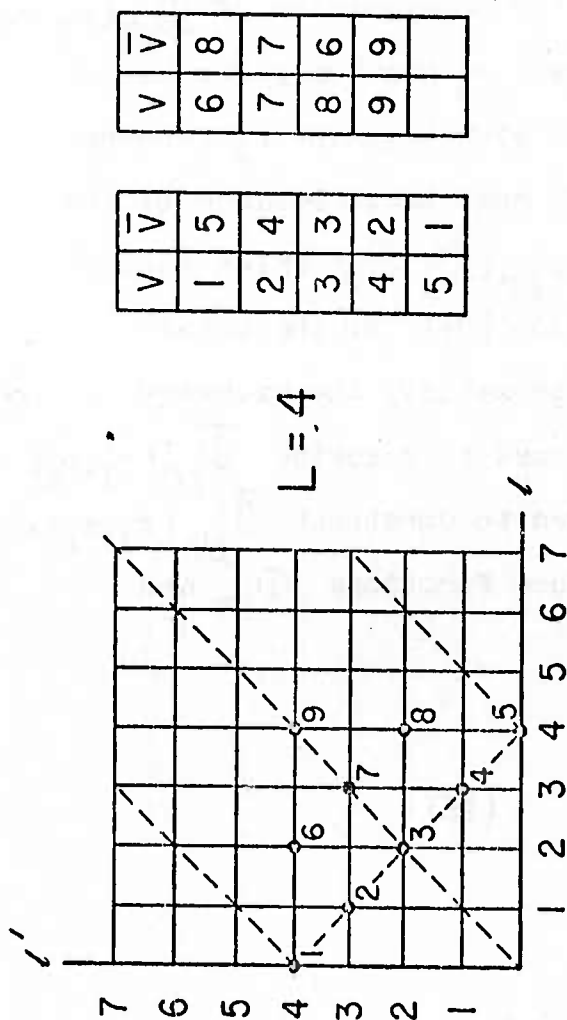


Fig. 2. Assignment of values for the running index v replacing the pair index $(l, l') \in [\mathcal{U}]$ for $L = 4$. By convention, $v = 1$ corresponds to the pair $(0, 1)$. The relationship between v and \bar{v} is also illustrated. Note that the points corresponding to the indices v and \bar{v} are symmetrically placed about the line $l = l'$. In this case the elements of the set V are the integers $1 - 9$.

to indicate the correspondence between v and the pair (ℓ, ℓ') . We also introduce V , the set of $v \rightarrow (\ell, \ell')$ for $(\ell, \ell') \in [\mathcal{V}]$.

We want to approximate $\Phi_{\ell\ell'}(r_1, r_2)$ by finite bilinear expansions of functions of the single arguments r_1 and r_2 . If a pair of such functions occurs in the construction of $\Phi_{\ell\ell'}(r_1, r_2)$ then the member bearing the coordinate r_1 must vary for small argument as $r_1^{\ell+1}$ while the function with argument r_2 behaves like $r_2^{\ell'+1}$ as r_2 approaches 0. This must be so because of the angular dependence of the function $Y_{\ell\ell'}(\Omega_1, \Omega_2)$ which accompanies $\Phi_{\ell\ell'}(r_1, r_2)$ in the expression (24) for the total wave function. Moreover, in order to satisfy the exchange condition, Eq. (25), the functions used to describe $\Phi_{\ell\ell'}(r_1, r_2)$ must be used with arguments exchanged to construct $\Phi_{\ell'\ell}(r_1, r_2)$. With these facts in mind, we introduce functions Φ_{vm} and $\Phi_{\bar{v}m}$, $m = 1, 2, \dots, N_v$,

$$\left. \begin{aligned} \Phi_{vm}(r) &\cong r^{\ell+1}, \\ \Phi_{\bar{v}m}(r) &\cong r^{\ell'+1}, \end{aligned} \right\} r \rightarrow 0, \quad (26)$$

where $v \rightarrow (\ell, \ell')$ and $\bar{v} \rightarrow (\ell', \ell)$.

As the notation indicates, the functions $\Phi_{vm}(r)$ depend upon both indices ℓ and ℓ' . We have introduced one set of functions for each point (ℓ, ℓ') of the set $[\mathcal{V}]$. To

construct the functions $\overline{\Phi}_{\ell\ell'}(r_1, r_2)$ and $\overline{\Phi}_{\ell\ell'}(r_1, r_2)$, both sets of functions Φ_{vm} and $\Phi_{\bar{v}m}$ are needed. In Fig. 2 for example, to construct $\overline{\Phi}_{0,4}(r_1, r_2)$ we use the products formed from $\Phi_{1m}(r_1)$ and $\Phi_{5n}(r_2)$, $m = 1, 2, \dots, N_1$; $n = 1, 2, \dots, N_5$; $N_1 = N_5$. All products are used which are not ruled out by the asymptotic behavior of the total wave function. Note that in this example, $v = 1 \rightarrow (0, 4)$ and $\bar{v} = 5 \rightarrow (4, 0)$. The same products with exchanged arguments are used to construct $\overline{\Phi}_{4,0}(r_1, r_2)$ where $v = 5 \rightarrow (4, 0)$ and $\bar{v} = 1 \rightarrow (0, 4)$. Note that if $v \rightarrow (\ell, \ell')$ and $w \rightarrow (\ell, \ell'')$, $\ell' \neq \ell''$, the two sets of functions $\Phi_{vm}(r)$ and $\Phi_{wn}(r)$ behave for small r like $r^{\ell+1}$ according to Eq. (26), yet these functions are in general completely different. This is a departure from the usual orbital model; it is adopted because of the greater flexibility afforded to the wave function and the ease of implementation in the two-electron case.

The approximations to the functions $\overline{\Phi}_{\ell\ell'}(r_1, r_2)$ are now given by

$$\overline{\Phi}_v(r_1, r_2) = (r_1 r_2)^{-1} \sum_{m=1}^{N_v} \sum_{n=1}^{N_{\bar{v}}} \Phi_{vm}(r_1) \Gamma_{vmn} \Phi_{\bar{v}n}(r_2), \quad (27)$$

where $v \rightarrow (\ell, \ell')$, $\bar{v} \rightarrow (\ell', \ell)$ and

$$\Gamma_{vmn} = (-1)^S \Gamma_{\bar{v}nm}. \quad (28)$$

Eq. (28) guarantees the exchange condition (18). Note that evidently,

$$N_v = N_{\bar{v}}. \quad (29)$$

In case $\ell' = \ell$ so that $\bar{v} = v \rightarrow (\ell, \ell)$, Eqs. (26) reduce to a single set and Eqs. (27,28) still apply;

$\bar{\Phi}_v(r_1, r_2)$ becomes a quadratic form in the functions $\Phi_{vm}(r)$, $m = 1, 2, \dots, N_v$.

According to Eqs. (19,20,21,23) which indicate the asymptotic behavior of ψ , two of the orbitals introduced have a special significance. The orbital $\Phi_{1,1}(r)$ is the hydrogenic ground state function $\Phi_{1s}(r)$, and $\Phi_{\bar{1},N_{\bar{1}}}$ is the continuum orbital $\Phi_{kL}(r)$:

$$\left. \begin{aligned} \Phi_{1,1}(r) &= \Phi_{1s}(r) = 2Z^{\frac{3}{2}} e^{-Zr}, \\ \Phi_{\bar{1},N_{\bar{1}}}(r) &= \Phi_{kL}(r) \cong \sin(kr + [Z-1]k^{-1} \ln r + \eta), \end{aligned} \right\} \quad (30)$$

$r \rightarrow \infty.$

We have adopted the convention that the fixed hydrogenic function $\Phi_{1s}(r)$ is numbered first among the functions $\Phi_{1n}(r)$, $n = 1, 2, \dots, N_1$ and the continuum orbital $\Phi_{kL}(r)$ is numbered last among the functions $\Phi_{\bar{1}m}$, $m = 1, 2, \dots, N_{\bar{1}}$. All of the remaining orbitals $\Phi_{vm}(r)$, $m = 1, 2, \dots, N_v$, $v \in V$, are square integrable functions. In scattering

processes, $\Phi_{1s}(r)$ describes the target, $\Phi_{kL}(r)$ describes the scattered electron at large distances from the target, and the remaining orbitals describe interactions taking place in the vicinity of the target; these include polarization, correlated motion, and resonance formation.

In the expansion (27) for $\bar{\Phi}_v(r_1, r_2)$, all possible products $\Phi_{vm}(r_1) \Phi_{\bar{v}n}(r_2)$ are used except those excluded by the asymptotic form given by Eqs. (19,23). This means that the continuum orbital $\Phi_{I, N_I}(r)$ can only be paired with the hydrogenic groundstate orbital $\Phi_{1,1}(r)$. This implies that

$$\Gamma_{I, N_I, n} = (-1)^{S_A} \delta_{n1} = (-1)^S \Gamma_{1, n, N_I} \quad (31)$$

All possible products between square integrable orbitals are permitted. Because all such products occur in (27), some auxiliary conditions must be imposed upon the $\Phi_{vm}(r)$ to guarantee an unambiguous expansion for $\bar{\Phi}_v(r_1, r_2)$: unique coefficients Γ_{vmn} can be specified only if some orthogonality and normalization requirements are placed upon the

$\Phi_{vm}(r)$. Even with normalization and orthogonality conditions imposed, the square integrable $\Phi_{vm}(r)$ can only be determined up to a unitary transformation, and further specification is necessary. For these reasons we require that, for fixed v , the square integrable functions (including $\Phi_{1s}(r)$ if $v = 1$)

are required to satisfy the equations

$$\left. \begin{aligned} \langle \Phi_{vm} | \mathcal{T}_{vn} \rangle &= \delta_{mn} , \\ \langle \Phi_{vm} | h_v | \Phi_{vn} \rangle &= \omega_{vm} \delta_{mn} , \end{aligned} \right\} \quad (32)$$

where

$$\left. \begin{aligned} 2h_v &= \frac{d^2}{dr^2} - \ell(\ell+1)r^{-2} + 2Zr^{-1} , \\ v &\rightarrow (\ell, \ell') . \end{aligned} \right\} \quad (33)$$

The particular choice of these conditions is dictated by the physical consideration that, as the incident electron's kinetic energy approaches the target excitation threshold, some of the $\Phi_{vm}(r)$ must become hydrogenic eigenfunctions. The conditions (32) allow this to happen in a natural way.

We wish to emphasize that the relations (32) required of the square integrable orbitals $\Phi_{vm}(r)$ apply only between functions bearing the same index v . Refer again to Fig. 2 where $v = 2$ corresponds to the pair $(\ell, \ell') = (1, 3)$, while $v = 7$ corresponds to the pair $(\ell, \ell') = (3, 3)$. The point $(\ell, \ell') = (3, 1)$ corresponds to $v = \bar{2} = 4$. The two sets of functions

$$\Phi_{4n}(r), \quad n = 1, 2, \dots, N_4,$$

$$\Phi_{7m}(r), \quad m = 1, 2, \dots, N_7,$$

have the same behavior for small argument; all of these functions start out near $r = 0$ proportional to r^4 . The

$\Phi_{4n}(r)$ form an orthonormal set which diagonalizes the operator

$$h_4 = \frac{1}{2} \frac{d^2}{dr^2} - 6r^{-2} + Zr^{-1},$$

in the Hilbert space available to them. According to Eqs.(32) with $v = 7$, the functions $\Phi_{7m}(r)$ are also an orthonormal set and diagonalize, in their Hilbert space, the same operator, yet they have no orthogonality relations with the $\Phi_{4n}(r)$.

The continuum orbital $\Phi_{KL}(r) = \Phi_{\bar{L}, N_{\bar{L}}}(r)$ is required to be orthogonal to the rest of the functions $\Phi_{\bar{L}n}(r)$:

$$\langle \Phi_{\bar{L}N_{\bar{L}}} | \Phi_{\bar{L}n} \rangle = 0. \quad (34)$$

In Fig. 2, $v = 1 \rightarrow (0,4)$, so that $\bar{v} = 5 \rightarrow (4,0)$. If there are $N_5 = N_1$ functions associated with the point $(4,0) \rightarrow 5$, then the continuum orbital is $\Phi_{5,N}(r)$ and is orthogonal to each function $\Phi_{5m}(r)$, $m = 1, 2, \dots, N_5 - 1$. Note that all of the other points in the diagram correspond to sets of square integrable functions only.

According to equations (24,27), the total wave function is given by

$$\psi(\vec{r}_1, \vec{r}_2) = (r_1 r_2)^{-1} \sum_{v \in V} \sum_{m=1}^{N_v} \sum_{n=1}^{N_v} \Phi_{vm}(r_1) \Gamma_{vmn} \Phi_{\bar{v}n}(r_2) Y_v(\Omega_1, \Omega_2). \quad (35)$$

To determine the functions $\Phi_{vm}(r)$ and the coefficients Γ_{vmn} we form the functional

$$L(\psi) = \int d^3\vec{r}_1 \int d^3\vec{r}_2 \psi^* [\mathcal{H} - E] \psi, \quad (36)$$

and calculate the first variation of L:

$$\begin{aligned} \delta L(\psi) = & 2 \int d^3\vec{r}_1 \int d^3\vec{r}_2 \delta\psi^* [\mathcal{H} - E] \psi \\ & - \int d^3\vec{r}_1 \oint_{\infty} d\sigma \left[\psi^* \frac{\partial \delta\psi}{\partial n_2} - \delta\psi \frac{\partial \psi^*}{\partial n_2} \right]. \end{aligned} \quad (37)$$

From this expression, we see that the function $\psi(\vec{r}_1, \vec{r}_2)$ for which $\delta L(\psi)$ vanishes for all variations $\delta\psi(\vec{r}_1, \vec{r}_2)$ such that the "surface term"

$$\int d^3\vec{r}_1 \oint_{\infty} d\sigma \left[\psi^* \frac{\partial \delta\psi}{\partial n_2} - \delta\psi \frac{\partial \psi^*}{\partial n_2} \right], \quad (38)$$

also vanishes, must satisfy the Schrödinger equation

$$[\mathcal{H} - E]\psi = 0. \quad (39)$$

We substitute $\psi(\vec{r}_1, \vec{r}_2)$ as given by Eq. (35) into Eq. (36) and carry out the variation (37), permitting only

variations in the radial functions $\Phi_{vm}(r)$ and the coefficients Γ_{vmn} . These variations are restricted so that the "surface term" (38) is always zero. We introduce for convenience, the functions $u_{vm}(r)$ defined by

$$u_{vm}(r) = \sum_{n=1}^{N_v} \Gamma_{vmn} \Phi_{vn}(r). \quad (40)$$

Note that according to Eq. (26),

$$u_{vm}(r) = r^{\ell'+1}, \quad r \rightarrow 0. \quad (41)$$

According to Eqs. (35,40), we may write

$$\psi(\vec{r}_1, \vec{r}_2) = (r_1 r_2)^{-1} \sum_{v \in V} \sum_{m=1}^{N_v} \Phi_{vm}(r_1) u_{vm}(r_2) Y_v(\Omega_1, \Omega_2). \quad (42)$$

The variational condition that $\delta L(\psi) = 0$ for all permitted variations $\delta\psi$ leads to the system of equations

$$[h_v - X(\Phi_{vm}, \Phi_{vm}) + \langle \Phi_{vm} | h_v | \Phi_{vm} \rangle + E] u_{vm} - \left\{ \sum_{w \in V} \sum_{n=1}^{N_w} X(\Phi_{vm}, \Phi_{wn}) u_{wn} + \delta_{vI} \langle \Phi_{mI} | h_I | \Phi_{IN_I} \rangle u_{IN_I} \right\} = 0, \quad (43)$$

for the functions $u_{vm}(r)$. Here $v \rightarrow (\ell, \ell')$, $v \in V$, $m = 1, 2, \dots, N_v$, but $(v, m) \neq (\bar{1}, N_{\bar{1}})$. The one-electron operator h_v is given by Eq. (33). The prime in Eq. (40) indicates that the term

$$X(\phi_{vm}, \phi_{vm})u_{vm},$$

is not included in the summation.

The auxiliary functions $X(\phi_{vm}, \phi_{wn})$ are defined by the equations

$$\left. \begin{aligned} X(\phi_{vm}, \phi_{wn}) &= \sum_v c_{vw}^v X^v(\phi_{vm}, \phi_{wn}), \\ X^v(\phi_{vm}, \phi_{wn}) &= (2v+1)^{-1} \left[r^v \int \phi_{vm}(s) s^{-(v+1)} \phi_{wn}(s) ds \right. \\ &\quad \left. + r^{-v-1} \int \phi_{vm}(s) s^v \phi_{wn}(s) ds \right], \\ c_{vw}^v &= (-1)^{L+v} (2\ell+1)(2\ell'+1)(2p+1)(2p'+1) [C(\ell p v, 000) \\ &\quad W(\ell \ell', pp', Lv) C(\ell' p' v, 000)] \end{aligned} \right\} (44)$$

where $v \rightarrow (\ell, \ell')$, $w \rightarrow (p, p')$ and $C(\ell p v, 000)$ and $W(\ell \ell', pp', Lv)$ are the well known Clebsh Gordan and Racah coefficients respectively.⁸

The index v in Eqs. (44) has the range specified by the conditions

$$\left. \begin{aligned} |\ell - p| &\leq v \leq \ell + p, \\ |\ell' - p'| &\leq v \leq \ell' + p', \\ (-1)^{\ell+p} &= (-1)^v = (-1)^{\ell'+p'}. \end{aligned} \right\} \quad (45)$$

There is one differential equation for each independent radial function. We see from Eq. (43) that there is no equation for $u_{\bar{I}, N_{\bar{I}}}(r)$. This is so because its functional form is prescribed by the dissociation requirement and cannot be varied. We obtain it from Eqs. (31,40):

$$u_{\bar{I}, N_{\bar{I}}}(r) = (-1)^{S_A} \phi_{1s}(r). \quad (46)$$

We wish to call attention to the terms in Eq. (43) of the form

$$\delta_{v\bar{I}} \langle \phi_{m\bar{I}} | h_{\bar{I}} | \phi_{1N_{\bar{I}}} \rangle u_{1N_{\bar{I}}}.$$

These terms occur in the system (43) because of the orthogonality condition (34) was imposed upon the continuum orbital $\phi_{kL}(r)$. These terms would not be present in Eq. (43) if, instead of Eq. (34), we required

$$\langle \Phi_{\bar{I}n} | h_{\bar{I}} + \frac{1}{2}k^2 | \Phi_{kL} \rangle = 0 ; \quad (47)$$

the resultant lack of orthogonality between $\Phi_{kl}(r)$ and the square integrable orbitals $\Phi_{\bar{I},n}(r)$, $n = 1, 2, \dots, N_1 - 1$, makes the determination of the functions $u_{vm}(r)$ more difficult in practice as the iterative scheme used to determine these functions tends to become unstable unless strict orthogonality is maintained between $\Phi_{kL}(r)$ and its square integrable companions. For this reason the condition (34) was adopted instead of (47).

The system (43) is solved iteratively: approximate orbitals $u_{vm}(r)$ and $\Phi_{vm}(r)$ must be in hand. The quantity in $\left\{ \right\}$ is computed using these approximate functions and then used as the "source term" in Eq. (43) which is treated as a second order ordinary differential equation for the function $u_{vm}(r)$. The "coulomb potential" $X(\Phi_{vm}, \Phi_{vm})$ is also computed using the approximate $\Phi_{vm}(r)$. This differential equation is numerically integrated to furnish an improved function $u_{vm}(r)$. For the square integrable functions, unique solutions, regular at the origin, are obtained. A unique improved continuum function $u_{1,1}(r)$ is also obtained if the condition of unit amplitude for large r is imposed. Once the improved

functions $u_{vm}(r)$ are obtained; a revised set of $\Phi_{vm}(r)$ are furnished by constructing appropriate linear combinations of the $u_{vm}(r)$ which satisfy the conditions (32,34). The expansion coefficients Γ_{vmn} are obtained by projection:

$$\Gamma_{vmn} = \langle u_{vm} | \Phi_{vn} \rangle, \quad m = 1, 2, \dots, N_v, \quad n = 1, 2, \dots, N_v. \quad (48)$$

The coefficients Γ_{1,n,N_I} and $\Gamma_{I,N_I,n}$ are, of course, fixed with values given by Eq. (31).

Once the Γ_{vmn} are obtained, they are forcibly symmetrized to guarantee that the exchange condition (28) is satisfied as the iteration proceeds. From the symmetrized Γ_{vmn} and the revised $\Phi_{vm}(r)$, a revised set of $u_{vm}(r)$ are constructed and the "source term" in (43) and the "coulomb potential" are recomputed. The process is repeated until convergence of the $\Phi_{vm}(r)$ and Γ_{vmn} is achieved.

The iterative process can be started by choosing for the square integrable $\Phi_{vm}(r)$ a suitable linear combination of Slater functions satisfying Eqs. (32), while for the continuum orbital $\Phi_{kL}(r)$ we start with

$$\Phi_{kL}^0(r) = u_{kL}^0(r) - \sum_{n=1} \langle u_{kL}^0 | \Phi_{In} \rangle \Phi_{In}(r), \quad (49)$$

where $u_{kL}^0(r)$ satisfies the "source free" equation:

$$\left[\frac{d^2}{dr^2} + 2Zr^{-1} - 2X(\Phi_{1s}, \Phi_{1s}) + k^2 \right] u_{kL}^0 = 0. \quad (50)$$

and the solution of Eq. (50), regular at the origin with unit amplitude for large r is chosen. The initial set of Γ_{vmn} can be taken as follows

$$\left. \begin{aligned} \Gamma_{1,1,N_I} &= 1 = (-1)^S \Gamma_{\bar{1},N_I,1} \\ \Gamma_{vmn} &= 0, \text{ all others.} \end{aligned} \right\} \quad (51)$$

Of course, other, more accurate starting sets may be used if they are available. All that is necessary is that the approximate $\Phi_{vm}(r)$ satisfy the conditions (32,34) and the Γ_{vmn} satisfy the exchange conditions (28).

RESULTS

Calculations were carried out for the $1s$ state of the system e^-H in the energy range $\epsilon_{1s} = E = \epsilon_{2s}$, using wave functions of increasing complexity. In Hartrees,

$$E = \epsilon_{1s} + k^2, \quad \epsilon_{1s} = -.500, \quad \epsilon_{2s} = -.125.$$

The wave functions used are labeled ψ_n , $n = 1, 2, \dots, 6$.

The structure of these wavefunctions is exhibited in Table I.

For example, the approximate wave function ψ_3 has the form

$$\begin{aligned} \psi_3(\vec{r}_1, \vec{r}_2) = (r_1 r_2)^{-1} & \left[\mathbb{O}_{1s}(r_1) u_{1s}(r_2) + \mathbb{O}_{2s}(r_1) u_{2s}(r_2) \right. \\ & \left. + \mathbb{O}_{ks}(r_1) u_{ks}(r_2) \right] Y_1(\Omega_1, \Omega_2) + \mathbb{O}_{2p}(r_1) u_{2p}(r_2) Y_2(\Omega_1, \Omega_2). \end{aligned} \quad (52)$$

Here we have departed from the formal notation of the text and adopted instead a "spectroscopic" notation. Table I gives the "spectroscopic" label corresponding to the pair (v, m) for each approximate wave function used. Thus for ψ_3 ,

$$\mathbb{O}_{1,1} = \mathbb{O}_{1s},$$

$$\mathbb{O}_{1,2} = \mathbb{O}_{2s},$$

$$\mathbb{O}_{1,3} = \mathbb{O}_{ks},$$

and

$$\Phi_{2,1} = \Phi_{2p}.$$

In all of these wavefunctions, Φ_{1s} is the hydrogen ground-state orbital and Φ_{ks} is the scattering orbital. The spectroscopic label on a u-function simply indicates which Φ -function is paired with it in the approximate wave function given by Eq. (42).

Because the $u_{vm}(r)$ are linear combinations of the $\mathcal{U}_{vm}(r)$ according to Eq. (40), the expression (42) for the total wave function is not manifestly symmetric in \vec{r}_1 and \vec{r}_2 . These functions nevertheless possess complete exchange symmetry according to Eqs. (28,35):

$$\psi_n(\vec{r}_1, \vec{r}_2) = \psi_n(\vec{r}_2, \vec{r}_1), \quad n = 1, 2, \dots, 6. \quad (53)$$

Only $\Phi_{1s}(r)$ among the functions $\Phi_{vm}(r)$ used in the construction of the wavefunctions has a prescribed form:

$$\Phi_{1s}(r) = 2re^{-r}. \quad (54)$$

Exchange symmetry of the functions $\psi_n(\vec{r}_1, \vec{r}_2)$ then

forces the function $u_{ks}(r)$ to have the same form:

$$u_{ks}(r) = \mathcal{O}_{1s}(r) . \quad (55)$$

The function $\mathcal{O}_{ks}(r)$ and therefore $u_{1s}(r)$ have the asymptotic behavior:

$$\left. \begin{aligned} \mathcal{O}_{ks}(r) &\simeq \sin(kr+\eta), \\ u_{1s}(r) &\simeq \sin(kr+\eta), \end{aligned} \right\} r \rightarrow \infty. \quad (56)$$

where we have imposed unit amplitude normalization on the total wave functions. The remaining functions are square integrable.

The function ψ_1 is identical to the "one state" close coupling function ψ_{1cc} and reproduces the phase shifts determined by other workers as is illustrated in Table III. If we compare ψ_1 with the corresponding close coupling function ψ_{1cc} :

$$\left. \begin{aligned} r_1 r_2 \psi_1(\vec{r}_1, \vec{r}_2) &= [\mathcal{O}_{1s}(r_1) u_{1s}(r_2) + \mathcal{O}_{ks}(r_1) u_{ks}(r_2)] Y_1(\Omega_1, \Omega_2), \\ r_1 r_2 \psi_{1cc}(\vec{r}_1, \vec{r}_2) &= [\mathcal{O}_{1s}(r_1) F_{1s}(r_2) + F_{1s}(r_1) \mathcal{O}_{1s}(r_2)] Y_1(\Omega_1, \Omega_2), \end{aligned} \right\} \quad (57)$$

we see that $\psi_1(\vec{r}_1, \vec{r}_2)$ is not manifestly symmetric in

r_1 and r_2 . This is a characteristic of all of the wave functions ψ_n when written in the form (42). The two functions ψ_1 and ψ_{1cc} are in fact identical and the connection between them is exhibited in the relations

$$\left. \begin{aligned} \Phi_{ks}(r) &= F_{1s}(r) - \langle F_{1s} | \Phi_{1s} \rangle \Phi_{1s}(r) , \\ u_{1s}(r) &= F_{1s}(r) + \langle F_{1s} | \Phi_{1s} \rangle \Phi_{1s}(r) . \end{aligned} \right\} \quad (58)$$

The continuum function $F_{1s}(r)$ of the close coupling model is determined from the differential equation

$$\begin{aligned} [h_1 - X(\Phi_{1s}, \Phi_{1s}) + \frac{1}{2}k^2]F_{1s} - X(\Phi_{1s}, F_{1s})\Phi_{1s} \\ + \langle \Phi_{1s} | h_1 | F_{1s} \rangle \Phi_{1s} = 0 , \end{aligned} \quad (59)$$

where

$$h_1 = \frac{1}{2} \frac{d^2}{dr^2} + r^{-1} , \quad (60)$$

while the equation

$$[h_1 - X(\Phi_{1s}, \Phi_{1s}) + \frac{1}{2}k^2]u_{1s} - X(\Phi_{1s}, \Phi_{ks})u_{ks} = 0, \quad (61)$$

supplemented by the linkage relations:

$$\left. \begin{aligned} \Phi_{ks}(r) &= u_{1s}(r) - \langle u_{1s} | \Phi_{1s} \rangle \Phi_{1s}(r) , \\ u_{ks}(r) &= \Phi_{1s}(r) , \end{aligned} \right\} \quad (62)$$

determine the functions $u_{1s}(r)$ and $\Phi_{ks}(r)$. Note that no term proportional to $\Phi_{1s}(r)$ appears in Eq. (61). This is so because $\Phi_{1s}(r)$ is an eigenfunction of h_1 and the two conditions (34) and (47) are, in this case, identical so that the term:

$$\langle \Phi_{1s} | h_1 | \Phi_{ks} \rangle u_{ks}$$

does not appear in Eq. (61).

We next compare ψ_2 with the corresponding "two state" close coupling function ψ_{2cc} . We have

$$\psi_2(\vec{r}_1, \vec{r}_2) = (r_1 r_2)^{-1} [\Phi_{1s}(r_1) u_{1s}(r_2) + \Phi_{2s}(r_1) u_{2s}(r_2) + \Phi_{ks}(r_1) u_{ks}(r_2)] Y_1(\Omega_1, \Omega_2),$$

$$\psi_{2cc}(\vec{r}_1, \vec{r}_2) = (r_1 r_2)^{-1} [\Phi_{1s}(r_1) F_{1s}(r_2) + \Phi_{2s}(r_1) F_{2s}(r_2) + F_{1s}(r_1) \Phi_{1s}(r_2) + F_{2s}(r_1) \Phi_{2s}(r_2)] Y_1(\Omega_1, \Omega_2), \quad (63)$$

where

$$\Phi_{1s}(r) = \Phi_{1s}(r) = 2re^{-r}, \quad (64)$$

$$\Phi_{2s}(r) = (2\sqrt{2})^{-1} (2r - r^2) e^{-.5r},$$

are hydrogenic radial eigenfunctions.

In the close coupling function ψ_{2cc} , both $F_{1s}(r)$ and $F_{2s}(r)$ are determined by solving coupled differential equations. Likewise, in ψ_2 , $u_{1s}(r)$ and $u_{2s}(r)$ are

similarly determined, the set of equations being

$$\left. \begin{aligned} [h_1 - X(\Phi_{1s}, \Phi_{1s}) + \frac{1}{2}k^2]u_{1s} - X(\Phi_{1s}, \Phi_{2s})u_{2s} \\ - X(\Phi_{1s}, \Phi_{ks})u_{ks} = 0, \\ [h_1 - X(\Phi_{2s}, \Phi_{2s}) + \langle \Phi_{2s} | h_1 | \Phi_{2s} \rangle + E]u_{2s} - X(\Phi_{2s}, \Phi_{1s})u_{1s} \\ - X(\Phi_{2s}, \Phi_{ks})u_{ks} + \langle \Phi_{2s} | h_1 | \Phi_{ks} \rangle u_{ks} = 0, \end{aligned} \right\} (65)$$

supplemented by the linkage relations:

$$\left. \begin{aligned} \Phi_{2s}(r) &= [u_{2s}(r) - \langle u_{2s} | \Phi_{1s} \rangle \Phi_{1s}(r)] N_{2s}^{-1} \\ \Phi_{ks}(r) &= u_{1s}(r) - \langle u_{1s} | \Phi_{1s} \rangle \Phi_{1s}(r) \\ &\quad - \langle u_{1s} | \Phi_{2s} \rangle \Phi_{2s}(r). \end{aligned} \right\} (66)$$

where

$$N_{2s} = (\langle u_{2s} | u_{2s} \rangle - \langle u_{2s} | \Phi_{1s} \rangle)^{\frac{1}{2}} \quad (67)$$

The function ψ_2 , involving only three pairs of functions is somewhat more compact than ψ_{2cc} . The important distinction however, between the two functions is that in ψ_2 the orbital $\Phi_{2s}(r)$ is not arbitrarily prescribed. Table III compares the phase shifts η obtained from both ψ_2 and ψ_{2cc} over a range of energies. As a benchmark for comparison we take the accurate Schwartz values.

A small but significant improvement in η_2 over η_{2cc} is noted throughout the energy range considered, namely $.1 \leq k \leq .8$.

Fig. 3 illustrates $\Phi_{2s}(r)$ for several values of k and also compares these functions with the hydrogenic orbital $\Phi_{2s}(r)$. A dramatic departure from $\Phi_{2s}(r)$ is exhibited for all k values examined. The more compressed appearance of $\Phi_{2s}(r)$ suggests that it is describing the close range interactions more adequately than is $\Phi_{2s}(r)$. The illustrated dependence of $\Phi_{2s}(r)$ on wave number, shows that the compression increases toward low k values. Even for $k = .8$ which is fairly close to the $1s \rightarrow 2s$ excitation threshold, the appearance of $\Phi_{2s}(r)$ is still quite compressed when compared with $\Phi_{2s}(r)$. These results are in agreement with the "orbital energies"

$$\lambda_{2s} = - \langle \Phi_{2s} | h_1 | \Phi_{2s} \rangle, \quad (68)$$

which are given in Table II. For the hydrogenic function

$\Phi_{2s}(r)$, $\lambda_{2s} = \epsilon_{2s} = -.1250$. We see from Table II that positive values of λ_{2s} are obtained for low k values, indicating that considerable continuum contribution is present in the function $\Phi_{2s}(r)$. On physical grounds, it might be expected that as k increases toward the $1s \rightarrow 2s$ excitation threshold of the atom core, the function $\Phi_{2s}(r)$

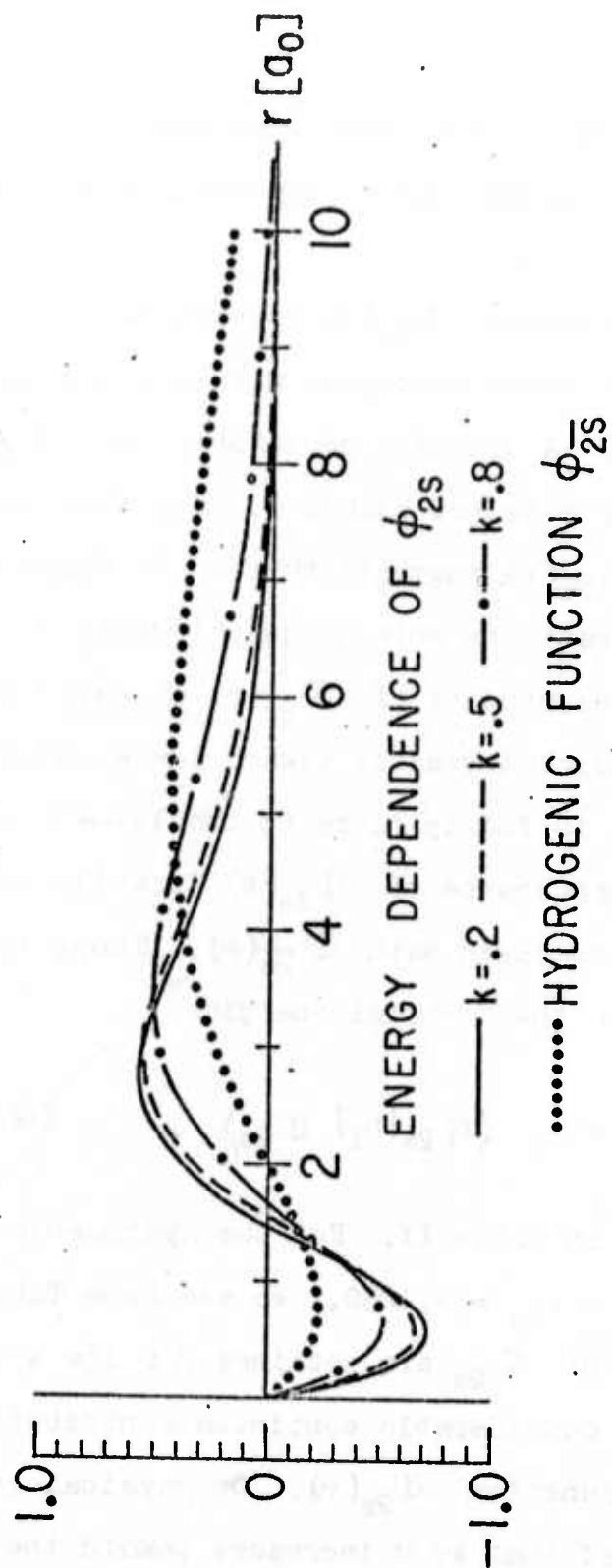


Fig. 3. From the wavefunction ψ_2

would tend to become the hydrogenic $\Phi_{2s}(r)$, while the function $u_{2s}(r)$ would expand to become a continuum orbital. This cannot happen for a wave function as simple in form as ψ_2 , because the linkage relations (66) demand that if $\Phi_{2s}(r)$ is square integrable, so also must be $u_{2s}(r)$.

More fundamentally, it is the exchange symmetry of ψ_2 which permits us to express u_{1s} , u_{2s} , and u_{ks} linearly in terms of Φ_{ks} , Φ_{2s} , and Φ_{1s} , but ψ_2 with only three pairs of functions comprising it, cannot exhibit proper behavior as threshold is crossed and still maintain its exchange symmetry. The difficulty is removed by adding an additional pair $\Phi_{3s}(r_1)u_{3s}(r_2)$ to ψ_2 . This gives a wave function of the form:

$$\psi(r_1, r_2) = [\Phi_{1s}(r_1)u_{1s}(r_2) + \Phi_{2s}(r_1)u_{2s}(r_2) + \Phi_{3s}(r_1)u_{3s}(r_2) + \Phi_{ks}(r_1)u_{ks}(r_2)] Y_1(\Omega_1, \Omega_2).$$

In this case, $u_{2s}(r)$ is a linear combination of $\Phi_{1s}(r)$, $\Phi_{2s}(r)$, and $\Phi_{3s}(r)$. The function $\Phi_{2s}(r)$ is now free to become the hydrogenic orbital $\Phi_{2s}(r)$ as k increases and threshold is crossed, while $\Phi_{3s}(r)$ and $u_{2s}(r)$ will become continuum orbitals. The other orbital $u_{3s}(r)$ will go over into a constant multiple of the hydrogenic orbital $\Phi_{2s}(r)$ and the entire wave function will become equivalent (above threshold) to the close coupling function ψ_{2cc} .

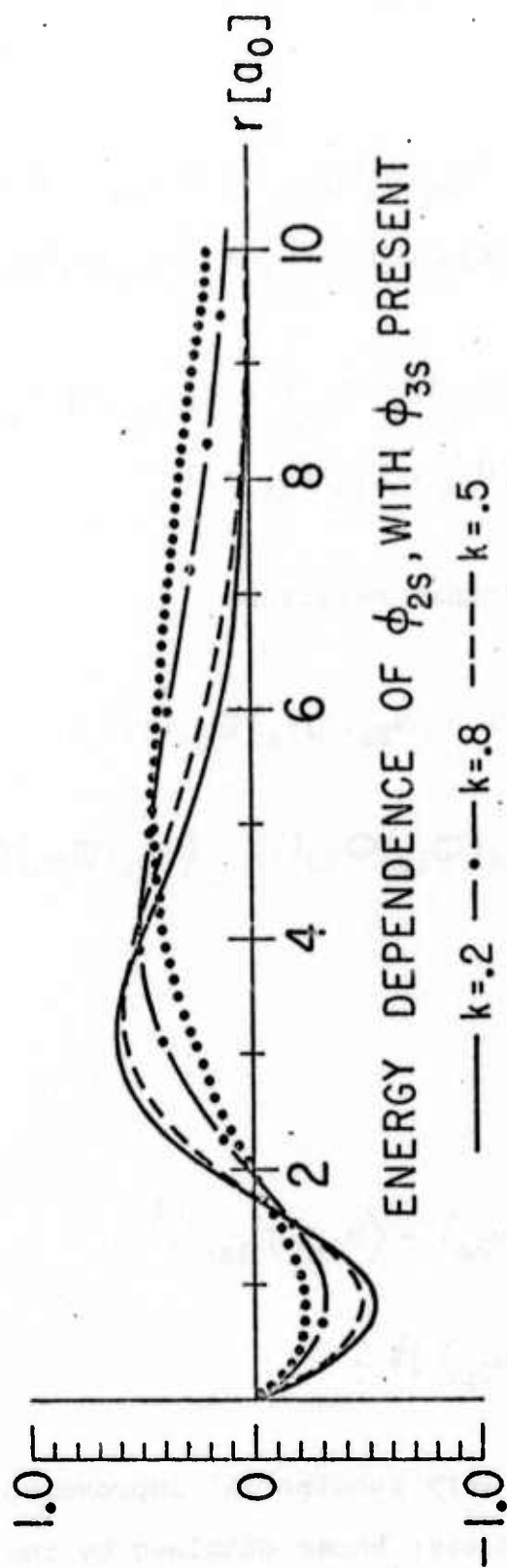
Fig. 4 illustrates the change in the form of Φ_{2s} when we add $\Phi_{3s}(r_1)u_{3s}(r_2)$ to ψ_2 . Table II shows the effect that this term has upon the 2s "orbital energy" λ_{2s} . We note that the addition of the Φ_{3s} function allows Φ_{2s} to relax toward larger values of r , although the compression of Φ_{2s} toward small r values still persists markedly for low k values. The 2s "orbital energy" λ_{2s} becomes lower throughout the examined energy range and as k approaches the $1s \rightarrow 2s$ excitation threshold, $\Phi_{2s}(r)$ bears a much stronger resemblance to the hydrogenic orbital $\Phi_{2s}(r)$.

We discuss now the function ψ_3 which includes a term

$$\Phi_{2p}(r_1)u_{2p}(r_2)Y_2(\Omega_1, \Omega_2), \quad (69)$$

designed to account for angular correlation. The index $v = 2$ on $Y_2(\Omega_1, \Omega_2)$ corresponds to the pair index $(l, l') = (1, 1)$. The functions $u_{1s}(r)$, $u_{2s}(r)$, and $u_{2p}(r)$ are determined from the system of equations:

$$\begin{aligned} [h_1 - X(\Phi_{1s}, \Phi_{1s}) + \frac{1}{2}k^2]u_{1s} - X(\Phi_{1s}, \Phi_{ks})u_{ks} - X(\Phi_{1s}, \Phi_{2s})u_{2s} \\ - X(\Phi_{1s}, \Phi_{2p})u_{2p} = 0, \end{aligned}$$



ENERGY DEPENDENCE OF ϕ_{2s} , WITH ϕ_{3s} PRESENT

— $k=0.2$ —•— $k=0.5$ --- $k=0.8$

..... HYDROGENIC FUNCTION ϕ_{2s}

Fig. 4. From the wavefunction $\psi_2 + \phi_{3s} u_{3s}$

$$[h_1 - X(\Phi_{2s}, \Phi_{2s}) + \langle \Phi_{2s} | h_1 | \Phi_{2s} \rangle + E]u_{2s} - X(\Phi_{2s}, \Phi_{ks})u_{ks} - X(\Phi_{2s}, \Phi_{1s})u_{1s} - X(\Phi_{2s}, \Phi_{2p})u_{2p} + \langle \Phi_{2s} | h_1 | \Phi_{ks} \rangle u_{ks} = 0,$$

$$[h_2 - X(\Phi_{2p}, \Phi_{2p}) + \langle \Phi_{2p} | h_2 | \Phi_{2p} \rangle + E]u_{2p} - X(\Phi_{2p}, \Phi_{ks})u_{ks} - X(\Phi_{2p}, \Phi_{2s})u_{2s} - X(\Phi_{2p}, \Phi_{1s})u_{1s} = 0,$$

(70)

supplemented by the linkage relations

$$\Phi_{2s}(r) = N_{2s}^{-1} [u_{2s}(r) - \langle u_{2s} | \Phi_{1s} \rangle \Phi_{1s}(r)],$$

$$\Phi_{ks}(r) = u_{1s}(r) - \langle u_{1s} | \Phi_{1s} \rangle \Phi_{1s}(r) - \langle u_{1s} | \Phi_{2s} \rangle \Phi_{2s}(r), \quad (71)$$

$$\Phi_{2p}(r) = N_{2p}^{-1} u_{2p}(r),$$

where

$$\left. \begin{aligned} N_{2s} &= (\langle u_{2s} | u_{2s} \rangle - \langle u_{2s} | \Phi_{1s} \rangle^2)^{\frac{1}{2}}, \\ N_{2p} &= (\langle u_{2p} | u_{2p} \rangle)^{\frac{1}{2}}. \end{aligned} \right\} \quad (72)$$

Table III shows a very substantial improvement in the calculated phase shifts over those obtained by the close coupling method. The orbitals Φ_{2s} , Φ_{ks} , and Φ_{2p} are illustrated for $k = .5$ in Fig. 5. Fig. 6 illustrates an

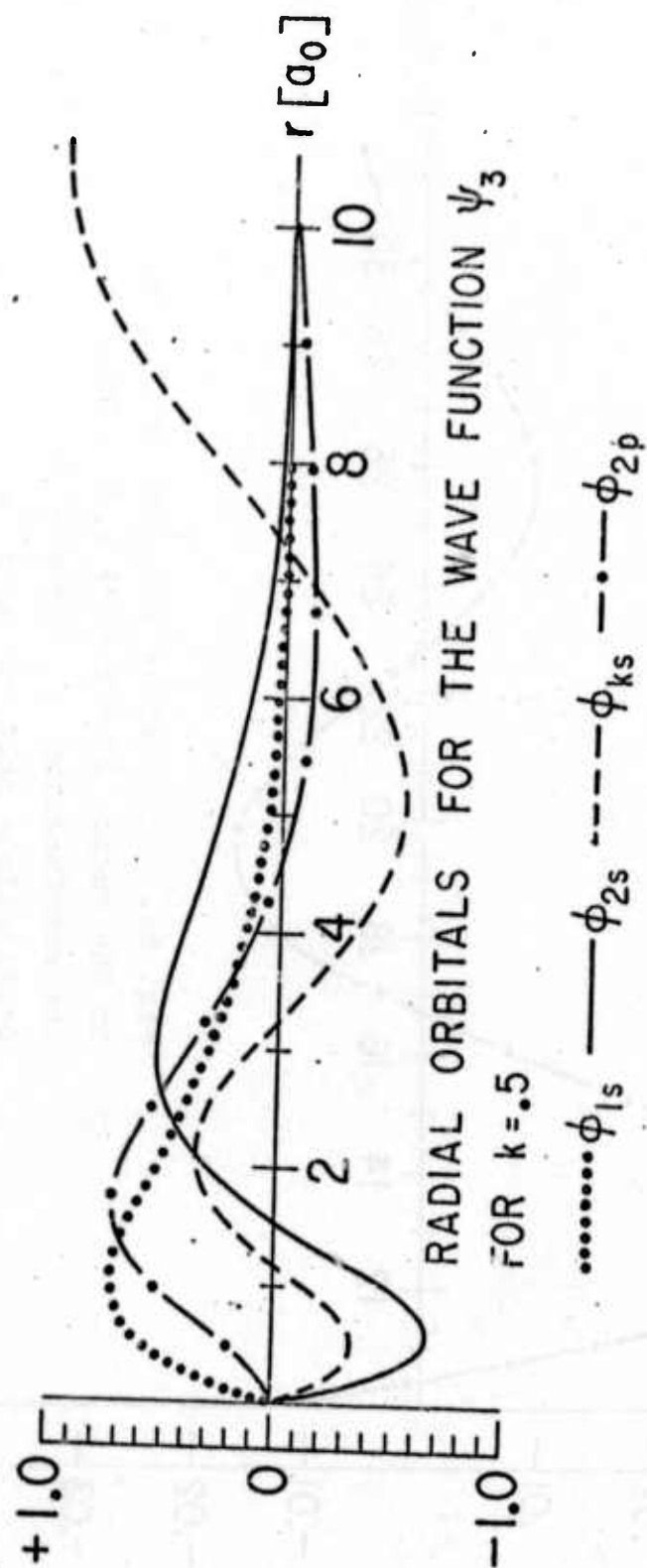


Fig. 5.

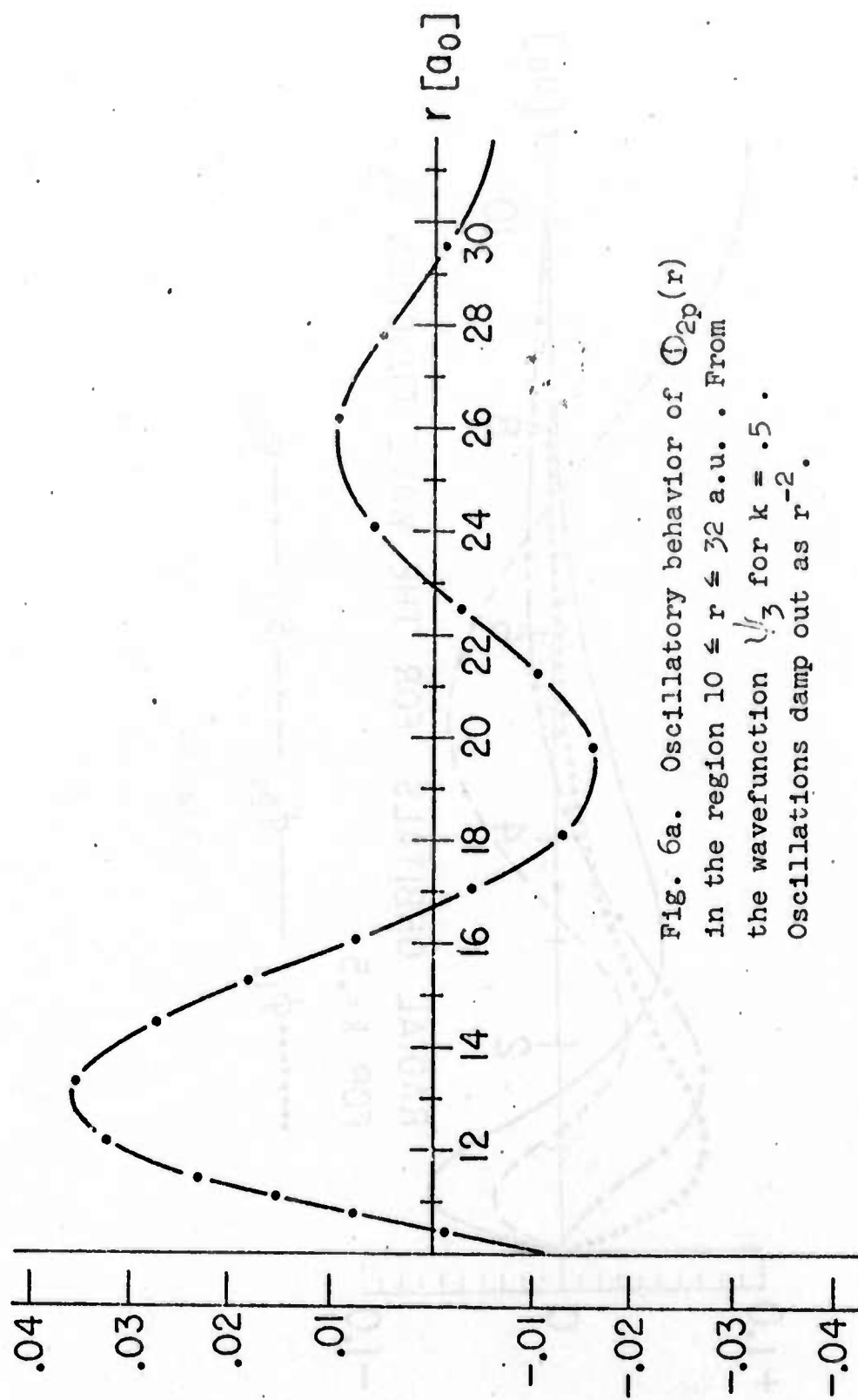


Fig. 6a. Oscillatory behavior of $\psi_3(r)$ in the region $10 \leq r \leq 32$ a.u. . From the wavefunction ψ_3 for $k = .5$. Oscillations damp out as r^{-2} .

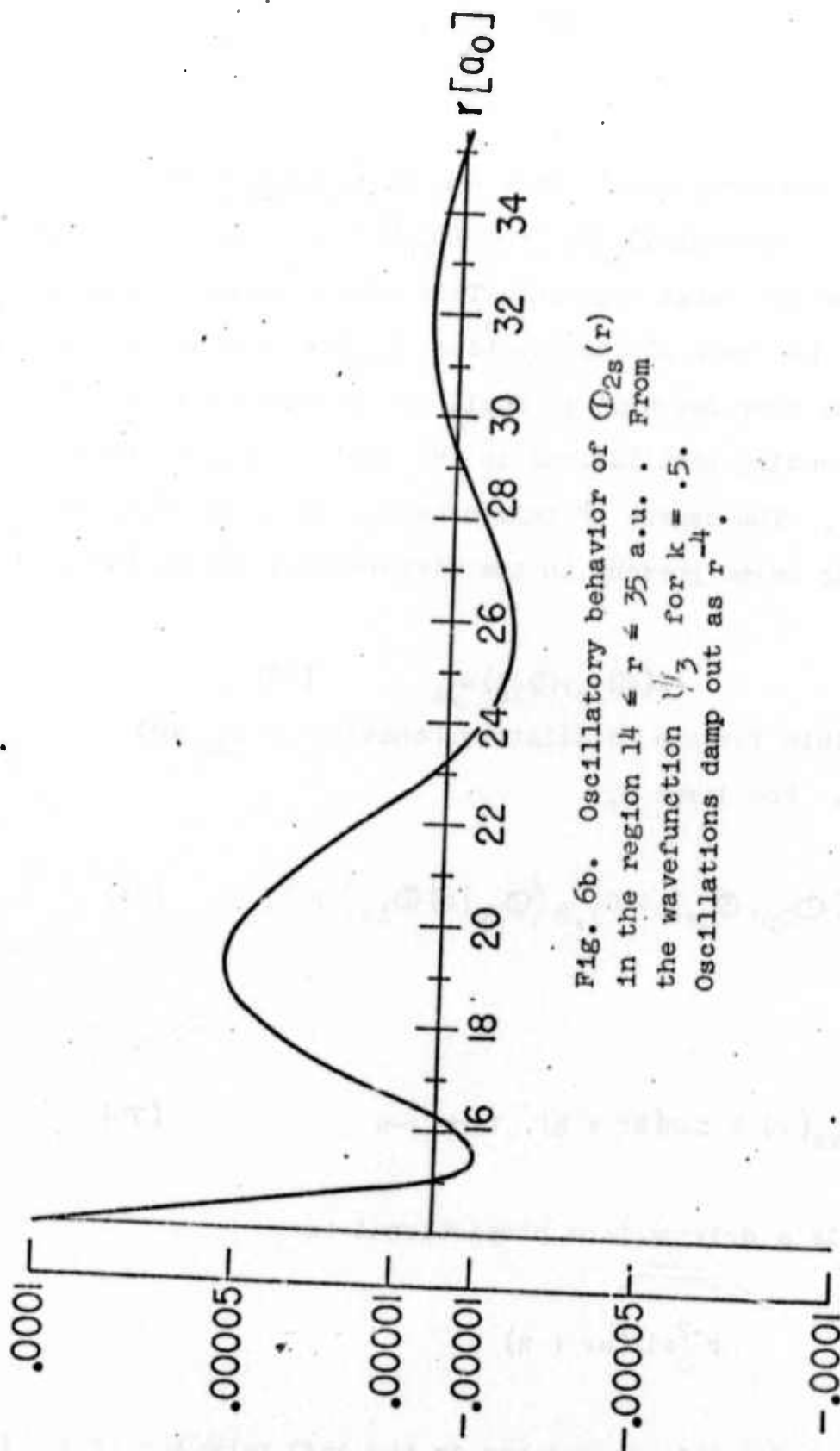


Fig. 6b. Oscillatory behavior of $\Phi_{2s}(r)$ in the region $14 \leq r \leq 35$ a.u. . From the wavefunction ψ_3 for $k = .5$. Oscillations damp out as r^{-4} .

interesting feature, namely that the variationally determined normalizeable orbitals $\Phi_{2s}(r)$ and $\Phi_{2p}(r)$ have damped oscillatory behavior for large argument. This effect is particularly striking in the case of the function $\Phi_{2p}(r)$, for which the oscillations damp out with an amplitude proportional to r^{-2} . The corresponding oscillations in the orbital $\Phi_{2s}(r)$ fall off like r^{-4} . The source of this behavior is to be found in the coupling terms present in the differential system (43). The term

$$X(\Phi_{2p}, \Phi_{1s}) u_{1s} \quad (73)$$

is responsible for the oscillatory behavior of u_{2p} and hence Φ_{2p} . For large r ,

$$X(\Phi_{2p}, \Phi_{1s}) \cong c_{1,2}^1 \langle \Phi_{2p} | r | \Phi_{1s} \rangle r^{-2}, \quad (74)$$

and

$$u_{ks}(r) \cong \sin(kr + \eta), \quad r \rightarrow \infty. \quad (75)$$

Thus (73) is a driving term proportional to

$$r^{-2} \sin(kr + \eta)$$

and accounts for this dependence in the tail behavior of $\Phi_{2p}(r)$.

Since $X(\Phi_{2s}, \Phi_{1s})$ decays exponentially for large r due to the orthogonality between $\Phi_{2s}(r)$ and $\Phi_{1s}(r)$, the direct coupling term involving $u_{ks}(r)$ does not function as a driving term which affects the tail behavior of $u_{2s}(r)$. The function $u_{ks}(r)$, of course, falls off as e^{-r} so that oscillatory behavior in $u_{2s}(r)$ and hence in $\Phi_{2s}(r)$ can only come from the coupling to $u_{2p}(r)$ through the term

$$X(\Phi_{2s}, \Phi_{2p}) u_{2p}. \quad (76)$$

As we have seen, for large r , and some constant α

$$u_{2p}(r) \cong \alpha r^{-2} \sin(kr + \eta), \quad r \rightarrow \infty, \quad (77)$$

also

$$X(\Phi_{2s}, \Phi_{2p}) \cong c_{1,2}^1 \langle \Phi_{2p} | r | \Phi_{2s} \rangle r^{-2}, \quad r \rightarrow \infty, \quad (78)$$

so that (76) represents a source term which for large r is proportional to

$$r^{-4} \sin(kr + \eta)$$

which accounts for this dependence in $\Phi_{2s}(r)$.

Fig. 7 illustrates the difference between $\Phi_{2p}(r)$ and the hydrogenic orbital $\Phi_{2p}(r)$ where

$$\Phi_{2p}(r) = (2\sqrt{6})^{-1} r^2 e^{-.5r}. \quad (79)$$

Again we note that the variationally determined orbital $\Phi_{2p}(r)$, illustrated for $k = .5$, has its peak much closer to the target atom than does the hydrogenic function $\Phi_{2p}(r)$. Use of the

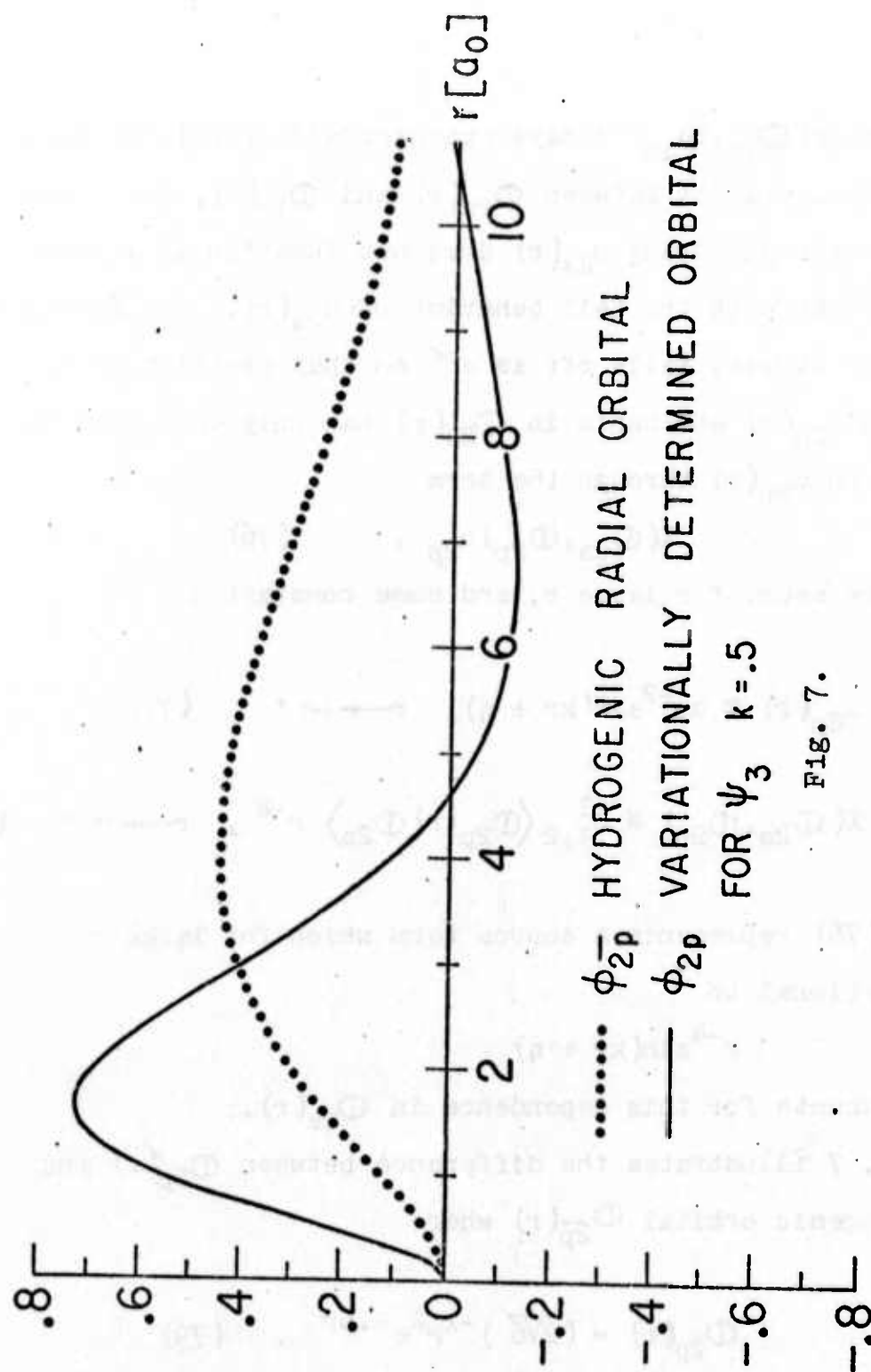


Fig. 7.

optimal orbital $\Phi_{2p}(r)$ accounts for the considerable improvement in the phase shift as compared against the close coupling results. Considerable continuum contribution is present in $\Phi_{2p}(r)$ as is indicated by its "orbital energy"

$$\lambda_{2p} = .182, \quad k = .5$$

which is to be compared with the value

$$\epsilon_{2p} = -.125$$

for the hydrogenic function.

Some idea of the efficiency of the present model wave functions can be obtained by comparing the phase shifts obtained using $\psi_3(\vec{r}_1, \vec{r}_2)$ with those obtained recently by Chung and Chen⁷. These workers used a wave function of the form

$$\begin{aligned} \psi(\vec{r}_1, \vec{r}_2) = & (r_1 r_2)^{-1} \left[\Phi_{1s}(r_1) G_{1s}(r_2) + G_{1s}(r_1) \Phi_{1s}(r_2) \right. \\ & \left. + Q \sum_{n=1} \sum_{\mu\nu} A_{\mu\nu}^n [r_1^\nu r_2^\mu e^{-(\alpha r_1 + \beta r_2)} + r_1^\mu r_2^\nu e^{-(\beta r_1 + \alpha r_2)}] P_n(\cos \Theta_{12}) \right]. \end{aligned} \quad (80)$$

In the summation, six terms of s-type and nine terms of p-type were included. The open channel function used was

$$\begin{aligned} G_{1s}(r) = & (\sin kr + \tan \eta \cos kr)(1 - e^{-\sigma r}) \\ & + \sum_n a_n r^n e^{-\sigma r}. \end{aligned} \quad (81)$$

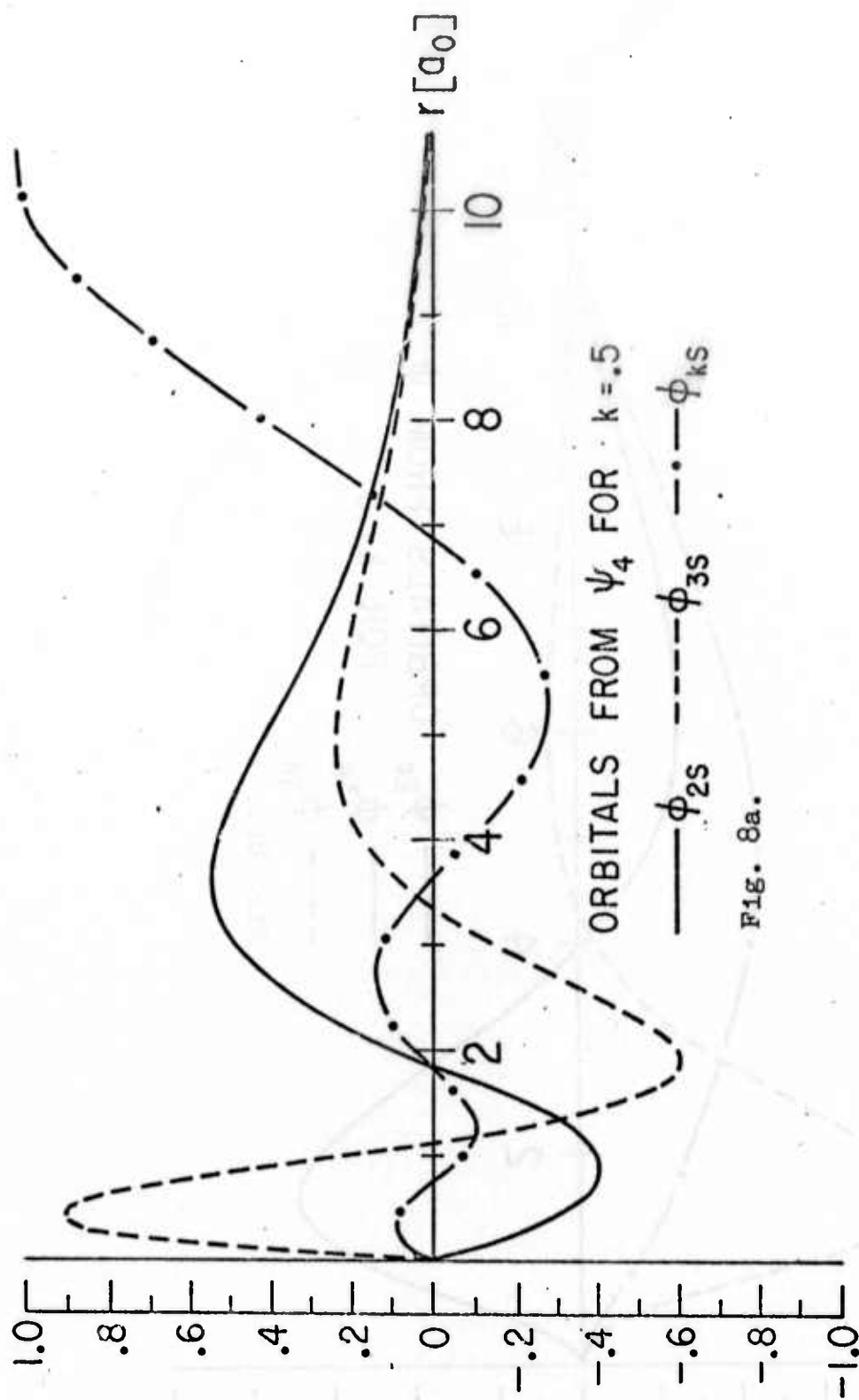
and Q is the projection operator:

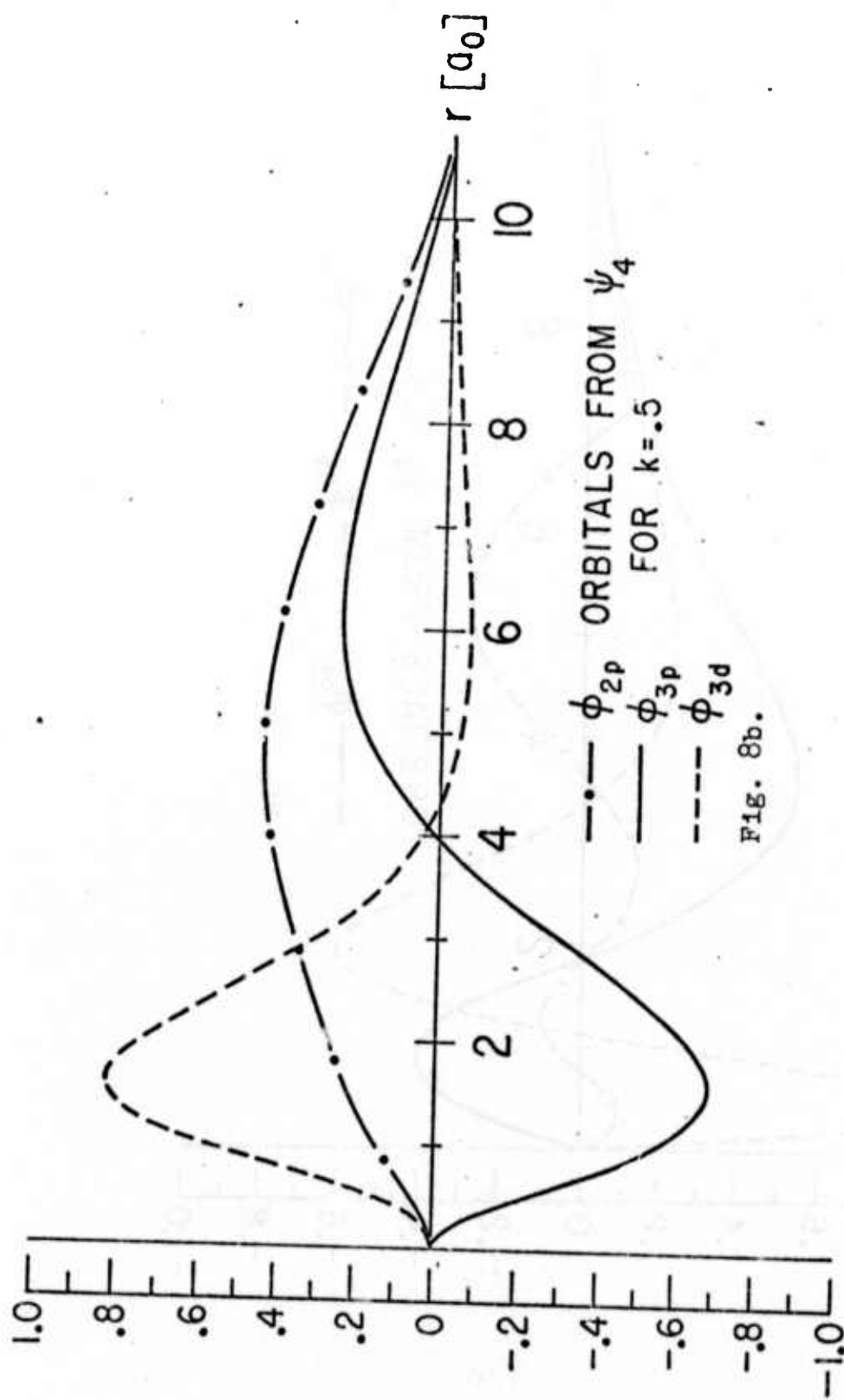
$$Q = [1 - |\phi_{1s}(r_1)\rangle\langle\phi_{1s}(r_1)|][1 - |\phi_{1s}(r_2)\rangle\langle\phi_{1s}(r_2)|]. \quad (82)$$

The coefficients $A_{\mu\nu}$ and d_n as well as the open channel parameter σ were calculated for each energy value considered in the range $.1 \leq k \leq .8$. The other two nonlinear parameters α and β were determined and used over the entire energy range. The phase shifts obtained with this wave function are compared with those obtained with ψ_3 in table III. These results show that the present model wavefunctions are quite efficient with respect to the number of terms required to produce phase shifts of comparable accuracy.

Further calculations were carried out with the more elaborate wavefunctions ψ_4 , ψ_5 , and ψ_6 . The results of these calculations are presented in table III where it is seen that accurate phase shifts are obtainable with short expansions within the present model. Even ψ_6 , the most elaborate wavefunction used, is constructed from only 11 optimal orbitals. In Fig 8, the optimal orbitals are illustrated for $k = .5$ using the wave function ψ_4 .

Table IV gives the expansion coefficients Γ_{vmn} for this wavefunction. Finally Table V presents the corresponding orbital energies.





ACKNOWLEDGEMENTS

Appreciation is expressed to Prof. C. C. J. Roothaan for sponsoring this research and for many helpful discussions. Thanks are also due to Deborah Rosenblatt for encouragement during the particularly vexing period when the computer program used in these calculations was being debugged.

REFERENCES

1. N. F. Mott and H. S. W. Massey, The Theory of Atomic Collisions (Clarendon Press, Oxford 1965). See esp p. 530.
 2. C. Schwartz, Phys. Rev. 124, 1468 (1961)
 3. R. L. Armstead, UCRL-11628 (1964)
 4. I. C. Percival and M. J. Seaton, Proc. Cambridge Phil. Soc. 53, 654 (1957).
P. G. Burke and H. M. Schey, Phys Rev. 126, 147 (1962)
K. Smith and L. A. Morgan, Phys. Rev. 165, 110 (1968)
 5. P. G. Burke and A. J. Taylor, Proc Phys Soc. 88 , 549 (1966)
A. J. Taylor, in Physics of Electronic and Atomic Collisions (Science Bookcrafters, N. Y. 1965) 27.
 6. M. Gaillitis, in Physics of Electronic and Atomic Collisions (Science Bookcrafters, N. Y. 1965) 10.
 7. K. T. Chung and J. C. Y. Chen, Phys Rev. A 6, 686 (1972)
 8. M. E. Rose, Elementary Theory of Angular Momentum (John Wiley and Sons Inc., N. Y. 1957).
- * Research supported in part by the Advanced Research Projects Agency through the U. S. Army Research Office (Durham), under Contract NOS. DA-31-124-ARO-D-447 and ARPA-S-D-89 and by the National Science Foundation under Grant NOS. NSF-GP-27138 and NSF-GP-15216.
- † Submitted in partial fulfillment of the requirements for the Ph. D.; Department of Physics, University of Chicago, Chicago, Ill.

FIGURE CAPTIONS

Fig. 1. Permitted pairs used in the construction of the angular two particle functions $Y_{LM\ell\ell'}(\Omega_1, \Omega_2)$, illustrated for $L = 0, 1, 2$.

Points indicated by \bullet are used for the "normal" terms for which

$$\phi_{Y_{LM\ell\ell'}} = (-1)^{L_Y} Y_{LM\ell\ell'}$$

Points indicated by \circ are used for the "abnormal" terms for which

$$\phi_{Y_{LM\ell\ell'}} = (-1)^{L+1} Y_{LM\ell\ell'}$$

Fig. 2. Assignment of values for the running index v replacing the pair index $(\ell, \ell') \in [N]$ for $L = 4$. By convention $v = 1$ corresponds to the pair $(0, L)$. The relationship between v and \bar{v} is also illustrated. Note that the points corresponding to the indices v and \bar{v} are symmetrically placed about the line $\ell = \ell'$. In this case the elements of the set V are the integers 1-9.

Fig. 6a. Oscillatory behavior of $\phi_{2p}(r)$ in the region $10 \leq r \leq 32$ a.u. (From the wavefunction ψ_3 for $k = .5$) Oscillations damp out as r^{-2} .

Fig. 6b Oscillatory behavior of $\phi_{2s}(r)$ in the region $14 \leq r \leq 35$ a.u. (From the wavefunction ψ_3 for $k = .5$) Oscillations damp out as r^{-4} .

The remaining figures are to be captioned simply as Fig. 3, Fig. 4, Fig. 5, Fig. 7, Fig. 8a, and Fig. 8b .

Table I. Structure of the Wavefunctions used.

(l, l')	$(0,0)$					$(1,1)$			$(2,2)$		$(3,3)$	
v	1					2			3		4	
m	1	2	3	4	5	1	2	3	1	2	1	
ψ_1	1s	ks										
ψ_2	1s	2s	ks									
ψ_3	1s	2s	ks			2p						
ψ_4	1s	2s	3s	ks		2p	3p		3d			
ψ_5	1s	2s	3s	ks		2p	3p	4p	3d			
ψ_6	1s	2s	3s	4s	ks	2p	3p	4p	3d	4d	4f	

TABLE III. Phase Shifts η for $1s$ elastic scattering of electrons from hydrogen atoms.

k	ψ_{1a}	ψ_{1cc}^b	ψ_{2cc}^b	ψ_{2a}	ψ_{3cc}^b	ψ_{3a}	15 term ^c	ψ_{4a}	50 term ^c	ψ_{5a}	ψ_{6a}	r_{12}^d
.1	2.396	2.404	2.420	2.491	2.537	2.539	2.539	2.548	2.550	2.549		2.553
.2	1.871	1.878	1.894	1.974	2.043	2.047	2.047	2.060	2.060	2.061		2.067
.3	1.508	1.519	1.533	1.596	1.673	1.673	1.673	1.688	1.690	1.690		1.696
.4	1.239	1.257	1.266	1.302	1.390	1.389	1.389	1.405	1.408	1.409	1.411	1.415
.5	1.031	1.046	1.062	1.092	1.172	1.174	1.174	1.189	1.192	1.194		1.202
.6	.869	.89	.906	.93	1.006	1.013	1.013	1.029	1.032	1.035		1.041
.7	.744	.77	.791	.82	.882	.902	.902	.919	.921	.924		.930
.8	.651	.70	.716	.77	.799	.857	.857	.875	.877	.879	.883	.886

^aPresent Model Wavefunctions

^bClose Coupling Wavefunctions, References 1,4

^cAnalytic Expansion Wavefunctions, Reference 7

^dSchwartz, Hylleraas-type Wavefunction, Reference 2

TABLE IV.
Expansion
coefficients for
 ψ_4 , $k = 0.5$

v	m	n	Γ_{vmn}
1	1	1	1.217
1	1	2	-0.859
1	1	3	0.746
1	1	4	1.000
1	2	2	-0.134
1	2	3	-0.029
1	2	4	0.
1	3	3	-0.032
1	3	4	0.
2	1	1	-0.085
2	1	2	-0.075
2	2	2	0.178
3	1	1	-0.031

TABLE II. Orbital energy of
the 2s orbital for different
k values.

k	$\lambda_{2s}(\psi_2)$	$\lambda_{2s}(\psi_2 + \psi_{3s} u_{3s})$
.2	.191	.026
.5	.117	-.025
.8	-.031	-.108

For the hydrogenic 2s orbital
 $\lambda_{2s} = \epsilon_{2s} = -.125$

TABLE V. Orbital energies
for the orbitals of the
wavefunction ψ_4
for $k = 0.5$

label	v	m	λ_{vm}
1s	1	1	-0.5000
2s	1	2	-0.0654
3s	1	3	1.0887
2p	2	1	-0.1120
3p	2	2	0.2088
3d	3	1	1.2299

INDEX TO HANDWRITTEN SYMBOLS

Ψ to be read Ψ

ψ to be read ψ

Φ to be read Φ

ϕ to be read ϕ

Γ to be read Γ

Ω to be read Ω

ω to be read ω

λ to be read λ

θ to be read θ

δ to be read δ

∂ to be read ∂

∞ to be read ∞

l to be read l

\mathcal{H} to be read "script" H

\mathcal{L} to be read "script" L

\mathcal{P} to be read "script" P

\mathcal{V} to be read "script" V